



VOLUME ONE HUNDRED AND TWENTY ONE

ADVANCES IN  
**HETEROCYCLIC CHEMISTRY**

**Heterocyclic Chemistry in the  
21st Century: A Tribute to  
Alan Katritzky**

## EDITORIAL ADVISORY BOARD

- A. T. Balaban *Galveston, Texas, United States of America*  
A. J. Boulton *Norwich, United Kingdom*  
M. Brimble *Auckland, New Zealand*
- D. L. Comins *Raleigh, North Carolina, United States of America*  
J. Cossy *Paris, France*  
J. A. Joule *Manchester, United Kingdom*  
V. I. Minkin *Rostov-on-Don, Russia*  
B. U. W. Maes *Antwerp, Belgium*
- A. Padwa *Atlanta, Georgia, United States of America*  
V. Snieckus *Kingston, Ontario, Canada*  
B. Stanovnik *Ljubljana, Slovenia*  
C. V. Stevens *Ghent, Belgium*
- J. A. Zoltewicz *Gainesville, Florida, United States of America*

VOLUME ONE HUNDRED AND TWENTY ONE

# ADVANCES IN HETEROCYCLIC CHEMISTRY

## Heterocyclic Chemistry in the 21st Century: A Tribute to Alan Katritzky

Editors

**ERIC F. V. SCRIVEN**

*Department of Chemistry,  
University of Florida,  
Gainesville, FL, USA*

**CHRISTOPHER A. RAMSDEN**

*Lennard-Jones Laboratories,  
Keele University, Staffordshire,  
United Kingdom*



**ACADEMIC PRESS**

An imprint of Elsevier  
elsevier.com

Academic Press is an imprint of Elsevier  
50 Hampshire Street, 5th Floor, Cambridge, MA 02139, United States  
525 B Street, Suite 1800, San Diego, CA 92101-4495, United States  
125 London Wall, London EC2Y 5AS, United Kingdom  
The Boulevard, Langford Lane, Kidlington, Oxford OX5 1GB, United Kingdom

First edition 2017

Copyright © 2017 Elsevier Inc. All rights reserved.

No part of this publication may be reproduced or transmitted in any form or by any means, electronic or mechanical, including photocopying, recording, or any information storage and retrieval system, without permission in writing from the publisher. Details on how to seek permission, further information about the Publisher's permissions policies and our arrangements with organizations such as the Copyright Clearance Center and the Copyright Licensing Agency, can be found at our website: [www.elsevier.com/permissions](http://www.elsevier.com/permissions).

This book and the individual contributions contained in it are protected under copyright by the Publisher (other than as may be noted herein).

### Notices

Knowledge and best practice in this field are constantly changing. As new research and experience broaden our understanding, changes in research methods, professional practices, or medical treatment may become necessary.

Practitioners and researchers must always rely on their own experience and knowledge in evaluating and using any information, methods, compounds, or experiments described herein. In using such information or methods they should be mindful of their own safety and the safety of others, including parties for whom they have a professional responsibility.

To the fullest extent of the law, neither the Publisher nor the authors, contributors, or editors, assume any liability for any injury and/or damage to persons or property as a matter of products liability, negligence or otherwise, or from any use or operation of any methods, products, instructions, or ideas contained in the material herein.

ISBN: 978-0-12-811174-1

ISSN: 0065-2725

For information on all Academic Press publications visit our website at <https://www.elsevier.com/>



Working together  
to grow libraries in  
developing countries

[www.elsevier.com](http://www.elsevier.com) • [www.bookaid.org](http://www.bookaid.org)

*Publisher:* Zoe Kruze

*Acquisition Editor:* Poppy Garraway

*Editorial Project Manager:* Shellie Bryant

*Production Project Manager:* Surya Narayanan Jayachandran

*Designer:* Greg Harris

Typeset by TNQ Books and Journals

# CONTRIBUTORS

**Saadia T. Chaudhry**

Department of Chemistry, Purdue University, West Lafayette, IN, USA

**Johannes G. de Vries**

Leibniz-Institut für Katalyse e.V. an der Universität Rostock, Rostock, Germany

**Andrew J.F. Edmunds**

Syngenta Crop Protection AG, Basel, Switzerland

**Jian-Bo Feng**

Leibniz-Institut für Katalyse e.V. an der Universität Rostock, Rostock, Germany

**Peter Maienfisch**

Syngenta Crop Protection AG, Basel, Switzerland

**Charles M. Marson**

Department of Chemistry, University College London, Christopher Ingold Laboratories, London, UK

**Colin H. McAteer**

Vertellus Specialties Inc., Indianapolis, IN, USA

**Jianguo Mei**

Department of Chemistry, Purdue University, West Lafayette, IN, USA

**Ramiah Murugan**

Vertellus Specialties Inc., Indianapolis, IN, USA

**Jean'ne M. Shreeve**

Department of Chemistry, University of Idaho, Moscow, ID, USA

**Yarlagadda V. Subba Rao**

Vertellus Specialties Inc., Indianapolis, IN, USA

**Xiao-Feng Wu**

Leibniz-Institut für Katalyse e.V. an der Universität Rostock, Rostock, Germany

**Ping Yin**

Department of Chemistry, University of Idaho, Moscow, ID, USA

**Tony Y. Zhang**

Small Molecule Design and Development, Lilly Research Laboratories, Eli Lilly and Company, Indianapolis, IN, USA

**Xikang Zhao**

Department of Chemistry, Purdue University, West Lafayette, IN, USA

## PREFACE

A short tribute to Alan Katritzky highlighting the aspects of his major work in heterocyclic chemistry (structure, mechanism, theory, QSAR, synthetic methods, applications, and the review literature) appeared in Volume 113 of *Advances in Heterocyclic Chemistry*. For over 50 years, Alan was at the forefront of advances in and applications of heterocyclic chemistry. He initiated the publication of *Advances in Heterocyclic Chemistry* in 1963 and personally commissioned and edited 112 volumes. When we considered what would be a fitting tribute to his contribution, we posed the question, as we felt Alan would have, “What is happening now, and what next?” In response to this question, we have been fortunate to receive chapters from leaders currently involved in heterocyclic chemistry and its applications. These cover the latest advances in the areas mentioned above together with a broad scope of new developments.

This, the third and final volume of the tribute, contains eight chapters which focus on synthetic approaches and applications of heterocycles with current or prospective commercial importance. The first chapter by Tony Zhang (Eli Lilly and Co.) contains an analysis of the structures of heterocyclic drugs and drug candidates, which illustrates the need for robust reactions that lead to more diverse structures. In Chapter 2, Charles Marson (University College London) reviews saturated heterocycles (with one heteroatom, spiroheterocyclic, and heterobicyclo systems) with applications in medicinal chemistry covering the period 2013–2015. Peter Maienfisch and Andrew Edmunds (Syngenta Crop Protection AG) present an account of the contribution of thiazoles and isothiazoles to crop protection in Chapter 3. Jean’ne Shreeve and Ping Yin (University of Idaho) (Chapter 4) review nitrogen-rich azoles as high-density energy materials. In Chapter 5, Jianguo Mei, Xikang Zhao, and Saadia Chaudhry (Purdue University) describe the use of five-membered ring heterocycles used as building blocks for production of organic semiconductors.

In Chapter 6, Colin McAteer, Ramiah Murugan, and Yarlagadda Subba Rao (Vertellus Specialties, Inc.) give a broad treatment of heterogeneously catalyzed synthesis of three- to seven-membered heterocycles including discussion of catalyst choice, process, and economic considerations. The main advances (2013–2015) in palladium-catalyzed carbonylative synthesis, especially of five- and six-membered heterocycles, is given by Xiao-Feng Wu and Jian-Bo Feng (Leibniz Institute for Catalysis, University of Rostock)

in Chapter 7. In the final chapter, Johannes de Vries (Leibnitz Institute for Catalysis, University of Rostock) discusses powerful new catalytic methods available and in development that allow the utilization of renewable resources, particularly 5-hydroxymethylfurfural as a platform chemical.

**Chris Ramsden and Eric Scriven**

September, 2016.



# The Evolving Landscape of Heterocycles in Drugs and Drug Candidates

Tony Y. Zhang<sup>a</sup>

Small Molecule Design and Development, Lilly Research Laboratories, Eli Lilly and Company,  
Indianapolis, IN, USA  
E-mail: zhang@lilly.com

## Contents

1. Introduction	2
2. Method	3
3. Results and Discussion	3
4. Conclusion	9
Acknowledgments	11
References	11

## Abstract

Substructure analysis of approved drugs and drug candidates in clinical trials was performed to illustrate the evolving roles of heterocycles in pharmaceutical research. The increasing representation of biaryls and heteroaromatics is noted and attributed predominantly to their better accessibility brought upon by advances in metal catalyzed cross-coupling and hetero-coupling reactions. Possible future focus of academic research is proposed for improving structural diversity and probability of success for drug research, and enhancing the impact of heterocyclic chemistry to the development of new medicines.

**Keywords:** Analysis; Biaryl; Cross-coupling; Drug; Drug candidates; Drug of the future; Heterocycle; Palladium catalysis; Pharmacophore; Pyrazole; Pyridine; Structural diversity; Substructures; Synthetic accessibility; Synthetic feasibility; Synthetic methodology development

<sup>a</sup> This paper is dedicated to the memory of Professor Alan R. Katritzky, from whom the author learned the reason of being for heterocycles.



## 1. INTRODUCTION

Heterocycles have played a prominent role among pharmaceuticals, as they have been essential in the perpetuation, propagation, and evolution of life in molecular forms such as nucleotides, carbohydrates, hemes, and amino acids. While most drugs achieve the desired therapeutic outcomes through interactions with proteins or DNA/RNA, the morphology of successful drugs does not necessarily resemble that of their biological targets. In fact, the shapes of drugs are heavily influenced by three artificial factors, i.e., (a) the structure of the initial hit or lead; (b) the synthetic feasibility for the intended structure; and (c) the availability of starting material for the preparation (Figure 1). The feedback loop connecting compound synthesis and biological testing during structural activity relationship (SAR) studies is still a relatively long and arduous process.

It is worth noting that all these three major factors are a culmination of historic synthetic chemistry efforts and natural product explorations in the last 200 years. As a result they tend to be biased toward certain chemical lineages, such as petroleum, coal tar, naval store chemicals, and existing drugs supply chain. For example, hits are usually obtained from screening an existing compound collection, which itself was collected through the years from various sources. We want to note that in recent years more tailor-designed libraries of hit structures, guided by insights into protein structures with the aid of computational chemistry and NMR techniques (e.g., fragment-based drug discovery/design) (2015DDT(20)1104) are matriculating into the

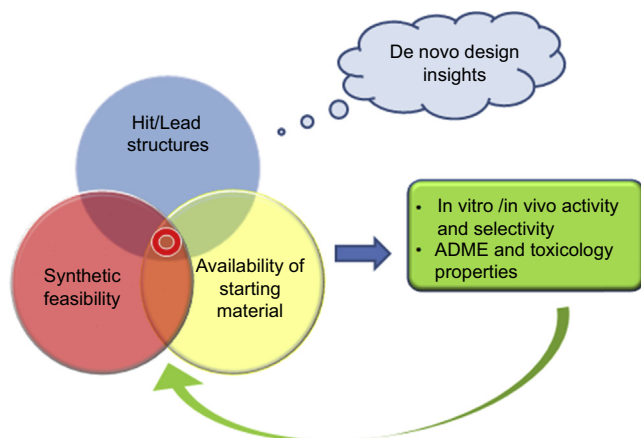


Figure 1 Major influencers of drug structures during the discovery process.

public and industrial collections to compliment compounds of natural and industrial origin. However, composition of these libraries is heavily influenced by high efficiency chemistry and separation technology that enabled their facile synthesis and purification. For SAR investigation, most chemists prefer reactions that are reliable and highly efficient, starting from commercially available starting materials. In other words, compounds that are easily synthesized are biased to have a better chance of progressing in the drug discovery journey.



---

## 2. METHOD

To have a more quantitative glimpse at the structural trend of drug molecules, we performed a substructure analysis of approved drugs as well as drug candidates currently in clinical and preclinical development using the Drug Data Report (MDDR) database (2016M11). MDDR is a commercial database that retrieves chemical structures from published documents. The database includes the respective therapeutic classes and status of development of drug candidates. It is difficult to compile a historical overview of snapshots of the shapes of molecules in development as the numbers are constantly changing. Therefore, we plot the data of all launched drugs ( $N = 1631$ ), those drugs that have been approved in the last decade (2005–2014,  $N = 221$ ); the previous decade (1995–2004,  $N = 331$ ); drug candidates currently in Phase III ( $N = 351$ ), Phase II ( $N = 1457$ ), and Phase I ( $N = 1161$ ); or in preclinical development ( $N = 17,580$ ), as of Sept 2015. Only compounds with defined structures were included and as a consequence large molecules such as antibodies and large peptides were omitted. The database also has a “Biological testing” category for development stage, which covers a broad range of the compounds that have not yet entered into preclinical development. They were not included in the analysis due to the lack of commonly accepted criteria for the milestone. Compounds with a development stage classified as “registered,” “pre-registered,” “recommended approval,” and those between phases were not included due to the small representation.



---

## 3. RESULTS AND DISCUSSION

Of the more than 22,000 compounds with defined structures in the selected dataset, a great majority (95%) contain at least one ring (top line,

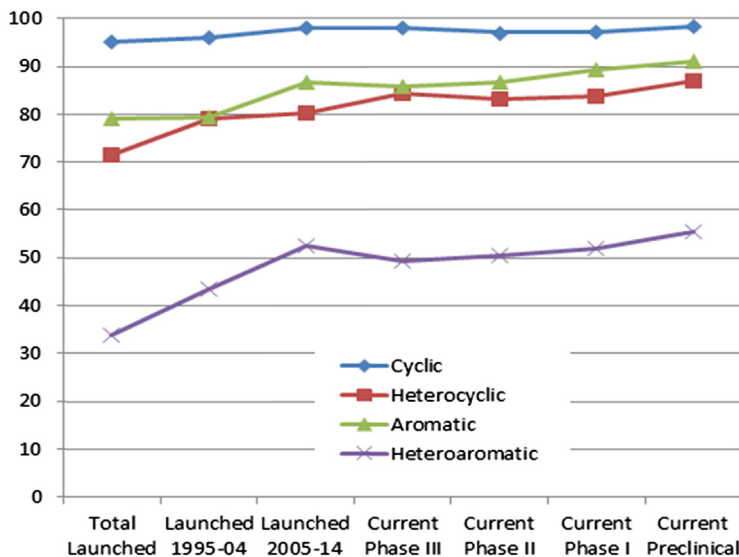


**Figure 2** Percentage of ring containing molecules by substructure analysis.

Figure 2). This percentage remains more or less constant if we look at newer drugs that have been approved in the last decade or earlier. Even for drugs that are still under various stages of clinical development, the ratio of cyclic compounds remains stable between 95% and 98%. The percentage of heterocyclic compounds, however, rose steadily from 71% to 87%. Compared to their linear counterparts of similar composition, cyclic compounds have fewer degrees of structural freedom, are more compact, and tend to be better binders with the protein targets. They are generally more bioavailable. Nevertheless, medicinal chemistry merits alone would not be able to account for their dominance. The percentage of aromatic compounds has also shown a dramatic increase from just under 80% for all marketed drugs to over 90% for drug candidates in preclinical development. This finding can be considered as a predictor for the structure of drugs in the near future. Considering the composition of drug candidates currently in Phase III clinical trials as a leading indicator for the types of future drugs to be approved, along with Phase II and Phase I molecules as yet a further indicator for what is coming down the road for the next generation of drugs, we can see the general trend towards more aromatic compounds. Interestingly this trend has been noted several years ago by Lovering, Bikker, and Humblet (2009JMC(52)6752). The drug discovery community has been alarmed by the increasing aromaticity or decreasing presence of saturation in drug

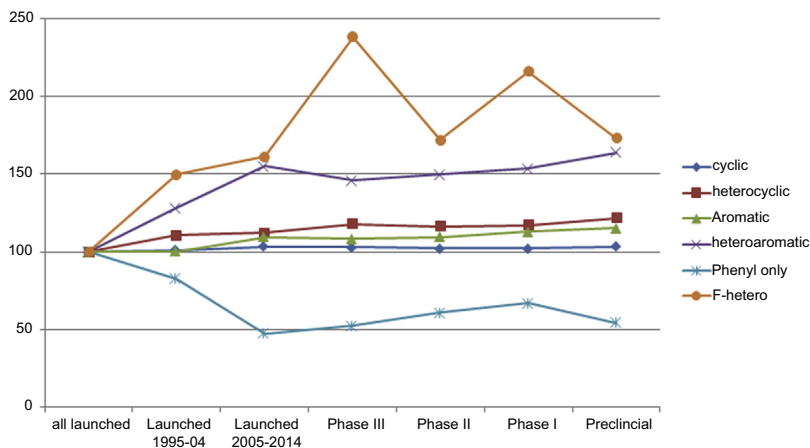


**Figure 3** Trends of ring containing compounds.

structures. The reason for concern is that the decrease in hydrogen atom saturation in drug candidates has been linked with poor solubility and high attrition rate during clinical development. However, the trend toward aromatization/unsaturation continues. The roles played by the synthetic feasibility for shaping this thread need to be delineated from the requirement of structural rigidity and hydrogen bonding capabilities (aromatic N atoms). The increasing proportion of therapeutic targets of drug discovery efforts toward oncology (i.e., large number of kinase targets) might also play a role in the molecular structure of drugs, leading to an increasing presence of  $sp^2$  hybridized nitrogen.

Instead of showing the absolute percentage of substructure representation, [Figure 3](#) illustrates the change across development stages. It is worth noting that 34% of all previously approved drugs contain at least one heteroaromatic ring. This number has increased by 54% for the compounds currently in preclinical testing. On the contrary, there is nearly a 50% drop for the simple, mono-substituted phenyl group. Explanation of this phenomenon is complex and needs to be nuanced. Contributing factors for the decreasing popularity of the plain phenyl might include the susceptibility toward metabolism, lack of binding specificity, too high a lipophilicity, or poor intellectual property positions.

One of the most prominent drug structure changes is the rise of biaryls ( $Ar-Ar'$ ). Biaryl as a pharmacophore obviously brings a combination of structural rigidity and flexibility around the “free” rotating single bond adjoining the two rings. However, its popularity has to be attributed to

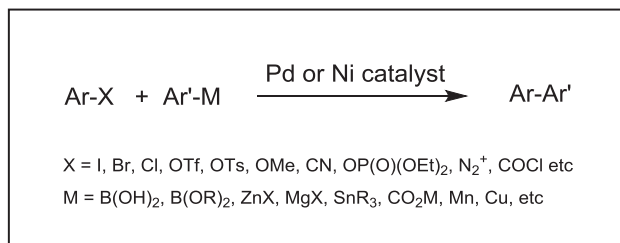


**Figure 4** Transition metal catalyzed crosscoupling reactions.

the advent of palladium cross-coupling reactions (Figure 4) (2012AGE(51)5062). Also, access to the nucleophilic aryl metals has been vastly improved through directed ortho metalation (2014MI1) and Rh- or Ir-facilitated direct borylation of arenes (2012ACR(45)864). In recent years, the scope of the Ir-catalyzed borylation reaction has been greatly expanded to accommodate unconventional “electrophiles” with leaving groups including OH, CN, and OMe. Biaryls (Ar-Ar') have also been obtained by Rh-catalyzed direct coupling of arenes (ArH) and aromatic aldehyde (Ar'CHO) coupling through a C-H activation mechanism (2010JA(132)12212).

As illustrated in Figure 5, the growth in biaryls is largely driven by the popularity of those containing a heteroaromatic ring. This is a class of compounds extremely difficult to selectively prepare without the aid of transition

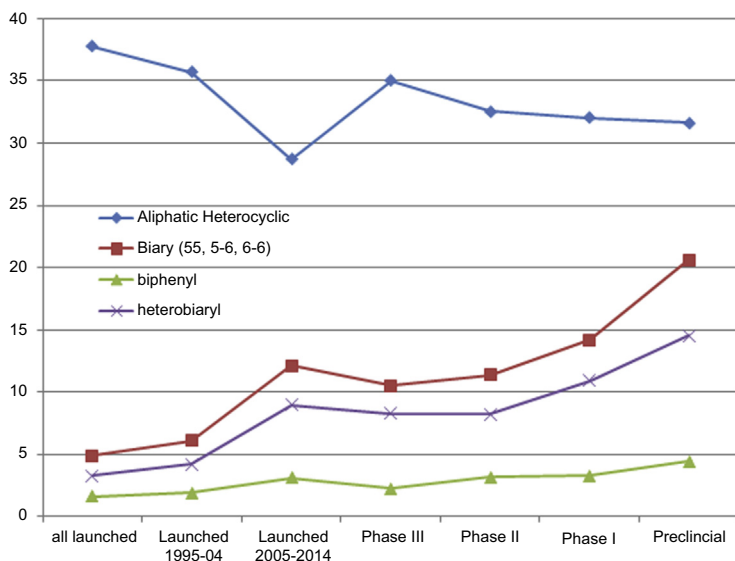


**Figure 5** The rise of biaryls (Ar-Ar').

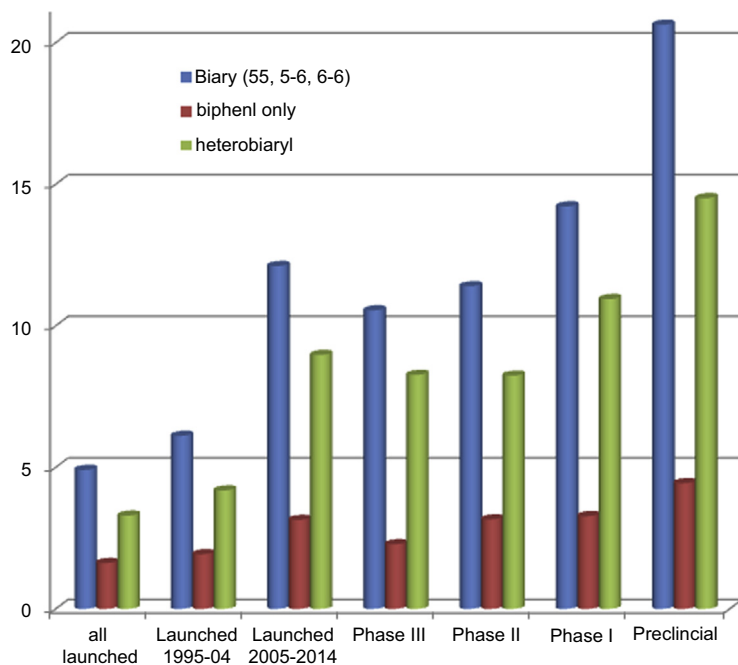


**Figure 6** The increasing presence of Ar–Ar' in drugs and drug candidates.

metal catalyzed cross-coupling. Concomitant with the rise of biaryls is the drop in the percentage of aliphatic heterocyclic compounds. Again data are lagging for concluding whether this is really a desirable phenomenon or not. The same data can be visualized in a columnar format to underscore the influence of cross-coupling reactions on the shape of drugs (Figure 6) (1982ACR(15)340, 2011AGE(50)6722). The popularity of biaryl in drugs corresponds well chronologically with the surge of published literature for this powerful and differentiating synthetic methodology (Figure 7) (2016MI2). Unequivocally, no other chemical transformation discovered in the last century has had such a profound impact on the shapes of drug molecules.

We then examined the representation by major heterocycle classes among the dataset across different development stages (Figure 8) and the results were intriguing. No significant changes were observed for the traditionally common pharmacophores such as piperidine, piperazine, indole, and pyrrolidine. However, pyridine has replaced piperidine as the most common heterocyclic pharmacophore. This is in line with the general trend of aromatization noted earlier. Again, how much of a bias toward aromatic compounds due to easier

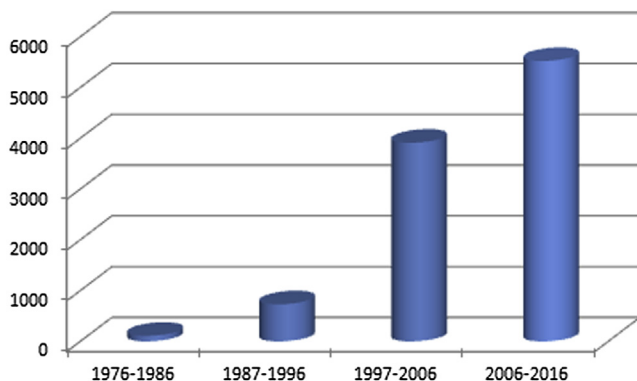


**Figure 7** Number of publications concerning palladium-catalyzed cross-coupling reactions.

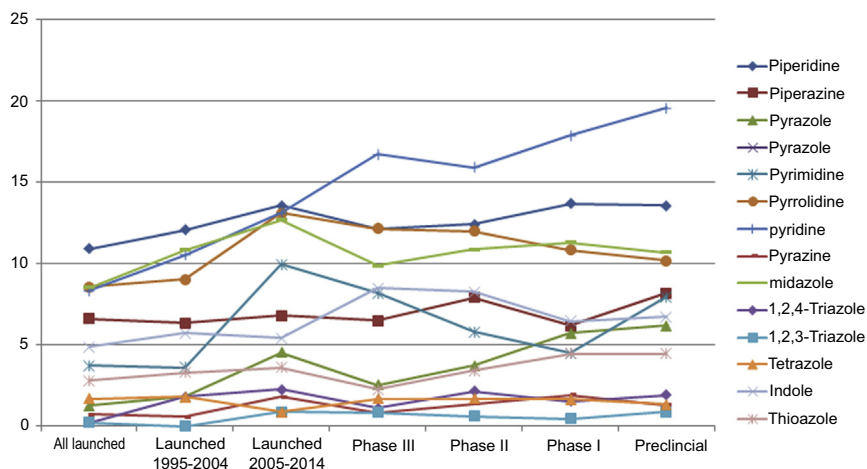


**Figure 8** Percentages of the major heterocyclic pharmacophores.

synthetic access of pyridines remains to be discerned in light of the ever strengthening repertoire of tools including aryl C–C bond cross-coupling (1982ACR(15)340, 2011AGE(50)6722), aryl C–N and C–O bond hetero-couplings (2006JA(128)3584, 2004ASC(346)1599), and aryl C–H activation (2014BMC(22)4445).

When the relative ratios (percentage) of a certain pharmacophore at a specific development stage are plotted against that of all launched drugs (Figure 9), we can see the emergence of small heteroaromatic system represented by pyrazole, triazoles, and tetrazole, all containing an N–N bond.

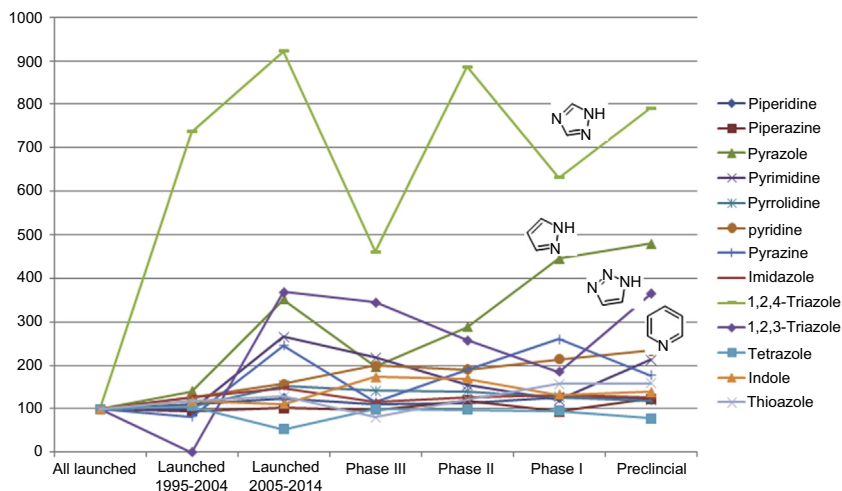


**Figure 9** Relative ratios of heterocyclic pharmacophores at stages of development.

Actually, the percentage of N–N bond containing molecules has doubled among preclinical compounds relative to that among launched drugs. Because of the lag time between the discovery and utilization of new synthetic methodologies and the manifestation of its impact on the structures of drug molecules, we may expect to see a rise of 1,2,3-triazoles in the future due to the power of Huisgen cycloaddition “Click chemistry” (2003DDT(8)1128), even though the current growth leader is clearly pyrazole for a variety of reasons, most notably metabolic stability.

## 4. CONCLUSION

In summary, we have uncovered some interesting trends in medicinal chemistry through a simple and very qualitative analysis of the phenotypic nature of drugs and drug candidates. While the phenotypic outcome is reasonably unambiguous, the underlying reasons affecting the design, preparation, selection, and attrition of drug molecules can be extremely complex (2009JMC(52)6752, 2003JMC(46)1250). We wish to highlight the unequivocal influence of synthetic accessibility, composed of facility of synthetic transformations and availability of starting materials. Understanding these biases and being conscientious of their merits and drawbacks will be instrumental in improving the efficiencies of drug discovery, and managing attritions of clinical candidates during development.



Drug discovery is a long and complex endeavor where decisions are often made with incomplete data and without the benefits of prompt feedbacks. Medicinal chemists have to constantly make tradeoffs between affinity, selectivity, physical and ADME properties (2003JMC(46)1250), toxicological findings, and synthetic route simplicity. It is noteworthy that all accumulated chemistry efforts in human history have barely scratched the surface of the vast possible chemical space. A case in point is that there are estimated fewer than 40 million compounds with known structures, and a typical compound collection for medicinal chemistry screening purpose is in the range of  $10^4$  to  $10^6$  scale. However, the enumerated number of possible structures with only 17 heavy atoms affording the typical size of drug like molecules would amount to 166 billion compounds (2012M11). The influence of synthetic accessibility has been very strong in the last few decades of modern drug discovery with more aromatic compounds getting into the pipeline. As a result there is a deviation from a natural product-like platform that tend to have higher  $sp^3/sp^2$  atom ratios. The unintended consequences include structural bulkiness, low aqueous solubility, and poor exposure. This general pattern has been stridently recognized if not widely heeded (2009JMC(52)6752, 2003JMC(46)1250, 2009JMC(52)2952, 2015JMC(58)4443, 2016JMC(59)4358).

Synthetic accessibility also influences the very early stage of drug discovery. Many of the intentionally designed diversity libraries lean toward ease of synthesis and purification efficiency. A common nexus for the combinatorial chemistry/parallel synthesis efforts is the reaction efficiency (e.g., using excess reagents to drive reactions to completion) and separation effectiveness (e.g., applying solid-phase-based reagents or scavengers). With the advent of computational chemistry and expansion of our knowledge base on protein structures, more fruitful de novo design of drug molecules is inevitable. However, this will only reduce the hit/lead bias as compared with biological screening of the actual compound collections. After in silico screening, selected compounds still need to be made in the laboratories to advance toward in vivo testing and ultimately human trials. The synthetic accessibility bias can only be overcome by the invention of more convenient methodologies with impact to that of the palladium-catalyzed cross-coupling reactions (e.g., Suzuki, Negishi, and Kumada couplings) for the preparation of biaryls. Besides fulfilling the need of medicinal chemists to incorporate a biaryl moiety into a molecular backbone, Suzuki couplings also has the advantages of being easy to perform (nonhydroscopic reaction conditions) and general applicability, having a growing supply of aryl halides and stable arylboronic

acids as coupling partners, and using a mild reaction condition compatible with many existing functional groups. This underscores the importance of robustness and generality of a new reaction. Medicinal chemists need more powerful, efficient, and convenient tools to prepare molecules that are more “natural product” like; have more  $sp^3$  atoms; and more flexible, diverse, unique, and intriguing structures. Transformations that enable functionalization of inactivated  $sp^3$  C–H bonds, stereoselective introduction of small alkyls onto saturated heterocyclic ring, and explorations of hitherto unknown heterocyclic rings (2009JMC(52)2952) are but just a few examples of current needs. Developers of synthetic methodologies will have a greater impact to the community if they align their expertise and curiosity with the current and strategic needs of medicinal chemists. More frequent dialogs and closer collaboration between industry and academia will undoubtedly benefit this goal.

## ACKNOWLEDGMENTS

The author wishes to dedicate this paper to Professor Alan R. Katritzky for his friendship and inspirations; and thank Drs. Eric Scriven, Christine Humblet, David Mitchell, Christopher Burcham, and Professor Victor Snieckus for their comments and review during the preparation of this manuscript.

## REFERENCES

- 1982ACR(15)340 E. Negishi, Palladium- or nickel-catalyzed cross coupling. A new selective method for carbon-carbon bond formation, *Acc. Chem. Res.*, **15**(11), 340–348 (1982).
- 2003DDT(8)1128 H.C. Kolb and K.B. Sharpless, The growing impact of click chemistry on drug discovery, *Drug Discovery Today*, **8**(24), 1128–1137 (2003).
- 2003JMC(46)1250 M.C. Wenlock, R.P. Austin, P. Barton, A.M. Davis, and P.D. Leeson, A comparison of physicochemical property profiles of development and marketed oral drugs, *J. Med. Chem.*, **46**(7), 1250–1256 (2003).
- 2004ASC(346)1599 B. Schlummer and U. Scholz, Palladium-catalyzed C–N and C–O coupling, a practical guide from an industrial vantage point, *Adv. Synth. Catal.*, **346**(13–15), 1599–1626 (2004).
- 2006JA(128)3584 S. Shekhar, P. Ryberg, J.F. Hartwig, J.S. Mathew, D.G. Blackmond, E.R. Strieter, and S.L. Buchwald, Reevaluation of the mechanism of the amination of aryl halides catalyzed by BINAP-ligated palladium complexes, *J. Am. Chem. Soc.*, **128**(11), 3584–3591 (2006).
- 2009JMC(52)2952 W.R. Pitt, D.M. Parry, B.G. Perry, and C.R. Groom, Heteroaromatic rings of the future, *J. Med. Chem.*, **52**(9), 2952–2963 (2009).
- 2009JMC(52)6752 F. Lovering, J. Bikker, and C. Humblet, Escape from flatland: increasing saturation as an approach to improving clinical success, *J. Med. Chem.*, **52**(21), 6752–6756 (2009).
- 2010JA(132)12212 S. Qi, L. Yang, X. Guo, O. Baslé, and C.J. Li, Rhodium-catalyzed oxidative C–H arylation of 2-arylpyridine derivatives via

- decarbonylation of aromatic aldehydes, *J. Am. Chem. Soc.*, **132**(35), 12212–12213 (2010).
- 2011AGE(50)6722 A. Suzuki, Cross-coupling reactions of organoboranes: an easy way to construct C–C bonds, *Angew. Chem. Int. Ed.*, **50**(30), 6722–6737 (2011).
- 2012ACR(45)864 J.F. Hartwig, Borylation and silylation of C–H bonds: a platform for diverse C–H bond functionalizations, *Acc. Chem. Res.*, **45**(6), 864–873 (2012).
- 2012AGE(51)5062 C.C. Johansson, M.O. Kitching, T.J. Colacot, and V. Snieckus, Palladium-catalyzed cross-coupling: a Historical contextual perspective to the 2010 Nobel Prize, *Angew. Chem. Int. Ed.*, **51**(21), 5062–5085 (2012).
- 2012MI1 L. Ruddigkeit, R. van Deursen, L.C. Blum, and J.L. Reymond, Enumeration of 166 billion organic small molecules in the chemical universe database GDB-17, *J. Chem. Inf. Model.*, **52**(11), 2864–2875 (2012).
- 2014BMC(22)4445 For a recent review in this exploding fields: see (a) M.E. Farmer, B.N. Laforteza, and J. Yu, Unlocking nature’s C–H bonds, *Bioorg. Med. Chem.*, **22**(16), 4445–4452 (2014).
- 2014MI1 V. Snieckus and E.J.–G. Anctil, The directed ortho metallation (DoM)-cross-coupling nexus. Synthetic methodology for the formation of aryl-aryl and aryl-heteroatom-aryl bonds, In A. De Meijere, S. Brase, and M. Oestreich, editors: *Metal-Catalyzed Cross-Coupling Reactions and More*, **3**, pp 1067–1133.
- 2015DDT(20)1104 For a recent review, see L. Oester, S. Tapani, Y. Xue, and H. Kaeck, Successful generation of structural information for fragment-based drug discovery, *Drug Discovery Today*, **20**(9), 1104–1111 (2015).
- 2015JMC(58)4443 D.G. Brown and J. Bostrom: Analysis of past and present synthetic methodologies on medicinal chemistry: where have all the new reactions gone? A Miniperspective. <http://dx.doi.org/10.1021/acs.jmedchem.5b01409>.
- 2016JMC(59)4358 This very relevant paper appeared after submission of this manuscript: N. Schneider, D.M. Lowe, R.A. Sayle, M.A. Tarselli, and G.A. Landrum. Big data from pharmaceutical patents: a computational analysis of medicinal chemists’ bread and butter. <http://dx.doi.org/10.1021/acs.jmedchem.6b00153>.
- 2016MI1 For provider website, see <http://accelrys.com/products/collaborative-science/databases/bioactivity-databases/mddr.html>.
- 2016MI2 SciFinder data, Chemical Abstract Services, (accessed February 2016).



# Saturated Heterocycles with Applications in Medicinal Chemistry

**Charles M. Marson**

Department of Chemistry, University College London, Christopher Ingold Laboratories, London, UK  
E-mail: c.m.marson@ucl.ac.uk

## Contents

1. Introduction	14
2. Ring Systems Containing One Heteroatom	15
2.1 Azetidines	15
2.2 Oxetanes	16
2.3 Pyrrolidines	17
2.4 Tetrahydrofurans	19
2.5 Piperidines	20
2.6 Tetrahydropyrans	21
3. Spirocyclic Heterocyclic Ring Systems	22
3.1 Introduction	22
3.2 Spirooxetanes	22
3.3 Spiropyrrolidines	22
3.4 Spiropiperidines	23
4. Heterobicyclo Systems	24
4.1 Azabicyclo[3.1.0]hexanes	24
4.2 Azabicyclo[2.2.1]heptanes	24
4.3 Azabicyclo[3.2.1]octanes	25
4.4 Azabicyclononanes	26
4.5 Miscellaneous Heterobicyclo Systems	27
5. Conclusions	27
References	28

## Abstract

In recent years, the advantages of incorporating saturated heterocyclic rings in therapeutic agents have become increasingly apparent, as compared to using only aromatic and heteroaromatic ring systems. In particular, saturated heterocyclic ring systems play a central role in medicinal chemistry; frequent advantages include improved aqueous

solubility and lower toxicity of metabolites, as well as the potential for greater diversity partly through stereoisomerism. This review illustrates examples of saturated heterocycles with relevance to medicinal chemistry as published in the years 2013–2015. The three main categories discussed are small and medium ring systems containing one heteroatom, spiroheterocyclic ring systems, and heterobicyclo systems.

**Keywords:** Heterobicyclo systems; Medicinal chemistry; Monocyclic heterocycles; Saturated rings; Spiroheterocycles



## 1. INTRODUCTION

The importance of saturated heterocyclic systems is well illustrated by the piperidine ring, long known in a medicinal context, and the most abundant saturated heterocyclic system in all current small-molecule therapeutic agents listed in the FDA Orange Book (2014JMC5845). Most pharmaceuticals contain between one and four rings (2014JMC5845), in part because of the lower conformational entropy to be overcome upon binding to the target. However, saturated rings tend to be inherently more drug-like than planar aromatic ones; toxic metabolites arising from arene oxidation are avoided, and saturation increases water solubility and imparts desirable three-dimensional occupancy of a drug target (2011PNAS6799), all factors that contribute to two recently formulated criteria that favor drug-likeness: a relatively high level of saturation and an asymmetric center. A case study of a large number of successful clinical candidates gave a ratio on 0.47 for the number of  $sp^3$  carbon atoms present to the total number of carbon atoms per drug molecule, which also typically contained at least one chiral center (2009JMC6752, 2013MCC515). Departure from using rings that are exclusively aromatic or heteroaromatic, such as benzene, imidazole, and pyridine has additional benefits, including greater diversity (through stereoisomerism) for a small increase in molecular weight, and structural novelty which can assist patentability. Consequently, the structural landscape of drug-like molecules is changing (2014JMC5845, 2011CSR5514), and has an increased emphasis on saturated ring systems, most of which are heterocyclic. To illustrate those points, this review covers some of the major saturated heterocycles (their low mass being a desirable drug-like feature) as well as more complex architecture present in saturated spiro and bicyclo heterocycles, especially where the constitution is novel or unusual.

## 2. RING SYSTEMS CONTAINING ONE HETEROATOM

### 2.1 Azetidines

In a study to optimize potent protein kinase C $\theta$  inhibitors with the potential to treat rheumatoid arthritis and inflammatory bowel disease, an azetidine ring was essential in order to obtain low nanomolar potency, as for compound **1**. Analogs where oxetane or cyclobutane replaced the azetidine ring were considerably less potent. Hydrogen bonding of such substituted azetidines to Asp, and in some cases also to an Asn residue, was confirmed by crystallography (2015JMC222) (Figure 1).

The azetidine **2** is a potent, selective and bioavailable antagonist of G-protein bile receptor 1, an important target in the treatment of diabetes (2014JMC3263). Analogs containing a piperidine ring in place of the azetidine ring were significantly less potent. However, in a study of the inhibition of sphingosine kinase 1, a target for fibrosis, inflammation, and cancer, while 2-substituted azetidine derivatives were potent, a 2-methylene-substituted pyrrolidine derivative afforded much greater inhibition of G-protein bile receptor 1, and was also highly selective for isoform 1 over isoform 2 (2015JMC1879).

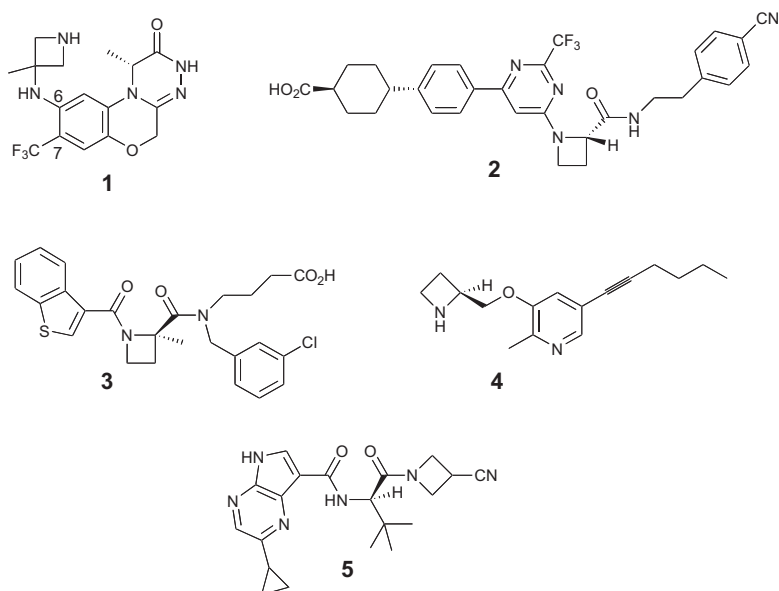


Figure 1 Enzyme inhibitors and receptor antagonists that contain an azetidine ring.

Azetidines are also a key feature of a class of free fatty acid receptor 2 antagonists, compound **3** showing promise for clinical development as an anti-inflammatory agent (2014JMC10044). In this series, the (*R*)-enantiomers were the more potent, and sometimes the (*S*)-enantiomers were inactive.

Nicotine addiction is mediated by nicotinic acetylcholine receptors which may also be involved in alcohol addiction. 3-(Azetidin-2-ylmethoxy)pyridine derivatives can show selective inhibition of the  $\alpha 4/\beta 2$  nicotinic acetylcholine receptor, and in a rat model of alcohol intake compound **4** showed greater selectivity for the  $\alpha 4/\beta 2$  receptor subtype and fewer side effects than the structurally related sazetidine-A (2013JMC3000). Other related compounds exhibited antidepressant properties in a mouse model (2013JMC5495).

A preclinical candidate for the treatment of Alzheimer's disease contained a 3-(1-isopropyl)azetidinyll subunit and inhibited gamma secretase but did not inhibit human CYP3A4 (which could lead to drug–drug interactions) as did other analogs in this series, presumably through binding to iron in the heme coenzyme (2013BMCL1621). In a series of 5-substituted benzimidazoles, a 3-(1-hydroxyethyl)azetidinyllsulfonyl subunit was found to confer potent selective agonism of the cannabinoid receptor (CB2) associated with irritable bowel syndrome; the agonist was effective (ED<sub>50</sub> 0.66 mg/kg) in a rat model of IBS and with few side effects (2015BMCL236).

Janus kinases (JAKs) are involved in signaling that is relevant to inflammatory diseases. The 3-cyanoazetidine **5** showed good selectivity for JAK3 while retaining potency against IL-2 signaling, indicating that such compounds could be useful probes of complex signaling pathways (2013JMC345).

## 2.2 Oxetanes

Synthetic routes to oxetanes and chemical transformations of oxetanes have developed markedly in recent years (2010AG(E)9052). Nucleophilic addition to the carbonyl group of oxetan-3-one can furnish a wide range of 3-substituted oxetane derivatives (2010JMC3227). The nickel-catalyzed Suzuki coupling of a (hetero)aryllboronic acid with 3-iodooxetane afforded 3-(hetero)aryloxetanes (2008OL3259).

The incorporation of an oxetane ring can greatly improve the drug-like properties of compounds (2006AG(E)7736), increasing solubility, and usually increasing metabolic stability, as well as typically lowering log P by about one unit (2010JMC3227). 3,3-Disubstituted oxetanes can be robust replacements either for a methylene group or a *gem*-dimethyl group, and in some cases also for a keto group (2010JMC3227). When a methylene group in an aliphatic chain is replaced by a 3-substituted oxetane a synclinal

conformation is adopted. The oxetane ring is sufficiently chemically inert to be found in natural products, and is thought to act as a conformational lock in paclitaxel, defining the orientation of the 2-benzoyl group and the C-13 side chain (1999BMCL3041), all key features in the binding of paclitaxel to tubulin.

In the progression of dual leucine zipper kinase inhibitors toward a new agent to treat neurodegeneration, the privileged 3-oxetanyl moiety was essential in obtaining potent inhibition of c-Jun N-terminal kinase and sub-nanomolar in vitro enzyme inhibition of dual leucine zipper kinase; both kinases are implicated in neurodegeneration, including Alzheimer's and Parkinson's diseases (2015JMC401). Appending the oxetane lowered the basicity of the piperidine ring and reduced efflux of compound **6** (Figure 2).

A 3-oxetanyl group, while not binding within the active site of the kinase mTOR which is a validated anticancer target, is a significant contributor to an improved PK/PD profile of a new mTOR inhibitor that also showed more potency than a previous preclinical candidate lacking an oxetane ring (2013JMC3090).

### 2.3 Pyrrolidines

In a series of 6-alkyl-2-amino-4-aminosubstituted pyrimidines designed as anti-inflammatory agents that target the histamine H4 receptor, compound **7** showed the best overall PK/PD profile, both the absolute configuration of the amino group and the pyrrolidine ring being crucial for potency and efficacy (the amino group is protonated and binds to Asp in the H4 active site). However, clinical progression of amine **7** during phase II evaluation against atopic dermatitis was halted following observation of drug-induced agranulocytosis in two patients (2014JMC2429) (Figure 3).

C<sub>2</sub>-symmetric pyrrolidine-based 3,4-bis-*N*-alkylsulfonamides, such as amine **8**, contain a novel and nonpeptidic scaffold. Amine **8** exhibits the most potent inhibition of the homodimeric human T-cell leukemia virus

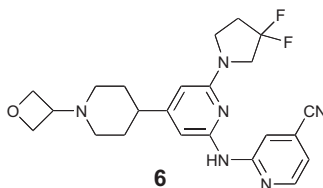


**Figure 2** A 3-substituted oxetane with neuroprotective properties.



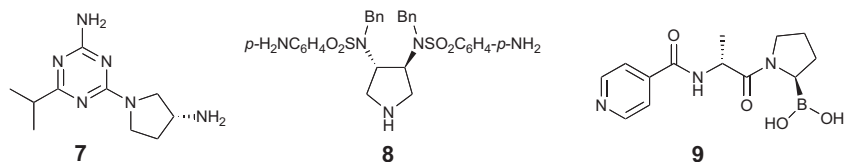


**Figure 3** Pyrrolidine receptor antagonists and protease inhibitors.

type 1 protease (an aspartate protease) currently known, each sulfonamide nitrogen atom binding to one of two aspartate residues in the catalytic site (2015JMC4845).

Disruption of the p53–MDM2 interaction, thereby restoring the tumor suppressor activity of p53, is seen as an appealing approach to cancer treatment. The difficulty of targeting the hydrophobic surface of the protein–protein interaction was met by appending suitably oriented lipophilic groups in a pentasubstituted pyrrole (Figure 4) (2013JMC5979). The nitrile group was found to be essential for achieving the required puckering of the pyrrolidine ring, and hence the appropriate dihedral angle of the two aryl substituents (2013JMC5979). This compound was highly effective when administered orally in an osteosarcoma mouse xenograft.

The post-proline serine protease fibroblast activation protein (FAP) is considered to contribute to tumor invasion and metastasis. The inhibitor 9 is a stable transition state analog that shows excellent selectivity for FAP

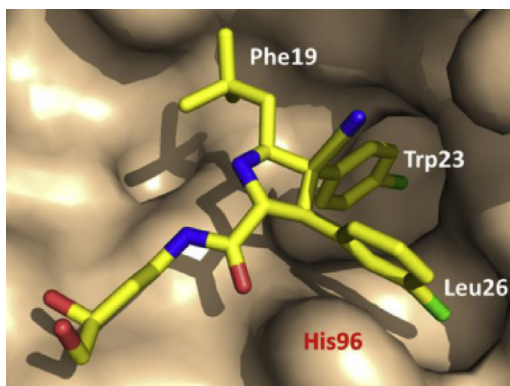


**Figure 4** A substituted pyrrolidine bound in MDM2: PDB 4JRG. Reprinted with permission from Q. Ding, Z. Zhang, J.-J. Liu, N. Jiang, J. Zhang, T. M. Ross, X.-J. Chu, D. Bartkovitz, F. Podlaski, C. Janson, C. Tovar, Z. M. Filipovic, B. Higgins, K. Glenn, K. Packman, L. T. Vassilev and B. Graves, *J. Med. Chem.* **2013**, *56*, 5979. Copyright (2013) American Chemical Society.

over several normal human dipeptidyl peptidases (DPP) and prolyl oligopeptidases (2013JMC3467). In a different series of proline-based FAP inhibitors, a 2-cyano-4,4-difluoropyrrolidine was found preferable to a 2-boronic acid derivative, and showed good potential for *in vivo* inhibition (2014JMC3053).

5,5-Fused systems containing one or more pyrrole rings are useful scaffolds in medicinal chemistry. Some octahydro-pyrrolo[3,4-*c*]pyrroles are selective antagonists of orexin-2, and a candidate for primary insomnia has progressed through phase I clinical trials (2015JMC5620). [3.3.0]-Octahydro-cyclopenta[*c*]pyrrole antagonists of retinol-binding protein 4 have potential for the treatment of atrophic age-related macular degeneration and Stargardt disease (2015JMC5863).

## 2.4 Tetrahydrofurans

The tetrahydrofuran ring present in RNA and DNA is a common scaffold in drug design targeting pathogenic nucleic acids. The tetrahydrofuran derivative **10** is a first-in-class nucleoside respiratory syncytial virus (RSV) polymerase inhibitor and has entered phase II clinical trials (2015JMC1862). Human RSV is associated with significant morbidity and mortality in childhood, and causes symptoms of the common cold in most patients. Other 2'-deoxy-2'- $\beta$ -fluoro-substituted nucleosides show promise for the treatment of hepatitis B (2015JMC3693).

Nucleoside analogs comprise the largest class of DNA methyltransferase inhibitors, and find use in the treatment of a variety of cancers, since promoter methylation can lead to inactivation of tumor suppressor genes (2015JMC2569) (Figure 5).

The (*R*)-enantiomer of a 2,2-diaryltetrahydrofuran is a good inhibitor of 5-lipoxygenase activating protein and has potential for the treatment of inflammatory diseases. Affinity (ligand lipophilic efficiency) was higher for the (*R*)-enantiomer than the (*S*)-enantiomer, suggesting that the ring oxygen atom forms a specific interaction within the receptor site (2015JMC897).

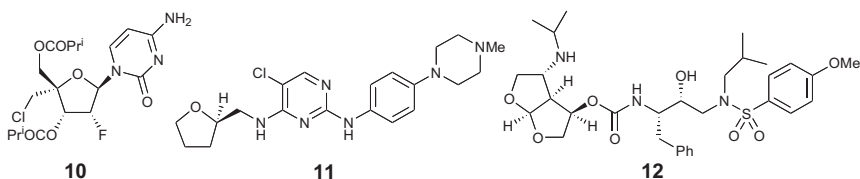


**Figure 5** Tetrahydrofuran-containing polymerase, kinase, and protease inhibitors.

In a hybrid approach to generating new inhibitors of the tyrosine kinase ACK1, implicated in signal transduction that sustains hormone-refractory cancers, the tetrahydrofuran **11**, containing the common 2-anilinopyrimidine unit that binds to peptide backbone regions of the kinase, showed potent in vitro inhibition of ACK1 and good antiproliferation in several cancer cell lines (2015JMC2746).

Several amino-bis-tetrahydrofuran derivatives such as the acetal **12** are very potent HIV-1 protease inhibitors that possess excellent antiviral properties. Although these compounds have the same ring systems and scaffold as darunavir, increased binding derives from the additional isopropylamino group hydrogen bonding with the active site backbone; enhanced lipophilicity of other substituents is also thought to contribute to the greater potency of derivative **12** and some analogs compared to darunavir (2015JMC6994).

## 2.5 Piperidines

Arginase overexpression is implicated in myocardial reperfusion injury. (*R*)-2-Amino-6-borono-2-(2-(piperidin-1-yl)-ethyl)hexanoic acid reduced infarct size in a rat model and is a potent inhibitor of arginase, its boronic acid group binding to manganese; there is also hydrogen bonding of water to the piperidine ring and two Asp residues in the active site (2013JMC2568).

The piperidine ring is often used as a linker, and a 4-aminopiperidine core was optimized for potency and efficacy against *Mycobacterium tuberculosis*; a 3-fluoro substituent on the piperidine ring lowered the lipophilicity and as expected also lowered hERG inhibition (2014JMC4889).

Making use of the finding by Zimmerman in the late 1970s that *N*-methyl-*trans*-3,4-dimethyl-4-(3-hydroxyphenyl)-piperidine was a pure antagonist of an opioid receptor, the same piperidine linker has been incorporated into a 3-isoquinoline carboxamide that is a very potent and highly selective antagonist of the  $\kappa$ -opioid receptor, considered to be a target in the treatment of anxiety, eating disorders, depression, and schizophrenia (2014JMC7367).

Antagonists of the G-protein-coupled receptor (GPCR) 119 stimulate glucose-dependent release of insulin, both directly in the pancreas, and indirectly by action in the gastrointestinal tract by promoting secretion of the incretin glucagon-like peptide-1 (GLP-1). Of a new class of GPR119 antagonists, pyridin-2-one **13** was effective in both chronic and acute models of rodent diabetes, and showed an increase in total GLP-1 plasma levels in healthy humans (2014JMC7499) (Figure 6).

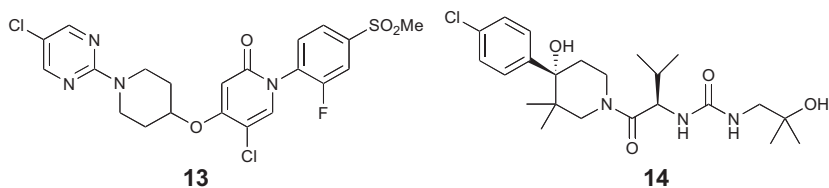


**Figure 6** Piperidine antagonists of two G-protein-coupled receptors.

CC chemokine receptor-1 (CCR1) is a GPCR linked with progression of several inflammatory diseases; the CCR1 antagonist **14** (BMS-817399), has entered phase 2 clinical trials for the treatment of rheumatoid arthritis (2014JMC7550). The axial hydroxy group on the piperidine ring of antagonist **14** binds to a His residue.

Polyhydroxylated piperidines such as nojirimycin are a rich source of glycosidase inhibitors. Several *N*-(4-biphenylmethyl)oxypentyl derivatives possessing a *D*-*gluco*-substituent assembly on the piperidine ring are potent inhibitors of intestinal glycosidases, and may have potential for development as agents to combat type 2 diabetes (2014JMC9096).

## 2.6 Tetrahydropyrans

Inhibitors of dipeptidyl peptidase 4 (DPP4) can be valuable in the treatment of diabetes. MK-3102 (omarigliptin) **15** progressed to phase 3 clinical evaluation in 2014 (2014JMC3205). Compared to Merck's previous inhibitors of DPP4 such as sitagliptin and saxagliptin, the primary amine is rigidified as part of a tetrahydropyran ring which in part led to improved pharmacokinetics and a longer half-life. The primary amine is engaged in hydrogen bonding with two Glu residues (2014JMC3205) (Figure 7).

Sodium-dependent glucose transporter (SGLT) inhibitors promote urinary excretion of glucose, thereby permitting an insulin-independent treatment of type 2 diabetes mellitus. Replacement of the ethyl group in dapagliflozin by trideuteromethyl gave derivative **16** which shows higher metabolic stability owing to the kinetic isotope effect, and is also a selective SGLT2 inhibitor of long duration of action (2014JMC1236).

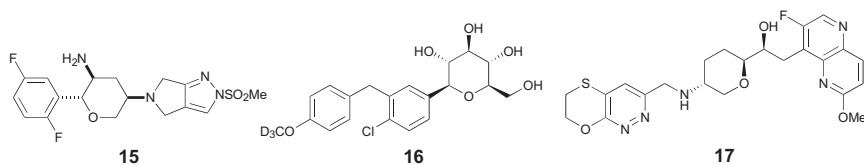


**Figure 7** Antidiabetic and antibacterial tetrahydropyrans.

Compound **17** and some analogs inhibit bacterial type II topoisomerases and are potent antibacterial agents against Gram-positive pathogens. The tetrahydropyran **17** showed no observable cross-resistance, only weakly inhibited hERG K<sup>+</sup> channels, and gave no observed adverse cardiovascular effects in guinea pigs (2015JMC927).



### 3. SPIROCYCLIC HETEROCYCLIC RING SYSTEMS

#### 3.1 Introduction

Spirocyclic scaffolds, in which a single atom is common to both rings, are a prime category of drug-like molecules (2014BMCL3673); they possess significant occupancy in each of three dimensions, and often have structural novelty that may also be accompanied by new synthetic methods of access. An example is the acetylcholinesterase inhibitor and antihypertensive agent spirapril which contains a spiro 1,3-dithiolane bonded to C-3 of a pyrrole ring.

#### 3.2 Spirooxetanes

The 2'-spirooxetane system was shown to be a moderately effective scaffold for the treatment of hepatitis C virus (2014JMC1826, 2014JMC1836). A 2'-oxetane cytidine triphosphate showed good inhibition of NS5B polymerase (IC<sub>50</sub> 8.5 μM), although modest replicon activity was found for the pyrimidine bases containing this spirooxetane unit (2014JMC1826). Some phosphoramidate prodrugs of 2'-deoxy-2'-spirooxetane ribonucleosides were more potent, having EC<sub>50</sub> values down to 0.2 μM in the Huh7-replicon cell line, and without any observed toxicity (2014JMC1836).

#### 3.3 Spiropyrrolidines

7-(1-Pyrrolidino)-4-oxyquinoline-2-carboxylic acids and their 8-aza derivatives are commonly used in the treatment of respiratory infections. In order to reduce toxicity in types that have fused cyclopropylamine units, spirocyclic pyrrolidines such as derivative **18** were synthesized and evaluated. The inability of compound **18** to undergo oxidation to an iminium ion is thought to contribute to its low toxicity. Spirocyclic **18** was effective in a murine model of multidrug-resistant streptococcal pneumonia (2013JMC1974) (Figure 8).

Some inhibitors of the interaction of MDM2 with p53 up-regulate the tumor suppressor and are in clinical trials (2015JMC1038). The most potent

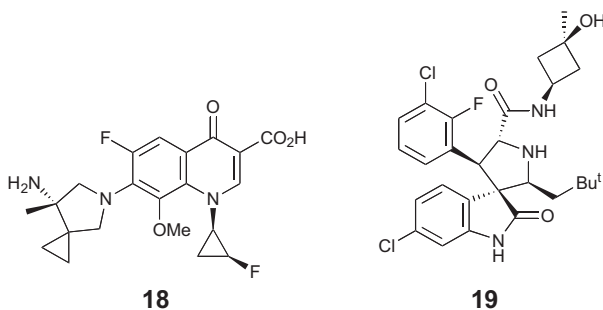


**Figure 8** Therapeutic agents containing a spirocyclic pyrrolidine unit.

inhibitor **19** of MDM2 ( $K_i$  0.44 nM) so far identified achieved complete and lasting tumor regression in xenograft models of osteosarcoma and lymphoblastic leukemia (2013JMC5553).

A spiroketal at the 3-position of a pyrrolidine ring was found to improve potency against mutants. The 1,4-dioxo-7-azaspiro[4.4]nonane unit maintained high inhibitory potency against genotypes 1a and 1b of the hepatitis C virus, as well as against Leu31Val and Tyr93His mutants (2014JMC2058). Potent suppression of hepatitis C viral RNA and the good pharmacokinetic and safety profile support clinical progression of the spiroketal.

### 3.4 Spiropiperidines

4-Spiropiperidines comprise a privileged scaffold, an example being the linkage of an indane at the 1-position with a piperidine at the 4-position.

Using a high-throughput cell-based reporter assay, a substituted 4-piperidinylpyridine shown to be a low micromolar inhibitor of WNT signaling was optimized to give the spiroactam **20**, a potent inhibitor of WNT signaling that displayed good oral pharmacokinetics and was effective in a solid tumor xenograft model (2015JMC1717) (Figure 9).

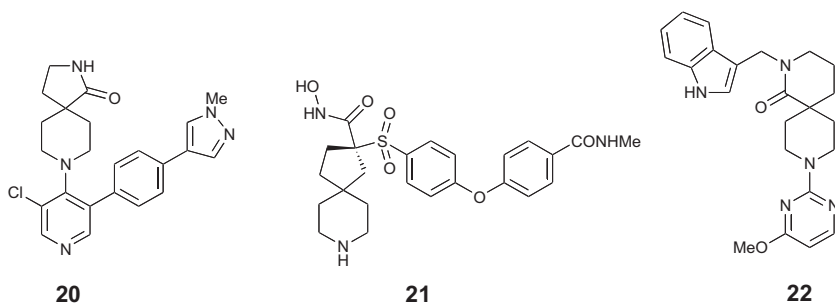


**Figure 9** 4-Spiropiperidine therapeutic agents.

Spirohydroxamic acid inhibitors were designed and synthesized on the basis of their potential to inhibit matrix metalloproteinases which are considered to exacerbate bleeding by delaying fibrinolysis (2015JMC2465, 2015JMC2941). The (*R*)-spirohydroxamic acid **21** was more effective in reducing fibrinolysis in vitro and showed fewer side effects than common current treatments using tranexamic acid or aprotinin; spiro piperidine **21** is a preclinical candidate for the treatment of acute hemorrhaging (2015JMC2465). The selective dual orexin receptor antagonist **22** induced mainly nonrapid eye movement sleep in mice, suggesting that such antagonists could find use in the treatment of insomnia (2013JMC7590).

A spiro[1*H*-isobenzofuran-3,4'-piperidine] with high aqueous solubility and negligible P-gp-mediated efflux is a potent antagonist of the human vasopressin 1a receptor. It showed good uptake in the brain, and is suitable for clinical studies in those with autism (2015JMC2275). The same spiro system, though with a different *N*-substituent and labeled with <sup>19</sup>F possesses low lipophilicity, is an effective tumor-imaging agent selective for the  $\sigma_1$  subtype of the opioid receptor (2015JMC5395).

## 4. HETEROBICYCLO SYSTEMS

### 4.1 Azabicyclo[3.1.0]hexanes

One advantage of the 3-azabicyclo[3.1.0]hexane system over the piperidine ring is that a 6-aryl substituent is conformationally locked in the equatorial position and can also be achiral. Such rigidity was found to be required for selective and highly potent inhibition of an opioid receptor (2012BMCL2200). The sensation in dogs of pruritus (intense itch), which by scratching can lead to secondary infections, is alleviated by the highly potent  $\mu$ -opioid receptor antagonist **23** ( $K_i$  0.2 nM), the increased lipophilicity of the indanyl ring enhancing the potency (2012BMCL2200) (Figure 10).

### 4.2 Azabicyclo[2.2.1]heptanes

Protonation of the bridgehead nitrogen atom of some 7-azabicyclo[2.2.1]heptane derivatives affords a rigid cycloalkylammonium cation that is

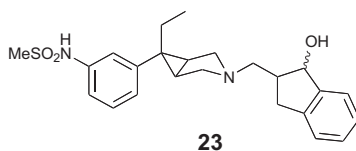


Figure 10 An antipruritic 3-azabicyclo[3.1.0]hexane derivative.

thought to form bifurcated bonds to the catalytic diad of Asp344 and Asp214 in plasmepsin, an aspartate protease of human hemoglobin that is degraded for growth and reproduction of *Plasmodium falciparum*, the most lethal parasitic conveyor of malaria (2015JMC5151). Other 7-azabicyclo[2.2.1]heptanes substituted at nitrogen with an electron-donating benzylic group show promise for selective inhibition of the  $\sigma_2$  receptor, relevant to CNS disorders including depression and anxiety (2012BMCL4059). 2-(4-Chloro-2-cyano-2-phenylbutyl)aziridines undergo one-step transformation by  $\text{LiAlH}_4$  into *exo*-2-aminomethyl-4-phenyl-1-azabicyclo[2.2.1]heptanes, some of which also show antimalarial properties (2013BMCL1507).

7-Azabicyclo[2.2.1]heptane-1-carboxylic acid and 1-azabicyclo[3.3.0]octane-5-carboxylic acid are conformationally locked versions of proline but were found to be poor inhibitors of proline racemases (2014BMCL390); computational studies suggest there is little room in the active site for proline or inhibitors of proline racemase to rotate (2009JA8513).

The 2-azabicyclo[2.2.1] system is present in ledipasvir (**24**), an extremely potent inhibitor of NS5A (GT1a replicon  $\text{EC}_{50}$  31 pM) that is in advanced clinical trials as an oral treatment for patients infected with genotype 1a hepatitis C virus (2014JMC2033). When used in combination with the NS5B nucleoside inhibitor sofosbuvir, the phase 2 efficacy of ledipasvir was outstanding in patients who had shown little or no response to a regimen of pegylated interferon and ribavirin (2014JMC2033) (Figure 11).

### 4.3 Azabicyclo[3.2.1]octanes

Tropanols of type **25** and **26** bind to the androgen receptor, but whereas **25** is an antagonist, **26** is an agonist (2015JMC1569). Tropanol **25** showed greater antagonistic behavior than did bicalutamide, a nonsteroidal clinical antiandrogen used in the treatment of prostate cancer. Additionally, **25** showed little agonism with the mutant Trp741Leu which is activated by bicalutamide and is detected in prostate cancer patients treated with bicalutamide (2015JMC1569) (Figure 12).

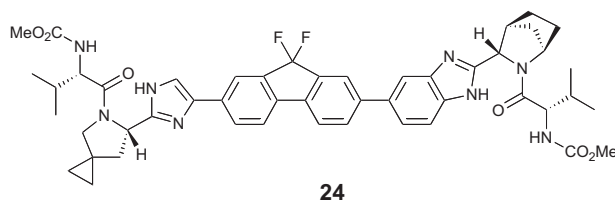
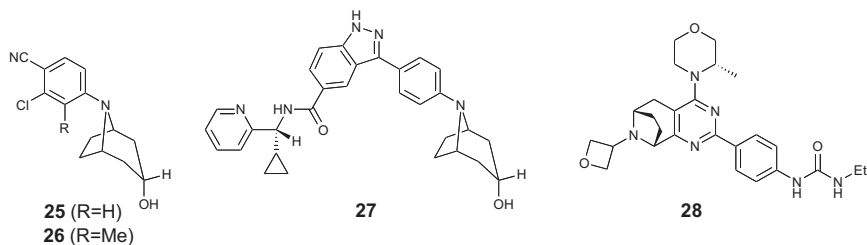


Figure 11 Ledipasvir, a clinical agent for the treatment of hepatitis C.





**Figure 12** Tropanols **25** and **27** as androgen receptor antagonists and anticancer agents **28** and **29**.

Some conventional sulfonamides were potent threonine tyrosine kinase inhibitors but only modestly attenuated the growth of cancer cells. However, removal of the sulfonamide group and replacement by an azabicyclo unit increased the lipophilicity, and lead optimization using crystallographic information led to the azabicyclooctane **27** with excellent potency in vitro and in cell-based assays, and good performance in a HCT116 xenograft tumor model (2015JMC3366).

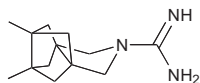
Bridging of a fused piperidine ring afforded the metabolically stable kinase inhibitor **28** with a fourfold increase in in vitro potency (mTOR  $K_i$  1.0 nM) and greatly increased reduction in cancer cell line proliferation to low nanomolar values (2013JMC3090).

#### 4.4 Azabicyclononanes

Chlorinated 2-azabicyclo[3.2.2]nonanes have shown good antitrypanosomal activity, whereas a 3-azabicyclo[3.2.2]nonane showed oral activity in a murine model of plasmodial infection (2015BMCL1390).

2-Azabicyclo[3.3.1]nonanes include the morphans, compounds that are often agonists or antagonists of one or more opioid receptors. The nonselective opioid receptor antagonist *N*-phenylpropyl-4 $\beta$ -methyl-5-(3-hydroxyphenyl)morphan was modified by addition of a 7 $\alpha$ -acylamino group to give a  $\kappa$ -selective antagonist; in contrast, addition of an amino, alkylamino, or dialkylamino group at the 7 $\alpha$ -position led to mainly  $\mu$  or  $\delta$  agonist properties admixed with agonism (2013JMC8826).

Activation of  $\alpha 4\beta 2$  nicotinic acetylcholine receptors is associated with improved cognitive performance. Of a new series of  $\alpha 4\beta 2$  nicotinic acetylcholine receptor agonists, 3-propionyl-3,7-diazabicyclo[3.3.0]octane showed improved memory in the performance of an object recognition task (2013BMCL3927). An exocyclic carbonyl group that functions as a hydrogen bond acceptor and a secondary amino group incorporated into this

**29**

**Figure 13** An M2 ion channel inhibitor for the treatment of influenza A virus.

scaffold, or into an azabicyclo system, were found to be requirements for potency (2013BMCL3927).

Some diazabicyclononanes show potency as antagonists of the orexin-1 and orexin-2 receptors, thought to be important targets for the treatment of various psychiatric disorders (2013BMCL4761).

#### 4.5 Miscellaneous Heterobicyclo Systems

Agonists of the GPCR G119 stimulate glucose-dependent secretion of insulin and release of incretin. Optimization of the 3-oxa-9-azabicyclo [3.3.1]nonan-9-ol scaffold led to the discovery of a potent and orally active agonist of G119 which significantly lowered blood glucose levels in a murine assay (2015BMCL5291).

Amantidine derivatives have often been used in the treatment of influenza; they inhibit the M2 ion channel essential for viral replication of the influenza A virus (Figure 13). However, the increase of viral strains resistant to amantidine derivatives was the drive for developing the first inhibitors of M2 that do not contain the adamantane ring system. 3-Azatetracyclo[5.2.1.1<sup>5,8</sup>.0.1<sup>5</sup>]undecane derivatives were proposed as structurally analogous to adamantane derivatives; indeed several including compound **29** showed low micromolar potency against the Val27Ala/M2 mutant channel (2013JMC9265).

Nicotinamide phosphoribosyltransferase catalyzes the formation of nicotinamide mononucleotide, a biochemical precursor of NAD. Tumor cells are more dependent upon this enzyme than are normal cells, and so are vulnerable to inhibition. 1-(4-{8-Oxa-3-azabicyclo[3.2.1]octane-3-sulfonyl}phenyl)-3-(pyridin-3-ylmethyl)urea is a low nanomolar inhibitor of nicotinamide phosphoribosyltransferase, and at an oral dosage of 125 mg/kg showed excellent efficacy in an A2780 ovarian tumor xenograft model (2013JMC4921).

## 5. CONCLUSIONS

Recent studies have shown major advantages in increasing the prominence of saturated rings in therapeutic agents compared to the more

conventional aromatic and heteroaromatic ring systems. Although the latter will always play a major role, alicyclic and saturated heterocyclic ring systems have already secured an essential place in medicinal chemistry. The need for saturated systems is driven by several factors, the most fundamental being that drug-likeness is in practice so often dependent upon appropriate chemical structure, in particular that the ratio of the total number of saturated heavy atoms to the total number of carbon atoms in an outstanding small-molecule therapeutic agent is seldom much lower than 0.47, and also that at least one chiral center is usually needed (2009JMC6752).

Other factors that favor the presence of saturated rings, especially heterocycles, include structural diversity, the need for a distinctive structural motif in a therapeutic agent, and the emerging possibility of tailoring the drug administered to the genetic profile of the particular patient, and with regard to the relevant isoforms or subtypes of the molecular target. Lastly, saturated heterocyclic systems often confer novelty through their structure or mode of synthesis, or both. For all those reasons, saturated heterocyclic systems have always been important in medicinal chemistry, and in the future will become even more essential.

## REFERENCES

- 1999BMCL3041 T.C. Boge, M. Hepperle, D.G. Vander Velde, C.W. Gunn, G.L. Grunewald, and G.L. Georg, *Bioorg. Med. Chem. Lett.*, **9**, 3041 (1999).
- 2006AG(E)7736 G. Wuitschik, M. Rogers-Evans, K. Müller, H. Fischer, B. Wagner, F. Schuler, L. Polonchuk, and E.M. Carreira, *Angew. Chem., Int. Ed.*, **45**, 7736 (2006).
- 2008OL3259 M.A. Duncton, M.A. Estiarte, D. Tan, C. Kaub, D.J.R. O'Mahony, R.J. Johnson, M. Cox, W.T. Edwards, M. Wan, J. Kincaid, and M.G. Kelly, *Org. Lett.*, **10**, 3259 (2008).
- 2009JA8513 A. Rubinstein and D.T. Major, *J. Am. Chem. Soc.*, **131**, 8513 (2009).
- 2009JMC6752 F. Lovering, J. Bikker, and C. Humblet, *J. Med. Chem.*, **52**, 6752 (2009).
- 2010AG(E)9052 J.A. Burkhard, G. Wuitschik, E.M. Carreira, M. Rogers-Evans, and K. Müller, *Angew. Chem., Int. Ed.*, **49**, 9052 (2010).
- 2010JMC3227 G. Wuitschik, E.M. Carreira, B. Wagner, H. Fischer, I. Parnilla, F. Schuler, M. Rogers-Evans, and K. Müller, *J. Med. Chem.*, **53**, 3227 (2010).
- 2011CSR5514 C.M. Marson, *Chem. Soc. Rev.*, **40**, 5514 (2011).
- 2011PNAS6799 A.W. Hung, A. Ramek, Y. Wang, T. Kaya, J.A. Wilson, P.A. Clemons, and D.W. Young, *Proc. Natl. Acad. Sci. U.S.A.*, **108**, 6799 (2011).
- 2012BMCL2200 G. Lunn, L.R. Roberts, S. Content, D.J. Critcher, S. Douglas, A.E. Fenwick, D.M. Gethin, G. Goodwin, D. Greenway, S. Greenwood, K. Hall, M. Thomas, S. Thompson, D. Williams, G. Wood, and A. Wylie, *Bioorg. Med. Chem. Lett.*, **22**, 2200 (2012).
- 2012BMCL4059 S.D. Banister, L.M. Rendina, and M. Kassiou, *Bioorg. Med. Chem. Lett.*, **22**, 4059 (2012).
- 2013BMCL1506 M. D'hooghe, K. Vervisch, K.W. Törnroos, T. Verhaeghe, T. Desmet, C. Lategan, P.J. Smith, K. Chibale, and N. De Kimpe, *Bioorg. Med. Chem. Lett.*, **23**, 1507 (2013).

- 2013BMCL1621 J.L. Hubbs, N.O. Fuller, W.F. Austin, R. Shen, J. Ma, Z. Gong, J. Li, T.D. McKee, R.M.B. Loureiro, B. Tate, J.A. Dumin, J. Ives, and B.S. Bronk, *Bioorg. Med. Chem. Lett.*, **23**, 1621 (2013).
- 2013BMCL3927 A.A. Mazurov, D.C. Kombo, S. Akireddy, S. Murthy, T.A. Hauser, K.G. Jordan, G.J. Gatto, and D. Yohannes, *Bioorg. Med. Chem. Lett.*, **23**, 3927 (2013).
- 2013BMCL4761 T.P. Lebold, P. Bonaventure, and B.T. Shireman, *Bioorg. Med. Chem. Lett.*, **23**, 4761 (2013).
- 2013JMC1974 T. Odagiri, H. Inagaki, Y. Sugimoto, M. Nagamochi, R.N. Miyauchi, J. Kuroyanagi, T. Kitamura, S. Komoriya, and H. Takahashi, *J. Med. Chem.*, **56**, 1974 (2013).
- 2013JMC2568 M.C. Van Zandt, D.L. Whitehouse, A. Golebiowski, M.K. Ji, M. Zhang, R.P. Beckett, G.E. Jagdmann, T.R. Ryder, R. Sheeler, M. Andreoli, B. Conway, K. Mahboubi, G. D'Angelo, A. Mitschler, A. Cousido-Siah, F.X. Ruiz, E.I. Howard, A.D. Podjarny, and H. Schroeter, *J. Med. Chem.*, **56**, 2568 (2013).
- 2013JMC3000 Y. Liu, J. Richardson, T. Tran, N. Al-Muhtasib, T. Xie, V.M. Yenugonda, H.G. Sexton, A.H. Rezvani, E.D. Levin, N. Sahibzada, K.J. Kellar, M.L. Brown, Y. Xiao, and M. Paige, *J. Med. Chem.*, **56**, 3000 (2013).
- 2013JMC3090 A.A. Estrada, D.G. Shore, E. Blackwood, Y.-H. Chen, G. Deshmukh, X. Ding, A.G. DiPasquale, J.A. Epler, L.S. Friedman, M.F.T. Koehler, L. Liu, S. Malek, J. Nonomiya, D.F. Ortwine, Z. Pei, S. Sideris, F. St-Jean, L. Trinh, T. Truong, and J.P. Lyssikatos, *J. Med. Chem.*, **56**, 3090 (2013).
- 2013JMC3467 S.E. Poplawski, J.H. Lai, Y. Li, Z. Jin, Y. Liu, W. Wu, Y. Wu, Y. Zhou, J.L. Sudmeier, D.G. Sanford, and W.W. Bachovchin, *J. Med. Chem.*, **56**, 3467 (2013).
- 2013JMC4921 X. Zheng, P. Bauer, T. Baumeister, A.J.K.H. Clodfelter, B. Han, Y.-C. Ho, N. Kley, J. Lin, D.J. Reynolds, G. Sharma, C.C. Smith, Z. Wang, P.S. Dragovich, A. Oh, W. Wang, M. Zak, J. Gunzner-Toste, G. Zhao, P. Yuen, and K.W. Bair, *J. Med. Chem.*, **56**, 4921 (2013).
- 2013JMC5495 H.-K. Zhang, L.-F. Yu, J.B. Eaton, P. Whiteaker, O.K. Onajole, T. Hania, D. Brunner, R.J. Lukas, and A.P. Kozikowski, *J. Med. Chem.*, **56**, 5495 (2013).
- 2013JMC5553 Y. Zhao, S. Yu, W. Sun, L. Liu, J. Lu, D. McEachern, S. Shargary, D. Bernard, X. Li, T. Zhao, P. Zou, D. Sun, and S. Wang, *J. Med. Chem.*, **56**, 5553 (2013).
- 2013JMC5979 Q. Ding, Z. Zhang, J.-J. Liu, N. Jiang, J. Zhang, T.M. Ross, X.-J. Chu, D. Bartkovitz, F. Podlaski, C. Janson, C. Tovar, Z.M. Filipovic, B. Higgins, K. Glenn, K. Packman, L.T. Vassilev, and B. Graves, *J. Med. Chem.*, **56**, 5979 (2013).
- 2013JMC7590 C. Betschart, S. Hintermann, D. Behnke, S. Cotesta, M. Fendt, C.E. Gee, L.H. Jacobson, G. Laue, S. Ofner, V. Chaudhari, S. Badiger, C. Pandit, J. Wagner, and D. Hoyer, *J. Med. Chem.*, **56**, 7590 (2013).
- 2013JMC8826 F.I. Carroll, M.G. Gichinga, J.D. Williams, E. Vardy, B.L. Roth, S.W. Mascarella, J.B. Thomas, and H.A. Navarro, *J. Med. Chem.*, **56**, 8826 (2013).
- 2013JMC9265 M. Rey-Carrizo, E. Torres, C. Ma, M. Barniol-Xicota, J. Wang, Y. Wu, L. Naesens, W.F. DeGrado, R.A. Lamb, L.H. Pinto, and S. Vázquez, *J. Med. Chem.*, **56**, 9265 (2013).
- 2013MCC515 F. Lovering, *Med. Chem. Commun.*, **4**, 515 (2013).
- 2013JMC345 M. Soth, J.C. Hermann, C. Yee, M. Alam, J.W. Barnett, P. Berry, M.F. Browner, K. Frank, S. Frauchiger, S. Harris, Y. He, M. Hekmat-

- Nejad, T. Hendricks, R. Henningsen, R. Hilgenkamp, H. Ho, A. Hoffman, P.-Y. Hsu, D.-Q. Hu, A. Itano, S. Jaime-Figueroa, A. Jahangir, S. Jin, A. Kuglstatter, A.K. Kutach, C. Liao, S. Lynch, J. Menke, L. Niu, V. Patel, A. Railkar, D. Roy, A. Shao, D. Shaw, S. Steiner, Y. Sun, S.-L. Tan, S. Wang, and M.D. Vu, *J. Med. Chem.*, **56**, 345 (2013).
- 2014BMCL390 M. Harty, M. Nagar, L. Atkinson, C.M. LeGay, D.J. Derksen, and S.J. Bearne, *Bioorg. Med. Chem. Lett.*, **24**, 390 (2014).
- 2014BMCL3673 Y. Zheng, C.M. Tice, and S.B. Singh, *Bioorg. Med. Chem. Lett.*, **24**, 3673 (2014).
- 2014JMC1236 G. Xu, B. Lv, J.Y. Roberge, B. Xu, J. Du, J. Dong, Y. Chen, K. Peng, L. Zhang, X. Tang, Y. Feng, M. Xu, W. Fu, W. Fu, W. Zhang, L. Zhu, Z. Deng, Z. Sheng, A. Welihinda, and X. Sun, *J. Med. Chem.*, **57**, 1236 (2014).
- 2014JMC1826 J. Du, B.-K. Chun, R.T. Mosley, S. Bansal, H. Bao, C. Espiritu, A.M. Lam, E. Murakami, C. Niu, H.M. Micolochick Steuer, P.A. Furman, and M.J. Sofia, *J. Med. Chem.*, **57**, 1826 (2014).
- 2014JMC1836 T.H.M. Jonckers, K. Vandyck, L. Vandekerckhove, L. Hu, A. Tahri, S. Van Hoof, T.-I. Lin, L. Vijgen, J.M. Berke, S. Lachau-Durand, B. Stoops, L. Leclercq, G. Fanning, B. Samuelsson, M. Nilsson, A. Rosenquist, K. Simmen, and P. Raboison, *J. Med. Chem.*, **57**, 1836 (2014).
- 2014JMC2033 J.O. Link, J.G. Taylor, L. Xu, M. Mitchell, H. Guo, H. Liu, D. Kato, T. Kirschberg, J. Sun, N. Squires, J. Parrish, T. Keller, Z.-Y. Yang, C. Yang, M. Matles, Y. Wang, K. Wang, G. Cheng, Y. Tian, E. Mogalian, E. Mondou, M. Cornpropst, J. Perry, and M.C. Desai, *J. Med. Chem.*, **57**, 2033 (2014).
- 2014JMC2058 W.M. Kazmierski, A. Maynard, M. Duan, S. Baskaran, J. Botyanszki, R. Crosby, S. Dickerson, M. Tallant, R. Grimes, R. Hamatake, M. Leivers, C.D. Roberts, and J. Walker, *J. Med. Chem.*, **57**, 2058 (2014).
- 2014JMC2429 B.M. Savall, F. Chavez, K. Tays, P.J. Dunford, J.M. Cowden, M.D. Hack, R.L. Wolin, R.L. Thurmond, and J.P. Edwards, *J. Med. Chem.*, **57**, 2429 (2014).
- 2014JMC3053 K. Jansen, L. Heirbaut, R. Verkerk, J.D. Cheng, J. Joossens, P. Cos, L. Maes, A.-M. Lambeir, I. De Meester, K. Augustyns, and P. Van der Veken, *J. Med. Chem.*, **57**, 3053 (2014).
- 2014JMC3205 T. Biftu, R. Sinha-Roy, P. Chen, X. Qian, D. Feng, J.T. Kueth, G. Scapin, Y.D. Gao, Y. Yan, D. Krueger, A. Bak, G. Eiermann, J. He, J. Cox, J. Hicks, K. Lyons, H. He, G. Salituro, S. Tong, S. Patel, G. Doss, A. Petrov, J. Wu, S.S. Xu, C. Sewall, X. Zhang, B. Zhang, N.A. Thornberry, and A.E. Weber, *J. Med. Chem.*, **57**, 3205 (2014).
- 2014JMC3263 D.P. Phillips, W. Gao, Y. Yang, G. Zhang, I.K. Lerario, T.L. Lau, J. Jiang, X. Wang, D.G. Nguyen, B.G. Bhat, C. Trotter, H. Sullivan, G. Welzel, J. Landry, Y. Chen, S.B. Joseph, C. Li, W.P. Gordon, W. Richmond, K. Johnson, A. Bretz, B. Bursulaya, S. Pan, P. McNamara, and H.M. Siedel, *J. Med. Chem.*, **57**, 3263 (2014).
- 2014JMC4889 P.S. Hameed, V. Patil, S. Solapure, U. Sharma, P. Madhavapeddi, A. Raichurkar, M. Chinnapattu, P. Manjrekar, G. Shanbhag, J. Puttur, V. Shinde, S. Menasinakai, S. Rudrapatana, V. Achar, D. Awasthy, R. Nandishaiah, V. Humnabadkar, A. Ghosh, C. Narayan, V.K. Ramya, P. Kaur, S. Sharma, J. Werngren, S. Hoffner, V. Panduga, C.N. Kumar, J. Reddy, K.N.M. Kumar, S. Ganguly, S. Bharath, U. Bheemaroo, K. Mukherjee, U. Arora, S. Gaonkar, M. Coulson, D. Waterson,

- V.K. Sambandamurthy, and S.M. de Sousa, *J. Med. Chem.*, **57**, 4889 (2014).
- 2014JMC5845 R.D. Taylor, M. MacCoss, and A.D.G. Lawson, *J. Med. Chem.*, **57**, 5845 (2014).
- 2014JMC7367 C.M. Kormos, M.G. Gichinga, R. Maitra, S.P. Runyon, J.B. Thomas, L.E. Brieady, S.W. Mascarella, H.A. Navarro, and F.I. Carroll, *J. Med. Chem.*, **57**, 7367 (2014).
- 2014JMC7499 D.A. Wacker, Y. Wang, M. Broekma, K. Rossi, S. O'Connor, Z. Hong, G. Wu, S.E. Malmstrom, C.-P. Hung, L. LaMarre, A. Chimalakonda, L. Zhang, L. Xin, H. Cai, C. Chu, S. Boehm, J. Zalaznick, R. Ponticello, L. Sereda, S.-P. Han, R. Zebo, B. Zinker, C.E. Luk, R. Wong, G. Everlof, Y.-X. Li, C.K. Wu, M. Lee, S. Griffen, K.J. Miller, J. Krupinski, and J.A. Robl, *J. Med. Chem.*, **57**, 7499 (2014).
- 2014JMC7550 J.B. Santella III, D.S. Gardner, J.V. Duncia, H. Wu, M. Dhar, C. Cavallaro, A.J. Tebben, P.H. Carter, J.C. Barrish, M. Yarde, S.W. Briceno, M.E. Cvijic, R.R. Grafstrom, R. Liu, S.R. Patel, A.J. Watson, G. Yang, A.V. Rose, R. D.Vickery, J. Caceres-Cortes, C. Caporuscio, D.M. Camac, J.A. Khan, Y. An, W.R. Foster, P. Davies, and J. Hynes Jr., *J. Med. Chem.*, **57**, 7550 (2014).
- 2014JMC9096 A.T. Ghisaidoobe, R.J.B.H.N. van den Berg, S.S. Butt, A. Strijland, W.E. Donker-Koopman, S. Scheij, A.M.C.H. van den Nieuwendijk, G.-J. Koomen, A. van Loevezijn, M. Leemhuis, T. Wennekes, M. van der Stelt, G.A. van der Marel, C.A.A. van Boeckel, J.M.F.G. Aerts, and H.S. Overkleeft, *J. Med. Chem.*, **57**, 9096 (2014).
- 2014JMC10044 M. Pizzonero, S. Dupont, M. Babel, S. Beaumont, N. Bienvenu, R. Blanqué, L. Cherel, T. Christophe, B. Crescenzi, E. De Lemos, P. Delerive, P. Deprez, S. De Vos, F. Djata, S. Fletcher, S. Kopiejewski, C. L'Ebraly, J.-M. Lefrançois, S. Lavazais, M. Manioc, L. Nelles, L. Oste, D. Polancec, V. Quénéhen, F. Soulas, N. Triballeau, E.M. van der Aar, N. Vandeghinste, E. Wakselman, R. Brys, and L. Saniere, *J. Med. Chem.*, **57**, 10044 (2014).
- 2015BMCL236 Y. Iwata, K. Ando, K. Taniguchi, N. Koba, A. Sugiura, and M. Sudo, *Bioorg. Med. Chem. Lett.*, **25**, 236 (2015).
- 2015BMCL1390 W. Seebacher, V. Wolking, J. Faist, M. Kaiser, R. Brun, R. Saf, F. Bucar, B. Gröblacher, A. Brantner, V. Merino, Y. Kalia, L. Scapozza, R. Perozzo, and R. Weis, *Bioorg. Med. Chem. Lett.*, **25**, 1390 (2015).
- 2015BMCL5291 X. Dai, A. Stamford, H. Liu, B. Neustadt, J. Hao, T. Kowalski, B. Hawes, X. Xu, H. Baker, K. O'Neill, M. Woods, H. Tang, and W. Greenlee, *Bioorg. Med. Chem. Lett.*, **25**, 5291 (2015).
- 2015JMC222 D.M. George, E.C. Breinlinger, M. Friedman, Y. Zhang, J. Wang, M. Argiadi, P. Bansal-Pakala, M. Barth, D.B. Duignan, P. Honore, Q.-Y. Lang, S. Mittelstadt, D. Potin, L. Rundell, and J.J. Edmunds, *J. Med. Chem.*, **58**, 222 (2015).
- 2015JMC401 S. Patel, F. Cohen, B.J. Dean, K. De La Torre, G. Deshmukh, A.A. Estrada, A.S. Ghosh, P. Gibbons, A. Gustafson, M.P. Huestis, C.E. Le Pichon, H. Lin, W. Liu, X. Liu, Y. Liu, C.Q. Ly, J.P. Lyssikatos, C. Ma, K. Scarce-Levie, Y.G. Shin, H. Solanoy, K.L. Stark, J. Wang, B. Wang, X. Zhao, J.W. Lewcock, and M. Siu, *J. Med. Chem.*, **58**, 401 (2015).
- 2015JMC897 M. Lemurell, J. Ulander, S. Winiwarter, A. Dahlén, O. Davidsson, H. Emtenäs, J. Broddefalk, M. Swanson, D. Hovdal, A.T. Plowright, A. Pettersen, M. Rydén-Landergren, J. Barlind, A. Llinas, M. Herslöf,

- T. Drmota, K. Sigfridsson, S. Moses, and C. Whatling, *J. Med. Chem.*, **58**, 897 (2015).
- 2015JMC927 J.-P. Surivet, C. Zumbunn, G. Rueedi, D. Bur, T. Bruyère, H. Locher, D. Ritz, P. Seiler, C. Kohl, E.A. Ertel, P. Hess, J.-C. Gauvin, A. Mirre, V. Kaegi, M. Dos Santos, S. Kraemer, M. Gaertner, J. Delers, M. Enderlin-Paput, M. Weiss, R. Sube, H. Hadana, W. Keck, and C. Hubschwerlen, *J. Med. Chem.*, **58**, 927 (2015).
- 2015JMC1038 Y. Zhao, A. Aguilar, D. Bernard, and S. Wang, *J. Med. Chem.*, **58**, 1038 (2015).
- 2015JMC1569 H. Sundén, M.C. Holland, P.K. Poutianinen, T. Jääskeläinen, J.T. Pulkkinen, J.J. Palmimo, and R. Olsson, *J. Med. Chem.*, **58**, 1569 (2015).
- 2015JMC1717 A. Mallinger, S. Crumpler, M. Pichowicz, D. Waalboer, M. Stubbs, O. Adeniji-Popoola, B. Wood, E. Smith, C. Thai, A.T. Henley, K. Georgi, W. Court, S. Hobbs, G. Box, M.-J. Ortiz-Ruiz, M. Valenti, A. De Haven Brandon, R. TePoele, B. Leuthner, P. Workman, W. Aherne, O. Poeschke, T. Dale, D. Wienke, C. Esdar, F. Rohdich, F. Raynaud, P.A. Clarke, S.A. Eccles, F. Stieber, K. Schiemann, and J. Blagg, *J. Med. Chem.*, **58**, 1717 (2015).
- 2015JMC1862 G. Wang, J. Deval, J. Hong, N. Dyatkina, M. Prhavic, J. Taylor, A. Fung, Z. Jin, S.K. Stevens, V. Serebryany, J. Liu, Q. Zhang, Y. Tam, S.M. Chanda, D.B. Smith, J.A. Symons, L.M. Blatt, and L. Beigelman, *J. Med. Chem.*, **58**, 1862 (2015).
- 2015JMC1879 N. N.Patwardhan, E.A. Morris, Y. Kharel, M.R. Raje, M. Gao, J.L. Tomsig, K.R. Lynch, and W.L. Santos, *J. Med. Chem.*, **58**, 1879 (2015).
- 2015JMC2275 H. Ratni, M. Rogers-Evans, C. Bissantz, C. Grundschober, J.-L. Moreau, F. Schuler, H. Fischer, R.A. Sanchez, and P. Schnider, *J. Med. Chem.*, **58**, 2275 (2015).
- 2015JMC2465 J. Orbe, J.A. Sánchez-Arias, O. Rabal, J.A. Rodríguez, A. Salicio, A. Ugarte, M. Belzunce, M. Xu, W. Wu, H. Tan, H. Ma, J.A. Páramo, and J. Oyarzabal, *J. Med. Chem.*, **58**, 2465 (2015).
- 2015JMC2569 A. Erdmann, L. Halby, J. Fahy, and P.B. Arimondo, *J. Med. Chem.*, **58**, 2569 (2015).
- 2015JMC2746 H.R. Lawrence, K. Mahajan, Y. Luo, D. Zhang, N. Tindall, M. Huseyin, H. Gevariya, S. Kazi, S. Ozcan, N.P. Mahajan, and N.J. Lawrence, *J. Med. Chem.*, **58**, 2746 (2015).
- 2015JMC2941 J. Orbe, J.A. Rodríguez, J.A. Sánchez-Arias, A. Salicio, M. Belzunce, A. Ugarte, H.C.Y. Chang, O. Rabal, J. Oyarzabal, and J.A. Páramo, *J. Med. Chem.*, **58**, 2941 (2015).
- 2015JMC3366 Y. Liu, Y. Lang, N.K. Patel, G. Ng, R. Laufer, S.-W. Li, L. Edwards, B. Forrest, P.B. Sampson, M. Feher, F. Ban, D.E. Awrey, I. Beletskaya, G. Mao, R. Hodgson, O. Plotnikova, W. Qiu, N.Y. Chirgadze, J.M. Mason, X. Wei, D.C.-C. Lin, Y. Che, R. Kiarash, B. Madeira, G.C. Fletcher, T.W. Mak, M.R. Bray, and H.W. Pauls, *J. Med. Chem.*, **58**, 3366 (2015).
- 2015JMC3693 Q. Yang, J. Kang, L. Zheng, X.-J. Wang, N. Wan, J. Wu, Y. Qiao, P. Niu, S.-Q. Wang, Y. Peng, Q. Wang, W. Yu, and J. Chang, *J. Med. Chem.*, **58**, 3693 (2015).
- 2015JMC4845 M. Kuhnert, A. Blum, H. Steuber, and W.E. Diederich, *J. Med. Chem.*, **58**, 4845 (2015).
- 2015JMC5151 A.P. Huizing, M. Mondal, and A.K.H. Hirsch, *J. Med. Chem.*, **58**, 5151 (2015).

- 2015JMC5395 F. Xie, R. Bergmann, T. Kniess, W. Deuther-Conrad, C. Mamat, C. Neuber, B. Liu, J. Steinbach, P. Brust, J. Pietzsch, and H. Jia, *J. Med. Chem.*, **58**, 5395 (2015).
- 2015JMC5620 M.A. Letavic, P. Bonaventure, N.I. Carruthers, C. Dugovic, T. Koudriakova, B. Lord, T.W. Lovenberg, K.S. Ly, N.S. Mani, D. Nepomuceno, D.J. Pippel, M. Rizzolio, J.E. Shelton, C.R. Shah, B.T. Shireman, L.K. Young, and S. Yun, *J. Med. Chem.*, **58**, 5620 (2015).
- 2015JMC5863 C.L. Cioffi, B. Racz, E.E. Freeman, M.P. Conlon, P. Chen, D.G. Stafford, D.M.C. Schwarz, L. Zhu, D.B. Kitchen, K.D. Barnes, N. Dobri, E. Michelotti, C.L. Cywin, W.H. Martin, P.G. Pearson, G. Johnson, and K. Petrukhin, *J. Med. Chem.*, **58**, 5863 (2015).
- 2015JMC6994 A.K. Ghosh, C.D. Martyr, H.L. Osswald, V.R. Sheri, L.A. Kassekert, S. Chen, J. Agniswamy, Y.-F. Wang, H. Hayashi, M. Aoki, I.T. Weber, and H. Mitsuya, *J. Med. Chem.*, **58**, 6994 (2015).





# Thiazole and Isothiazole Ring—Containing Compounds in Crop Protection

Peter Maienfisch\*, Andrew J.F. Edmunds

Syngenta Crop Protection AG, Basel, Switzerland

\*Corresponding author: E-mail: peter.maienfisch@syngenta.com

## Contents

1. Introduction	37
2. Thiazole and Isothiazole Ring—Containing Compounds in Crop Protection	39
3. Thiazole and Isothiazole as Bioisosteric Replacement	42
4. Synthesis of Thiazoles and Isothiazoles	44
4.1 Thiazoles	44
4.2 Isothiazoles	45
4.3 Benzothiazoles	47
4.4 Benzisothiazoles	48
5. Thiazole- and Isothiazole-Containing Insecticides	49
5.1 Thiamethoxam	50
5.1.1 Discovery	50
5.1.2 Synthesis	51
5.1.3 Structure—Activity Relationships	52
5.2 Clothianidin	53
5.2.1 Discovery	53
5.2.2 Synthesis	54
5.2.3 Structure—Activity Relationships	54
5.3 Dicloromezotiaz	55
5.3.1 Discovery	55
5.3.2 Synthesis	57
5.3.3 Structure—Activity Relationships	58
6. Thiazole- and Isothiazole-Containing Fungicides	58
6.1 Thiabendazole	58
6.1.1 Discovery	59
6.1.2 Synthesis	59
6.1.3 Structure—Activity Relationships	60
6.2 Thifluzamide	60
6.2.1 Discovery	61
6.2.2 Synthesis	61
6.2.3 Structure—Activity Relationships	61

<b>6.3</b>	Ethaboxam	63
6.3.1	<i>Discovery</i>	63
6.3.2	<i>Synthesis</i>	63
6.3.3	<i>Structure—Activity Relationships</i>	64
<b>6.4</b>	Benthiavalicarb	64
6.4.1	<i>Discovery</i>	65
6.4.2	<i>Synthesis</i>	65
6.4.3	<i>Structure—Activity Relationships</i>	66
<b>6.5</b>	Isotianil	66
6.5.1	<i>Discovery</i>	66
6.5.2	<i>Synthesis</i>	67
6.5.3	<i>Structure—Activity Relationships</i>	67
<b>6.6</b>	Oxathiapiprolin	68
6.6.1	<i>Discovery</i>	68
6.6.2	<i>Synthesis</i>	69
6.6.3	<i>Structure—Activity Relationships</i>	69
<b>7.</b>	Thiazole- and Isothiazole-Containing Herbicides	69
<b>7.1</b>	Methabenzthiazuron	71
7.1.1	<i>Discovery</i>	73
7.1.2	<i>Synthesis</i>	73
7.1.3	<i>Structure—Activity Relationships</i>	74
<b>7.2</b>	Mefenacet	74
7.2.1	<i>Discovery</i>	74
7.2.2	<i>Synthesis</i>	75
7.2.3	<i>Structure—Activity Relationships</i>	75
<b>8.</b>	Thiazole- and Isothiazole-Containing Nematicides	77
<b>8.1</b>	Fluensulfone	77
8.1.1	<i>Discovery</i>	78
8.1.2	<i>Synthesis</i>	78
8.1.3	<i>Structure—Activity Relationships</i>	78
<b>8.2</b>	Benclonthiaz	78
8.2.1	<i>Discovery</i>	79
8.2.2	<i>Synthesis</i>	79
8.2.3	<i>Structure—Activity Relationships</i>	80
<b>9.</b>	Conclusions	80
	References	81

## Abstract

Organic compounds containing five-membered aromatic heterocyclic rings play an important role in life science. Among them thiazole and isothiazole heterocycles are present in many pharmaceutical drugs and crop protection compounds and have sparked over past years an enormous interest on these scaffolds. In agrochemicals these moieties are found in 11 commercial products as well as in two development compounds. A thiazole moiety is present in seven currently marketed agrochemicals, namely the

insecticides thiamethoxam and clothianidin, the fungicides thiabendazole, thifluzamide, ethaboxam, and oxathiapiprolin, and the nematocide fluensulfone, as well as in the development compound dicloromezotiaz. One compound, the fungicide isotianil, contains an isothiazole ring and three compounds a benzothiazole ring, namely the fungicide ben-thiavalicarb and the herbicides methabenzthiazuron and mefenacet. A benzisothiazole ring is not yet present in any commercial product, however, is found in the former nematocide development compound benclotiaz.

Interestingly thiazole and isothiazole heterocycles are much less frequently found in agrochemicals than pyridine and pyrazole despite their bioisosteric relationship, which may indicate that these heterocycles have still not been explored to their full scope in crop protection lead discovery and optimization.

Detailed information on the discovery, synthesis, and the structure–activity relationships of thiazole- and isothiazole-containing agrochemicals is provided in this review.

**Keywords:** Agrochemicals; Benzisothiazole; Benzothiazoles; Bioisosterism; Discovery; Isothiazoles; Structure–activity relationships; Synthesis; Thiazoles



## 1. INTRODUCTION

Thiazoles (1,3-thiazoles) and isothiazoles (1,2-thiazoles) belong to the group of azole heterocycles, that include also imidazoles and oxazoles. They are aromatic five-membered ring heterocycles containing one sulfur and one nitrogen atom (Figure 1). In recent years thiazoles and their derivatives and isomers have found applications in different fields, such as medicinal chemistry (2015EJMC(97)699), agrochemicals (2008ANK(36)14389), and biologically active natural products (2003JNP(66)1022, 2015JMC(97)911), as well as in materials science especially in liquid crystals (1979JPR(321)643, 2001JOM(66)7925, 2003JA(125)1700), molecular switches (2014AGE(53)2090), sensors (2015HSA(B)(206)430), or sunscreens in the cosmetic industry (2000TL(41)1707).

In medicinal chemistry thiazole-containing compounds have been described to possess pronounced activity as antioxidants, analgesics, antiinflammatories, antimicrobials, antifungals, antivirals, diuretics, anticonvulsants, and as neuroprotective, antitumor, or cytotoxic drugs (2015EJMC(97)699, 2015JMC(97)911, 2015EJMC(92)1, 2015MCR(21)2123, 2013SI(4)253, 2011IJDDR(3)55, 2009IJPSD(1)136, 2011PCh(1)523). Some prominent

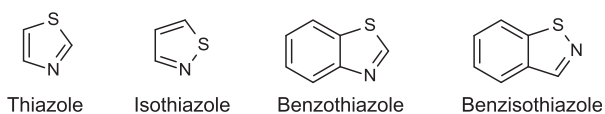


**Figure 1** Generic structures of thiazole and isothiazole ring-containing heterocycles included in this review.

examples are ritonavir (anti-human immunodeficiency virus drug), nizatidine (antiulcer agent), fatostatin (sterol regulatory element-binding proteins (SREBPs) inhibitor), febuxostat (treatment of chronic gout and hyperuricemia), tiazofurin and dasatinib (antineoplastic agents), fanetizole, meloxicam, and fentiazac (antiinflammatory agents), sulfathiazole (antimicrobial drug), abafungin and ravuconazole (antifungal agents), and nitazoxanide (antiparasitic agent). In many of these chemistries modifications of the thiazole ring have resulted in improved potency and reduced toxicity.

For isothiazole derivatives, a range of biological properties have been claimed, such as antimicrobial, antibacterial, antifungal, antiviral, antiproliferative, and antiinflammatory activities (2007THC(9)179, 2015JBPS(2)149). Furthermore isothiazoles have been described to act as inhibitors of proteases, for the treatment of anxiety and depression, as inhibitors of aldose reductase, and as 5-hydroxytryptamine receptor antagonists (2015AP(248)155).

Benzothiazoles and benzisothiazoles (Figure 1) are bicyclic compounds consisting of a benzene and a thiazole or isothiazole ring, respectively, and described to also possess a wide range of biological activities including anticancer, antimicrobial, antidiabetic, anticonvulsant, antiinflammatory, antiviral, and antitubercular properties (1981PMC(18)117, 2016CCR(308)32, 2012COC(16)789).

The thiazole moiety is also found in vitamin B1 and many biologically active natural products (2003JNP(66)1022, 2015JMC(97)911). More recent examples of biologically active natural products are: Hoiamide A, a novel cyclic depsipeptide that activates sodium influx in mouse neocortical neurons and that also exhibits modest cytotoxicity to cancer cells; nocardithiocin, a novel thiopeptide containing six thiazole rings, which is an antibiotic highly active against rifampicin-susceptible and resistant *Mycobacterium tuberculosis* strains as well as thiazomycin B, a novel antibiotic exhibiting antibacterial activity comparable to thiazomycin.

The pronounced biological effects observed with thiazole- or isothiazole-containing compounds have sparked over past years an enormous interest on these scaffolds especially in pharmaceutical and crop protection lead discovery and optimization which resulted in a steady increase in the number of related patent applications as well as in the successful introduction of thiazole- or isothiazole-containing pharmaceutical drugs and crop protection compounds to the market.

This development has been facilitated by a huge arsenal of cost-efficient synthetic methods for the preparation of thiazole and isothiazole ring-containing compounds and the versatility of these heterocyclic scaffolds as

synthons in organic transformations (2015EJMC(97)699, 2016CCR(308)32, 2012COC(16)789, 2013HCDD283). Today thiazole and isothiazole heterocycles are important scaffolds in research especially as pharmacophoric and bioisosteric elements, and also as spacers (2014JCSP(36)150, 2014MI(33)458, 1995ACS(SS584)15, 1991PDR(37)287). Furthermore thiazole and isothiazole rings as part of bioactive compounds can strongly impact the physicochemical and pharmacokinetic properties.

This review provides an up-to-date overview on thiazole and isothiazole ring-containing compounds in crop protection. In-depth information on the synthesis and the structure-activity relationships (SARs) of these compounds as well as on thiazole and isothiazole bioisosterism is included.

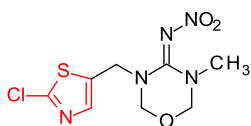


## 2. THIAZOLE AND ISOTHAZOLE RING-CONTAINING COMPOUNDS IN CROP PROTECTION

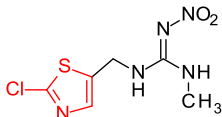
In agrochemicals the thiazole and isothiazole moieties are found in 11 commercial products as well as in two development compounds (Figure 2). A thiazole moiety is present in seven currently marketed agrochemicals, namely the insecticides thiamethoxam and clothianidin, the fungicides thiabendazole, thifluzamide, ethaboxam, and oxathiapiprolin, and the nematocide fluensulfone, as well as in the development compound dicloromezotiaz. One compound, the fungicide isotianil, contains an isothiazole ring and three compounds a benzothiazole ring, namely the fungicide benthialicarb and the herbicides methabenzthiazuron and mefenacet. A benzisothiazole ring is not yet present in any commercial product, however, is found in the former nematocide development compound benclotiaz. Among these compounds, only the insecticides thiamethoxam and clothianidine belong to the 15 best-selling compounds in their indication (2015PMcD(weblink)) (Table 1).

An analysis of the 157 compounds proposed for International Organization for Standardization (ISO) common name between 2000 and 2015 showed that 111 (70.7%) compounds contain a heterocyclic group, but only three compounds (1.9%) contain a thiazole and one compound (0.6%) an isothiazole moiety, whereas 25 compounds (15.9%) possess a pyridine, 26 (16.6%) a pyrazole, 6 (3.8%) a pyrimidine, and 5 (3.2%) a thiophene ring (Table 1, Figure 3).

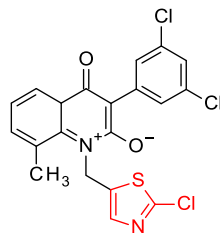
Despite the steady increase of publications and patent applications on biologically active thiazole and isothiazole ring-containing compounds and the demonstrated market value of such compounds, it appears that these heterocycles have still untapped potential especially when compared to pyridine and

**INSECTICIDES**

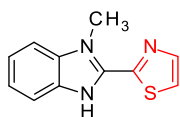
Thiamethoxam



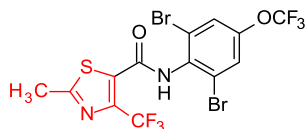
Clothianidin



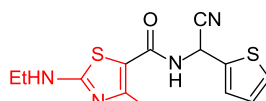
Diclomezotiaz

**FUNGICIDES**

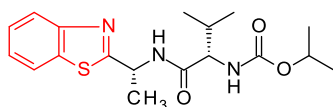
Thiabendazole



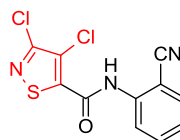
Thifuzamide



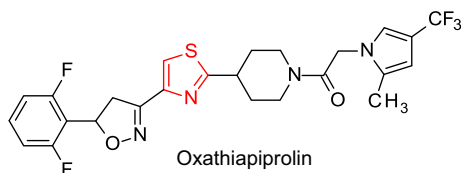
Ethaboxam



Benthiavalicarb



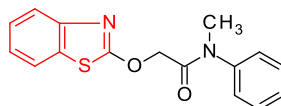
Isotianil



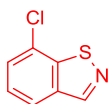
Oxathiapiprolin

**HERBICIDES**

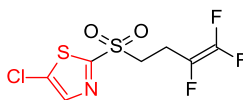
Methabenzthiazuron



Mefenacet

**NEMATOCIDES**

Benclothiaz



Fluensulfone

**Figure 2** Thiazole and isothiazole ring-containing agrochemicals.

**Table 1** Occurrence of thiazole- and isothiazole-containing compounds

	<b>No. of chemicals</b>	<b>No. of compounds containing a heterocycle (%)</b>	<b>No. of compounds containing an (iso-) thiazole group (%)</b>	<b>No. of compounds containing a pyridyl group (%)</b>	<b>Other major heterocycles (No.)</b>
Leading fungicides 2014 (top 15 products)	14	10 (71.4)	0	2 (14.3)	Triazole (5)
Leading herbicides 2014 (top 15 products)	15	7 (46.7)	0	3 (20.0)	—
Leading insecticides 2014 (top 15 products)	15	9 (60.0)	2 (13.3)	4 (26.7)	Pyrazole (2)
New ISO common names 2000–15	157	111 (70.7)	4 (2.5)	25 (15.9)	Pyrazole (26) Pyrimidine (6) Thiophene (5) Triazine (3) Thiophene (5)

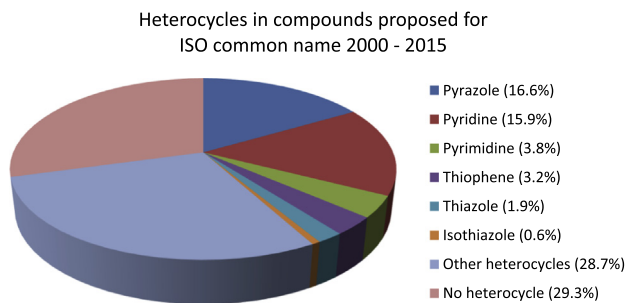


**Figure 3** Frequency of aromatic heterocyclic rings in compounds proposed for ISO common name in the period 2000–15, which includes a total of 157 compounds with 111 (70.7%) compounds containing a heterocyclic group.

pyrazole compounds. This is perhaps surprising considering the bioisosteric relationship between these heterocyclic moieties. Furthermore, it is apparent that isothiazole, benzothiazole, or benzisothiazole heterocycles thus far are of lower importance in crop protection than the isomeric thiazoles.

### 3. THIAZOLE AND ISOTHIAZOLE AS BIOISOSTERIC REPLACEMENT

The concept of bioisosterism is based on the replacement of an atom or a group in an active molecule by another electronically and/or sterically similar atom or group with retention of the biological activity. This concept is well established, and has been widely applied as a successful strategy in lead optimization in pharmaceutical and crop protection research. Bioisosteric replacements can lead to an increase of potency and improved physicochemical, pharmacokinetic, and/or toxicological properties of lead compounds (2014JCS(36)150, 2014MI(33)458, 1995ACS(SS584)15, 1991PDR(37)287, 2011PHARM(1)272).

The basic principles of bioisosteric replacements involve ring-to-ring transformations and ring-to-chain transformations. The following replacements in ring-to-ring transformations are well established:

- |                                |                                    |
|--------------------------------|------------------------------------|
| • Bivalent atom replacements:  | –S–, –O–, –NH–, –CH <sub>2</sub> – |
| • Trivalent atom replacements: | –N=, –CH=                          |
| • Other replacements           | –S–, –CH=CH–<br>–N=, –CH=          |



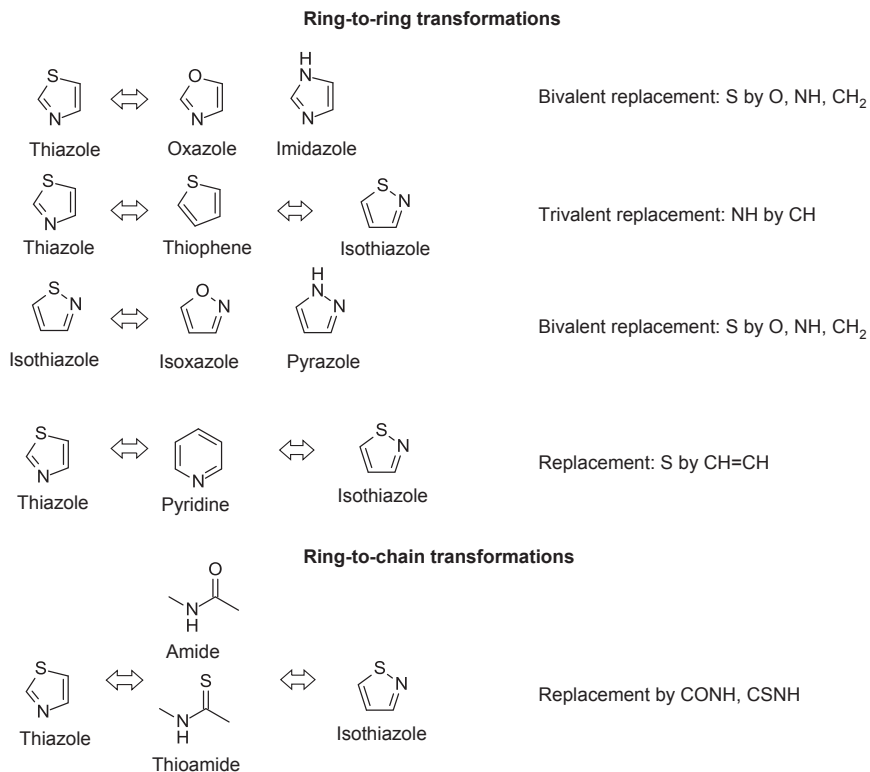


**Figure 4** Major bioisosteric replacements of thiazole and isothiazole ring equivalents and open-chain bioisosteres.

Applying these principles to thiazole and isothiazoles indicates that oxazoles and imidazoles are potentially ideal bioisosteres of thiazoles; isoxazoles and pyrazoles of isothiazoles; and pyridine and thiophene of both thiazoles and isothiazoles (Figure 4). Thiazole and isothiazole can also serve as bioisosteric replacements of several open-chain substituents such as amides and thioamides.

Successful examples of bioisosteric replacements of the thiazole ring, and also to some extent of the isothiazole ring, are documented in the literature:

- Replacement of five- and six-membered aromatic rings like pyridine, oxazole, furan, thiophene, 1,2,4-oxadiazoles, imidazole, and even benzene with thiazole and isothiazole (1991PDR(37)287, 2011PHARM(1) 272, 2001CODDD(4)471, 2004CUZ(38)320, 2004BMC(38)320, 2012CB(9)2442).

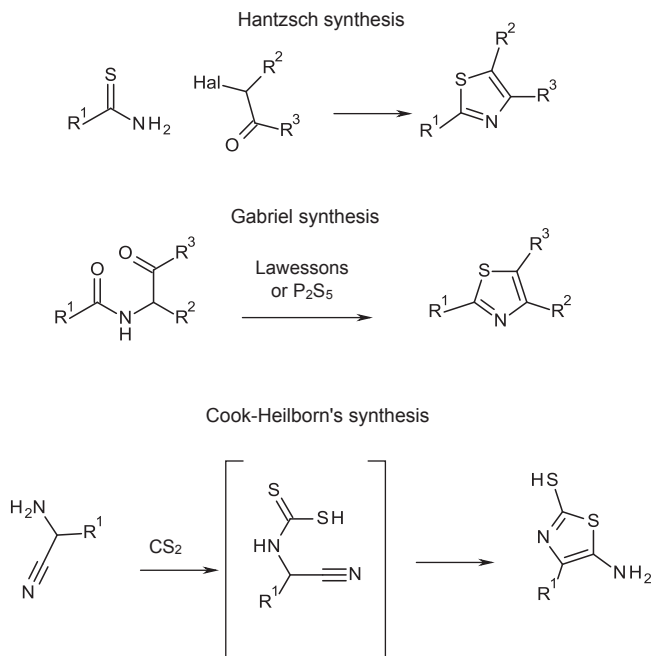
- Replacement of an amide, ester, sulfonamide, or a carbonyl group by thiazole (2012CB(9)2442, 2012JMC(55)2301, 1990JMC(33)2715).

Further examples of bioisosteric replacements of various groups with thiazole or isothiazole rings in crop protection products will be discussed in the following sections.

## 4. SYNTHESIS OF THIAZOLES AND ISOTHAZOLES

### 4.1 Thiazoles

Thiazole heterocycles can easily be prepared by well-known methods such as Hantzsch synthesis, Gabriel synthesis, or Cook–Heilborn’s synthesis (Scheme 1). The Hantzsch approach involves cyclization and condensation of haloketones with thioamide (1945OS(V3)332). In Gabriel synthesis, thiazoles are formed from  $\alpha$ -acylaminoketones after treatment with stoichiometric amounts of  $P_2S_5$  or Lawesson’s reagent (2009JOC(74)8988). Cook–Heilborn’s synthesis is a versatile method for the synthesis of substituted aminothiazoles involving the reaction of  $\alpha$ -aminonitriles with dithioacids or esters, carbon disulfide, carbonyl sulfide, and isothiocyanates

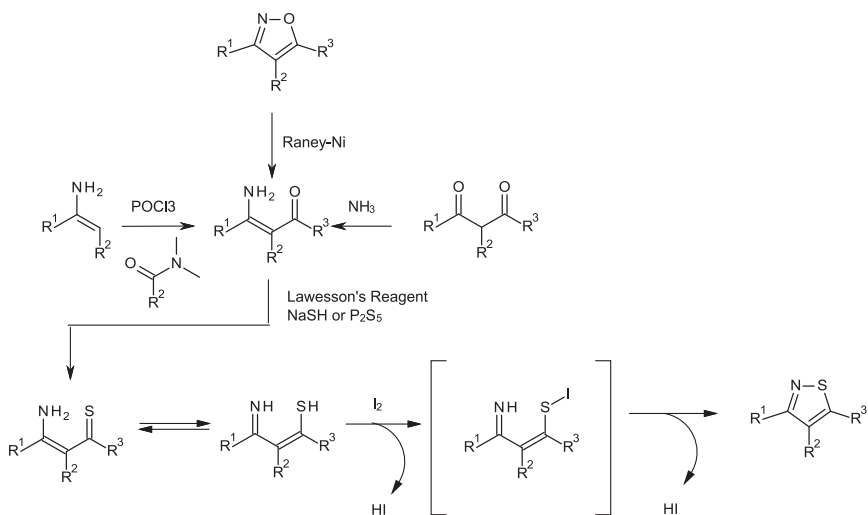


**Scheme 1** General syntheses of thiazoles.

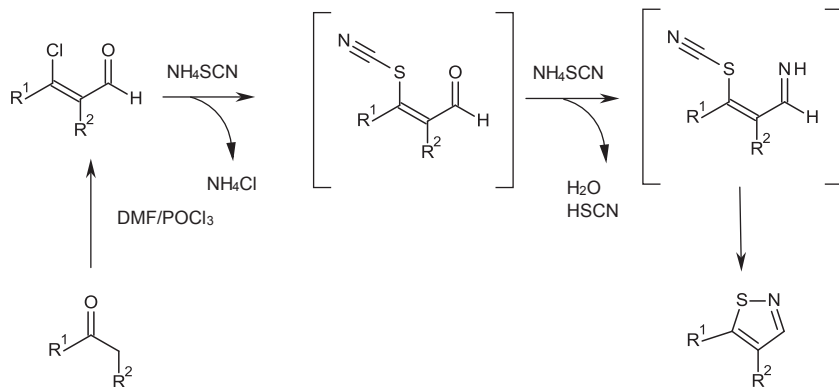
under mild conditions as illustrated in [Scheme 1](#) with carbon disulfide (1949JCS1064). Details on more recent synthetic methodologies for the synthesis of thiazole derivatives has been described in several review articles (2015EJMC(97)699, 2016CCR(308)32, 2013HCDD283, 2011PHC(22)259, 2001SCM10).

## 4.2 Isothiazoles

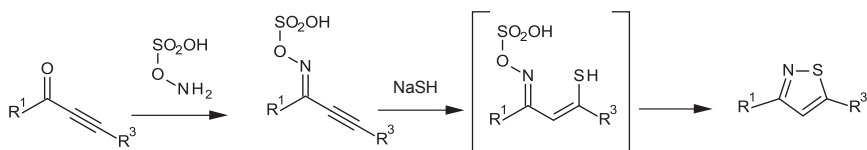
The most common strategies for the synthesis of isothiazoles (2002SS(11)507) are illustrated in [Schemes 2–5](#). Among them, the oxidative C-N coupling of  $\beta$ -amino thiones is of special importance (2003CH(2ndEd)162). The oxidation in principle adds a leaving group to the sulfur in the isomeric thiol form of the  $\beta$ -amino thione which then can undergo intramolecular ring closure. This is illustrated for oxidation with iodine (2002SS(11)507) in [Scheme 2](#). The  $\beta$ -amino thiones are readily prepared from  $\beta$ -diketones by treatment with ammonia and then a sulfenating reagent such as Lawesson's reagent. Alternatively,  $\beta$ -amino thiones can be prepared by a Vilsmeier reaction of enamines, hydrolysis, and treatment with an appropriate sulfenating reagent. As the synthesis of isoxazoles is well established, it may also sometimes be useful to convert these to isothiazoles, by reductive ring-opening of the isoxazole, and then treating the  $\beta$ -ketoenamine with a sulfenating reagent, followed by oxidative S-N bond formation (1969T(25)389).



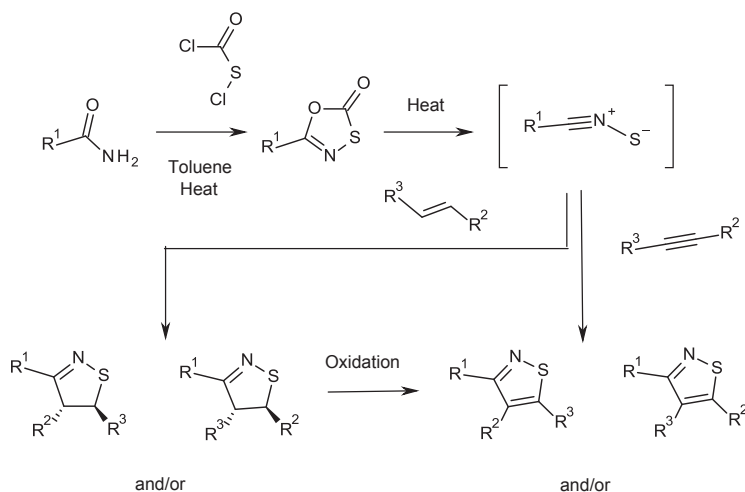
**Scheme 2** Syntheses of isothiazoles via oxidative C-N coupling of  $\beta$ -amino thiones.



**Scheme 3** Syntheses of isothiazoles from chlorovinyl aldehydes.



**Scheme 4** Syntheses of isothiazoles from acetylene aldehydes or ketones.



**Scheme 5** Syntheses of isothiazoles from amides and acetylenes.

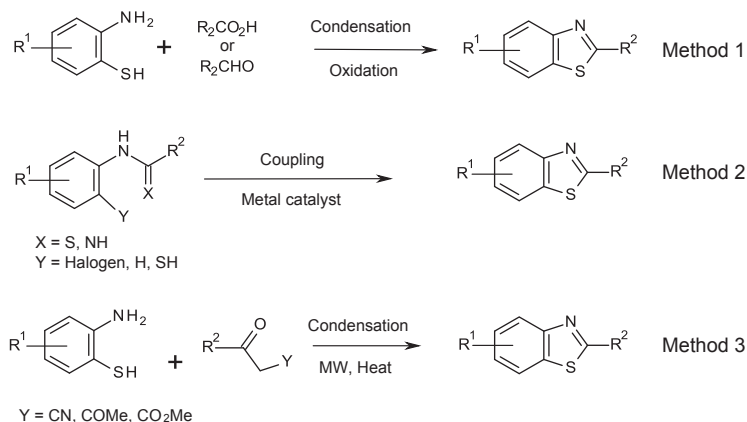
A similar strategy involves the reaction of chlorovinyl aldehydes, which can readily be obtained by Vilsmeier reaction of  $\alpha$ -methylene ketones, with two equivalents of ammonium thiocyanate (Scheme 3) (2002SS(11)507).

In another strategy starting from alkynones and alkynals, a leaving group attached to the nitrogen of the reagent is introduced, which after Michael addition of a sulfur nucleophile, enables spontaneous S-N bond formation (Scheme 4) (1989H(29)97).

A very elegant synthesis of isothiazoles involves a 1,3 dipolar cycloaddition of nitrile sulfides with acetylenes (Scheme 5) (1978JOC(43)3736, 1970TL1381, 1973JCS(CC)524). Judicious choice of the acetylenes allows for good regioselectivity in the reactions. Microwave versions of the reaction have also been reported (2012COC(16)789). The reaction can also be carried out with olefins, which can then be readily oxidized to the corresponding isothiazoles (Scheme 5) (1978JOC(43)3736).

### 4.3 Benzothiazoles

Benzothiazoles (2002SS(11)507) are usually synthesized by one of the general strategies highlighted in Scheme 6. The first method involves the condensation reactions of 2-amino thiophenols with carboxylic acids (2009SC(39)860, 2012TL(53)2440, 1982CL1225) or aldehydes (2009OL(11)2039, 2010SC(40)206, 2013TL(54)579) under oxidative conditions, the second method involves the transition-metal-catalyzed intramolecular cyclization of 2-haloanilide analogues (2009OC(74)8719, 2004CC446, 2003TL(44)6073, 2010TL(51)5009, 2007OL(9)3687, 2009AGE(48)4222, 2007S819),



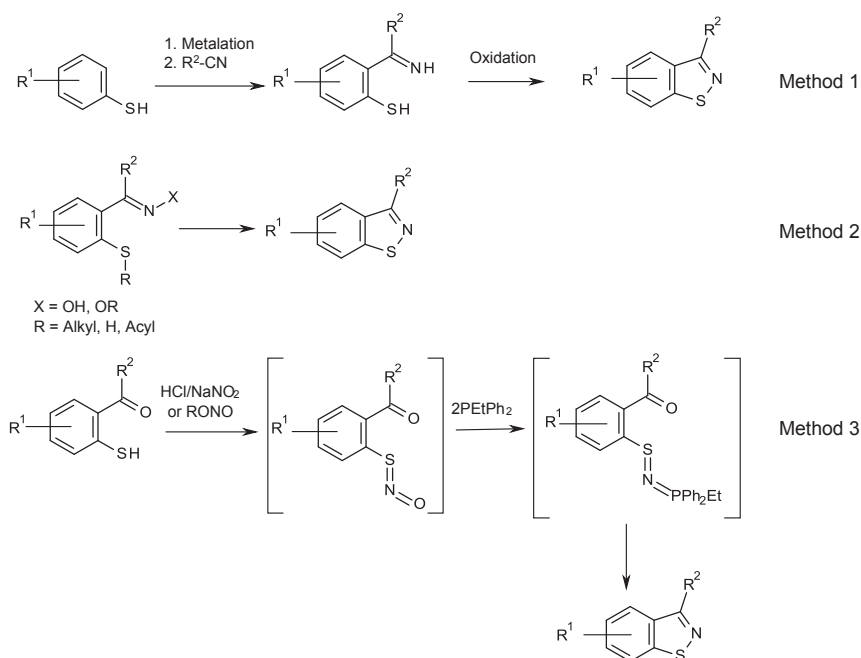
Scheme 6 Strategies for synthesis of benzothiazoles.

and the third method involves the condensation reactions of 2-aminothiophenols with  $\beta$ -ketonitriles (2006JHC(43)1609),  $\beta$ -ketoesters (2005H(65)2119, 2011CJC(29)1880), or  $\beta$ -diketones (2005JHC(42)1001, 2014OL(16)764) under microwave radiation and high-temperature conditions.

#### 4.4 Benzisothiazoles

The most usual general strategies for the preparation of benzisothiazoles (2002SS(11)507, 2002SS(11)835) are similar to those for isothiazoles and are shown in Scheme 7.

The first method involves intramolecular oxidative ring closure of imine with thiophenols (1995JHC(32)1683). A second strategy involves forming the S-N bond by having a leaving group attached to the nitrogen, followed by intramolecular ring closure (1973JCS(PT1OBOC4)356, 2011JA(133)6403, 1978S(1)58, 1982PS(12)357, 1988CJC(66)1405). A further strategy for the synthesis of benzisothiazoles involves reduction of nitrosothiols, formation of an aza Wittig reagent with subsequent intramolecular ring closure (Method 3) (2010OL(12)752). Formation of the S-N bond to generate in situ S-NH<sub>2</sub> moieties, which then intramolecularly cyclize with ketone/aldehydes is also known (1993TL(34)6525).



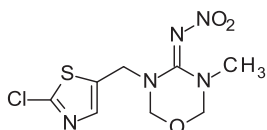
Scheme 7 Strategies for synthesis of benzisothiazoles.

Further details on the synthesis of thiazoles, isothiazoles, benzothiazoles, and benzisothiazoles are provided in the following sections.

## 5. THIAZOLE- AND ISOTHIAZOLE-CONTAINING INSECTICIDES

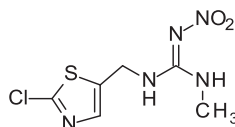
The global market for insecticides in 2014 was valued at \$18,619 million, equivalent to 29.5% of the total agrochemical market (2015PMcD([weblink](#))). The most important chemical classes are neonicotinoids (mode of action: modulators of nicotinic acetyl choline receptors; market share: 18.0% of the total market), pyrethroids (modulators of voltage-gated sodium channels; 17.0%), organophosphates (inhibition of acetylcholinesterase; 15.3%), carbamates (inhibition of acetylcholinesterase; 6.7%), fermentation products (6.7%), and several other chemical classes having less than 5% market share each. A thiazole ring is present in only two insecticide sales products, thiamethoxam and clothianidin, as well as in the development compound dicloromezotiaz ([Figure 5](#)). All these compounds belong to the chemical class of the neonicotinoids.

Currently no isothiazole-containing insecticide is on the market or thought to be in development.



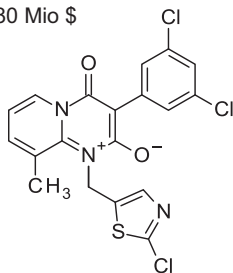
### Thiamethoxam

Syngenta  
 Launch: 1998  
 Chemical Class: Neonicotinoid  
 Sales 2014: 1.180 Mio \$  
 Rank: 2



### Clothianidin

Sumitomo / Bayer  
 Launch: 2001  
 Chemical Class: Neonicotinoid  
 Sales 2014: 460 Mio \$  
 Rank: 10



### Dicloromezotiaz

DuPont  
 Chemical Class: Neonicotinoid  
 In development

**Figure 5** Thiazole-containing insecticides.

## 5.1 Thiamethoxam

Thiamethoxam (Figure 5) (2001PMS(57)165, 2001PMS(57)906, 2006ZN(B61)353) belongs to the chemical class of the neonicotinoids and possess broad-spectrum insecticidal activity. It was introduced to the market in 1998 and is used by foliar or soil application as well as a seed treatment against a wide spectrum of pests in many crops.

The neonicotinoids are currently the most successful chemical class of insecticides reaching sales of more than 3.345 biodollars in 2014 (2015PMcD(weblink)), mainly due to the excellent market performance of thiamethoxam and imidacloprid as leading products. Both these products reach sales of more than \$1 billion and have been the second and third best-selling insecticides in 2014.

Other products from this class include acetamiprid, nitenpyram, and thiacloprid possessing, as imidacloprid, a pyridyl moiety instead of the thiazole ring and clothianidin and dinotefurane, which have a thiazole and tetrahydrofuran ring, respectively (2012MCPC(2nd Ed, 3)1165).

Neonicotinoids bind selectively to insect nicotinic acetylcholine receptors (nAChRs) with nanomolar affinity. However, they do not act as a homogenous class of insecticides. Recent findings suggest that thiamethoxam binds, compared to the other neonicotinoid sales products, in a different way, possibly to a different site of the receptor in aphids (2004PMS(60)959, 2004PMS(60)945, 2016PMS(in press)).

### 5.1.1 Discovery

Thiamethoxam was discovered as part of a research program to investigate novel innovative variations of the nitroimino-heterocycle of imidacloprid (2001PMS(57)165). In a first optimization cycle, the 4-nitroimino-1,3,5-oxadiazinane ( $X=O$ ), 4-nitroimino-hexahydro-1,3-pyrimidine ( $X=CH_2$ ), 4-nitroimino-hexahydro-1,3,5-triazine ( $X=NR$ ), and 4-nitroimino-1,3,5-thiadiazinane ( $X=S$ ) analogues of imidacloprid were prepared. Bioassays revealed that among these compounds, the 4-nitroimino-1,3,5-oxadiazinane analogue exhibits the best insecticidal activity, and that its potency was close to imidacloprid. Further chemical and biological exploration showed that replacement of the 6-chloro-3-pyridyl group by a 2-chloro-5-thiazolyl moiety resulted in a strong increase of the activity against chewing insects and that the introduction of a methyl group at the nitroguanidine moiety increased the activity against sucking pests. The combination of these two favorable modifications led to thiamethoxam (Figure 6).



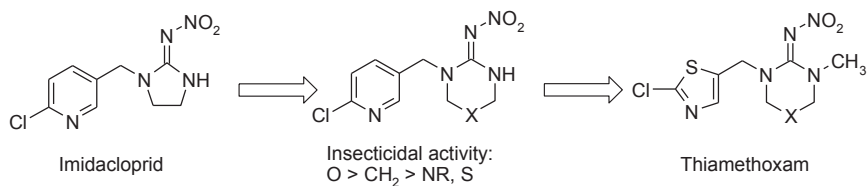
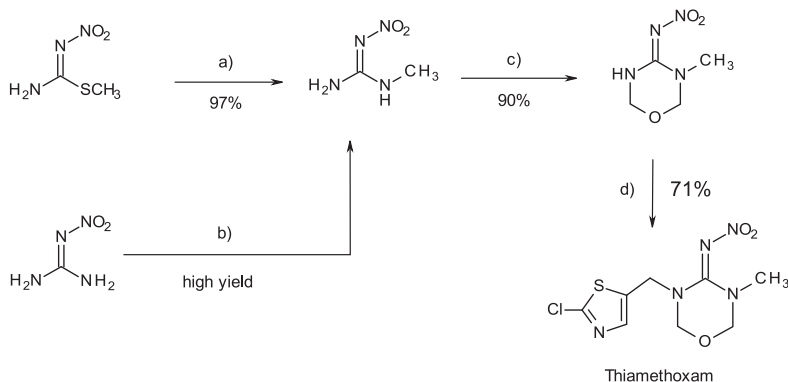


**Figure 6** Discovery of thiamethoxam.

### 5.1.2 Synthesis

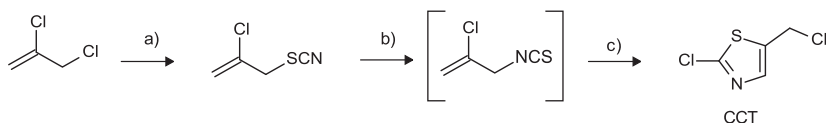
Thiamethoxam can be synthesized in only a few steps from easily accessible starting materials as shown in [Scheme 8 \(2001PMS\(57\)165\)](#). *N*-methylnitroguanidine is converted to the corresponding 4-nitroimino-oxadiazinane by a Mannich-type cyclization reaction with formaldehyde in the presence of formic acid. Subsequent alkylation in dimethylformamide with potassium carbonate as a base afforded thiamethoxam in good yields.

The key intermediate 2-chlorothiazol-5-ylmethyl chloride (CCT) is an intermediate not only for the synthesis of thiamethoxam, but also for the production of clothianidin. The most cost-efficient process has been developed by Takeda (now Sumitomo). Starting from 2,3-dichloro-1-propene CCT can be prepared in three steps and high yield as shown in [Scheme 9 \(CA 115 280011 \(1991\)\)](#).



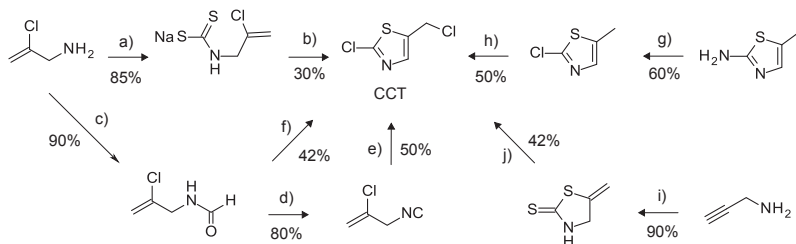
**Reagents and conditions:** a) CH<sub>3</sub>NH<sub>2</sub>, EtOH, 80°C, b) CH<sub>3</sub>NH<sub>2</sub>, Δ, c) HCHO, HCO<sub>2</sub>H, 50°–80°C, d) 2-Chlorothiazol-5-ylmethyl chloride, K<sub>2</sub>CO<sub>3</sub>, DMF, 50°C.

**Scheme 8** Synthesis of thiamethoxam.



**Reagents and conditions:** a) KSCN, b) Δ, c) Chlorination

**Scheme 9** Synthesis of 2-chlorothiazol-5-ylmethyl chloride.



**Reagents and conditions:** a) H<sub>2</sub>O, NaOH, CS<sub>2</sub>, 85%, b) H<sub>2</sub>O, KI, I<sub>2</sub>, then CH<sub>2</sub>Cl<sub>2</sub>, SO<sub>2</sub>Cl<sub>2</sub>, 30%, c) HCO<sub>2</sub>C<sub>2</sub>H<sub>5</sub>, reflux, 12 hr, 90%, d) DMF, SOCl<sub>2</sub>, Na<sub>2</sub>CO<sub>3</sub>, 12 hr, 80%, e) CCl<sub>4</sub>, SCl<sub>2</sub>, 40 °C, 4 hr, 50%, f) SOCl<sub>2</sub>, SCl<sub>2</sub>, reflux, 24 hr, 42%, g) t-BuONO, CuCl<sub>2</sub>, CH<sub>3</sub>CN, 60%, h) N-chlorosuccinimide, dibenzoylperoxide, CCl<sub>4</sub>, reflux, 50%, i) CS<sub>2</sub>, EtOH, ambient temperature, 2hr, 90%, j) CH<sub>2</sub>Cl<sub>2</sub>, H<sub>2</sub>O, SO<sub>2</sub>Cl<sub>2</sub>, 1 hr, 80%. (laboratory yields – not optimized)

**Scheme 10** Alternative syntheses of 2-chlorothiazol-5-ylmethylchloride.

In the course of the optimization of the production costs for thiamethoxam alternative syntheses of 2-chlorothiazol-5-ylmethyl chloride starting from five different precursors were investigated and a wide choice of additional practical methods for large-scale production of this key intermediate became available (1999PS1999) (Scheme 10).

### 5.1.3 Structure–Activity Relationships

The SARs for the thiazole heterocycle in thiamethoxam was investigated in detail (2001PMS(57)906) (Figure 7). Best potency and broadest insecticidal spectrum is achieved with the 2-chloro-5-thiazolyl ring. The 2-chloro-5-pyridyl analogue is the best alternative, but overall is somewhat less active. Replacement of the chloro substituent by hydrogen, methyl, trifluoromethyl, hydroxy, or methoxy led to a clear decrease in activity. Changing the 2-chloro-5-thiazolyl ring into a 2-chloro-3-pyridyl or a 2-chloro-4-pyridyl resulted in a drastic loss of activity. Replacement of the 2-chloro-5-thiazolyl

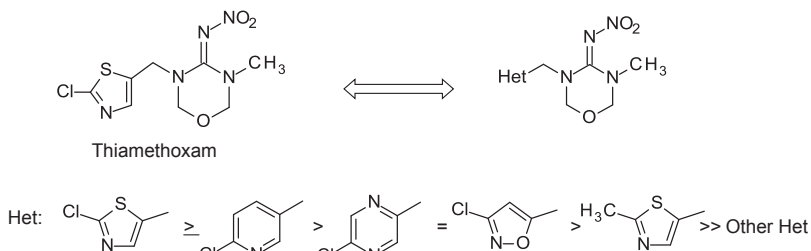


**Figure 7** Structure–activity relationships of thiamethoxam.

or the 2-chloro-5-pyridyl group by a 5-chloro-2-pyrazinyl or a 3-chloro-5-isoxazolyl group led to compounds also showing good, but somewhat reduced activity and spectrum.

The SARs show that a chloro substituent at the heterocyclic group is required and that the pyridyl, pyrazinyl, and isoxazolyl groups can be regarded as bioisosteric replacements of the thiazolyl ring.

## 5.2 Clothianidin

Clothianidin (Figure 5) (2006SK20, 2011JAF(59)2931, 2003PNB(56)5) belongs, as thiamethoxam, to the chemical class of the neonicotinoids and possesses broad-spectrum insecticidal activity. It was jointly developed by Takeda (now Sumitomo) and Bayer and was first introduced in 2002 in Japan by Takeda for use in rice and turf, and in 2003 by Bayer in the United States as a seed treatment. In 2014 clothianidin reached sales of \$460 million and has been the 10th best-selling insecticide (2015PMcD([weblink](#))).

### 5.2.1 Discovery

Inspired by patent applications from Bayer on neonicotinoid insecticides together with some in-house leads having an acyclic nitromethylene moiety Takeda (now Sumitomo) started in the mid-1980s an optimization program on neonicotinoids and prepared acyclic nitromethylenes and later acyclic nitroguanidines (2011JAF(59)2931). Initial success was achieved with the discovery of nitenpyram, a neonicotinoid insecticide which was introduced to the market in 1995. This compound has several attractive features such as high activity against *Hemiptera* and low mammalian toxicity. However, its insecticidal spectrum and physicochemical properties, such as photostability and lack of persistence, were insufficient for further progression, and thus further optimization was performed. Replacing the nitromethylene pharmacophore by a nitroguanidine moiety, as present in imidacloprid and thiamethoxam, and changing the heterocyclic group from chloropyridyl to chlorothiazolyl resulted in the discovery of clothianidin, a new neonicotinoid with strongly improved spectrum and persistence compared to the acyclic neonicotinoid nitenpyram (Figure 8).

Besides Takeda and Bayer, Ciba (now Syngenta) also had the same design idea and performed at the same time independent research on acyclic nitromethylene and nitroguanidine compounds which resulted in a series of overlapping patent applications. However, both compounds, nitenpyram and clothianidin, were first disclosed in Takeda patent applications.

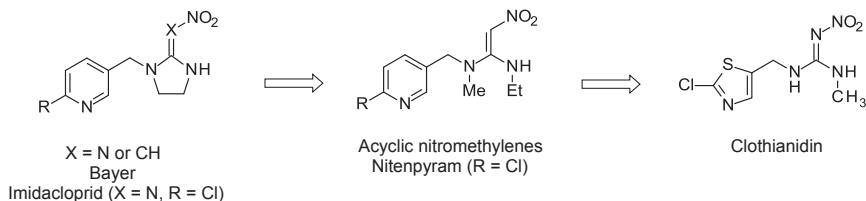


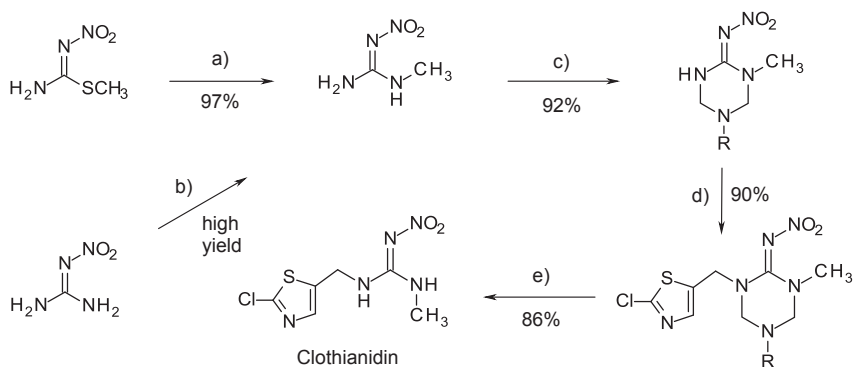
**Figure 8** Discovery of clothianidin.

### 5.2.2 Synthesis

Many different synthetic routes have been reported by Takeda for the synthesis of the key building block 2-chlorothiazolyl-5-methylchloride (see also Schemes 9 and 10) and the further conversion to clothianidin starting from *S*-methyl-*N*-nitrosothiourea and *O*-methyl-*N*-nitrosourea, respectively (2011JAFC(59)2931). Furthermore, a very cost-efficient process has been developed and patented by Ciba (now Syngenta) which involves the synthesis of a hexahydro-1,3,5-triazine intermediate from the readily available *N*-methyl-*N'*-nitroguanidine via Mannich-type cyclization reaction, followed by alkylation with 2-chlorothiazolyl-5-methylchloride and N-CH<sub>2</sub>-N bond cleavage under acetic condition. By this method clothianidin is accessible in only four steps and an overall laboratory yield of 69% (Scheme 11) (2000TL(41)7187).

### 5.2.3 Structure–Activity Relationships

The presence of an electron-withdrawing group is essential, with the nitroimino group delivering the best activity and broadest spectrum. The SARs



**Reagents and conditions:** a) CH<sub>3</sub>NH<sub>2</sub>, EtOH, 80°C, b) CH<sub>3</sub>NH<sub>2</sub>, Δ, c) *n*-PrNH<sub>2</sub>, HCHO, EtOH, 50°C, (R = *n*-Pr), d) 2-Chlorothiazol-5-ylmethyl chloride, K<sub>2</sub>CO<sub>3</sub>, DMF, 50°C (R = *n*-Pr), e) 1N HCl, EtOH, r.t.

**Scheme 11** Synthesis of clothianidin.

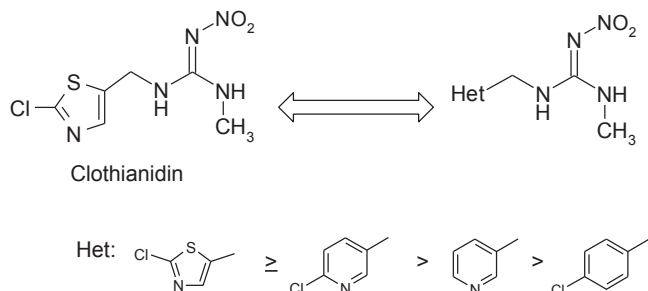


**Figure 9** Structure–activity relationships of clothianidin.

for the thiazole heterocycle in clothianidin follows the standard SAR observed in the chemical class of the neonicotinoids. The 2-chloro-5-thiazolyl is the most preferable heterocycle, followed by 6-chloro-3-pyridyl (Figure 9). A chloro substituent at the 2-position of the 5-thiazole ring is the first choice, a bromine atom is slightly inferior, followed in decreasing order by  $\text{CF}_3$ , H,  $\text{CH}_3$ ,  $\text{CH}_3\text{S}$ , and  $\text{C}_6\text{H}_5$  (2011JAF(59)2931).

The SARs observed for acyclic neonicotinoids confirm the value of the thiazolyl ring as bioisosteric replacement of the pyridine ring.

### 5.3 Dicloromezotiaz

The development compound dicloromezotiaz (Figure 5) (CA 154 250059 (2011)) is the second mesoionic insecticide from Du Pont, which targets the acetylcholine receptor but with a physiological action which is distinct from that of neonicotinoids, and as such has the same mode of action as triflumezopyrim (2014IUPAC836). The compound is structurally very similar to triflumezopyrim (Figure 10), having a mesoionic central core, a meta-substituted aromatic ring (in this case a dichloro benzene ring) and a methylene heteroaryl substituent on the nitrogen. The only other difference is the additional methyl substituent on the amino pyridyl moiety. Dicloromezotiaz has a much weaker hopper activity, but good activity on a range of lepidopteran species.

#### 5.3.1 Discovery

The discovery of dicloromezotiaz started from the mesoionic lead structure shown in Figure 10. Initial scoping of this lead included addition of aryl substituents which led to an increase of insecticidal activity. At this stage, the classical neonicotinoid  $\text{CH}_2$ -hetaryl substituents were tested which led to drastic improvements in insecticidal activity. Further optimization of the phenyl moiety led to the development compound (2014IUPAC446).

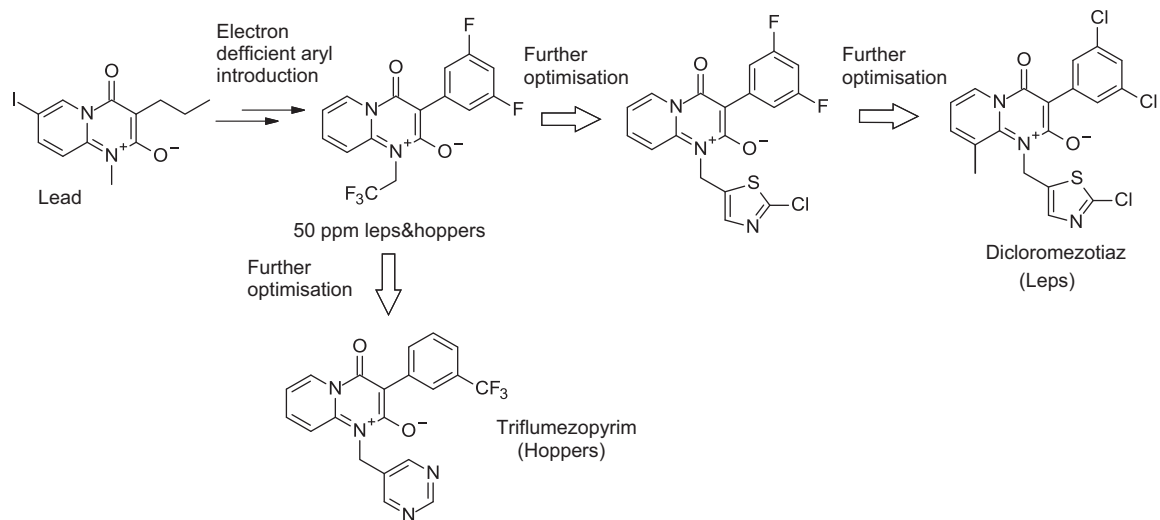
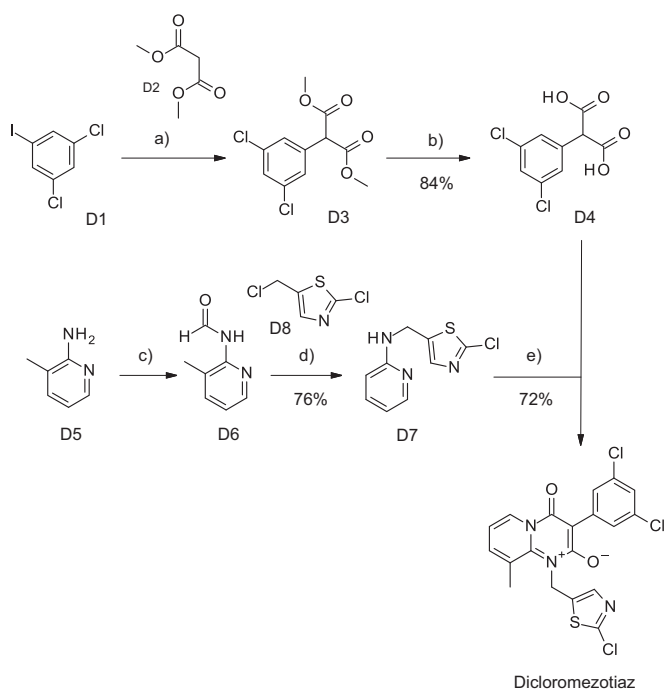


**Figure 10** Discovery of dicloromezotiaz.

### 5.3.2 Synthesis

A convergent synthesis of dicloromezotiaz begins with a copper catalyzed coupling of dimethyl malonate D2 with the iodide D1. The crude product D3 is directly hydrolyzed to the diacid D4 in overall yield of 84% for the two steps. The required coupling partner D7 is prepared efficiently by formamide protection of D5. The thiazole moiety is introduced by a building block strategy, i.e., phase transfer catalyzed alkylation of D6 with 2-chlorothiazol-5-ylmethyl chloride (D9), building block well known from classical neonicotinoid chemistry. In situ deprotection of the formyl group gives D7 in 76% yield. To complete the synthesis, the diacid is activated as the diacid chloride and treated with D7 in toluene in the presence of triethyl amine. This yields dicloromezotiaz in 72% yield as a single crystal polymorph (2016BMC(24)317) (Scheme 12).



**Reagents and conditions:** a)  $\text{Cs}_2\text{CO}_3$ , 2-picolinic acid (cat.), CuI (cat.), dioxane,  $90^\circ\text{C}$ . b) NaOH,  $\text{H}_2\text{O}$ , MeOH, r.t.;  $10^\circ\text{C}$ , then HCl,  $\text{H}_2\text{O}$ . c)  $\text{HCO}_2\text{H}$ , Ac<sub>2</sub>O, EtOAc, r.t.  $\rightarrow 46^\circ\text{C}$ . d) 1)  $\text{K}_2\text{CO}_3$ , Bu<sub>4</sub>N<sup>+</sup>Br<sup>-</sup> (cat.), Me<sub>2</sub>CHOH, r.t.  $\rightarrow 75^\circ\text{C}$ ; 2) NaOH,  $\text{H}_2\text{O}$ ,  $50^\circ\text{C}$ . e) 1) Oxallyl chloride, DMF (cat.),  $\text{CH}_2\text{Cl}_2$ , reflux. 2) Et<sub>3</sub>N, Toluene, r.t.

Scheme 12 Synthesis of dicloromezotiaz.

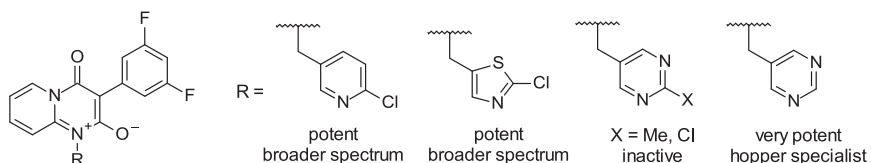


**Figure 11** Structure–activity relationships of dicloromezotiaz.

### 5.3.3 Structure–Activity Relationships

Regarding the methylene hetaryl substituent, shifts in pest spectrum are observed depending on the nature of the heterocycle. Pyridyl and thiazole give broad-spectrum insecticides, while surprisingly a naked pyrimidine gives a potent hopper specialist. The naked pyrimidine is not a usual heterocycle seen in classical neonicotinoid chemistries, and is even more surprising given that the chloro- and methyl-substituted pyrimidines are inactive (2014IUPAC446) (Figure 11).

## 6. THIAZOLE- AND ISOTHIAZOLE-CONTAINING FUNGICIDES

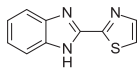
The global market for fungicides in 2014 was valued at \$16,365 million, equivalent to 25.9% of the total agrochemical market (2015PMcD(weblink)). The most important chemical classes are strobilurins (mode of action: inhibitors of mitochondrial synthesis at the cytochrome bc1 complex; 22.9% of the total market), triazoles (C14 demethylase inhibitors of the sterol biosynthesis pathway; 21.2%), succinate dehydrogenase inhibitors (inhibition of succinic acid oxidation during metabolic respiration; 8.4%), azoles (C14 demethylase inhibitors of the sterol biosynthesis pathway; 7.9%), dithiocarbamates (multi-site contact; 5.4%), and several other chemical classes having less than 5% market share each.

Five fungicides contain thiazole heterocycles, namely thiabendazole, thi-fluzamide, ethaboxam, benthiavalicarb, and oxathiapiprolin, and one compound, isotianil, contains an isothiazole ring (Figure 12). None of these fungicides have yet reached sales of more than \$35 million and as such can be regarded as specialist fungicides for some specific uses.

### 6.1 Thiabendazole

Thiabendazole (Figure 12) was introduced by Merck in 1964, the first benzimidazole to be commercialized, and was acquired as part of this business by Novartis (now Syngenta) in 1997. The major uses are as a seed treatment and



**FUNGICIDES****Thiabendazole**

Syngenta

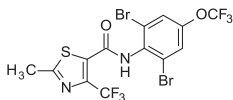
Launch: 1964

Chemical Class:

Sales 2014:

Benzimidazoles

35 Mio \$

**Thifluzamide**

Nissan, Dow

Launch:

Chemical Class:

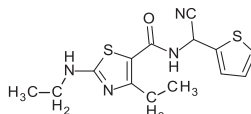
Sales 2014:

1997

Succinate

dehydrogenase inhibitors

&lt;30 Mio \$

**Ethaboxam**

LG Chemicals

Launch:

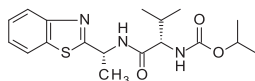
Chemical Class:

Sales 2014:

1999

Carboxamide

&lt;10 Mio \$

**Benthiavalicarb**

Kumiai, Bayer

Launch:

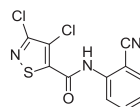
Chemical Class:

Sales 2014:

2004

Carbamate

&lt;30 Mio \$

**Isotianil**

Bayer, Sumitomo

Launch:

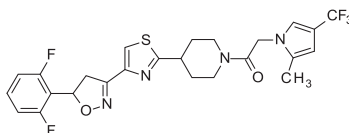
Chemical Class:

Sales 2014:

2010

Others

&lt;30 Mio \$

**Oxathiapiprolin**

DuPont, Syngenta

Launch:

Chemical Class:

Sales 2014:

2015

Piperidinyl thiazole isoxazolines

**Figure 12** Thiazole- and isothiazole-containing fungicides.

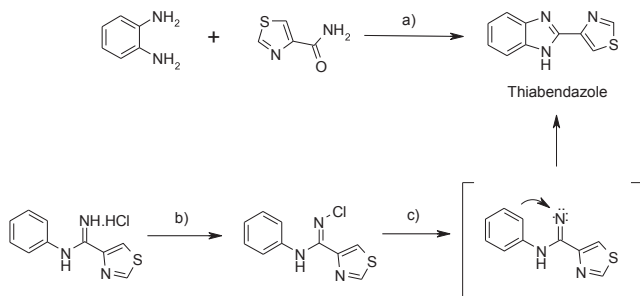
for postharvest disease control, mostly on fruit and vegetables, but also on cereals (2015PMcD(weblink)). The mode of action of benzimidazoles has been described in several comprehensive reviews and it appears that they are inhibitors of microtubule assembly by specific binding to the  $\beta$ -subunit of fungal tubulin (1995MSF305, 1984BMAP382, 1986ARP24).

**6.1.1 Discovery**

Thiabendazole was originally introduced as an anthelmintic (CA 56 79451 (1962)), and it was only later that its fungicidal properties were discovered (1964ID(42)479, 1964PP(13)163, 1968PHYT(58)860).

**6.1.2 Synthesis**

Thiabendazole has been prepared by heating thiazole-4-carboxamide and benzene-1,2-diamine in polyphosphoric acid (Scheme 13) (1961JA(83) 1764). An alternative synthesis involves 4-carboxythiazole (CA 162 590253 (2015), CA 62 90958 (1964)) or 4-cyanothiazole (CA 130



Reagents and Conditions: a) Polyphosphoric acid, heat. b) NaOCl. c) NaOH

**Scheme 13** Synthesis of thiabendazole.

110264 (1996), CA 121 57510 (1994)) as starting materials. A different approach to the synthesis of thiabendazole has been described starting from *N*-arylamidines; in the presence of sodium hypochlorite and a base, *N*-arylamidine hydrochlorides are transformed to benzimidazoles via formation of *N*-chloroamidine intermediate followed by ring closure in a stepwise or concerted mechanism (1965JOC(30)259).

### 6.1.3 Structure–Activity Relationships

The antifungal SARs of benzimidazoles have scarcely been described (1985UKZ(2)18) and mostly rely on the information available in the patent literature or in publications on mode of action/resistance studies. On the contrary, a vast literature is available on benzimidazoles as basic structure for active ingredients in the pharmaceutical and animal health industries, which is outside the scope of our chapter.

## 6.2 Thifluzamide

Thifluzamide (Figure 12) was discovered by Monsanto in the early 1990s (1992BCPC(PD1)427), but acquired by Rohm & Haas in 1994 and became part of the Dow portfolio, although in 2010 most uses were divested to Nissan. The product has been introduced in East Asian and Latin American countries for sheath blight control on rice; the major markets are Japan and Brazil (2015PMcD(weblink)). Thifluzamide possesses broad-spectrum fungicidal activity and has been registered in mixture formulations for rice nursery boxes in Japan in combinations with imidacloprid and carpropamid, and also imidacloprid and spinosad. It was introduced by Insecticides India as Pulsor in India in 2012. Thifluzamide belongs to the class of succinate dehydrogenase inhibitors (SDHI). Succinate dehydrogenase (Complex II or

succinate ubiquinoneoxidoreductase) is the smallest complex in the respiratory chain and transfers the electrons derived from succinate directly to the ubiquinone pool. Succinate dehydrogenase fungicides specifically inhibit fungal respiration by blocking the ubiquinone-binding sites in the mitochondrial complex II (2007MCPC(1st Ed, 2)496).

### 6.2.1 Discovery

The first SDHI fungicide was carboxin (1966SCI659), followed by oxycarboxin (CA 65 38564 (1966)), mepronil (CA 82 155895 (1975)), flutolanil (CA 96 137998 (1981)), and then thifluzamide (CA 96 137998 (1981)) (Figure 13). It is apparent that as this class evolved, the aromatic portions on each side of the amide bond were optimized. This class of fungicides is still of high interest, and since the discovery of thifluzamide, more potent, broad-spectrum fungicides have reached the market place (2007MCPC(1st Ed, 2)496).

### 6.2.2 Synthesis

The synthesis of thifluzamide is shown in Scheme 14 (CA 163 65941 (2015), CA 113 191337 (1990)). The key thiazole was prepared by chlorination of a  $\beta$ -keto ester and then treatment with thioacetamide to give the thiazole with complete regioselectivity.

### 6.2.3 Structure–Activity Relationships

The SARs of the thiazole carboxanilide fungicides is illustrated in Figure 14 (1993PS(38)1). It is apparent how this SAR, which is based on in vitro data,

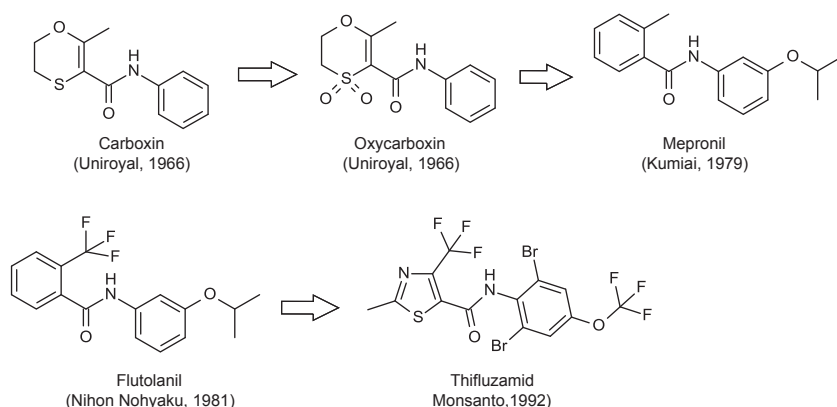
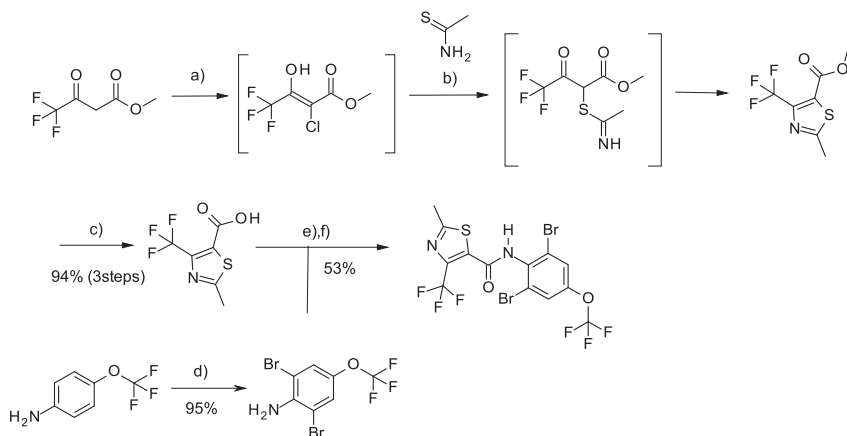
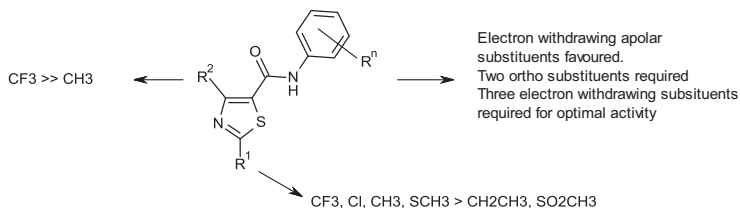


Figure 13 Discovery of thifluzamide.



**Reagents and Conditions:** a)  $\text{SOCl}_2$ , rt  $\rightarrow$   $-15^\circ\text{C}$ . b) EtOH, 12 h,  $15^\circ\text{C}$   $\rightarrow$  reflux. c) NaOH,  $\text{H}_2\text{O}$ , reflux. d) NaOAc,  $\text{Br}_2$ , AcOH,  $60^\circ\text{C}$ . e).  $\text{SOCl}_2$ , reflux. f) Xylene, reflux.

**Scheme 14** Synthesis of thifluzamide.



**Figure 14** Structure–activity relationships of thifluzamide.

led to thifluzamide as an optimum. The SDHI fungicides are still a very important class of fungicides and several new products have been introduced to the market (2014FCP(2nd Ed)88). The trifluoromethyl-substituted thiazole has been replaced in the newest SDHIs with a fluoroalkyl substituted pyrazole, and with a lipophilic anilide moiety, as illustrated in Figure 15 for sedaxane and penthiopyrad. This is a nice illustration of a thiazole functioning as an isosteric replacement of a pyrazole.

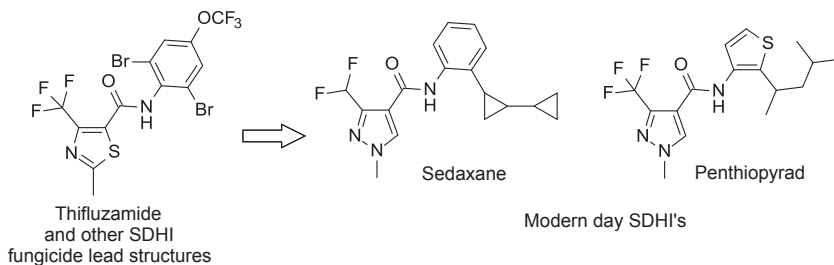


**Figure 15** Latest evolution of SDHI fungicides.

## 6.3 Ethaboxam

Ethaboxam (Figure 12) is an Oomycetes fungicide discovered by LGCI, Korea, in 1993 and controls various diseases caused by Oomycetes including potato late blight and grape downy mildew as well as other vegetable diseases (2015PMcD(weblink)).

### 6.3.1 Discovery

The benzamide fungicides were discovered at ICI (now Syngenta) in the late 1970s/early 1980s, as a result of speculative chemistry carried out in an attempt to make novel cyano imines (1992ACS(SS504)443). The products of trapping these imines with alcohols turned out to have interesting fungicidal and herbicidal activity. After a careful study of the SARs, highly active fungicides were found for the control of Oomycete fungi, and the compound 4-chloro-*N*-[cyano(ethoxy)methyl]benzamide (zarilamide) was chosen as a development candidate. Further evolution of the class (as shown in Figure 16) showed that the alkoxy group could be replaced by a heterocycle (thiophene), and further modifications of the phenyl group led eventually to ethaboxam. As with other compounds within this class, ethaboxam is a  $\beta$ -tubulin inhibitor, thus affecting fungal mitosis and cell division (2012MCPC(2nd Ed, 2)739).

### 6.3.2 Synthesis

The synthesis of ethaboxam is shown in Scheme 15. The key thiazole portion of the molecule is formed by Hantzsch synthesis (2004PMS(60)1007).

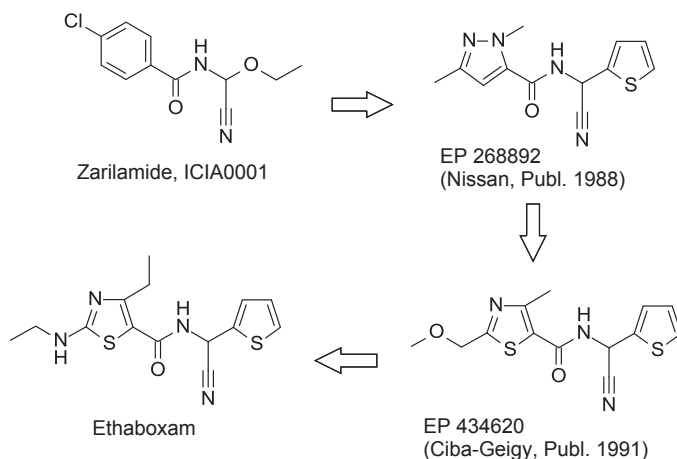
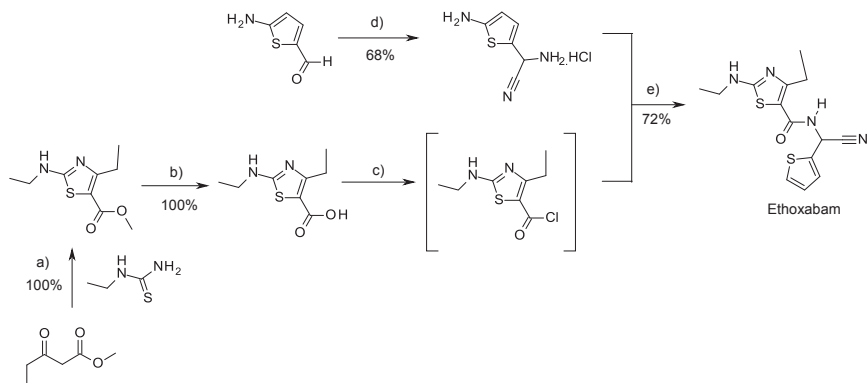


Figure 16 Discovery of ethaboxam.



**Reagents and Conditions:** a) MeOH, reflux. b) NaOH, MeOH, reflux. c) SOCl<sub>2</sub>, CH<sub>2</sub>Cl<sub>2</sub>, reflux. d) NH<sub>4</sub>Cl, NaCN, NH<sub>3</sub>(aq.), toluene, r.t. e) Pyridine, CH<sub>2</sub>Cl<sub>2</sub>, 10 °C.

**Scheme 15** Synthesis of ethoxabam.

### 6.3.3 Structure–Activity Relationships

The SAR of this class of fungicides is shown in [Figure 17 \(1992ACS\(SS504\) 443\)](#). Compounds where Ar<sub>2</sub> is thiophene and Ar<sub>1</sub> is thiazole and pyrazole possess the optimum fungicidal activity. Phytotoxicity was a problem with Ar<sub>1</sub> as pyrazole, but this could be circumvented with a thiazole groups as Ar<sub>1</sub>. Further optimization led to ethaboxam.

## 6.4 Benthiavalicarb

Benthiavalicarb ([Figure 12](#)) entered the oomycete disease control sector in 2004 following co-development by Kumiai and Bayer ([2003BCPC\(1\) 105](#)). Benthiavalicarb is a member of the amino acid amide carbamate group of fungicides, which includes iprovalicarb ([1998BCPC\(2\)367](#)) and valifenal ([CA 133 105348\(2000\)](#)), and is effective against all Oomycete fungal plant pathogens except *Pythium* spp. The mode of action of benthiavalicarb-isopropyl is to inhibit the incorporation of precursors required for phospholipid biosynthesis ([2012MCPC\(2nd Ed, 2\)651](#)).

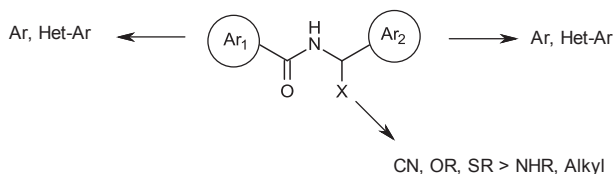


**Figure 17** Structure–activity relationships of ethaboxam and other benzamide fungicides.

### 6.4.1 Discovery

Benthiavalicarb was discovered by classical patent follow-up from iprovalicarb (Figure 18). Replacing the phenyl group by benzofuran led to active fungicides. Further derivatization resulted in the identification of benzothiazole as heterocyclic ring which had the optimal properties for further development (2010JPS(35)488).

### 6.4.2 Synthesis

The synthesis of benthiavalicarb is shown in Scheme 16 (2010N(9)174, 2015MCR(24)3660). The benzothiazole ring is generated by condensation of a 2-amino thiophenol with (4R)-4-methyloxazolidine-2,5-dione.

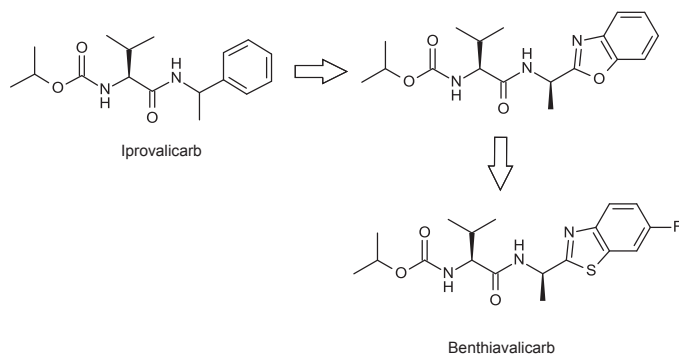
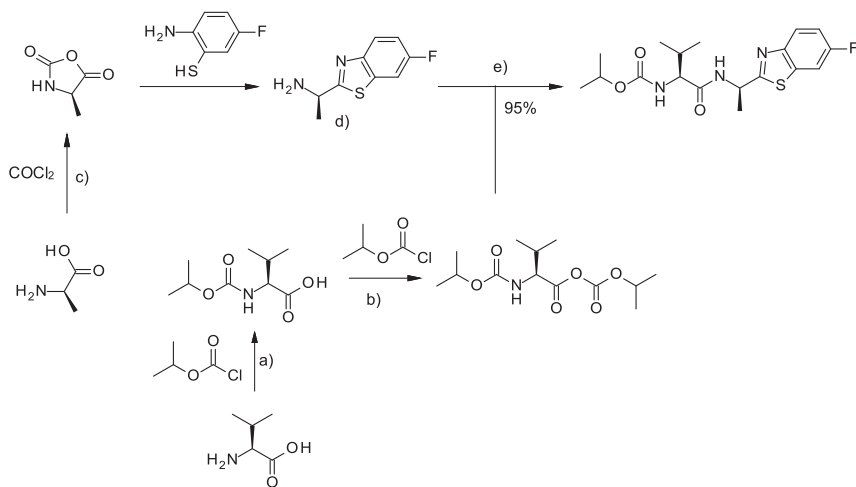
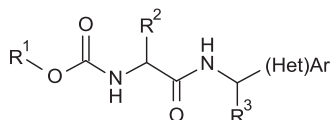


Figure 18 Discovery of benthiavalicarb.



**Reagents and Conditions:** a) 1) NaOH, H<sub>2</sub>O, b) rt → 0°C 2) HCl, H<sub>2</sub>O, pH 2. b) Et<sub>3</sub>N, Toluene, rt. c) THF, rt, d) HCl, H<sub>2</sub>O, THF, rt. e) Toluene, r.t.

Scheme 16 Synthesis of benthiavalicarb.



**Figure 19** General structure of amino acid amide carbamates.

### 6.4.3 Structure–Activity Relationships

The general structure of amino acid amide carbamates is shown in [Figure 19](#). Good activity is found when  $R^1$  is an  $\alpha$ -branched alkyl chain. Valine or isoleucine amino acids ( $R^2=i$ -Pr or *sec*-butyl) are the favored amino acid residues for fungicidal activity. Finally, the use of an  $\alpha$ -branched aryl or hetaryl ethyl amine ensures optimal activity ([2012MCPC\(2nd Ed, 2\)651](#)). It was found that the most active heteroaryl compounds were benzofuran and benzothiazole ([2010JPS\(35\)488](#)), the latter having a 6-fluoro substituent which is envisaged to improve the physical properties of the molecule to improve translocation.

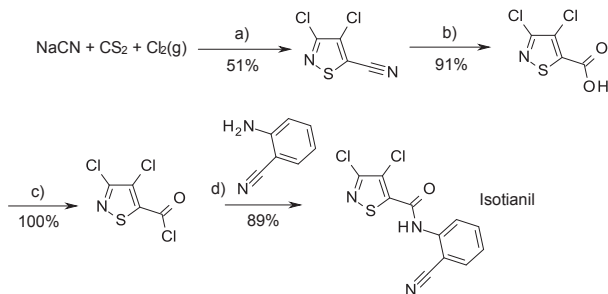
## 6.5 Isotianil

Isotianil ([Figure 12](#)) entered the rice blast control sector in 2010, having been co-developed by Bayer and Sumitomo Chemical ([2014ACS\(AGRO-744\)](#), [2011SUMR&DRep1](#)). It can be used as a seed treatment as well as in rice nursery boxes, reportedly at low application rates. Isotianil was first launched in Korea and Japan in 2010. In 2011, Nissan Chemical introduced the product in a mixture with imidacloprid, spinosad, and thifluzamide as SHARID™ in Japan for rice nursery box application. Commercial introduction in other major rice growing countries in Asia is expected to follow. Bayer is introducing isotianil in a mixture with cyantraniliprole as ROUTINE™ Duo Box GR ([2015PMcD\(weblink\)](#)).

### 6.5.1 Discovery

Isothiazoles are known to have a range of agrochemical activities, a fact that was apparent to chemists at Bayer CropScience ([2014ACS\(AGRO-744\)](#)). In what appears to be a chemistry-driven project starting from a cheap known building block, 3,4-dichloroisothiazole-5-carbonitrile ([Scheme 17](#)) ([CA 130 338103 \(1999\)](#), [1956CIL1232](#)), a comprehensive search for isothiazole-based compounds was undertaken, and from this program isotianil was discovered ([2011SUMR&DRep1](#)). The compound is





**Reagents and Conditions:** a) NaCN, CS<sub>2</sub>, Cl<sub>2</sub>, DMF, 60 °C. b) 45%NaOH in H<sub>2</sub>O, 40 °C. c) SOCl<sub>2</sub>, DMF (cat), reflux. d) Pyridine, 10 °C.

**Scheme 17** Synthesis of isotianil.

structurally related to tiadinil, and like tiadinil, probenazole, and acibenzolar-*S*-methyl (CA 146 121958 (2007)) activates defense responses against a wide range of additional pathogens. Moreover, isotianil does not show any direct antimicrobial activity against bacteria and fungi. Its efficiency against rice blast seems unusually high, as lower dosages of isotianil are needed than of any other existing plant defense activators mentioned earlier (2011SUMR&DRep1).

### 6.5.2 Synthesis

The synthesis of isotianil is shown in Scheme 17. The isothiazole ring is constructed from chlorine, CS<sub>2</sub>, and sodium cyanide (1956CIL1232, CA 146 121958 (2007)). Modern variants of this reaction have also been published (CA 160 559314 (2014), CA 153 600769 (2010)). With the nitrile isothiazole in hand, hydrolysis to the acid, followed by amide bond coupling yields isotianil in high yields (CA 130 338103 (1999)).

### 6.5.3 Structure–Activity Relationships

Isotianil does not show any fungicidal activity as such, as it is a synthetic plant defense elicitor, for which biological testing is much more complex. There are no studies on the SAR of this molecule. However, compared to the other plant activators probenazole, acibenzolar *S*-methyl, and tiadinil, isotianil has a relatively high logP and low water solubility, which is suggested to reduce loss of the active ingredient into the environment and thus allows a residual preventive effect (2011SUMR&DRep1).

## 6.6 Oxathiapiprolin

Oxathiapiprolin (Figure 12) is the first member of a new class of piperidinyl thiazole isoxazoline fungicides (2014ACS(AGRO-622)). It selectively controls plant pathogens of the Oomycete genus by inhibition of oxysterol-binding protein, a novel mode of action for the fungicide market (2014ACS(AGRO-911)). The compound shows excellent preventative, curative, and residual efficacy against key diseases of grapes, potatoes, and vegetables. Oxathiapiprolin is being developed globally as Zorvec™ with 2016 expected launches in China, Japan, Mexico, Colombia, Australia, Vietnam, and Argentina (2016BACC(weblink)).

### 6.6.1 Discovery

Modern agrochemical companies have various sources to obtain new lead compounds. These include biorational design, natural products, competitor patents and literature, and screening of external vendor libraries. The discovery of oxathiapiproline can be traced back to the last of these approaches. DuPont obtained a library of chemicals from an external vendor and observed that a compound showed up as a weak hit in their fungicidal assays (2016BMC(24)354, 2015ACS(SS1204)149). Furthermore, the hit provided optimal properties for optimization as the central orthogonally protected thiazole core could be derivatized in both directions. This is summarized in Figure 20.

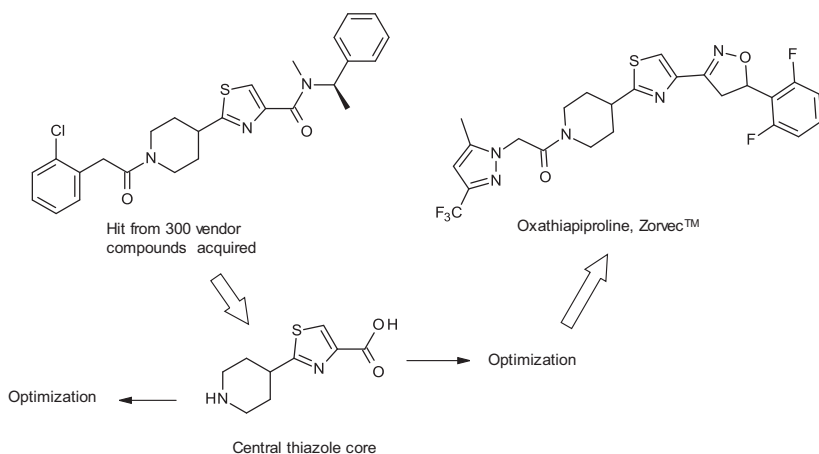


Figure 20 Discovery of oxathiapiprolin.

### 6.6.2 Synthesis

The key orthogonally protected thiazole building block for this optimization was synthesized by classical Hantzsch synthesis as shown in [Scheme 18](#). The acid functionality can be revealed by base hydrolyzes, and the resultant acid coupled to an amine by standard amide coupling. The tert-butyloxycarbonyl protecting group (BOC group) is cleaved under acid conditions to give the free piperidine, which is then reacted with an acid under standard amide coupling conditions to give the general lead structure. Alternatively, the BOC group of the orthogonally protected thiazole building block can first be cleaved, followed by amine coupling, ester hydrolysis, and amide formation to give the same lead structure ([2016BMC\(24\)354](#), [2015ACS\(SS1204\)149](#)). This chemistry is ideal to enable optimization of either the amide group  $R_3$ , keeping  $\text{CONR}_1R_2$  constant, or the amide moiety  $\text{CONR}_1R_2$ , keeping  $R_3$  constant.

A possible synthesis of oxathiapipronil is shown in [Scheme 19](#), where it can be seen that the thiazole amide moiety was eventually replaced by an amide bond isostere, an isoxazoline ([2016BMC\(24\)317](#)).

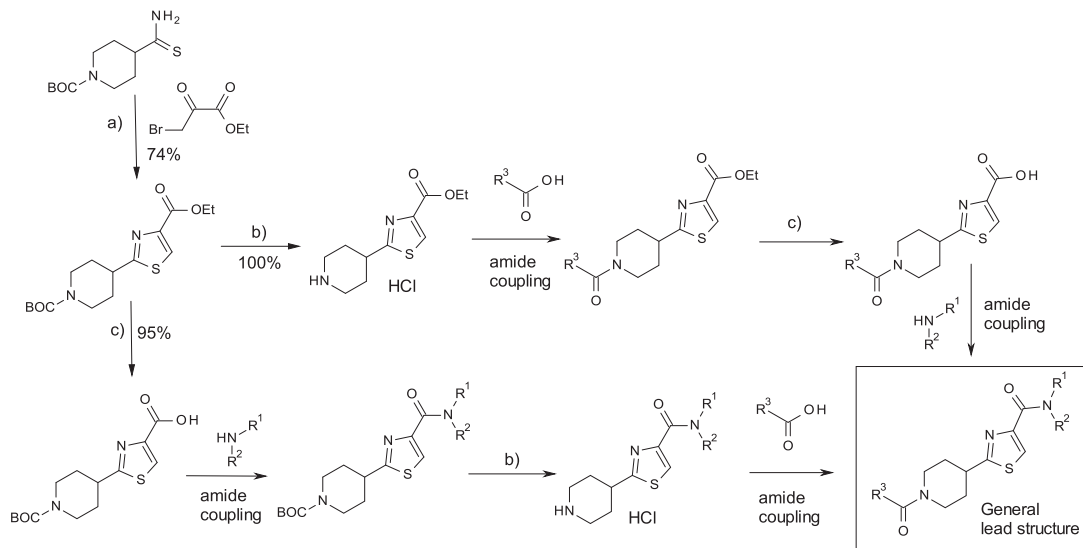
### 6.6.3 Structure–Activity Relationships

A detailed SAR analysis of oxathiapiprolin and its analogues has been published ([2016BMC\(24\)354](#), [2015ACS\(SS1204\)149](#)). Relevant to this article is the SAR of the thiazole central core. Keeping the left and right hand parts constant, and varying only the central thiazole core it was found that several other five-membered rings with similar exit vectors also led to highly active compounds, including isomeric thiazoles ([Figure 21](#)). If the exit vectors were changed, for example incorporating six-membered rings or alternatively substituted five-membered rings, this led to less active compounds. This illustrated the requirement for the correct geometry of the molecule. Although many highly active compounds were found that did not have a thiazole core, the decision to develop oxathiapiprolin over other similarly active compounds was due in part to the fact that it has not only excellent fungicidal activity, but also an excellent mammalian and environmental toxicity profile.



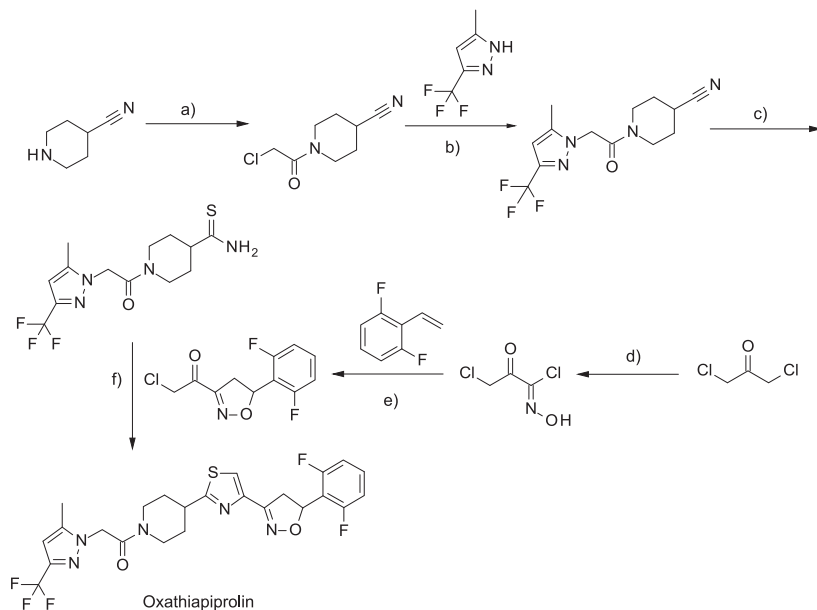
## 7. THIAZOLE- AND ISOTHIAZOLE-CONTAINING HERBICIDES

The global market for herbicides in 2014 was valued at \$26,440 million, equivalent to 41.8% of the total agrochemical market ([2015PMcD\(weblink\)](#)). The most important chemical classes are amino



**Reagents and conditions:** a). EtOH, 0°C →rt overnight. b) . HCl/Et<sub>2</sub>O, rt. c). NaOH, H<sub>2</sub>O/Dioxane, r.t.

**Scheme 18** Synthesis of general lead structure of oxathiapiprolin.



**Reagents and conditions:** a)  $\text{ClH}_2\text{CCOCl}$ ,  $\text{K}_2\text{CO}_3$ ,  $\text{CH}_2\text{Cl}_2$ ,  $-10^\circ\text{C}$ . b)  $\text{KOH}$ ,  $\text{H}_2\text{O}$ ,  $\text{DMF}$ ,  $5^\circ\text{C}$ . c)  $\text{H}_2\text{S}$ ,  $\text{NH}(\text{CH}_2\text{CH}_2\text{OH})_2$ ,  $\text{DMF}$ ,  $50^\circ\text{C}$ . d)  $t\text{-BuONO}$ ,  $\text{HCl}$ ,  $\text{Et}_2\text{O}$ ,  $\text{H}_2\text{O}$ ,  $15^\circ\text{C}$ . e)  $\text{NaHCO}_3$ ,  $\text{MeCN}$ , r.t. f)  $\text{NaBr}$ ,  $\text{Me}_2\text{CO}$ , reflux.

### Scheme 19 Synthesis of oxathiapiiprolin.

acids (mode of action: inhibition of 5-enolpyruvylshikimate-3-phosphate (EPSP) synthase/glutamine synthase; 23.8% of the total market), sulfonylureas (inhibition of acetolactate synthase (ALS); 8.7%), imidazolinones and other ALS inhibitors (inhibition of acetolactate synthase; 8.1%), acetamides (inhibition of cell division; 7.7%), PPO inhibitors (inhibition of protoporphyrinogen oxidase; 6.5%), HPPD inhibitors (inhibition of hydroxyphenyl pyruvate deoxygenase; 5.3%), pyridines (synthetic auxin action/microtubule assembly inhibition; 5.0%), and several other chemical classes having less than 5% market share each.

Two herbicides contain thiazole heterocycles, namely methabenzthiazuron and mefenacet. Currently no isothiazole-containing herbicide is on the market or thought to be in development. (Figure 22).

## 7.1 Methabenzthiazuron

Methabenzthiazuron (Figure 22) is a member of the urea group of herbicides (1.6% market share) and has the inhibition of photosynthesis at photosystem II as a mode of action. It was introduced by Bayer CropScience in 1968 and

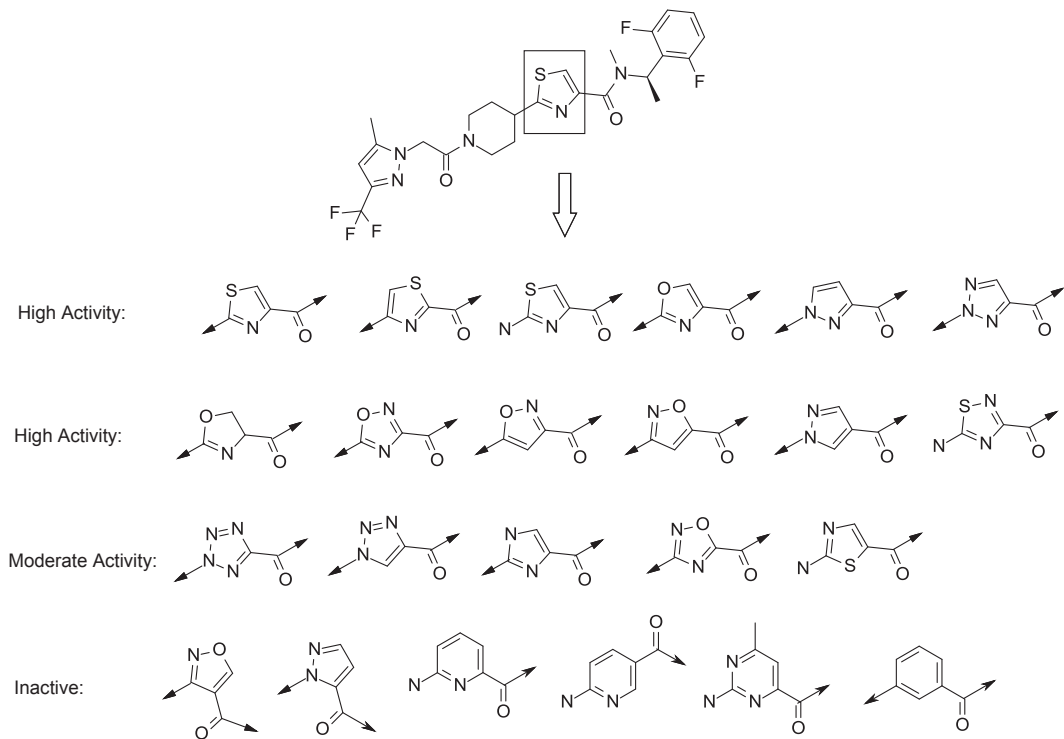


**Figure 21** Structure–activity relationships of the central thiazole core of oxathiapiprolone.

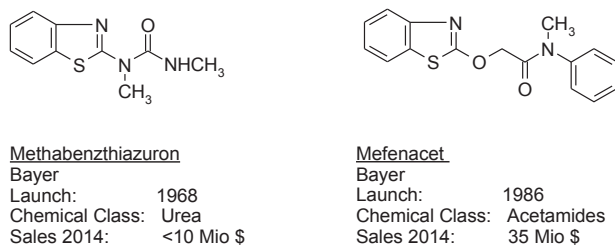


Figure 22 Thiazole-containing herbicides.

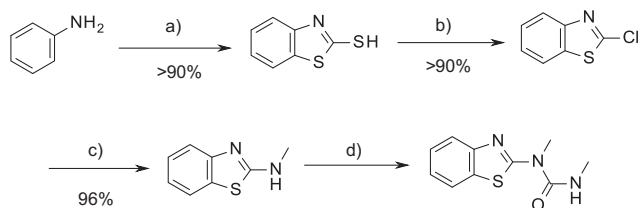
was used as a broadleaf weed herbicide in crops such as corn, vegetables, and in vineyards (1969BN(22)341). Methabenzthiazuron has since been withdrawn for use in Europe (2010BP(2009)26, 2014JES(26)757) and is only of limited commercial significance.

### 7.1.1 Discovery

The phenyl urea herbicides were discovered by the Grasselli Chemical Company (which later became DuPont) shortly after World War II in a random screening of chemicals to find compounds with herbicidal properties (1988SCSDuPont451). This work led to the discovery of monuron in 1951, followed by a whole series of other phenyl urea herbicides, including linuron, fenuron, and chloroxuron, among many others. It was not surprising that other ureas were discovered with substituents other than phenyl such as noruron (1967ICPP446) and of course methabenzthiazuron (1969BN(22)341).

### 7.1.2 Synthesis

The synthesis of methabenzthiazuron is shown in Scheme 20. The benzothiazole is synthesized by treatment of aniline with carbon disulfide and sulfur at high temperature and under high pressure (1996PSH42, 2002SS(11)835). Several patents have appeared recently regarding this process (CA 156 452144 (2012), CA 153 620652(2010), CA 149 203017(2007), CA



**Reagents and Conditions:** a) S, CS<sub>2</sub>, rt → 245°C, 7.5 MPa. b) SOCl<sub>2</sub>, rt. c) K<sub>2</sub>CO<sub>3</sub>, CuI, DMSO, 120°C. d) Methyl isocyanate

Scheme 20 Synthesis of methabenzthiazuron.

152 290557 (2010)). Introduction of the chlorine can be achieved by a variety of chlorinating agents, and copper catalysis is used to bring about methyl amine substitution (2013ASC(355)3263). Reaction with methyl isocyanate provides methabenzthiazuron.

### 7.1.3 Structure–Activity Relationships

The general structure of a phenylurea herbicide is (substituted) phenyl–NH–C(=O)–NHR<sub>2</sub>. The phenyl ring is often substituted with chlorine or bromine atoms, but methoxy, methyl, trifluoromethyl, or 2-propyl substitution also gives active compounds. Most phenyl ureas are *N*-dimethyl-phenyl-urea, but a combination of a methyl substituent and another group is also allowed. Substituents other than phenyl are known, such as heterocyclic aromatic ring systems and unsaturated bicyclic carbon ring systems (2011UP-SPA(weblink)). Methabenzthiazuron resulted from a successful bioisosteric replacement of the substituted phenyl moiety by benzothiazole.

## 7.2 Mefenacet

Mefenacet (Figure 22) is the first oxyacetamide herbicide which was developed by Bayer CropScience for the control of grass weeds in rice and introduced to the market in 1986 mainly for barnyard grass control in rice (1984MFLRG(49)1075). In 2014 mefenacet reached sales of \$35 million (2015PMcD(weblink)). This herbicide exerts its herbicidal activity by inhibition of cell division (inhibition of very-long-chain fatty acid synthesis) and as such belongs to the same class of herbicides as the chloroacetamides, such as metolachlor (2012MCPC(2nd Ed, 1)316).

### 7.2.1 Discovery

The discovery of mefenacet had an element of serendipity (2012MCPC(2nd Ed, 1)316). It began in 1976 when scientists from Bayer CropScience were carrying out patent follow-up on oxyacetamide phosphates (Figure 23) from Nihon Tokushu Nouyaku Seizo (now Bayer CropScience) (CA 87 67841(1977)). These phosphate compounds already showed good activity as herbicides along with rice selectivity. The first stage of the modifications

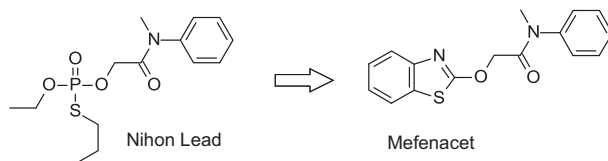
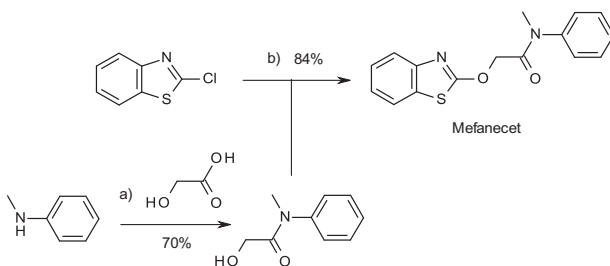


Figure 23 Discovery of mefenacet.





**Reagents and Conditions:** a) H<sub>2</sub>O, 175°C b) 45% aq. NaOH.

**Scheme 21** Synthesis of mefenacet.

included replacement of the phosphate group with various sulfur-containing heterocycles. The heterocycle chosen for development was the benzothiazole, which had the optimal properties to make it one of the leading paddy rice herbicides over the last three decades.

### 7.2.2 Synthesis

The synthesis of mefenacet utilizes the same 2-chlorobenzothiazole used in the synthesis of methabenzthiazuron (Scheme 21, see also Scheme 20). This is reacted with 2-hydroxy-*N*-methyl-*N*-phenyl-acetamide in 45% aqueous sodium hydroxide (CA 126 157288(1997)). The former is obtained by reaction of an aqueous solution of glycolic acid with *N*-methyl-aniline at 175 °C with simultaneous removal of water (CA 97 127633(1982)) (1985US4509971).

### 7.2.3 Structure–Activity Relationships

Mefenacet shows excellent activity as a paddy rice herbicide against barnyard grass (*Echinochloa crus-galli*), as well as on other grasses such as *Cyperus difformis* and *Scirpus juncooides* (1995BCPC(1)43). It also has activity on some broad-leaved weeds (*Monochoria vaginalis* and *Lindernia pyxidaria*). In parallel with the development of mefenacet, Bayer CropScience was nevertheless interested in further exploring the potential of the oxyacetamide class for use in dry rice planting areas, as well as exploring potential of the class in other crops. It was found that monocyclic rings were superior to the bicyclic heterocyclic ring in terms of herbicidal activity, and the CF<sub>3</sub> substituted thiadiazole ring gave the best activity (Figure 24). The anilide moiety was important for both selectivity and herbicidal activity, and it was found that the combination of an isopropyl anilide with a 4-F substituent gave overall the best herbicidal activity and crop tolerance (2012MCPC(2nd Ed, 1)316). In this way fufenacet was discovered (Figure 24) (1995BCPC(1)43).

Thus, while mefenacet is principally used in paddy rice at rates of 1–1.2 kg/ha, flufenacet is used as a selective herbicide in corn, cereals,

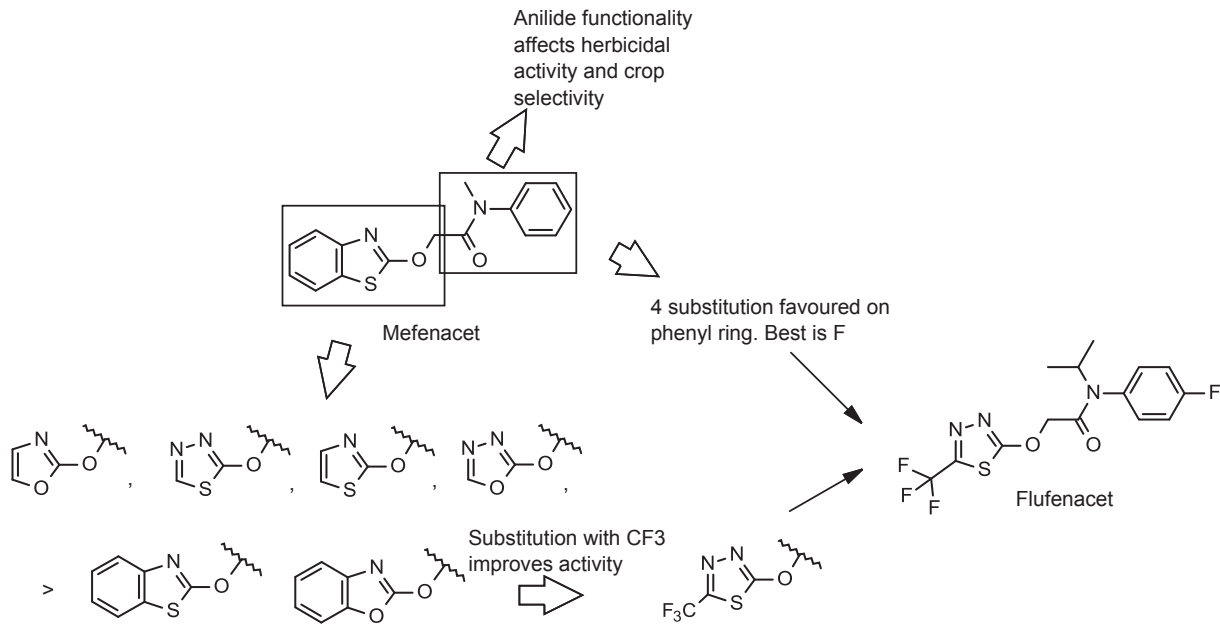


Figure 24 Structure–activity relationships in mefenacet.

soybeans, cotton, and sunflower to control grass and broadleaf weeds at rates of only 125–250 g/ha (2012MCPC(2nd Ed, 1)316).

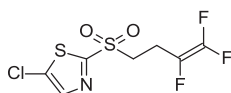
As shown by the SARs of mefenacet, the benzoxazole heterocycle is a valuable bioisosteric replacement of the benzothiazoles ring, as well as some aromatic five-ring heterocycles such as oxazole, thiadiazole, thiazole, and oxadiazole.

## 8. THIAZOLE- AND ISOTHIAZOLE-CONTAINING NEMATICIDES

The global market for nematicides is valued at \$1.110 billion in 2014 and estimated to strongly grow over the next years to reach \$1.350 billion by 2020 (2015MM(weblink)). Two types of chemical products are used to manage nematodes, namely soil fumigants and nonfumigant (or contact) nematicides, both of which can provide an excellent control of plant-parasitic nematodes. The most important chemical classes are the carbamates, organophosphates, and mectins, with Abamectin (trade name: Avicta<sup>®</sup>) being the leading product (2012MCPC(2nd Ed, 3)1367). A thiazole ring is present in only two compounds, the recently launched nematicide fluensulfone and the former development compound benclonthiaz (Figure 26).

### 8.1 Fluensulfone

Fluensulfone (product name Nimitz<sup>®</sup>) (Figure 25) offers a new mode of action for control of a range of plant-parasitic nematodes and belongs to the chemical class of the fluoroalkenyl sulfones (2012MCPC(2nd Ed, 3)1367). It causes irreversible nematicidal activity resulting in pest mortality within 1–2 days by paralysis leading to cessation of feeding, whilst also affecting eggs, impacting laying, hatching, and development. The mode of action remains unknown, although it has been postulated that it may be related to the inhibition of medium-chain acyl-coenzyme A dehydrogenases (2014PBP(109)44, 2004C(58)108, 2013PMS(69)1225).

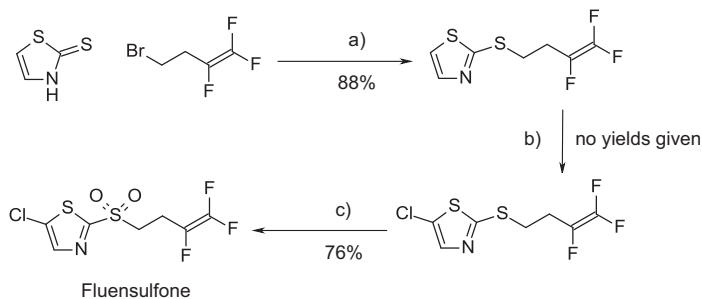


**Fluensulfone**  
Adama  
Launch: 2014  
Chemical Class: Fluoroalkenyl sulfone



**Benclonthiaz**  
Chemical Class: Benzisothiazole  
Development discontinued

**Figure 25** Thiazole- and isothiazole-containing nematicides.



**Reagents and conditions:** a)  $\text{K}_2\text{CO}_3$ ,  $\text{CH}_3\text{CN}$ , reflux, b) 1.2 eq. NCS,  $\text{CCl}_4$ ,  $\Delta$ , c) 3 eq. 31% aq.  $\text{H}_2\text{O}_2$ , AcOH,  $60^\circ\text{C}$ .

**Scheme 22** Synthesis of fluensulfone.

### 8.1.1 Discovery

Fluensulfone was discovered in 2001 by Nihon Bayer (2001CA(134)100860), started being developed by Makhteshim Agan (now Adama) in 2008 and entered the US and Canadian markets in 2014.

### 8.1.2 Synthesis

Fluensulfone can be synthesized from 2-mercaptothiazole and 4-bromo-1,1,2-trifluorobutene in only a few steps from easily accessible starting materials as shown in Scheme 22 (2016BMC(24)317).

### 8.1.3 Structure—Activity Relationships

From the general structure—activity profile for fluoroalkenyl sulfone nematocides it can be concluded that a trifluorovinyl or a difluorovinyl moiety is required for good activity, sulfide, sulfoxide, and sulfone can be used as tethers, and that many variations of the heterocyclic ring are tolerated (2012MCPC(2nd Ed, 3)1367). In the patent literature many compounds containing five- or six-membered aromatic and nonaromatic heterocycles different from thiazole are described to exhibit nematocidal activity (Figure 26). This includes the classical bioisosteric thiazole replacements oxazole and pyridine and other heterocycles being derived from further bivalent or trivalent atom replacements.

## 8.2 Benclonthiaz

Benclonthiaz (Figure 25) (2012MCPC(2nd Ed, 3)1367) belongs to the chemical class of the benzisothiazoles and is highly active against the southern root knot nematode (*Meloidogyne incognita*) and the soybean cyst nematode (*Heterodera glycines*). As yet, the mode of action of benclonthiaz remains unknown.

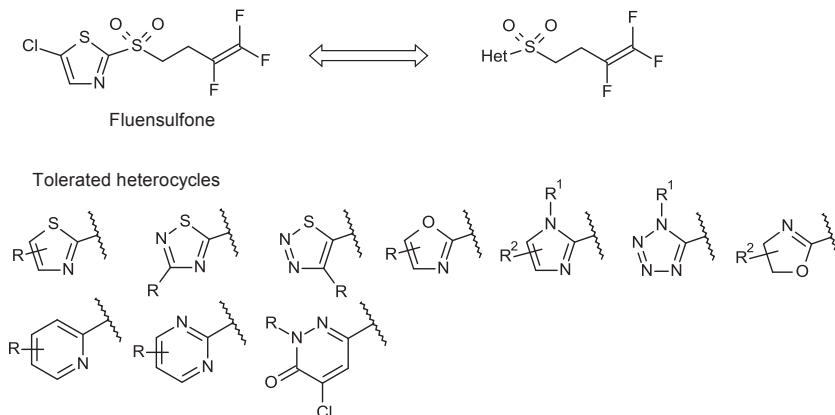


**Figure 26** Structure–activity relationships of fluensulfone.

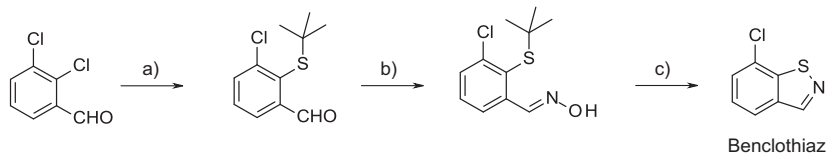
In 2002, Syngenta applied for an ISO common name for benclotiaz (developmental code CGA 235860, IUPAC name: 7-chloro-1,2-benzothiazole); however, it has later terminated further development of this compound. Further evaluation and development work were performed by Mitsubishi Chemical Corp. and Sumitomo Seika Chemicals Co., Ltd., in 2002 and 2006, which resulted in additional process patent applications (CA 136 183810 (2002), CA 145 8157 (2006), CA 116 106280 (1991)). No further reports on benclotiaz have been published in recent years and considerable data gaps regarding its environmental fate and its toxicity still exist. Consequently registration has not been approved for use in most of the developed world and benclotiaz can be regarded as an obsolete nematicide.

### 8.2.1 Discovery

The nematicidal activity of benzisothiazoles was discovered by Ciba-Geigy (now Syngenta) in 1991 (CA 116 106280 (1991)). Among a series of substituted benzisothiazoles described in the scope of this patent application benclotiaz was found to give the best overall nematicidal activity. Benclotiaz was first synthesized in 1963 by Ricci et al., as part of a program to investigate synthetic methodologies for the preparation of benzisothiazoles (1963AC(R)(53)1860).

### 8.2.2 Synthesis

Benclotiaz is prepared in three steps from commercially available 2,3-dichlorobenzaldehyde (Scheme 23) (2012MCPC(2nd Ed, 3)1367, CA 123 83358 (1995)). The key cyclization reaction of 2-mercapto-benzaldehyde oxime to afford the benzisothiazole was achieved in *n*-propanol as



**Reagents and conditions:** a) *t*-BuSH, K<sub>2</sub>CO<sub>3</sub>, DMF, b) NH<sub>2</sub>OH, *n*-PrOH, c) 0.05 eq. PPTS, *n*-PrOH, 90%.

**Scheme 23** Synthesis of benclotiaz.

solvent in the presence of a catalytic amount of pyridine *p*-toluenesulfonic acid (PPTS). Applying these mild reaction conditions gave yields in excess of 90% and delivered much better results compared to the standard conditions which involve the use of a large excess of strong acid and consequently in a difficult work-up procedure.

### 8.2.3 Structure–Activity Relationships

To date no information has been disclosed on SARs of benzisothiazole nematocides. However, it appears that the benzisothiazole heterocycles are required for good activity and that not many modifications are tolerated (2012MCPC(2nd Ed, 3)1367).

## 9. CONCLUSIONS

Eleven commercial agrochemicals as well as two development compounds contain thiazole or isothiazole heterocycles. A thiazole moiety is present in seven currently marketed agrochemicals, namely the insecticides thiamethoxam and clothianidin, the fungicides thiabendazole, thifluzamide, ethaboxam, and oxathiapiprolin, and the nematocide fluensulfone, as well as in the development compound dicloromezotiaz. One compound, the fungicide isotianil, contains an isothiazole ring and three compounds a benzothiazole ring, namely the fungicide bentiavalicarb and the herbicides methabenzthiazuron and mefenacet. A benzisothiazole ring is not yet present in any commercial product, however, is found in the former nematocide development compound benclotiaz.

The thiazole ring can successfully be applied as bioisosteric replacements of the heterocycles pyridine, thiophene, oxazole, imidazole, and others, as well as of many functional groups such as amide, thioamide, and even ester. Many such bioisosteric replacements were instrumental in the discovery of crop protection products. The isothiazole ring can serve as a bioisosteric

replacement of pyridine, thiophene, isoxazole, pyrazole, and the functional groups amide, thioamide, and esters; however, these replacements have only been rarely applied in crop protection research.

Although the value of the thiazole and isothiazole moiety as bioisosteric replacements is well documented in crop protection research and highlighted herein, it appears that there is still much scope to explore these (benz)thiazoles and (benz)isothiazoles as bioisosteric replacements in many areas of agrochemical research. It is hoped that some of the data presented here will inspire scientists to think of employing such heterocycles in their design of agrochemicals of the future.

## REFERENCES

- 1945OS(V3)332  
1949JCS1064  
1956CIL1232  
1961JA(83)1764  
1963AC(R)(53)1860  
1964ID(42)479  
1964PP(13)163  
1965JOC(30)259  
1966SCI659  
1967ICPP446  
1968PHYT(58)860  
1969BN(22)341  
1969T(25)389  
1970TL1381  
1973JCS(CC)524  
1973JCS(PT1OBOC4)356  
1978JOC(43)3736  
1978S(1)58  
1979JPR(321)643  
1981PMC(18)117  
1982CL1225  
1982PS(12)357  
G. Schwarz, *Org. Synth. Coll.*, **3**, 332 (1945).  
A.H. Cook, I. Heilbron, S.F. MacDonald, and A.P. Mahadevan, *J. Chem. Soc.*, 1064 (1949).  
A. Adams and R. Slack, *Chem. Ind.*, 1232 (1956).  
H.D. Brown, A.R. Matzuk, I.R. Ilves, L.H. Peterson, S.A. Harris, and L.H. Sarett, *J. Am. Chem. Soc.*, **83**, 1764 (1961).  
A. Ricci, A. Martani, O. Graziani, and M.L. Oliva, *Ann. Chim. (Rome)*, **53**, 1963 (1860).  
H.J. Robinson, H.C. Stoerk, and O.E.J. Graessle, *Invest. Dermatol.*, **42**, 479 (1964).  
T. Staron and C. Allard, *Phytriatri. Phytopharm.*, **13**, 163 (1964).  
V.J. Grenda, R.E. Jones, G. Gal, and M. Sletzing, *J. Org. Chem.*, **30**, 259 (1965).  
B. Von Schmeling and M. Kulka, *Science*, **659** (1966).  
A. Fischer, *Abstr. Int. Congr. Plant Prot.*, **446** (1967).  
D.D. Erwin, J.J. Sims, and J.J. Partridge, *Phytopathology*, **58**, 860 (1968).  
H. Hack, *Pflanz. Nachr. Bayer (Engl. Ed.)*, **22**, 341 (1969).  
D.N. McGregor, U. Corbin, J.E. Swigor, and L.C. Cheney, *Tetrahedron*, **25**, 389 (1969).  
J.E. Franz and L.L. Black, *Tetrahedron Lett.*, 1381 (1970).  
R.K. Howe and J.E. Franz, *J. Chem. Soc. Chem. Commun.*, 524 (1973).  
K. Clarke, C.G. Hughes, and R.M. Scrowston, *J. Chem. Soc. Perkin. Trans. 1 Org. Bio-Org. Chem.*, **4**, 356 (1973).  
R.K. Howe, T.A. Gruner, L.G. Carter, L.L. Black, and J.E. Franz, *J. Org. Chem.*, **43**, 3736 (1978).  
O. Meth-Cohn and B. Tarnowski, *Synthesis*, **1**, 58 (1978).  
K. Dolling, H. Zschke, and H. Schubert, *J. Prakt. Chem.*, **321**, 643 (1979).  
A. De, *Progress Med. Chem.*, **18**, 117 (1981).  
K. Yamamoto and H. Watanabe, *Chem. Lett.*, **1225** (1982).  
A.J. Lawson, *Phosp. Sulf. Rel. Elem.*, **12**, 357 (1982).

- 1984BMAP382 J.R. Corbett, In K. Wright and A.C. Baillie, editors: *The Biochemical Mode of Action of Pesticides*, Academic Press: New York (1984), p 382.
- 1984MFLRG(49)1075 R.R. Schmidt, *Meded. Fac. Landbouwwet. Rijksuniv. Gent*, **49**, 1075 (1984).
- 1985UKZ(2)18 L.A. Tyurina and C.S. Kadyrov, *Uzbekskii Khimicheskii Zhurnal*, **2**, 18 (1985).
- 1985US4509971 H. Forster, W. Hofer, V. Volker Mues, and R.R. Schmidt, *US Patent Application, US 4509971*.
- 1986ARP24 L.C. Davidse, *Ann. Rev. Phytopathol.*, **24** (1986).
- 1988CJC(66)1405 D.M. McKinnon and K.R. Lee, *Can. J. Chem.*, **66**, 1405 (1988).
- 1988SCSDuPont451 D.A. Hounshell and J.K. Smith, *Science and Corporate Strategy: Du Pont R and D 1902–1980*, Cambridge University Press (1988), p 451.
- 1989H(29)97 F. Lucchesini, N. Picci, M. Pocci, A. De Munno, and V. Bertini, *Heterocycles*, **29**, 97 (1989).
- 1990JMC(33)2715 T. Rosen, A.A. Nagel, J.P. Rizzi, J.L. Ives, J.B. Daffeh, A.H. Ganong, K. Guarino, J. Heym, S. McLean, J.T. Nowakowski, A.W. Schmidt, T.F. Seeger, C.J. Siok, and L.A. Vincent, *J. Med. Chem.*, **33**, 2715 (1990).
- 1991PDR(37)287 A. Burger, *Prog. Drug Res.*, **37**, 287 (1991).
- 1992ACS(SS504)443 D. Bartholomew, P.J. Crowley, and T. Kay, In *ACS Symposium Series, Synthesis and Chemistry of Agrochemicals IV*, **Vol. 504**, p 443.
- 1992BCPC(PD1)427 P. O'Reilly, S. Kobayashi, S. Yamane, W. Phillips, P. Raymond, and B. Castanho, *Br. Crop. Prot. Conf. Pest Dis.*, **1**, 427 (1992).
- 1993PS(38)1 W.G. Phillips and M. Rejda-Heath, *Pestic. Sci.*, **38**, 1 (1993).
- 1993TL(34)6525 D.M. Fink and J.T. Strupczewski, *Tetrahedron Lett.*, **34**, 6525 (1993).
- 1995ACS(SS584)15 T. Koyanagi and T. Haga, In *ACS Symposium Series, Synthesis and Chemistry of Agrochemicals IV*, **Vol. 584**, p 15.
- 1995BCPC(1)43 R. Deege, H. Foester, R.R. Schmidt, W. Thielert, A.M. Tice, G.J. Agesen, J.R. Bloomberg, and H.J. Santel, In *Brighton Crop Protection Conference—Weeds*, **Vol. 1**, p 43.
- 1995JHC(32)1683 L.E. Brieady and K.H. Donaldson, *J. Heterocycl. Chem.*, **32**, 1683 (1995).
- 1995MSF305 L.C. Davidse and H. Ishi, In H. Lyr and H. Gustav, editors: *Modern Selective Fungicides*, Fischer Verlag (1995), p 305.
- 1996PSH42 T.A. Unger, *Pesticide Synthesis Handbook*, Noyes Publications: New Jersey (1996), p 42.
- 1998BCPC(2)367 K. Stenzel, *Proc. Br. Crop Prot. Conf. Pests Dis.*, **2**, 367 (1998).
- 1999PS1999 T. Gobel, L. Gsell, O.F. Huter, P. Maienfisch, R. Naef, A.C. O'Sullivan, T. Pitterna, T. Rapold, G. Seifert, and M. Senn, et al., *Pestic. Sci.*, 355 (1999).
- 2000TL(41)1707 T. Bach and S. Heuser, *Tetrahedron Lett.*, **41**, 1707 (2000).
- 2000TL(41)7187 P. Maienfisch, H. Huerlimann, and J. Haettenschwiler, *Tetrahedron Lett.*, **41**, 7187–7191 (2000).
- 2001CA(134)100860 Y. Watanabe, K. Ishikawa, Y. Otsu, and K. Shibuya, In *PCT Int. Appl., WO 2001/02378, 2001 (Nihon Bayer Agrochem K.K.)*, *Chem. Abstr.* **Vol. 134**, p 100860.



- 2001CODDD(4)471  
2001JOM(66)7925  
2001PMS(57)165  
2001PMS(57)906  
2001SCM10  
2002SS(11)507  
2002SS(11)835  
2003BCPC(1)105  
2003CH(2ndEd)162  
2003JA(125)1700  
2003JNP(66)1022  
2003PNB(56)5  
2003TL(44)6073  
2004BMC(38)320  
2004C(58)108  
2004CC446  
2004CUZ(38)320  
2004PMS(60)1007  
2004PMS(60)945  
2004PMS(60)959  
2005H(65)2119  
2005JHC(42)1001  
2006JHC(43)1609  
2006SK20  
2006ZN(B61)353  
2007MCPC(1st Ed, 2)496
- P.H. Olesen, *Curr. Opin. Drug Discovery Dev.*, **4**, 471 (2001).  
A.A. Kiryanov, P. Sampson, and A.J. Seed, *J. Org. Chem.*, **66**, 7925 (2001).  
P. Maienfisch, H. Huerlimann, A. Rindlisbacher, L. Gsell, H. Dettwiler, J. Haettenschwiler, E. Sieger, and M. Walti, *Pest Manag. Sci.*, **57**, 165 (2001).  
P. Maienfisch, M. Angst, F. Brandl, W. Fischer, D. Hofer, H. Kayser, W. Kobel, A. Rindlisbacher, R. Senn, A. Steinemann, and H. Widmer, *Pest Manag. Sci.*, **57**, 906 (2001).  
I. Grayson, *Specialty Chemicals Magazine*, p 10.  
D.W. Brown and M. Sainsbury, *Sci. Synth.*, **11**, 507 (2002).  
H. Ullrich, *Sci. Synth.*, **11**, 835 (2002).  
Y. Miyake, J. Saiki, I. Miura, and K. Nagayam, In *Proc. Br. Crop Prot. Conf Int. Congr. Glasgow*, **Vol. 1**, p 105.  
T. Eicher and S. Hauptmann, *The Chemistry of Heterocycles*, 2nd Ed., Wiley: Germany (2003), p 162.  
A. Mori, A. Sekiguchi, K. Masui, T. Shimada, M. Horie, K. Osakada, M. Kawamoto, and T. Ikeda, *J. Am. Chem. Soc.*, **125**, 1700 (2003).  
D.J. Newman, G.M. Cragg, and K.M. Snader, *J. Nat. Prod.*, **66**, 1022e1037 (2003).  
P. Jeschke, H. Uneme, J. Benet-Buchholz, J. Stoelting, W. Sirges, M.E. Beck, and W. Etzel, *Pflanz. Nachr. Bayer (Engl. Ed.)*, **56**, 5 (2003).  
C. Benedí, F. Bravo, P. Uriz, E. Fernández, C. Claver, and S. Castellón, *Tetrahedron Lett.*, **44**, 6073 (2003).  
N.A. Colabufo, M. Contino, M. Cantore, E. Capparelli, M.G. Perrone, G. Cassano, G. Gasparre, M. Leopoldo, F. Berardi, and R. Perrone, *Bioorg. Med. Chem.*, **21**, 1324 (2013).  
T. Pitterna, M. Böger, and P. Maienfisch, *Chimia*, **58**, 108 (2004).  
L.L. Joyce, G. Evindar, and R.A. Batey, *Chem. Commun.*, 446 (2004).  
C.D. Siebert, *Chem. Unserer Zeit*, **38**, 320 (2004).  
D.S. Kim, S.J. Chun, J.J. Jeon, S.W. Lee, and G.H. Joe, *Pest Manag. Sci.*, **60**, 1007 (2004).  
H. Kayser, C. Lee, A. Decock, M. Baur, J. Haettenschwiler, and P. Maienfisch, *Pest Manag. Sci.*, **60**, 945 (2004).  
H. Wellmann, M. Gomes, C. Lee, and H. Kayser, *Pest Manag. Sci.*, **60**, 959 (2004).  
S. Kamila, H. Zhang, and E.R. Biehl, *Heterocycles*, **65**, 2119 (2005).  
Z.-X. Wang and H.-L. Qin, *J. Heterocycl. Chem.*, **42**, 1001 (2005).  
S. Kamila, B. Koh, and E.R. Biehl, *J. Heterocycl. Chem.*, **43**, 1609 (2006).  
H. Uneme, M. Konobe, A. Akayama, T. Yokota, and K. Mizuta, *Sumitomo Kagaku (Osaka Jpn.)*, **20** (2006).  
P. Maienfisch, *Z. Naturforsch. B Chem. Sci.*, **61**, 353 (2006).  
J. Rheinheimer, In W. Krämer and U. Schirmer, editors: *Modern Crop Protection Compounds*, **Vol 2**, Wiley-VCH: Weinheim, Germany (2007), p 496.

- 2007OL(9)3687  
2007S819  
2007THC(9)179
- 2008ANK(36)14389  
2009AGE(48)4222
- 2009IJPSD(1)136  
2009JOC(74)8988
- 2009OC(74)8719
- 2009OL(11)2039
- 2009SC(39)860
- 2010BP(2009)26
- 2010JPS(35)488
- 2010N(9)174
- 2010OL(12)752  
2010SC(40)206  
2010TL(51)5009
- 2011CJC(29)1880
- 2011IJDDR(3)55  
2011JA(133)6403
- 2011JAF(59)2931  
2011PCh(1)523
- 2011PHARM(1)272
- 2011PHC(22)259
- 2011SUMR&DRep1
- 2011UP-SPA(webblink)
- 2012CB(9)2442
- T. Itoh and T. Mase, *Org. Lett.*, **9**, 3687 (2007).  
D.S. Bose, M. Idrees, and B. Srikanth, *Synthesis*, **819** (2007).  
F. Clerici, M.L. Gelmi, S. Pellegrino, and D. Pocar, In *Topics in Heterocyclic Chemistry*, Bioactive Heterocycles III, **Vol. 9**, p 179.  
X. Sun and J. Zhou, *Anhui Nongye Kexue*, **36**, 14389 (2008).  
D. Ma, S. Xie, P. Xue, X. Zhang, J. Dong, and Y. Jiang, *Angew. Chem. Int. Ed.*, **48**, 4222 (2009).  
N. Siddiqui, *Int. J. Pharm. Sci. Drug Res.*, **1**, 136 (2009).  
J.F. Sanz-Cervera, R. Blasco, J. Piera, M. Cynamon, I. Ibáñez, M. Murguía, and S. Fustero, *J. Org. Chem.*, **74**, 8988 (2009).  
P. Saha, T. Ramana, N. Purkait, A.M. Ashif, R. Paul, and T.J. Punniyamurthy, *Org. Chem.*, **74**, 8719 (2009).  
A.J. Blacker, M.M. Farah, M.I. Hall, S.P. Marsden, O. Saidi, and J.M. Williams, *J. Org. Lett.*, **11**, 2039 (2009).  
H. Sharghi and O. Asemani, *Synth. Commun*, **39**(860), 2009 (2009).  
P. Brandt, *Berichte Zu Pflanzenschutzmitteln 2009: Wirkstoffe in Pflanzenschutzmitteln; Zulassungshistorie und Regelungen der Pflanzenschutz-Anwendungsverordnung*, Springer (2010), p 26.  
J. Sakai, I. Miura, M. Shibata, N. Yonekura, H. Hiyoshi, M. Takagaki, and K. Nagayama, *J. Pestic. Sci.*, **35**, 488 (2010).  
F. Yang, D. Liao, W. Shi, S. Liu, and M. Du, *Nongyao*, **9**, 174 (2010).  
N.O. Devarie-Baez and M. Xian, *Org. Lett.*, **12**, 752 (2010).  
S.S. Patil and V.D. Bobade, *Synth. Commun.*, **40**, 206 (2010).  
E.A. Jaseer, D.J.C. Prasad, A. Dandapat, and G. Sekar, *Tetrahedron Lett.*, **51**, 5009 (2010).  
L. Cai, X. Ji, Z. Yao, F. Xu, and Q. Shen, *Chin. J. Chem.*, **29**, 2011 (1880).  
N. Siddiqui, *Int. J. Drug Dev. Res.*, **3**, 55 (2011).  
Z. Zhang, G.M. Lindale, and L.S. Liebeskind, *J. Am. Chem. Soc.*, **133**, 6403 (2011).  
H. Uneme, *J. Agric. Food Chem.*, **59**, 2932 (2011).  
A. Zagade and G.P. Senthilkumar, *Pharma Chem.*, **3**, 523 (2011).  
R. Bhatia, V. Sharma, B. Shrivastava, and R.K. Singla, *Pharmacologyonline*, **1**, 272–299 (2011).  
Y.-J. Wu and V.Y.B.V. Yang, *Prog. Heterocycl. Chem.*, **22**, 259 (2011) (Thiazole and Isothiazole).  
M. Ogawa, K. Kadowaki, and O. Kadooka, *Sumitomo Kagaku, R&D Report*, 1–16 (May 31, 2011). Retrieved from the Internet: URL:[http://www.sumitomo-chem.co.jp/english/rd/report/theses/docs/2011-1E\\_01.pdf](http://www.sumitomo-chem.co.jp/english/rd/report/theses/docs/2011-1E_01.pdf).  
S. Morais, M. Correia, V. Domingues, and C. Delerue-Matos, In M. Stoytcheva, editor: *Urea Pesticides, Pesticides – Strategies for Pesticides Analysis*, ISBN 978-953-307-460-3. Available from: <http://www.intechopen.com/books/pesticides-strategies-for-pesticides-analysis/ureapesticides>.  
U. Yngvea, P. Şçdermana, M. Svenssona, S. Rosqvist, and P.I. Arvidsson, *Chem. Biodiversity*, **9**, 2442 (2012).

- 2012COC(16)789 R. Sakhuja, S.S. Panda, and K. Bajaj, *Curr. Org. Chem.*, **16**, 789 (2012).
- 2012JMC(55)2301 U.J.Y. Hwang, R.R. Attia, F. Zhu, L. Yang, A. Lemoff, C. Jeffries, M.C. Connelly, and R.K. Guy, *J. Med. Chem.*, **55**, 2301 (2012).
- 2012MCPC(2nd Ed, 1)316 Y. Watanabe, In 2nd Ed., In W. Krämer, U. Schirmer, P. Jeschke, and M. Witschel, editors: *Modern Crop Protection Compounds*. 2nd Ed., **Vol. 1**, Wiley-VCH: Weinheim (2012), p 316.
- 2012MCPC(2nd Ed, 2)651 U. Gisi, C. Lamberth, A. Mehl, and T. Seitz, In 2nd Ed., In W. Krämer, U. Schirmer, P. Jeschke, and M. Witschel, editors: *Modern Crop Protection Compounds*. 2nd Ed., **Vol. 2**, Wiley-VCH: Weinheim (2012), p 651.
- 2012MCPC(2nd Ed, 2)739 D.H. Young, In 2nd Ed., In W. Krämer, U. Schirmer, P. Jeschke, and M. Witschel, editors: *Modern Crop Protection Compounds*. 2nd Ed., **Vol. 2**, Wiley-VCH: Weinheim (2012), p 739.
- 2012MCPC(2nd Ed, 3)1165 P. Jeschke, In 2nd Ed., In W. Krämer, U. Schirmer, P. Jeschke, and M. Witschel, editors: *Modern Crop Protection Compounds*. 2nd Ed., **Vol. 3**, Wiley-VCH: Weinheim (2012), p 1165.
- 2012MCPC(2nd Ed, 3)1367 O. Loiseleur, B. Slaats, and P. Maienfisch, In W. Krämer, U. Schirmer, P. Jeschke, and M. Witschel, editors: *Modern Crop Protection Compounds*, Wiley-VCH: Weinheim (2012), p 1367.
- 2012TL(53)2440 X. Wen, J. El Bakali, R. Deprez-Poulain, and B. Deprez, *Tetrahedron Lett.*, **53**, 2440 (2012).
- 2013ASC(355)3263 S. Toulot, T. Heinrich, and F. Leroux, *Adv. Syn. Catal.*, **355**, 3263 (2013).
- 2013HCDD283 N.B. Ambhaukar, In J.J. Li, editor: *Heterocyclic Chemistry in Drug Discovery*, p 283.
- 2013PMS(69)1225 Y. Oka, S. Shuker, and N. Tkachi, *Pest Manag. Sci.*, **69**, 1225 (2013).
- 2013SI(1)253 V. Gupta and V. Kant, *Sci. Int.*, **1**, 253 (2013).
- 2013TL(54)579 S.M. Inamdar, V.K. More, and S.K. Mandal, *Tetrahedron Lett.*, **54**, 579 (2013).
- 2014ACS(AGRO-622) R.J. Pasteris and M.A. Hanagan, In *248th ACS National Meeting & Exposition, Abstracts of Papers AGRO-622*. San Francisco, CA, United States.
- 2014ACS(AGRO-744) G. Zong, Z. Fan, X. Ji, F. Li, Y. Zhu, and L. Chen, In *248th ACS National Meeting & Exposition, Abstracts of Papers, AGRO-744*. San Francisco, CA, USA.
- 2014ACS(AGRO-911) J. Sweigard, J. Andreassi, S. Pember, S. Gutteridge, R. Pasteris, M.A. Hanagan, A. Carrol, J. Sopa, and D. Nesnow, In *248th ACS National Meeting & Exposition, Abstracts of Papers AGRO-911*. San Francisco, CA, United States.
- 2014AGE(53)2090 Y. Wu, Y. Xie, Q. Zhang, H. Tian, W. Zhu, and A.D.Q. Li, *Angew. Chem. Int. Ed.*, **53**, 2090 (2014).
- 2014FCP(2nd Ed)88 P. Richard and H.G.H. Oliver, *Fungicides in Crop Protection*, 2nd Ed., p 88.

- 2014IUPAC446 C.W. Holyoke, W. Zhang, T.F. Pahutski, G.P. Lahm, M.-H.T. Tong, D. Cordova, M.E. Schroeder, E.A. Benner, J.J. Rauh, R.F. Dietrich, R.M. Leighty, R.F. Daly, R.M. Smith, and D.R. Vincent, In *13th International Congress on Pesticide Chemistry, Abstract 446, San Francisco, CA, USA*.
- 2014IUPAC836 D. Cordova, E.A. Benner, M.E. Schroeder, C.W. Holyoke, W. Zhang, G.P. Lahm, M.-H.T. Tong, T.F. Pahutski, D.R. Vincent, and R.M. Leighty, In *IUPAC – 13th International Congress on Pesticide Chemistry, Abstract 836, San Francisco, CA*.
- 2014JCSP(36)150 A. Gowhar, S. Fazal, U.I. Nazar, K. Inamullah, R. Khalid, Samiullah, A. Muzaffar, and R. Abdur, *J. Chem. Soc. Pak.*, **36**, 150 (2014).
- 2014JES(26)757 J. Fenoll, F. Pilar, H. Pilar, J. Hernandez, and S. Navarro, *J. Environ. Sci.*, **26**, 757 (2014).
- 2014MI(33)458 N. Brown, *Mol. Inf.*, **33**, 458 (2014).
- 2014OL(16)764 M.S. Mayo, X. Yu, X. Zhou, X. Feng, Y. Yamamoto, and M. Bao, *Org. Lett.*, **16**, 764 (2014).
- 2014PBP(109)44 J. Kearns, E. Ludlow, J. Dillon, V. O'Connor, and L. Holden-Dye, *Pest. Biochem. Phys.*, **109**, 44 (2014).
- 2015ACS(SS1204)149 R.J. Pasteris, M.A. Hanagan, J.J. Bisaha, B.L. Finkelstein, L.E. Hoffman, V. Gregory, C.P. Shepherd, J.L. Andreassi, J.A. Sweigard, and B.A. Klyashchitsky, In P. Maienfisch and T.M. Stevenson, editors: *Discovery and Synthesis of Crop Protection Products*, ACS Symposium Series, **Vol. 1204**, p 149.
- 2015AP(248)155 R.K. Gill, R.K. Rawal, and J Bariwal, *Arch. Pharm.*, **348**, 155 (2015).
- 2015EJMC(92)1 M. Tiwari, *Eur. J. Med. Chem.*, **92**, 1e34 (2015).
- 2015EJMC(97)699 A. Ayati, S. Emami, A. Asadipour, A. Shafiee, and A. Foroumadi, *Eur. J. Med. Chem.*, **97**, 699e718 (2015).
- 2015HSA(B)(206)430 B.-Y. Kim, H.-S. Kim, and A. Helal, *Sens. Actuators B Chem.*, **206**, 430 (2015).
- 2015JBPS(2)149 G.N. Raju and R.R. Nadendla, *Eur. J. Biomed. Pharm. Sci.*, **2**, 149 (2015).
- 2015JMC(97)911 C. Tanyeli, *Eur. J. Med. Chem.*, **97**, 911e927 (2015).
- 2015MCR(21)2123 S.J. Kashyap, *Med. Chem. Res.*, **21**, 2123 (2012).
- 2015MCR(24)3660 V. Pechal, M. Pejchalova, and Z. Ruzickova, *Med. Chem. Res.*, **24**, 3660 (2015).
- 2015MM(weblink) Marketsandmarkets.com, Report code AGI 2533, publishing date September 2015, <http://www.marketsandmarkets.com/Market-Reports/nematicides-market-193252005.html>.
- 2015PMcD P. McDougall, *Industry Overview, 2013 Market*. [http://www.academia.edu/8024371/Industry\\_Overview\\_of\\_timorex\\_gold](http://www.academia.edu/8024371/Industry_Overview_of_timorex_gold).
- 2016BACC(weblink) J. Collins, In *Bank of America Merrill Lynch – Global Agriculture and Chemicals Conference, Ft. Lauderdale, Florida, USA*. Link to the full presentation: [http://s2.q4cdn.com/752917794/files/doc\\_presentations/2016/2016-BAML-Conference-FINAL.pdf](http://s2.q4cdn.com/752917794/files/doc_presentations/2016/2016-BAML-Conference-FINAL.pdf).
- 2016BMC(24)317 S. Jeanmart, E.F. Edmunds, C. Lamberth, and M. Pouliot, *Bioorg. Med. Chem.*, **24**, 317 (2016).

- 2016BMC(24)354 R.J. Pasteris, M.A. Hanagan, J.J. Bisaha, B.L. Finkelstein, L.E. Hoffman, V. Gregory, J.L. Andreassi, J.A. Sweigard, B.A. Klyashchitsky, Y.T. Henry, and R.A. Berger, *Bioorg. Med. Chem.*, **24**, 354 (2016).
- 2016CCR(308)32 L.M.T. Frija, *Coord. Chem. Rev.*, **308**, 32 (2016).
- 2016PMS(in press) H. Kayser, K. Lehmann, W. Schleicher, K. Dotzauer, M. Moron, M. Gomes, and P. Maienfisch, *Pest Manag. Sci.*, (2016) (in press).
- CA 56 79451 (1962) L.H. Sarett and H.D. Brown, *US 3017415*.
- CA 62 90958 (1964) NL 6405730, *No Inventor Data Available*.
- CA 65 38564 (1966) B. Von Schmeling, M. Kulka, D.S. Thiara, and W.A. Harrison, *US 3249499*.
- CA 82 155895 (1975) I. Chiyomaru, S. Kawada, and K. Takita, *DE 2434430*.
- CA 96 137998 (1981) JP 56167606, *No Inventor Data Available*.
- CA 97 127633(1982) S. Thomas, *Japan Patent Application, Jpn. Kokai Tokkyo Kwon, JP S57-93969*, (1982).
- CA 113 191337 (1990) G.H. Alt, J.K. Pratt, W.G. Phillips, and G.H. Srouji, *EP371950*.
- CA 115 280011 (1991) H. Uneme, N. Higuchi, and I. Minamida, *EP 446913 A1, 910918*, Takeda Chem. Ind., Ltd. (1991).
- CA 116 106280 (1991) M. Sutter and W. Kunz, *European Patent Application EP 454, 621*, Ciba-Geigy AG (1991).
- CA 121 57510 (1994) P.A. Parziale, T.C. Chang, and L.E. Applegate, *US 5310924*.
- CA 123 83358 (1995) H.-R. Kaenel, A. Wegmann, and D. Neff, *European Patent Application EP 655, 446*, Ciba-Geigy AG (1995).
- CA 126 157288(1997) A. Dierdorf and T. Papenfuhs, *European Patent Application EP 753507 A1*.
- CA 130 110264 (1996) S. Li, G. Lu, Y. Li, and Y. Deng, *Faming Zhuanli Shenqing Gongkai Shuomingshu, CN1121516*.
- CA 130 338103 (1999) L. Assmann, D. Kuhnt, H.-L. Elbe, C. Erdelen, S. Dutzmann, G. Hanssler, K. Stenzel, A. Mauler-Machnik, Y. Kitagawa, and H. Sawada, *WO 9924413*.
- CA 133 105348(2000) L. Filippini, M. Gusmeroli, S. Mormile, L. Colombo, and L. Mirena, *Jpn. Kokai Tokkyo Koho JP 2000198797*, (2000).
- CA 136 183810 (2002) K. Okano, A. Miyauchi, and T. Tanaka, *Japan Patent Application JP 2002/053,563*, Mitsubishi Chemical Corp. (2002).
- CA 145 8157 (2006) M. Tanaka, H. Kagano, K. Nakayama, and S. Fukutome, *Japan Patent Application JP 2006/131,593*, Sumitomo Seika Chemicals Co., Ltd. (2006).
- CA 146 121958 (2007) T. Himmler, *Patent Application DE 102005031348*.
- CA 149 203017(2007) S. Podmanicky, K. Jurkovic, J. Dziacek, M. Machajova, and S. Krska, *SK 285783 B6*.
- CA 152 290557 (2010) J. Miao, Z. Liu, K. Wang, J. Zhang, and Y. Xue, *Faming Zhuanli Shenqing Gongkai Shuomingshu, CN 101638396 A*.
- CA 153 600769 (2010) T. Nakamura, O. Kumagai, and M. Ogawa, *Patent Application WO 2010126170*.
- CA 153 620652(2010) A.A. Brunkin, *Patent Application RU 2404171 C2*.
- CA 154 250059 (2011) W. Zhang, C.W. Holyoke, K.A. Hughes, G.P. Lahm, T.F. Pahutski, M.-H. T. Tong, and M. Xu, *PCT Int. Appl., WO2011/017342*, Assignee: E. I. du Pont de Nemours and Company, USA (2011).

- CA 156 452144 (2012) J. An, *Faming Zhuanli Shenqing*, Patent application CN 102391205 (2012).
- CA 160 559314 (2014) T. Abe, *Patent Application WO 2014054294*.
- CA 162 590253 (2015) H. Bi, C. Zhi, and Y. Zhang, *Faming Zhuanli Shenqing Gongkai Shuomingshu*, CN 104557902.
- CA 163 65941 (2015) T. Zheng, S. Ye, and X. Wang, *Faming Zhuanli Shenqing*, CN 104672168.



# Nitrogen-Rich Azoles as High Density Energy Materials: Reviewing the Energetic Footprints of Heterocycles

Ping Yin, Jean'ne M. Shreeve\*

Department of Chemistry, University of Idaho, Moscow, ID, USA

\*Corresponding author: E-mail: jshreeve@uidaho.edu

## Contents

1. Introduction	89
2. Pyrazole-Based Energetic Materials	92
3. Imidazole-Based Energetic Materials	104
4. Triazole-Based Energetic Materials	109
5. Tetrazole-Based Energetic Materials	123
6. Summary	127
Acknowledgments	129
References	129

## Abstract

In this contribution, recent developments of azole-based high energy density materials are reviewed. A variety of azoles, e.g., pyrazole, imidazole, triazole, and tetrazole, were used as nitrogen-rich backbones and were functionalized with explosives. The synthetic methods, experimental properties, and theoretical calculations are discussed leading to panoramas of these promising energetic materials.

**Keywords:** High energy density materials; Imidazole; Pyrazole; Tetrazole; Triazole

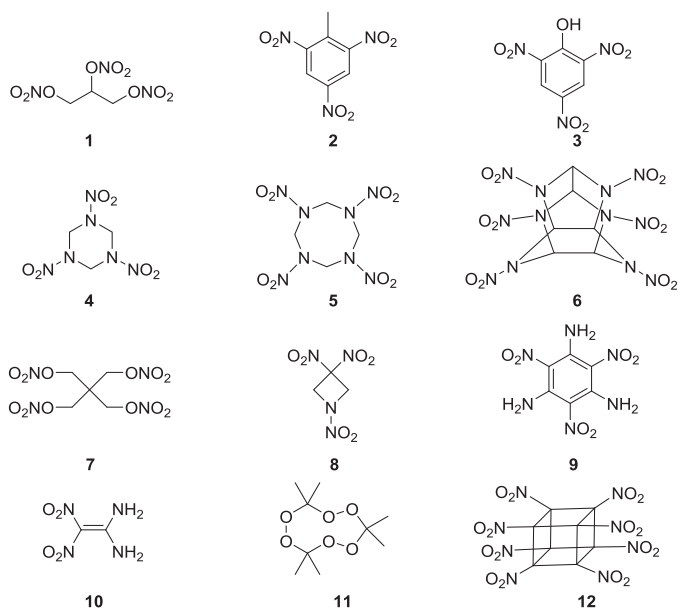


## 1. INTRODUCTION

As the most well-known energetic material historically, black powder was invented by mixing flammable charcoal and sulfur with oxidant potassium nitrate. With the development of synthetic chemistry, both fuel and oxidizer moieties are capable of being assembled into the same molecule,

thereby raising the curtain on the new age of modern explosives. In general, most currently used energetic materials are composed of an organic backbone with versatile energetic functionalized groups, so-called explosophores. Under certain conditions, e.g., heat, friction, shock, and electrostatic discharge, energetic compounds decompose with huge amounts of chemical energy. The rapid energy release mainly arises from self-oxidation and the formation of  $N\equiv N$  bonds.

Reflecting on the history of energetic materials, the most well-known work was contributed by the pioneer scientist, Alfred Nobel, who developed nitroglycerine in the 1860s (Scheme 1, **1**). At the same time, another classic explosive, 2,4,6-trinitrotoluene (TNT, **2**), which was first synthesized in 1863 and then applied in melt-pour explosives (1863ACP178). More interestingly, after serving as yellow dyes for more than 100 years, the detonating features of picric acid (PA, **3**) were proved in 1873 (1873JCS796) and were exploited as high-performance explosives in the late nineteenth century. Although cyclotrimethylenetrinitramine (RDX, **4**) was first claimed as a potential medicine in 1899, its excellent energetic performance was tested on the battlegrounds of the two world wars (1943CPE396). Octahydro-1,3,5,7-tetranitro-1,3,5,7-tetrazocine (HMX, **5**) was discovered from



Scheme 1 Representative energetic compounds in the recent two centuries.



the side products of RDX, and later study indicated that an increased percentage of HMX in RDX improved the detonation properties (1996EE). Hexanitrohexaazaisowurtzitane (HNIW, **6**) is one of the most powerful explosives and has attracted great interest by the U.S. Navy and other communities since it was first reported in 1987 (1989PCE|7). In addition to nitramine-based energetic materials, pentaerythritol tetranitrate (PETN, **7**) is one of the last representatives in the family of nitrate esters which shows higher detonation performance than **1** and the impact and friction sensitivities are superior to those of **1** (2009JA7490). In order to find high-performance melt-pour explosives, 1,3,3-trinitroazetidine (TNAZ, **8**) was synthesized and characterized. Its low melting point and excellent detonation properties may enable it as a TNT replacement (2004JHM35).

Along with the increasing requirement for advanced energetic materials, diversified energetic compounds were synthesized to meet ever-changing criteria, e.g., safe production and storage, low cost, and reduced pollution for the environment. Amino and nitro groups play roles as a hydrogen bond donor and a hydrogen bond acceptor, respectively, thereby providing the most efficient approach to the design of high-performance insensitive energetic materials (HIEMs). 2,4,6-Triamino-1,3,5-trinitrobenzene (TATB, **9**) and 1,1-diamino-2,2-dinitroethene (FOX-7, **10**) are the two most representative energetic molecules with  $\text{NH}_2\text{-NO}_2$ -based hydrogen bond strategies (2010JHM1, 1998T11525). While 1,3,5-trinitrobenzene has a density of  $1.676 \text{ g/cm}^3$ , TATB has a remarkably high density of  $1.937 \text{ g/cm}^3$  because of the additional amino functionalities (1972AC193, 1965AC485, 2010JPCA2727, 2010PEP15). Similarly, the unique structure of FOX-7 provides a modular design to balance between detonation properties and sensitivity.

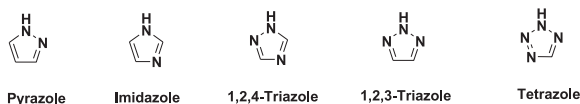
While most explosives are nitrogen-containing compounds, acetone peroxide is an unusual energetic molecule composed of carbon, hydrogen, and oxygen. 3,3,6,6,9,9-Hexamethyl-1,2,4,5,7,8-hexaoxacyclononane (TATP, **11**), a trimer of acetone peroxide, is used for practical production because it shows better stability than the other polymers of acetone peroxide (1959JA6461). In 2000, the discovery of a long awaited energetic material, i.e., octanitrocubane (ONC, **12**) was considered to be a milestone achievement (2000AN401). Although ONC has a predicted density of  $2.20 \text{ g/cm}^3$ , the measured crystal density of  $1.96 \text{ g/cm}^3$  is even lower than that of heptanitrocubane ( $2.03 \text{ g/cm}^3$ ). Hence, the scientific communities continue to search for a higher dense form of ONC by improving the efficiency of crystal packing.

Accompanying the growing demands of a new generation of advanced energetic materials, the rational assembly of explosophores with diversified backbones is highly appealing to integrate performance. No doubt the field of high energy density materials (HEDMs) has been boosted by the advent of multifunctionalized N-heterocycles. There are two main advantages in N-heterocycle-based energetic materials; on the one hand, N-heterocycles have a higher nitrogen content, heat of formation, and density than those of carbocyclic compounds; on the other hand, most energetic functionalized groups, i.e., nitro, nitramino, azo, azoxy, amino, and azido group are compatible with N-heterocycles, thereby extending greatly the design of energetic compounds. Among these N-heterocycles, the most commonly used energetic backbones are five-membered azoles, such as pyrazole, imidazole, 1,2,4-triazole, 1,2,3-triazole, and tetrazole (Scheme 2).

In 2011, we examined the progress of energetic five-membered azole salts (2011CR7377). However, a closer look at energetic azole chemistry reveals a great advance for both molecular and ionic compounds in the ensuing 5 years. In this contribution, the recent developments of azole-based energetic materials are reviewed. Unlike most general overviews, attention is mainly focused on high-dense energetic heterocycles with densities ranging between 1.80 and 2.00 g/cm<sup>3</sup>. Meanwhile, the insight structure–property relationship for a better understanding for the future design of energetic materials is discussed.

## 2. PYRAZOLE-BASED ENERGETIC MATERIALS

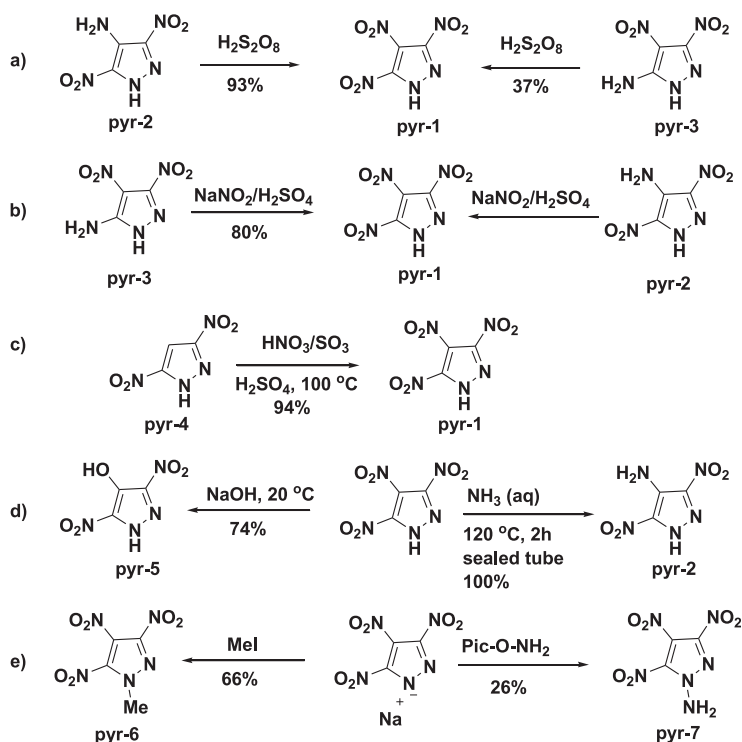
As an ideal combination of organic framework and explosophores, the all-carbon-nitrated arenes have attracted much attention for a long time. In such energetic molecules, a large number of nitro groups not only increases the density greatly, but also provides sufficient oxygen sources to give proper oxygen balance, thereby maximizing the detonation performance in energy release. However, a general screening of all-carbon-nitrated arenes indicates that many nitro-functionalized azoles, such as 2,4,5-trinitroimidazole, 3,4-dinitro-1,2,3-triazole, 3,5-dinitro-1,2,4-triazole, 5-nitrotetrazole, and



Scheme 2 Some commonly used azole backbones in energetic materials.

1,2,3,4-tetranitropyrrole, do not meet the integrated requirements of energetic materials for practical application because of the low thermal stabilities and poor sensitivities (1992JHC1721, 1970SKGS259, 1992BR751, 1997RJOC1771). Similarly, hexanitrobenzene, albeit with a fairly high density of  $1.985 \text{ g/cm}^3$ , is very moisture and impact sensitive (1986JOC3261). Differently from other all-carbon-nitrated analogs, 3,4,5-trinitro-1*H*-pyrazole (TNP) exhibits unexpected favorable thermal, chemical, and mechanical stability (2010AN3177). Various synthetic routes, including oxidation, diazotization, and direct nitration, have been investigated for selective syntheses of 3,4,5-trinitro-1*H*-pyrazole (Scheme 3(a–c)). In addition, both nucleophilic substitutions and electrophilic reactions can be carried out with different reagents (Scheme 3(d) and (e)) to yield a variety of energetic derivatives of TNP.

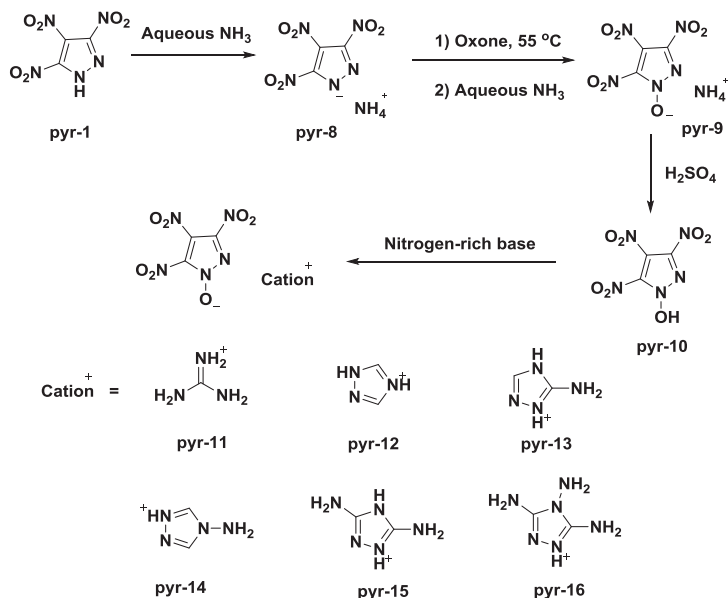
Unlike other nitroazoles with strong acidity, TNP is a relatively weak acid which is compatible with other energetic ingredients. With respect to the stability of energetic compounds, decomposition temperature ( $T_d$ ),



Scheme 3 Selective Preparation of 3,4,5-Trinitro-1*H*-Pyrazole and its derivatives.

and impact and friction sensitivities (IS and FS) are significant criteria. Compared to some classical performance explosives, such as HMX and RDX, TNP shows comparable thermal, chemical, and mechanical stabilities (HMX,  $T_d$ , 286 °C, IS, 7 J, FS, 120 N; RDX,  $T_d$ , 205 °C, IS, 7 J, FS, 120 N; TNP,  $T_d$ , 258 °C, IS, 17 J, FS, 92 N). The energy parameters, e.g., detonation velocity ( $v_D$ ), detonation pressure ( $P$ ), and specific impulse ( $I_{sp}$ ), were evaluated by theoretical calculation (CHEETAH) based on experimental density. The detonation performance of TNP is superior to RDX, but somewhat lower than HMX (HMX,  $P$ , 39.5 GPa,  $v_D$ , 9320 m/s; RDX,  $P$ , 34.9 GPa,  $v_D$ , 8748 m/s; TNP,  $P$ , 38.6 GPa,  $v_D$ , 9253 m/s). With higher oxygen content and oxygen balance, the specific impulse of TNP-containing formulations is greater than those of HMX and RDX.

Continuing research interest in exploring new energetic derivatives was stimulated by the unusual physicochemical properties of TNP. Using Oxone<sup>®</sup> as the oxidizing reagent, the N-OH group was successfully introduced into TNP (Scheme 4). The combination of the oxygen-rich TNP backbone with the additional N-O functionality enhances the oxygen content and oxygen balance of 3,4,5-trinitro-1*H*-pyrazol-1-ol, thus making it very promising as a new energetic oxidizer (2012JMC12659). In spite of

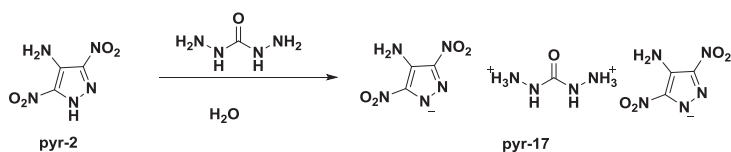


Scheme 4 Synthesis of 3,4,5-trinitropyrazole-1-ol and its salts.

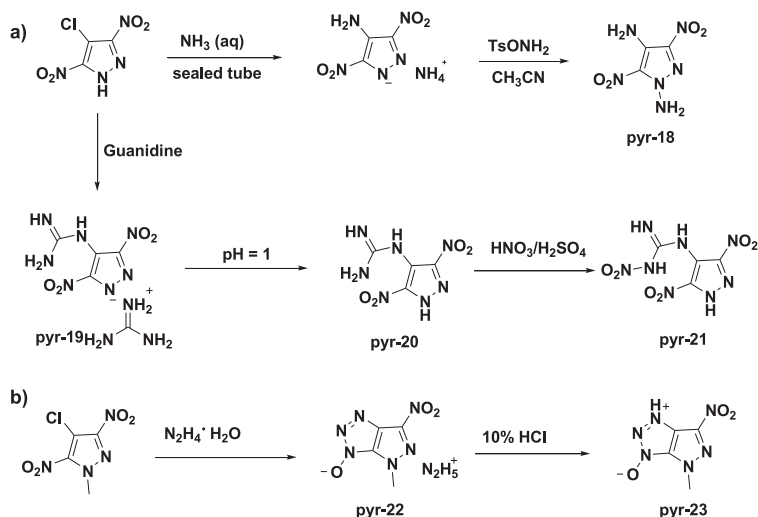
the high density of  $1.90 \text{ g/cm}^3$ , the application of 3,4,5-trinitro-1*H*-pyrazol-1-ol may be precluded by the fact that it is very impact sensitive ( $IS = 1 \text{ J}$ ). However, incorporation of a variety of nitrogen-rich bases to form energetic salts is a promising tool in modifying the sensitivity of energetic materials. As expected, 3,4,5-trinitro-1*H*-pyrazol-1-ol-based energetic salts show lower impact sensitivities ranging between 6 and 40 J.

High detonation performance and insensitivity are two of the most important characteristics for HEDMs but these are often contradictory with each other. Although energetic salts show better impact sensitivities than their molecular precursors, the density and detonation performances are usually decreased. Hence, searching for high-density energetic salts is one of the most challenging issues in energetic salt formation. While the high densities of TNP and 3,4,5-trinitropyrazole-1-ol originate from multiple nitro groups, 4-amino-3,5-dinitropyrazole is featured with enhanced density by virtue of hydrogen-bond interactions. Incorporating the carbohydrazinium cation with the 4-amino-3,5-dinitropyrazolate anion results in salt **pyr-17** which has a high density of  $1.84 \text{ g/cm}^3$  (Scheme 5) (2011JMC6891). More importantly, the excellent detonation properties ( $P$ , 32.6 GPa,  $v_D$ , 8743 m/s) and high impact insensitivity ( $IS > 60 \text{ J}$ ) highlight **pyr-17** as a potential replacement for some currently used explosives, e.g., TATB and RDX.

Among the azole frameworks, the three catenated carbon atoms of pyrazole endow the backbone with a unique opportunity for diversified functionalizations. Recently, a new family of energetic pyrazoles were synthesized from a readily prepared precursor, i.e., 4-chloro-3,5-dinitropyrazole (2013JMCA2863). In the presence of aqueous ammonia, 4-chloro-3,5-dinitropyrazole was converted to ammonium 4-amino-3,5-dinitropyrazolate in a sealed tube at  $130 \text{ }^\circ\text{C}$ . Amination was carried out using *O*-tosylhydroxylamine to give 1,4-amino-3,5-dinitropyrazole (**pyr-18**). In a similar manner, 4-guanidinyll- and 4-nitroguanidinyll (**pyr-21**)-substituted products were prepared in good yields (Scheme 6).



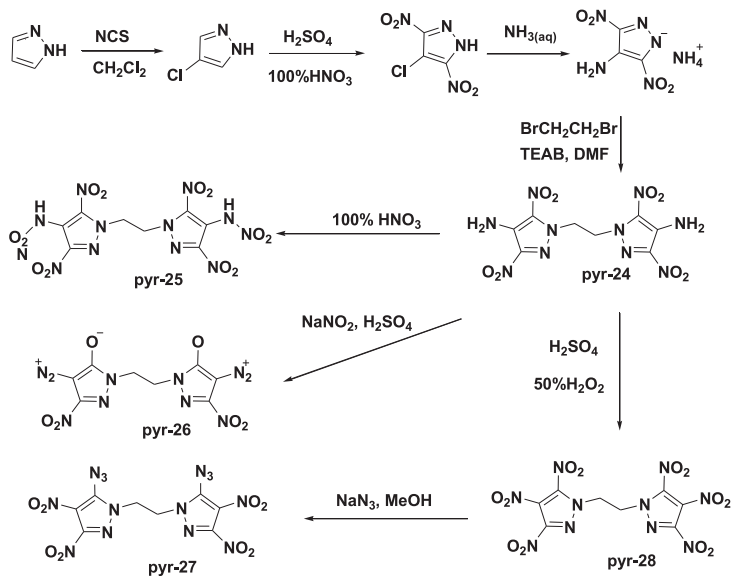
**Scheme 5** Synthesis of the high-performance insensitive energetic salt carbohydrazinium 4-amino-3,5-dinitropyrazolate.



**Scheme 6** Nucleophilic reactions of 4-chloro-3,5-dinitropyrazole and *N*-methyl 4-chloro-3,5-dinitropyrazole.

Both **pyr-18** and **pyr-21** have high densities, positive heats of formation, good detonation performance, and low impact sensitivities. Using hydrazine monohydrate as a nucleophile, reaction of *N*-methyl 4-chloro-3,5-dinitropyrazole formed a novel fused pyrazole-triazole backbone (**pyr-22**, **pyr-23**) (2016JMCA1514).

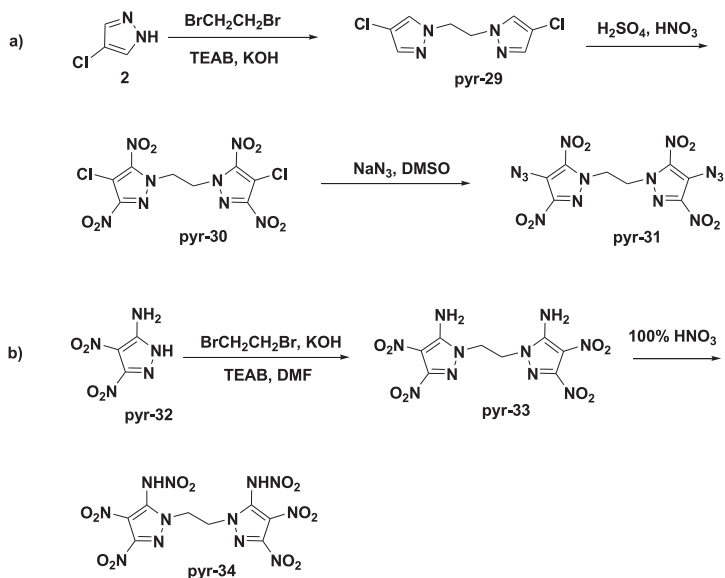
Development of *N,N'*-bridged azoles enriches the synthetic strategies to construct various energetic compounds. A variety of *N,N'*-ethylene-bridged tetrazoles were synthesized and their energetic properties evaluated by both experimental and theoretical investigations, which indicated the *N,N'*-ethylene bridge can balance energetic performance and molecular stability. Inspired by the advantage of an *N*-bridging functionality, extensive study on the pyrazole framework was developed. Employing the easily prepared ammonium 4-amino-3,5-dinitropyrazolate as the key intermediate, versatile functional group transformations gave a family of new *N,N'*-ethylene-bridged pyrazoles with diversified functionalities and energetic properties (Scheme 7) (2014CEJ16529). With energy levels analogous to RDX, nitro-amino-, azido-, and nitro-functionalized *N,N'*-ethylene-bridged pyrazoles can be classified as high explosives. However, with respect to thermal, chemical, and mechanical stabilities, the nitro-functionalized product, **pyr-28**, is superior to those of the nitroamino- and azido-functionalized analogs.



**Scheme 7** Synthesis of *N,N'*-ethylene-bridged 4,4'-diaminobis(pyrazole) and its derivatives.

Using sodium nitrite/sulfuric acid and sodium azide, the initial attempt to prepare 4,4'-diazido bis(pyrazole) compound resulted in an unexpected diazonium salt (**pyr-26**). Then, an alternative three-step synthesis gave rise to desired product, **pyr-31**, from 4-chloropyrazole. Also, an *N,N'*-ethylene bridge was used successfully to link the 5-amino 3,4-dinitropyrazole moieties, whereas the nitramino product, **pyr-34**, was readily obtained by the treatment of **pyr-33** with 100% nitric acid (Scheme 8).

Although the nitro group is the most favorable functionality in the construction of energetic molecules, the investigation of the nitramino functionality has become the new hot spot toward next generation of HEDMs. From a traditional industrial standpoint, nitramino-functionalized heterocycles are not good candidates for HEDMs because of some fatal flaws, e.g., sensitivity and strong acidity. However, energetic salt formation represents a new promising opportunity to apply nitramino compounds in the design of high-energy nitro-rich materials. In the presence of mixed acid, 4-amino 3,4-dinitropyrazole is readily converted to 4-nitramino-3,4-dinitropyrazole (2012CEJ987). Unfortunately, like many other nitramino compounds, 4-nitramino-3,4-dinitropyrazole is not stable and must be stored in ether solution at low temperature. The reaction of nitramine

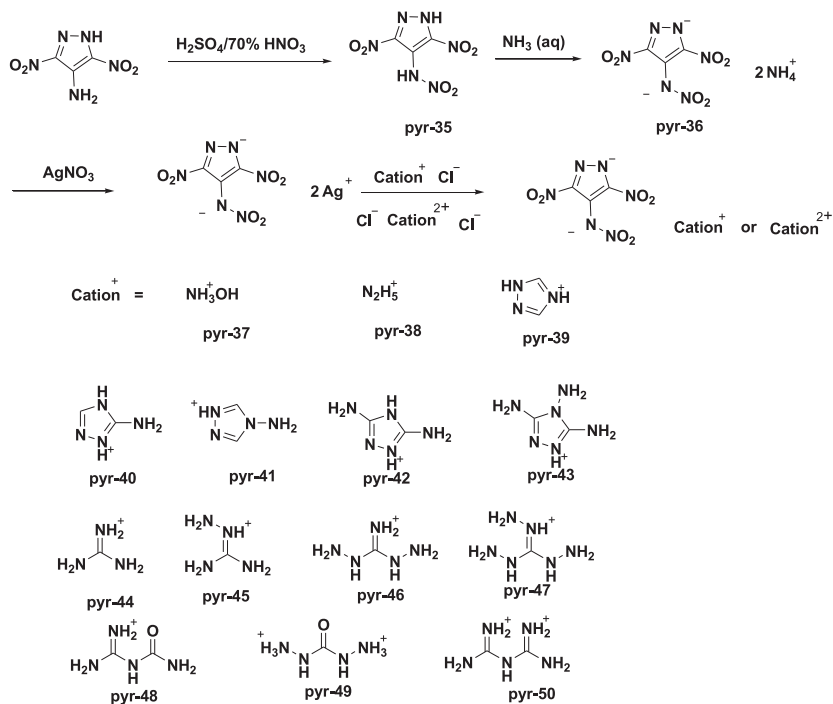


**Scheme 8** (a) Synthesis of *N,N'*-ethylene-bridged 4,4'-diazidobis(pyrazole) (**pyr-31**). (b) Synthesis of *N,N'*-ethylene-bridged 5,5'-diaminobis(pyrazole) (**pyr-33**) and its nitramine derivative (**pyr-34**).

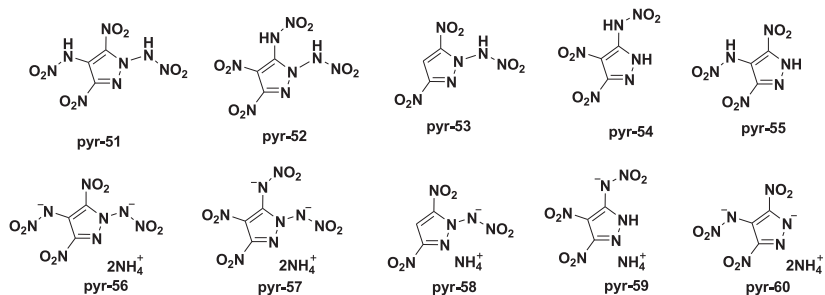
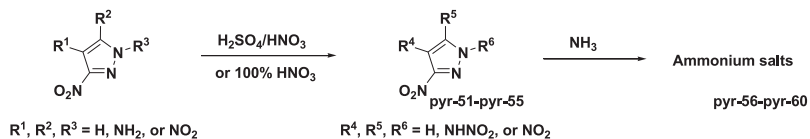
(**pyr-35**) with concentrated aqueous ammonia resulted in a more chemically and thermally stable product, ammonium 4-nitramino-3,4-dinitropyrazolate (**pyr-36**). Employing metathesis reactions of silver 4-nitramino-3,4-dinitropyrazolate, a variety of nitrogen-rich salts were prepared (Scheme 9). Of them, hydroxylammonium 4-nitramino-3,4-dinitropyrazolate (**pyr-37**) exhibits excellent detonation performance ( $P$ , 37.4 GPa,  $v_D$ , 9013 m/s) and relatively ideal impact sensitivity (IS = 30 J).

In the framework of crystal engineering science, hydrogen bonding is one of the most significant interactions in order to understand the structural features of solid-state compounds. In most cases, the nitroamino compounds show strong hydrogen-bonding interactions in their crystal structures. A comparative investigation involving several nitraminopyrazoles (**pyr-51**–**pyr-55**) demonstrated diversified energetic properties and molecular stabilities (Scheme 10) (2015JA4778). Of them, **pyr-54** with a unique “NO<sub>2</sub>-NHNO<sub>2</sub>-NH” structure shows high detonation performance with acceptable stability, whereas other nitramino analogs are not stable at room temperature. In comparison, all nitraminopyrazole-based ionic derivatives show enhanced stability with good energetic properties (Scheme 11a).

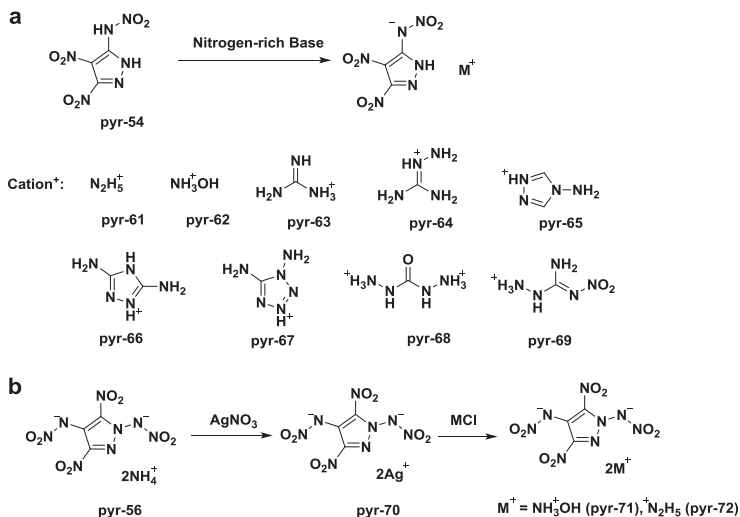




**Scheme 9** Synthesis of 4-nitramino-3,5-dinitroprazole (pyr-35) and its salts.



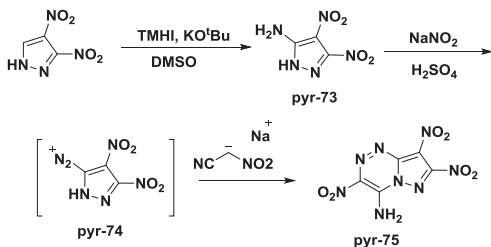
**Scheme 10** Synthesis of multifunctionalized nitraminopyrazoles and their ammonium salts.



**Scheme 11** (a) Synthesis of monocationic 5-nitramino 3,4-dinitropyrazolates. (b) Synthesis of 1,4-nitramino 3,5-dinitropyrazole-based salts.

It is worth mentioning that the remarkably high density of **pyr-54** ( $2.032 \text{ g/cm}^3$  at 150 K;  $1.97 \text{ g/cm}^3$  at 298 K) is higher than any reported CHNO-based azoles to date. In addition, the dihydroxylammonium salt, **pyr-71**, and dihydrazinium salt, **pyr-72**, were prepared and their detonation pressures and velocities were calculated by EXPLO 5 v6.01 (**pyr-71**,  $P$ , 40.2 GPa,  $v_D$ , 9410 m/s; **pyr-72**,  $P$ , 33.8 GPa,  $v_D$ , 9040 m/s) (Scheme 11b).

A clever application of vicarious nucleophilic substitution enables 3,4-dinitropyrazole to be easily converted to 5-amino-3,4-dinitropyrazole, **pyr-73** (Scheme 12) (2015JMCA17693), and an exciting new energetic derivative was synthesized and fully characterized. The following one-pot procedure involving diazotization and cycloaddition gave 4-amino-3,7,8-trinitropyrazolo-[5,1-*c*] [1,2,4]triazine (**pyr-75**). Single-crystal X-ray

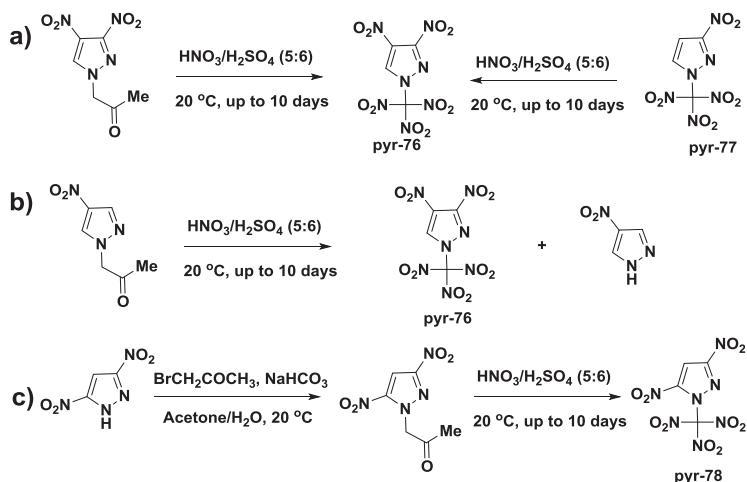


**Scheme 12** Synthesis of 4-amino-3,7,8-trinitropyrazolo-[5,1-*c*] [1,2,4]triazine via a vicarious nucleophilic substitution route.

diffraction of **pyr-75** shows the planarity of the fused-ring structure and a high density ( $2.006 \text{ g/cm}^3$  at 100 K;  $1.946 \text{ g/cm}^3$  at 300 K), which exceed that of the classic explosive HMX ( $1.904 \text{ g/cm}^3$  at 298 K). Furthermore, with good detonation performance, its excellent thermal stability, low sensitivity to impact, friction, and spark highlight the safety margins for practical applications.

In addition to nitramines and fused rings, the trinitromethyl functionality was also utilized to improve the molecular energy of pyrazole-based compounds. In 2015, an effective synthetic methodology of *N*-trinitromethyl nitropyrazoles was developed by the Sheremetev research group (2015CAJ1987). Treated with a mixture of  $\text{HNO}_3/\text{H}_2\text{SO}_4$ , 3,4-dinitro- and 3,5-dinitro-1-(trinitromethyl)pyrazoles were prepared by destructive nitration of the corresponding 1-acetylpyrazoles. Compounds **pyr-76** and **pyr-78** have remarkable positive oxygen balances ( $\Omega_{\text{CO}_2} = +7.8\%$ ;  $\Omega_{\text{CO}} = +28.7\%$ ), thereby suggesting their application potential as high-energy dense oxidizers (Scheme 13).

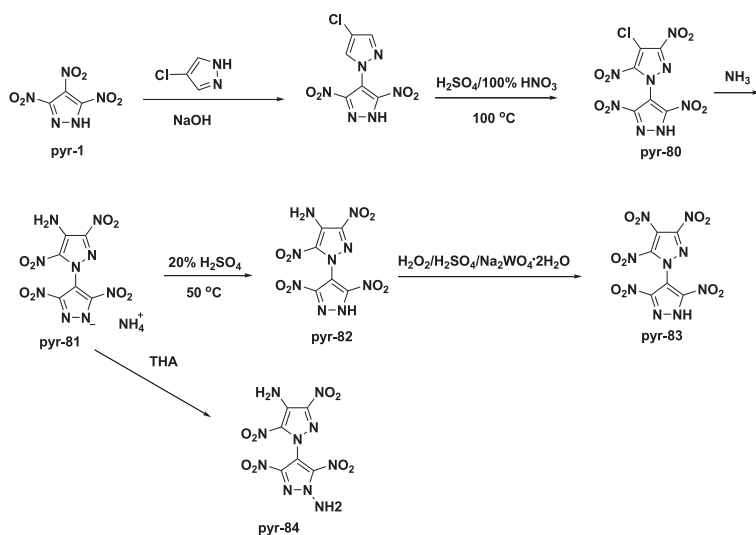
A bis(heterocycle) is one of the most attractive energetic backbones due to its favorable thermal stability and high density. Reaction of TNP with various azoles undergoes regiospecific nucleophilic substitution to yield some novel bis(azole) frameworks (2010MC355). However, the attempted nucleophilic substitution of TNP with highly dense 4-amino 3,4-dinitropyrazole fails to yield the target bispyrazole, **pyr-82**. Instead, by using 4-chloro-3',5'-dinitro-1'-H-1,4'-bipyrazole as the intermediate, ammonium



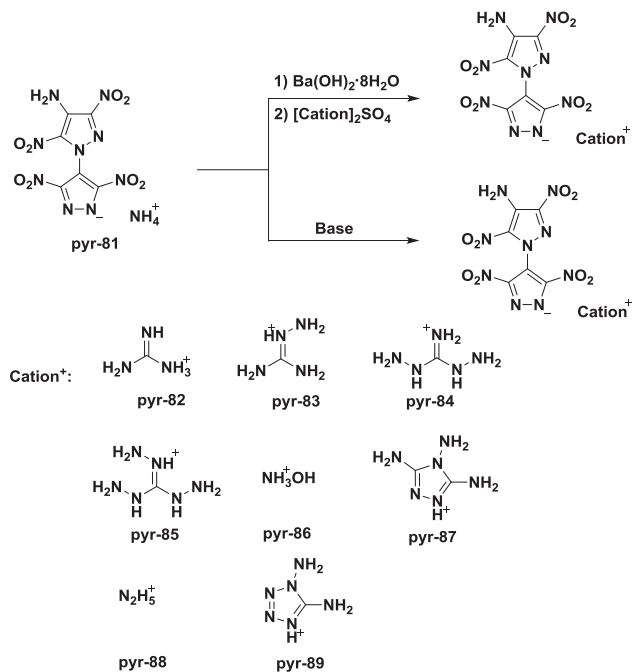
Scheme 13 Preparation of 3,4-dinitro- and 3,5-dinitro-1-(trinitromethyl)pyrazoles.

pyrazolate (**pyr-81**) was successfully prepared in two synthetic steps (Scheme 14) (2014JMCA18907). By employing freshly prepared *O*-tosylhydroxylamine, the *N*-amino group was introduced into **pyr-81** to give **pyr-84**. In the oxidative system consisting of concentrated sulfuric acid, sodium tungstate dihydrate, and 30% hydrogen peroxide, oxidation of the amino group gave rise to the crude product pentanitro-bispyrazole **pyr-83**, which can be purified by further recrystallization in a mixture of ethanol and water. The key energetic parameters of these new bispyrazoles, e.g., thermal stabilities, impact sensitivities, densities, and detonation performances, were comparable or even superior to those of RDX. More importantly, nitrogen-rich salts of **pyr-82** exhibit low impact sensitivities, which are favorable for safety preparation and storage (Scheme 15).

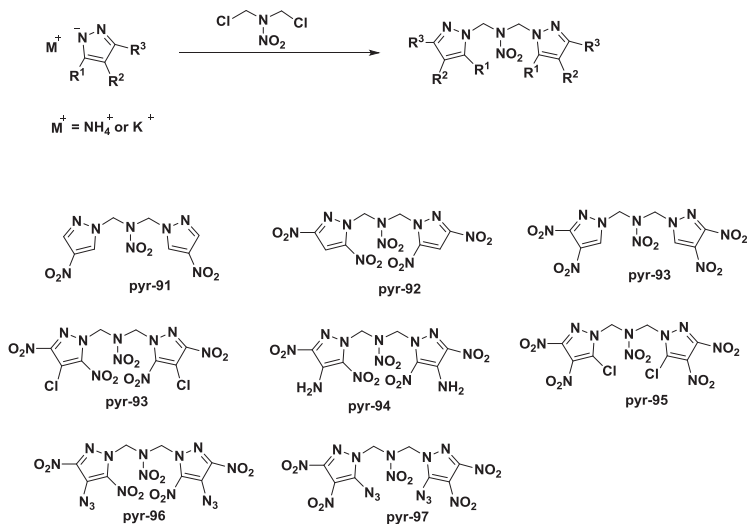
Because of high density and low sensitivity, more research interest was focused on bispyrazole-based HEDMs. While the direct C–N bond was used as a link to connect two pyrazole rings in **pyr-82**, a more energetic building block, i.e., *N,N'*-2-nitrazapropyl, was employed in the construction of new bispyrazoles (Scheme 16) (2013CEJ8929, 2013EJOC4667). The side chlorination at 5-position was observed in the *N*-alkylation of TNP, giving rise to di(3,4-dinitro-5-chloropyrazole)-*N*-nitromethanamine (**pyr-95**), which can be converted to highly energetic and extremely sensitive 5,5'-diazo product, **pyr-97**. Of these bridged bispyrazoles, **pyr-97** has



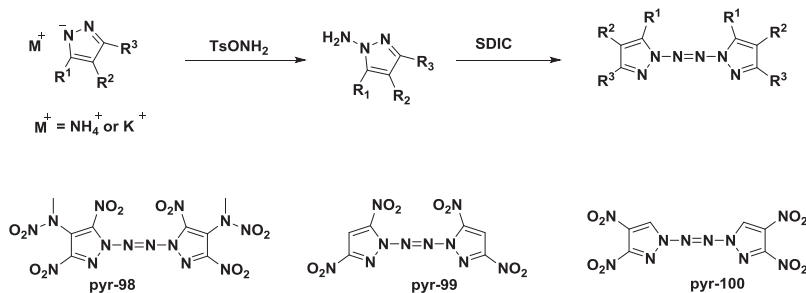
Scheme 14 Synthesis of polynitro-substituted bispyrazoles.



**Scheme 15** Synthesis of energetic salts from ammonium 4-(4'-amino-3',5'-dinitro-1'-pyrazol)-3,5-dinitro-1H-pyrazolate (**pyr-81**).



**Scheme 16** Synthesis of *N,N'*-2-nitrazapropyl-bridged bis(pyrazoles).



the best overall energetic properties ( $d$ , 1.86 g/cm<sup>3</sup>;  $P$ , 34.7 GPa,  $v_D$ , 8639 m/s; IS > 40 J), which are superior to those of the insensitive explosive TATB and are comparable to those of the high explosive RDX.

In addition to the *N,N'*-2-nitrazapropyl bridge, the *N,N'*-azo group is another promising building block to link two azole rings. In comparison to *N,N'*-alkyl compounds, a unique feature of the *N,N'*-azo functionality is that it leads to the formation of planar molecules which are conducive in improving thermal and mechanical stabilities. *N,N'*-azo-bridged bispyrazoles were synthesized by *N*-amination of potassium or ammonium pyrazolates followed by oxidative coupling with sodium dichloroisoocyanurate (SDIC) (Scheme 17) (2014CEJ6707). Compounds **pyr-99** and **pyr-100** exhibit high density, excellent thermal stability, and favorable detonation velocity and pressure, with concomitant acceptable impact and friction sensitivities.

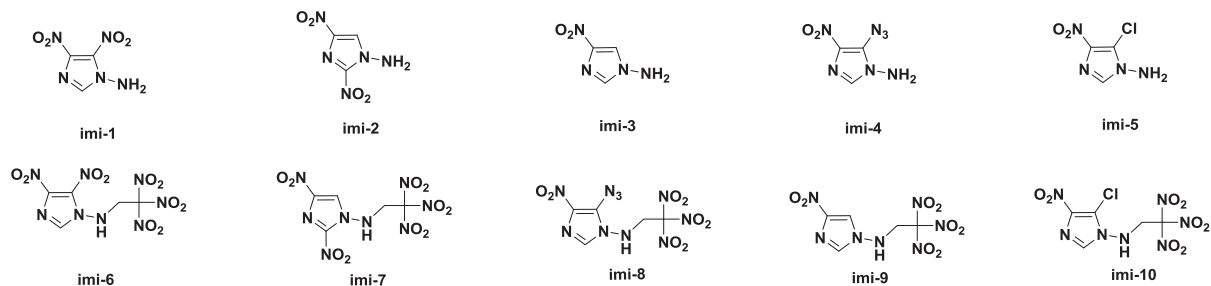
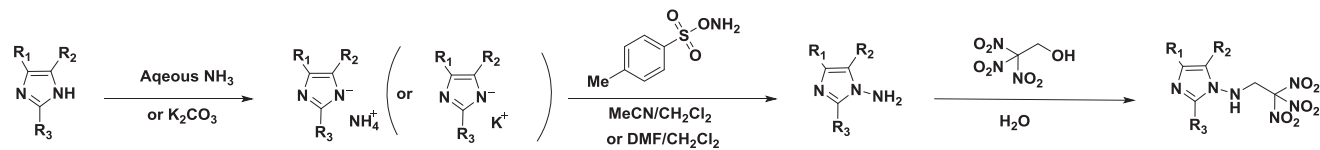
### 3. IMIDAZOLE-BASED ENERGETIC MATERIALS

Research interest in imidazole compounds is mainly focused on the application of chemical and pharmaceutical intermediates. As an isomer of pyrazole, imidazole also has two nitrogen atoms but the density and thermal stabilities are usually superior to those of pyrazole, for example, the density of 1*H*-pyrazole (1.12 g/cm<sup>3</sup>) is slightly lower than that of 1*H*-imidazole (1.23 g/cm<sup>3</sup>). Based on some previous comparative studies involving trinitropyrazolates and trinitroimidazolates, it can also be concluded that the densities and detonation properties of trinitroimidazolates are higher than those of its pyrazole analogs (2010CEJ10778). However, pyrazole-based materials have some advantages which are superior to imidazole, such as higher heats of formation. Considering the

complexity of energetic molecules, rationally selecting functional groups and backbones can provide a shortcut to maximizing performance with smaller losses in stability.

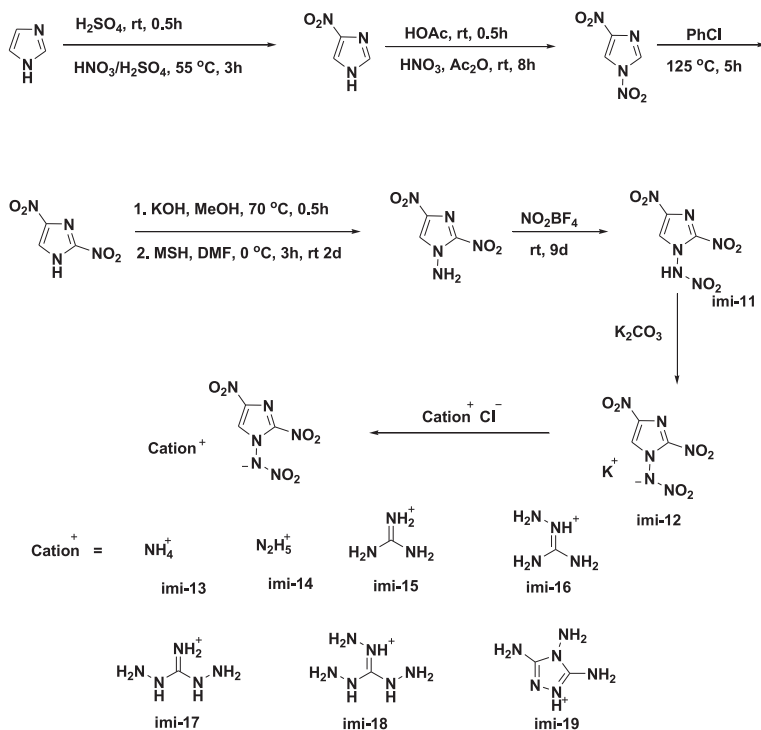
Investigations of the trinitroethyl functionality have demonstrated it to be a promising explosophore to improve energetic properties (2009AFM347). Introduction of the trinitroethyl group into nitrogen-rich heterocycles enhances both density and oxygen balance because of the greater numbers of nitro groups. As a result, the detonation pressure and velocity are improved, in spite of the slight decrease in heat of formation. A multistep synthetic procedure including salt formation and *N*-amination followed by trinitroethylation has been investigated (2013JMCA7500). *N*-Trinitroethylamination of imidazoles provided a new strategy for designing high-performance energetic materials. While *N*-aminoimidazoles (**imi-1–imi-5**) exhibit moderate densities and are insensitive, *N*-trinitroethylaminoimidazoles (**imi-6–imi-10**) have excellent densities with moderate sensitivities (Scheme 18). Of these compounds, **imi-6** and **imi-7** are featured with high densities (**imi-6**, *d*, 1.867 g/cm<sup>3</sup> at 293 K, 1.909 g/cm<sup>3</sup> at 150 K; **imi-7**, *d*, 1.869 g/cm<sup>3</sup> at 293 K, 1.923 g/cm<sup>3</sup> at 100 K), and positive oxygen balances ( $\Omega_{\text{co}}$ ) based on carbon monoxide (**imi-6**,  $\Omega_{\text{co}}$ , +14.29%; **imi-7**,  $\Omega_{\text{co}}$ , +14.29%), which show potential as high-dense energetic oxidizers. In the case of *N*-trinitroethylamino functionalization, the density of **imi-7** (*d*, 1.869 g/cm<sup>3</sup>) is remarkably higher than its pyrazole-based isomer, 3,4-dinitro-*N*-(2,2,2-trinitroethyl)-1*H*-pyrazol-1-amine (*d*, 1.78 g/cm<sup>3</sup>) (2014JMCA3200).

Another promising route to improve energetic performance has been developed by the introduction of the *N*-nitramino functionality to nitroimidazoles (2013RA10859). 2,4-Dinitroimidazole was used as the precursor because of good density and low sensitivity. By carefully controlling the temperature at 0 °C, reaction of potassium 2,4-dinitroimidazolate with *O*-mesitylsulfonyl hydroxylamine gave 1-amino 2,4-dinitroimidazole in 45% yield. As the *N*-amino group is more sensitive than the *C*-amino group in acidic media, the nitration was accomplished by using the mild reagent, nitronium tetrafluoroborate. Compound **Im-11** was examined as a precursor to salt formation with various nitrogen-rich compounds (**imi-13–imi-19**) (Scheme 19). Of them, hydrazinium 1-amino 2,4-dinitroimidazolate (**imi-14**) has a high density of 1.93 g/cm<sup>3</sup>, which exceeds that of HMX (*d*, 1.90 g/cm<sup>3</sup>). With excellent detonation performance (*P*, 40.5 GPa,  $\nu_{\text{D}}$ , 9209 m/s) and relatively low impact sensitivity (IS, 12 J), **imi-14** is a potential candidate as a high-performance energetic material.



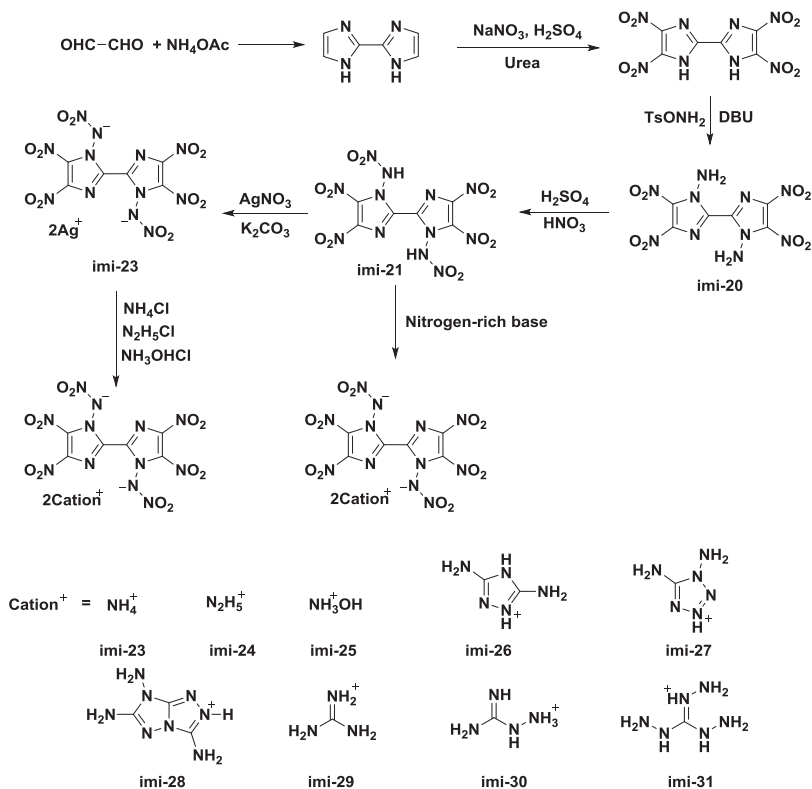
Scheme 18 *N*-trinitroethylation of nitroimidazoles.





**Scheme 19** High energy density energetic salts based on 1-nitramino-2,4-dinitroimidazole.

Compared to fully C-nitrated TNP, trinitroimidazole is less stable both thermally and chemically. However, the fully C-nitrated bisimidazole, i.e., 4,4',5,5'-tetranitro-1*H*,1'*H*-2,2'-biimidazole competes well with respect to energetic performance and sensitivity and has been studied as a precursor to nitrogen-rich salts (2012ZAAC1278). Further research efforts in searching for bisimidazole-based HEDMs are focused on the utilization of the *N*-nitramino functionality. Analogous to the *N*-amination reported previously, the *N,N'*-diamino compound (**imi-20**) was obtained in moderate yield (Scheme 20). A modified nitration using concentrated sulfuric acid and fuming nitric acid gave the *N,N'*-dinitramino compound **imi-21** in 81% yield (2016CEJ2108). The most exciting feature of **imi-20** and **imi-21** is the high experimental densities which exceed that of HMX (**imi-20**, *d*, 1.93 g/cm<sup>3</sup>; **imi-21**, *d*, 1.94 g/cm<sup>3</sup>; HMX, *d*, 1.90 g/cm<sup>3</sup>). Compound **imi-21** was further confirmed by single-crystal X-ray crystallography. For **imi-21**, the crystal density of 2.007 g/cm<sup>3</sup> at 100 K matches the

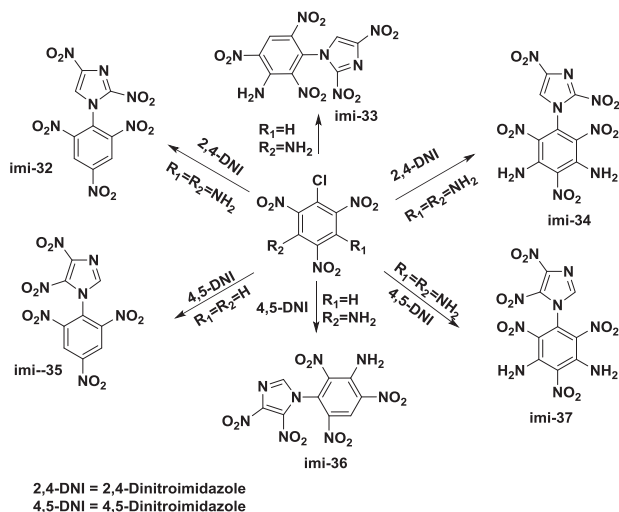


**Scheme 20** Synthesis of *N,N'*-nitroamino 4,4',5,5'-tetranitro-2,2'-biimidazole and its energetic salts.

experimental data and ranks the highest in any reported imidazole-based CHNO compounds.

As a result of high density and positive heat of formation, **imi-21** exhibited excellent detonation performance and could be classified as a high explosive. Furthermore, energetic salts prepared from **imi-21** show good densities and favorable detonation properties ( $P$ , 29.5–38.2 GPa,  $\nu_D$ , 8409–9169 m/s), with moderate to good impact and friction sensitivities (IS, 5–30 J; FS, 60–240 N). Compared to expensive nitronium tetrafluoroborate, the nitration of the acid-sensitive *N*-amino group using H<sub>2</sub>SO<sub>4</sub>/HNO<sub>3</sub> at low temperature enables an economical route to nitrogen and oxygen-rich energetic materials.

Nucleophilic aromatic substitution plays a pivotal role in the design of advanced energetic compounds by virtue of C–N bond formation. Chloro-substituted polynitrobenzenes are featured with high reaction



**Scheme 21** Synthesis of *N*-nitrobenzyl imidazole derivatives.

activity with some energetic nucleophilic reagents. A family of new energetic benzene-imidazoles were obtained from dinitroimidazole with diversified chloro-substituted polynitrobenzenes (Scheme 21) (2013NJC2837). X-ray crystallographic analysis indicated good to excellent experimental densities ranging between 1.75 and 1.84 g/cm<sup>3</sup> for these bicyclic energetic molecules (**imi-32**–**imi-37**). Of them, **imi-34** has the highest density of 1.842 g/cm<sup>3</sup> with detonation properties ( $P$ , 32.49 GPa;  $\nu_D$ , 8440 m/s) comparable to TATB.

## 4. TRIAZOLE-BASED ENERGETIC MATERIALS

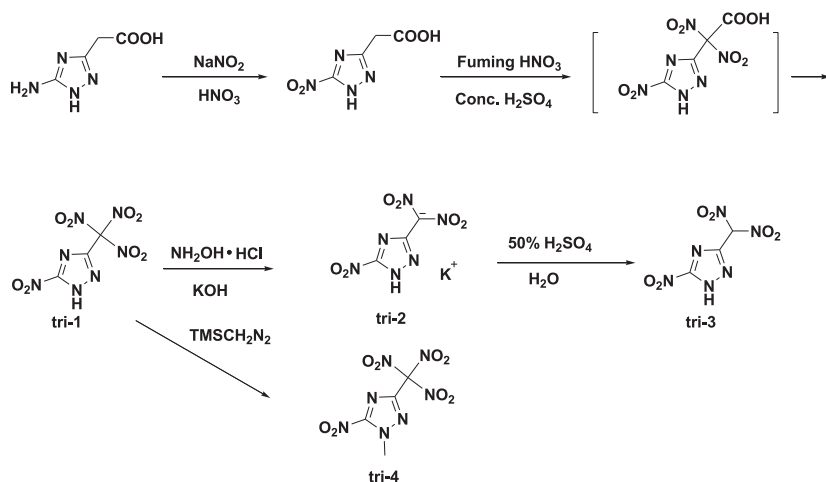
Triazoles are five-membered heterocycles containing three nitrogen atoms and two carbon atoms, which are either 1,2,3-triazole and 1,2,4-triazole. In general, the heat of formation and density of 1,2,3-triazole is higher than that of 1,2,4-triazole. Currently, there is a much larger number of energetic 1,2,4-triazole derivatives than energetic 1,2,3-triazole derivatives due to the synthetic difficulty for 1,2,3-triazole. In comparison to imidazole, pyrazole, and tetrazole, triazole has a moderate nitrogen content, which may be conducive to finding a balance between performance and stability.

With high oxygen content, positive oxygen balance, and low production cost, ammonium perchlorate (AP) has long been used as the preferred

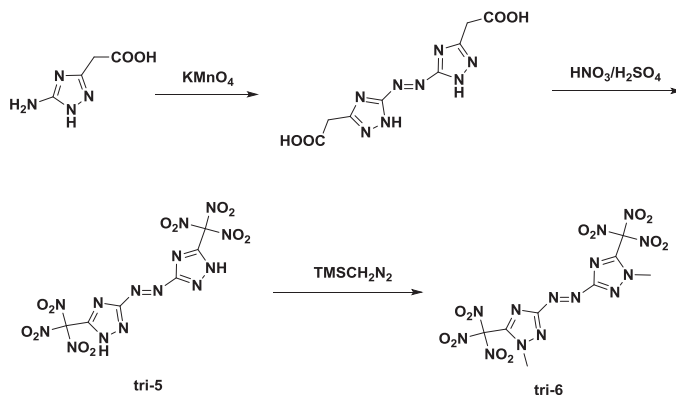
oxidizer in solid rocket and missile propellants. Nevertheless, the decomposition product of AP, i.e., hydrogen chloride leads to serious environmental concerns (2014JA16102). Driven by the increasing demands for seeking green propellants, the scientific community pays more attention to alternative solid oxidizers to replace AP. Polynitromethyl moieties, such as trinitromethyl and dinitromethyl groups, are considered to be promising functionalities needed to provide an adequate oxygen supply in the design of green energetic oxidizers.

Given the promising density and stability of 1,2,4-triazoles, introduction of a polynitromethyl functionality is a highly appealing strategy toward high-density oxidizers. The first attempt at destructive nitration of 2-(5-amino-1*H*-1,2,4-triazol-3-yl)acetic acid failed to yield the desired trinitromethyl product (2011JA6464). Under similar nitrating conditions, 2-(5-nitro-1*H*-1,2,4-triazol-3-yl)acetic acid was converted to the desired product **tri-1** via a dinitro intermediate (Scheme 22). Using hydroxylammonium chloride in aqueous potassium hydroxide, potassium dinitro(5-nitro-1*H*-1,2,4-triazol-3-yl)methanidate (**tri-2**) was obtained and following acidification with 50% H<sub>2</sub>SO<sub>4</sub> resulted in the dinitromethyl product **tri-3**. Treated with commercially available trimethylsilyl diazomethane, the *N*-methyl product **tri-4** was obtained and, as expected, showed better impact sensitivity than that of **tri-3**.

Other than nitro-substituted azoles, destructive nitration also leads to bis(1,2,4-triazole), giving the azo-bridged product **tri-5** (Scheme 23).



**Scheme 22** Synthesis of trinitromethyl and dinitromethyl 1,2,4-triazoles.

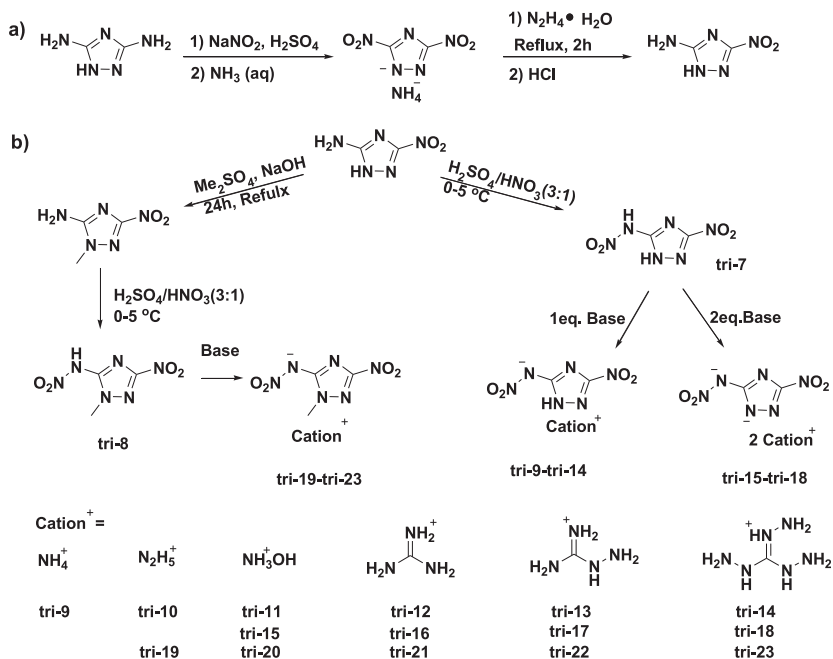


**Scheme 23** Synthesis of azo-bridged trinitromethyl 1,2,4-triazoles.

Also, a similar methylation of **tri-5** was tried using trimethylsilyl diazomethane to yield **tri-6**. Through experimental and theoretical studies, these polynitro-substituted 1,2,4-triazoles exhibited excellent energetic properties, such as density, detonation performance, and impact sensitivity. Based on the high density of  $1.94 \text{ g/cm}^3$  and a positive oxygen balance of +9.12% (based on carbon dioxide), **tri-1** may be an appealing replacement of AP as a solid rocket oxidizer.

5-Amino-3-nitro-1,2,4-triazole (ANTA), which can be prepared easily by a two-step synthesis from 3,5-diamino-1,2,4-triazole, is one of the most promising compounds among the triazole-based energetic materials because of the high density and low sensitivity (2012EJIC2429). In a mixture of 98%  $\text{H}_2\text{SO}_4$  and 100%  $\text{HNO}_3$  in a molar ratio of 3:1, nitration of ANTA gives 3-nitro-5-nitramino-1*H*-1,2,4-triazole (**tri-7**) (Scheme 24) in an isolated yield of 76%. Undergoing *N*-methylation and nitration, 1-methyl-5-nitramino-3-nitro-1,2,4-triazole (**tri-8**) was prepared from ANTA. Using nitrogen-rich bases, a series of monocationic and dicationic energetic salts (**tri-9**–**tri-23**) were obtained from **tri-7** and **tri-8**. Compound **tri-7** showed a rather high density of  $1.938 \text{ g/cm}^3$  with a high impact sensitivity of 1 J, whereas its energetic salts showed moderate densities and better sensitivities, falling between  $1.69$ – $1.75 \text{ g/cm}^3$  and 6–40 J, respectively.

As promising energetic precursors, ANTA and 3,5-dinitro-1,2,4-triazole were functionalized using 1,3-dichloro-2-nitrazapropane. *N*-Alkylation of ANTA gives rise to the desired product **tri-24** with a minority of isomer (Scheme 25) (2013EJIC4667). In the preparation of 1,3-bis(3,5-dinitro-1,2,4-triazol-1-yl)-2-nitrazapropane (**tri-24**), the high reaction temperature

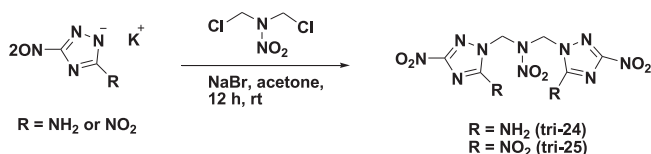


**Scheme 24** Synthesis of 3-nitro-5-nitramino-1*H*-1,2,4-triazole and 1-methyl-5-nitramino-3-nitro-1,2,4-triazole-based energetic salts.

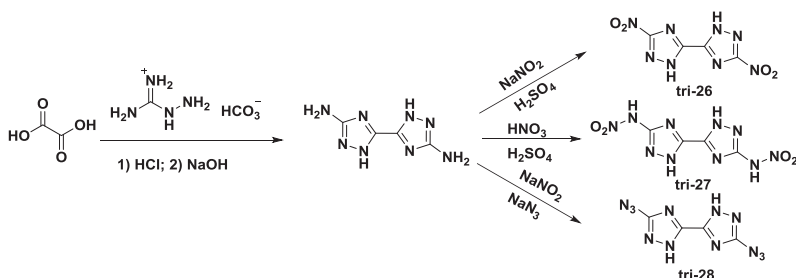
led to chloro-substitution as a side reaction, whereas the reaction carried out at room temperature gave the pure product in a lower yield. With respect to energetic properties, **tri-24** exhibited higher density and detonation performance than **tri-23** (**tri-23**,  $d$ , 1.69 g/cm<sup>3</sup>,  $P$ , 25.0 GPa,  $v_D$ , 8012 m/s; **tri-24**,  $d$ , 1.90 g/cm<sup>3</sup>,  $P$ , 37.3 GPa,  $v_D$ , 9089 m/s).

The preparation procedure for 5,5'-diamino bis(1,2,4-triazoles) was modified recently and nitro-, nitramino-, and azido-substituted derivatives (**tri-26**–**tri-28**) were obtained by virtue of functional group transformations (Scheme 26) (2012CEJ16742).

In comparison, the synthetic approach to 5,5'-dinitromethyl bis(1,2,4-triazole) (**tri-29**) is more complicated. Diethyl oxalimidate was first formed



**Scheme 25** Syntheses of energetic nitrotriazoles from 1,3-dichloro-2-nitrazopropane.



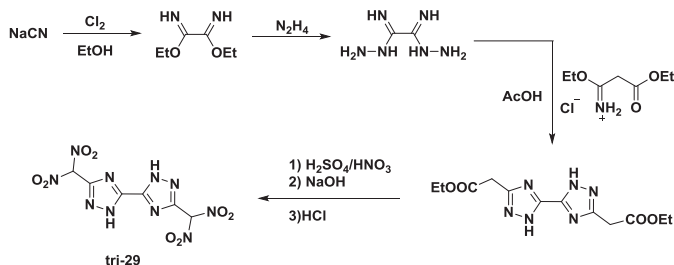
**Scheme 26** Synthesis of the energetic bis(1,2,4-triazole) derivatives.

by chlorination of sodium cyanide in ethanol, and the subsequent reactions with hydrazine and 3-ethoxy-3-iminopropionic acid ethyl ester hydrochloride gave rise to the diacetate intermediate, which was then converted to **tri-29** via nitration, decarboxylation, and acidification (Scheme 27). Compound **tri-29** has an outstanding density of  $1.95 \text{ g/cm}^3$  and an impact sensitivity of 20 J.

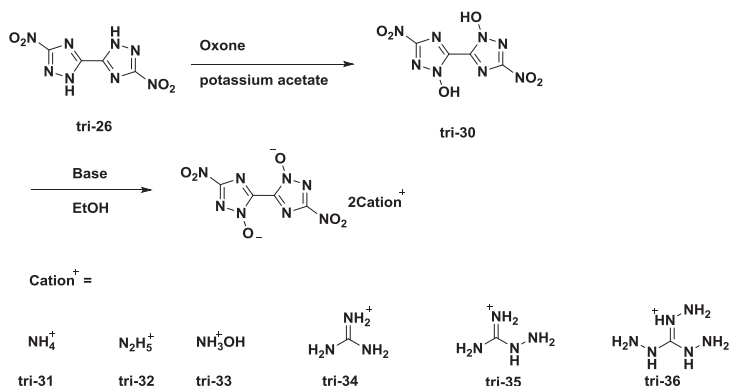
Generally, the introduction of the N-O functionality into energetic heterocycles has a major positive impact on density. Employing potassium acetate as the pH buffer, reaction of Oxone<sup>®</sup> and **tri-26** resulted in dinitro-bis-1,2,4-triazole-1,1'-diol (**tri-30**) in 81% yield (Scheme 28) (2013JA9931).

Subsequent reactions of **tri-31** with various nitro-rich reagents, such as hydrazine monohydrate, guanidinium bicarbonate, and triaminoguanidinium chloride, resulted in a family of new HIEMs. Of them, the overall energetic properties of **tri-33** are superior to the currently used RDX (**tri-33**,  $d$ ,  $1.90 \text{ g/cm}^3$ ,  $P$ , 39.0 GPa,  $v_D$ , 9087 m/s, IS, 40 J, FS, 360 N; RDX,  $d$ ,  $1.81 \text{ g/cm}^3$ ,  $P$ , 34.9 GPa,  $v_D$ , 8748 m/s, IS, 7 J, FS, 120 N).

In addition to introducing the N-O functionality, N-N functionalization of mono- and bis-1,2,4-triazoles was reported. The N-amino, N-nitro,



**Scheme 27** Synthesis of high-density 5,5'-dinitromethyl bis(1,2,4-triazole).



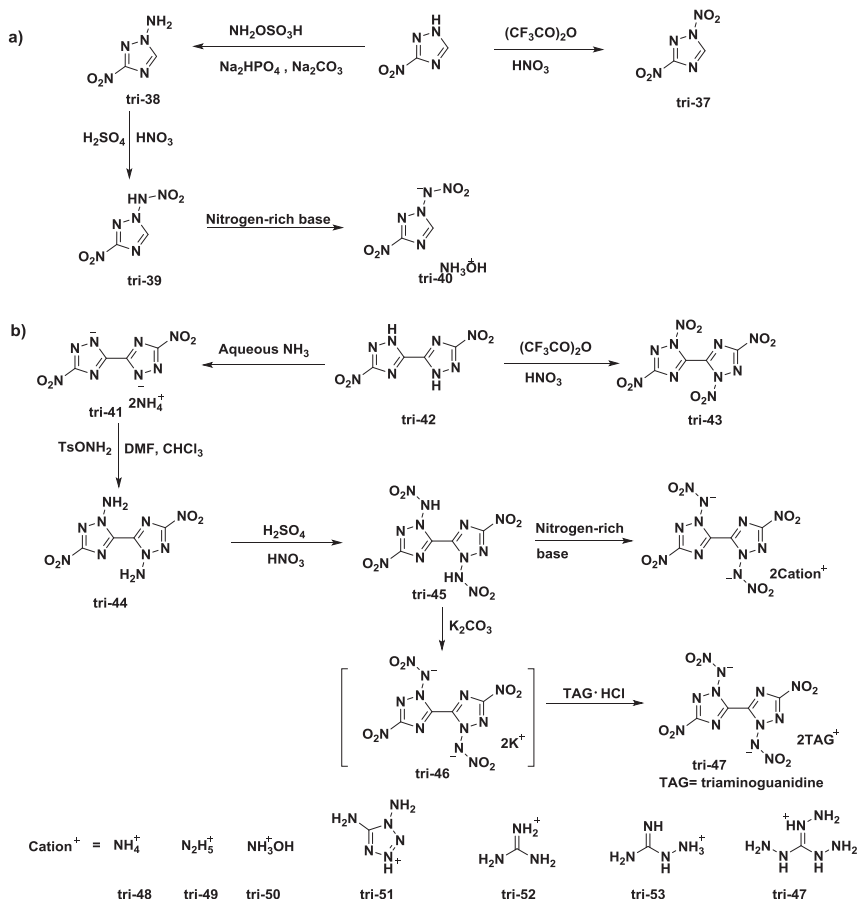
**Scheme 28** Synthesis of dinitro-bis-1,2,4-triazole-1,1'-diol and its energetic salts.

and *N*-nitramino groups were introduced and the resulting compounds were fully characterized. The *N*-amino products, **tri-38** and **tri-44**, have low sensitivities with moderate densities and detonation performances (Scheme 29) (2015AN14721). While most nitro-substituted energetic molecules are more stable than the nitramino analogs, the stability of the *N,N'*-nitramino compound, **tri-45**, shows better chemical and thermal stabilities in comparison to the *N,N'*-nitramino compound, **tri-43**. By pairing with nitrogen-rich cations, the stability of the energetic salts is enhanced by the increasing hydrogen-bonding interactions. Based on the evaluation of integrated properties, the hydroxylammonium salt, **tri-50**, is comparable to the high explosive HMX (**tri-50**,  $d$ , 1.86 g/cm<sup>3</sup>,  $P$ , 39.1 GPa,  $v_D$ , 9330 m/s, IS, 8 J, FS, 120 N; HMX,  $d$ , 1.90 g/cm<sup>3</sup>,  $P$ , 39.5 GPa,  $v_D$ , 9320 m/s, IS, 7 J, FS, 120 N)

In 2009, a novel synthetic methodology enabling the introduction of a nitrogen-rich tetrazole moiety into secondary amines was developed (2015JMCA163). An extensive study involving the reaction of ANTA with cyanogen azide demonstrated a facile synthesis of 3-nitro-1-(2H-tetrazol-5-yl)-1*H*-1,2,4-triazol-5-amine (**tri-54**) (Scheme 30). The energetic salts of **tri-54** have promising detonation properties and low impact sensitivities, indicating their application potentials as RDX replacements.

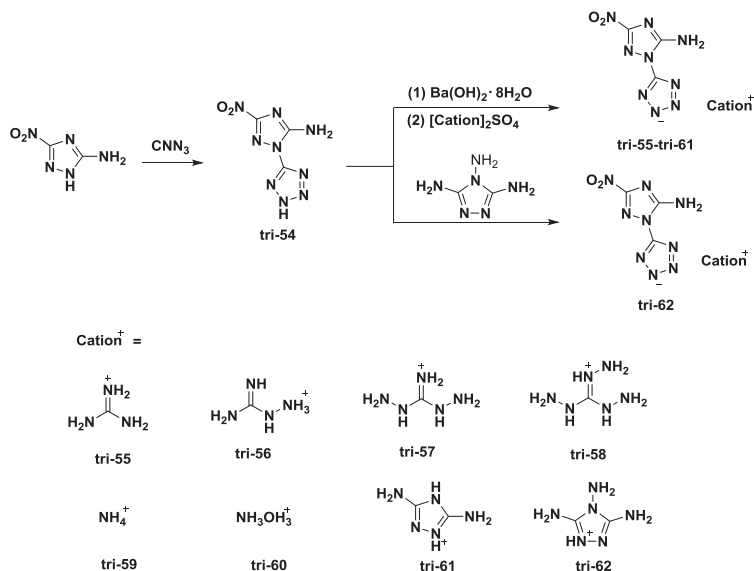
Oxidative coupling transformation from the amino group to the azo group is one of the most important reaction types in construction of high-nitrogen energetic materials. Although azo formation from the C-NH<sub>2</sub> moiety has been well established for a long time, recent intensive studies of *N*-NH<sub>2</sub> compounds illustrated a favorable pathway to a novel family of catenated nitrogen-atom chain-based HEDMs (2014CEJ6707).





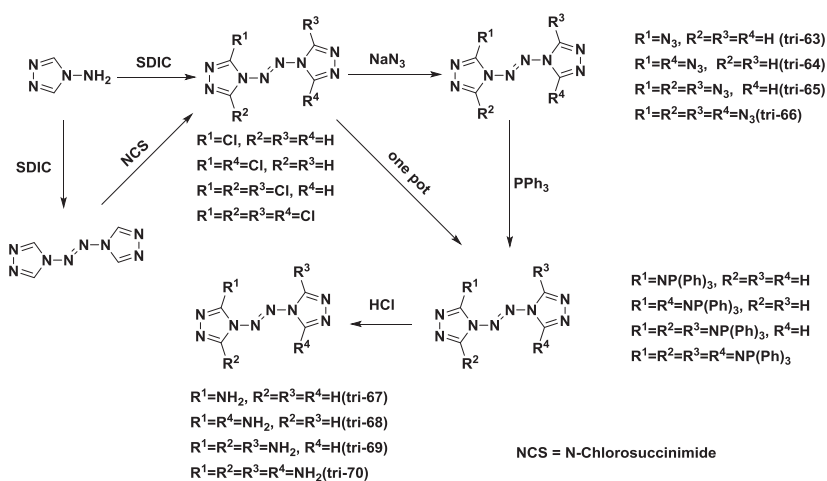
By employing chlorine-containing oxidants, i.e., SDIC, trichloroisocyanuric acid, or tert-butyl hypochlorite (t-BuOCl), a series of *N,N'*-azo-bridged compounds was synthesized by forming an *N,N'*-azo bridge between two azole rings.

By a simultaneous chlorination and N-oxidation, a series of *N,N'*-azo-bridged chloro bis (1,2,4-triazoles) was obtained using SDIC as the key reagent. Treated with sodium azide in dimethylformamide (DMF) at room temperature, the azido substituted derivatives (**tri-63–tri-66**) were readily prepared and the following reduction using triphenyl phosphine and diluted aqueous HCl gave rise to the corresponding amino substituted compounds (**tri-67–tri-70**) (Scheme 31) (2012CEJ16562).



**Scheme 30** 3-Nitro-1-(2H-tetrazol-5-yl)-1H-1,2,4-triazol-5-amine and its energetic salts.

Through a theoretical evaluation, 3,3',5,5'-tetra-(azido)azo-1,2,4-triazole (**tri-66**) has the highest positive heat of formation of 6933 kJ/kg (2274 kJ/mol) among the reported energetic materials so far. With a nitrogen content of 85.36% and a good density of 1.79 g/cm<sup>3</sup>, the detonation velocity and detonation pressure of **tri-66** competes well with HMX.

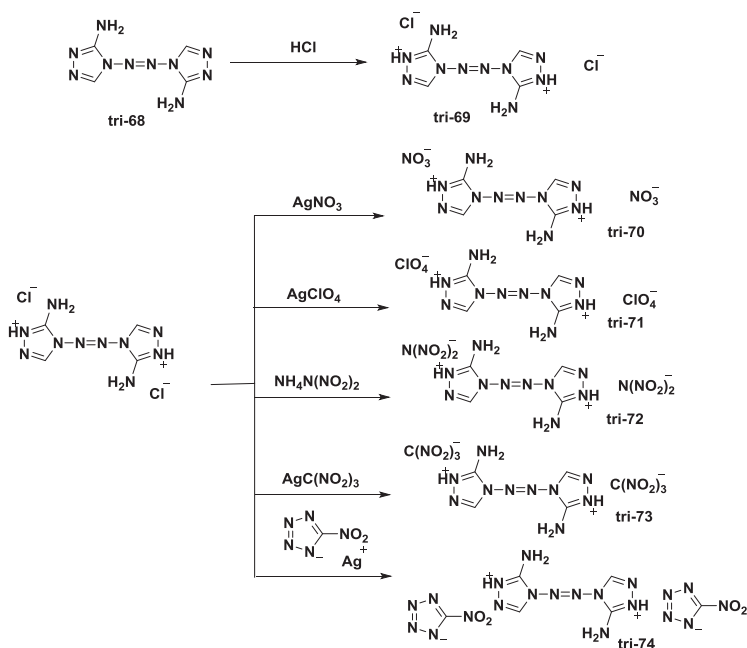


**Scheme 31** Synthesis of polysubstituted derivatives based on the *N,N'*-azo link.

Featured with outstanding thermal stability and nitrogen content, **tri-68** was used as a high-energy cation to react with various anions, including nitrate, perchlorate, dinitroamide, trinitromethylate, and 5-nitro tetrazolate (2014JMCA15978). With an excellent density of 1.87 g/cm<sup>3</sup> and a positive oxygen balance of 6.4%, energetic salt, **tri-72**, exhibits the highest detonation properties ( $P$ , 42.9 GPa;  $v_D$ , 9569 m/s) (Scheme 32). Additionally, **tri-70** has good detonation performance and mechanical sensitivities, which are superior to RDX and HMX.

A significant feature of aromatic azoles is the coplanar structure, which is conducive to lowering the mechanical sensitivity, as well as improving the packing coefficient. However, compared to monocyclic azole rings, the C–C-bridged bis(azoles) are not able to retain planarity due to the rotation at the C–C bond. In addition, some functionalities, such as trinitromethyl and trinitroethyl groups, are not coplanar with the heterocyclic backbones because of steric hindrance.

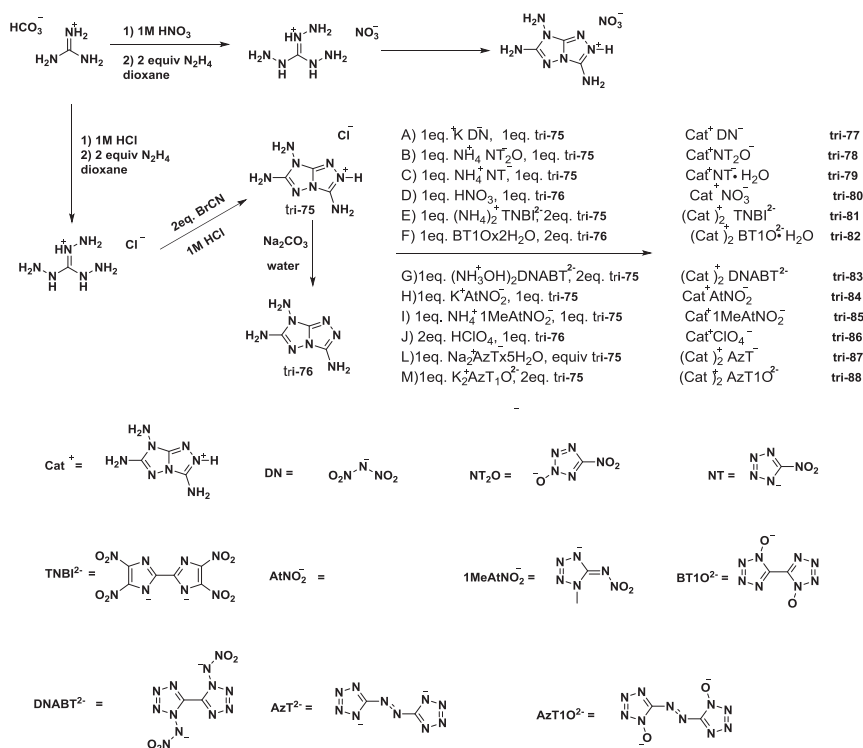
Fused azoles are a unique class of energetic backbones. By sharing two carbon or nitrogen atoms, two neighboring rings are coplanar with each



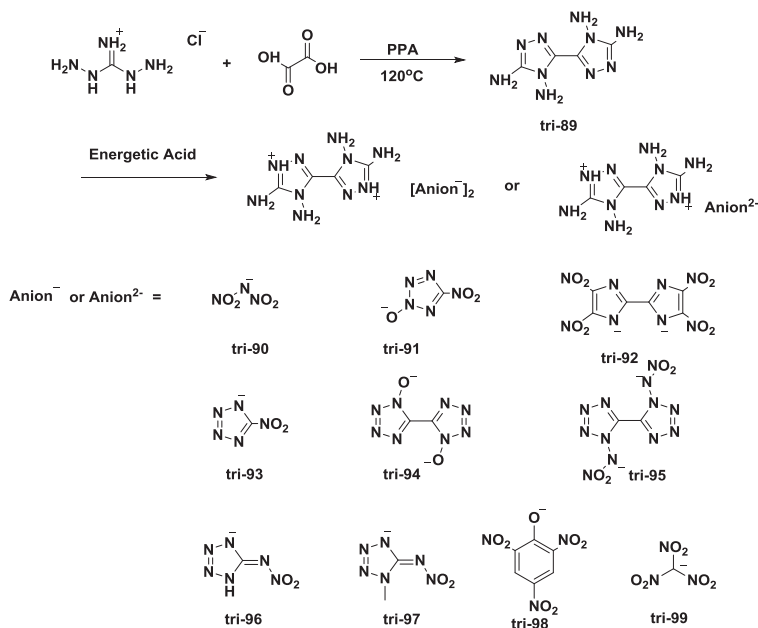
**Scheme 32** Synthesis of energetic salts based on 3,3'-diamino-4,4'-azobis-1,2,4-triazole.

other. 3,6,7-Triamino-[1,2,4]triazolo[4,3-*b*] [1,2,4]triazole is the most promising representative compound in the recent study of energetic materials (2015CEJ9219, 2015JMCA2685, 2015JMCA8606). The fused azole-based energetic salts feature high density, positive heat of formation, and good detonation performance. 3,6,7-Triamino-[1,2,4]triazolo[4,3-*b*] [1,2,4]triazolium nitrate (**tri-77**) shows strikingly high thermal and insensitive behavior with a decomposition temperature of 280 °C and an impact sensitivity of 40 J (Scheme 33). In addition, the calculated detonation velocity of **tri-80** is slightly superior to that of RDX.

Because the nitrogen-rich 1,2,4-triazolium cations show great potential in the design of thermally stable HEDMs, continuing studies of ionic derivatives based on 4,4',5,5'-tetraamino-3,3'-bi-2,4-triazolium cation were reported (2015JMCA2685). When the bistriazole cation was combined with a variety of oxygen-rich counteranions, the energetic salts were readily obtained and their physicochemical properties fully



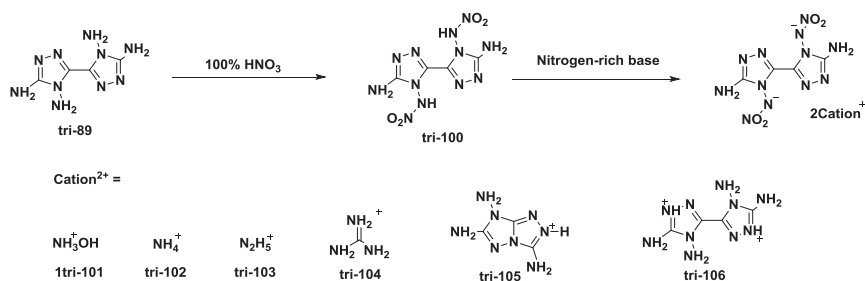
**Scheme 33** Synthesis of energetic salts based on 3,6,7-triamino-[1,2,4]triazolo[4,3-*b*] [1,2,4]triazole.



**Scheme 34** Ionic derivatives based on 4,4',5,5'-tetraamino-3,3'-bi-2,4-triazolium cation.

characterized. With a high decomposition temperature ( $T_d$ , 200 °C), the thermal behavior of the dinitramide salt, **tri-90**, is superior to nearly all the known energetic dinitramides (Scheme 34).

In addition to playing the role of energetic cation, **tri-89** was used as precursor for nitramine-based HEDMs (2016CAJ844). In the presence of 100%  $\text{HNO}_3$ , selective *N*-amino nitration of **tri-89** gave the *N,N'*-dinitramino compound, **tri-100**, which has enhanced energetic performance and retained thermal stability (Scheme 35). Among the energetic salts prepared



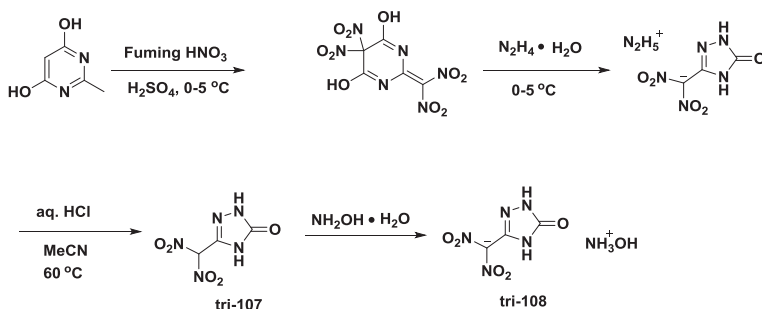
**Scheme 35** Synthesis of 5,5'-diamino-4,4'-dinitramino-3,3'-bi-1,2,4-triazole and its energetic salts.

from **tri-100**, the hydroxylammonium salt, **tri-101**, has a higher density and detonation performance than those of the molecular form **tri-100** (**tri-100**,  $d$ , 1.756 g/cm<sup>3</sup>,  $P$ , 31.2 GPa,  $\nu_D$ , 8846 m/s; **tri-101**,  $d$ , 1.763 g/cm<sup>3</sup>,  $P$ , 34.0 GPa,  $\nu_D$ , 9313 m/s).

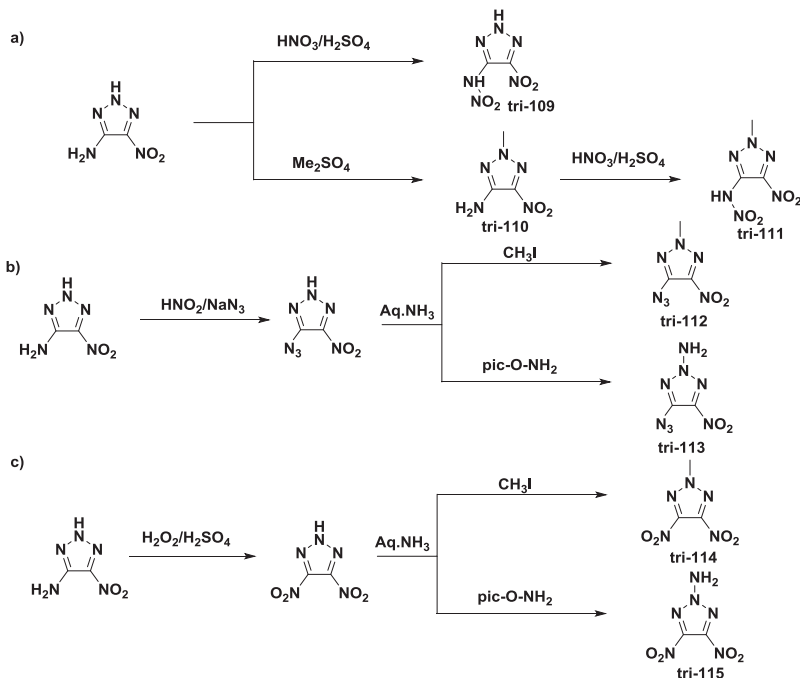
Generally, ionic CHNO explosives have lower densities than their parent nonionic molecules. An exciting energetic compound, hydroxylammonium 3-dinitromethyl-1,2,4-triazolone (**tri-108**), was synthesized and a comparative study with its nonionic precursor **tri-107** was carried out (Scheme 36) (2015JA1697). Compared to **tri-107**, **tri-108** exhibits several advantages, e.g., higher density, higher detonation performance, enhanced thermal stability, and lower impact and friction sensitivities, which was further supported by theoretical calculations associated with the analysis of hydrogen bonding and  $\pi$  stacking interactions.

Featuring three contiguous nitrogen atoms, the 1,2,3-triazole ring is rather stable as a highly energetic backbone. In some cases, the thermal stability of 1,2,3-triazole compounds is even better than those of their isomer, 1,2,4-triazole. For example, the decomposition temperature of 4-amino-5-nitro-1,2,3-2*H*-triazole ( $T_d$ , 297 °C) is higher than that of ANTA (243 °C) (2013JMCA585). Utilizing nitration, methylation, or amination, several energetic functionalities were easily introduced (Scheme 37). The symmetric compound, **tri-115**, is the most favorable analog in the derivatives of 5-nitro-1,2,3-2*H*-triazole, as confirmed by the overall properties which are higher than RDX (**tri-115**,  $d$ , 1.868 g/cm<sup>3</sup>,  $P$ , 36.2 GPa,  $\nu_D$ , 8843 m/s, IS, 30 J; RDX,  $d$ , 1.81 g/cm<sup>3</sup>,  $P$ , 34.9 GPa,  $\nu_D$ , 8748 m/s, IS, 7 J).

N-Functionalization of nitrogen-rich heterocycles offers a diversified designing strategy of HEDMs. By constructing versatile bonds, such as N–C, N–N, and N–O bonds, the properties of energetic materials are



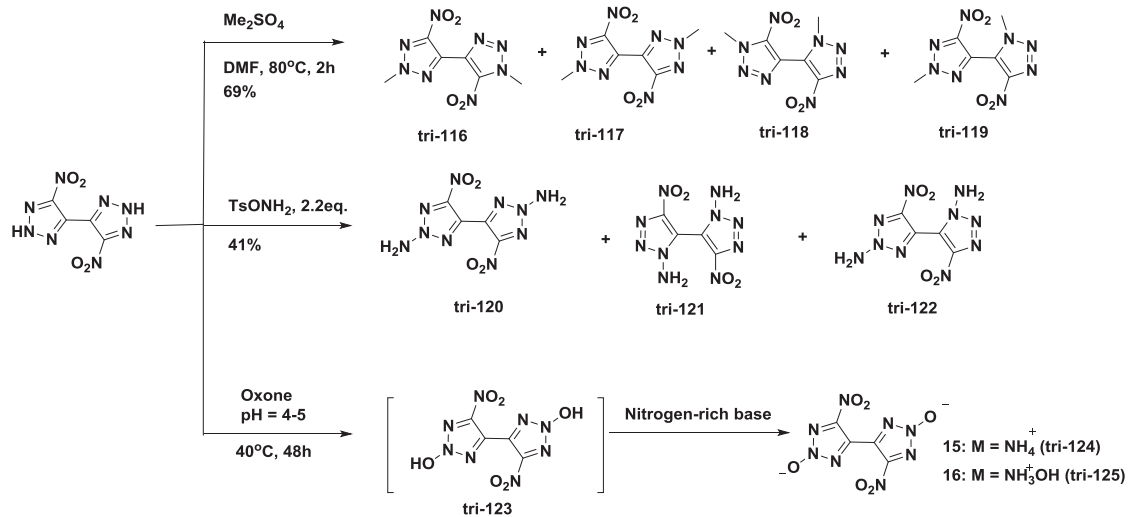
**Scheme 36** Synthesis of 3-dinitromethyl-1,2,4-triazolone (**tri-107**) and its hydroxylammonium salt (**tri-108**).



Scheme 37 Derivatives of 5-nitro-1,2,3-2H-triazole.

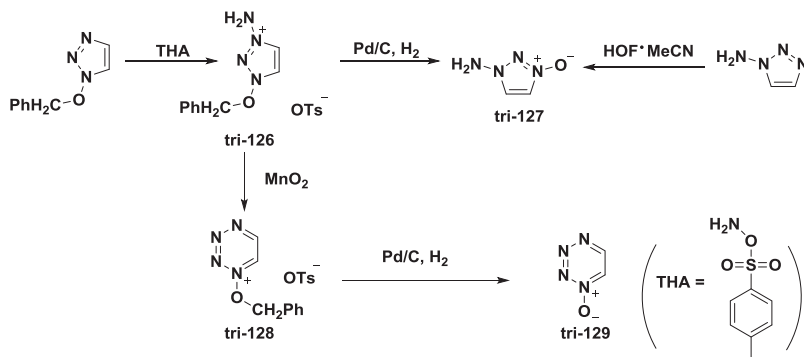
modified for different applications. The *N*-methylation of 4,4'-bis(5-nitro-1,2,3-2H-triazole) gives rise to four isomers (**tri-116**–**tri-119**), which have moderate densities and detonation performances, but with excellent low sensitivities (Scheme 38) (2015AN6260). Similar isomers are found with *N*-amination and three isomers can be isolated. Treated with Oxone<sup>®</sup> in pH buffer, the *N*-oxidized product **tri-123** is too unstable to be isolated neat. To obtain more stable derivatives, two energetic salts, **tri-124** and **tri-125**, were prepared and their energetic properties were evaluated. Among these ionic derivatives, the hydroxylammonium salt **tri-125** exhibited the highest detonation performance (*P*, 39.1 GPa, *v*<sub>D</sub>, 9171 m/s).

1-Amino-1,2,3-triazole-3-oxide (**tri-126**) was first prepared from 1-amino-1,2,3-triazole by virtue of hypofluorous acid oxidation (Scheme 39) (2015PEP491). Alternatively, **tri-127** could be obtained from 1-(benzyloxy)-1,2,3-triazole using *N*-amination and hydrogenation reduction. Meanwhile, the intermediate **tri-128** was used to synthesize 1,2,3,4-tetrazine-1-oxide (**tri-129**), undergoing spontaneous nitrene formation and ring expansion, with Pd/C catalyzed reduction. In addition to NMR spectra, **tri-127** was further confirmed by single-crystal X-ray structure.



Scheme 38 Energetic derivatives of 4,4'-bis(5-nitro-1,2,3-*H*-triazole).



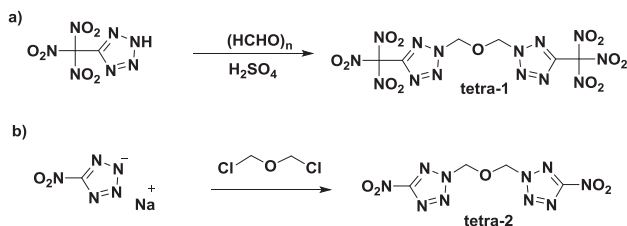


**Scheme 39** The transformation from 1,2,3-triazole to 1,2,3,4-tetrazine.

## 5. TETRAZOLE-BASED ENERGETIC MATERIALS

As a promising nitrogen-rich backbone, the nitrogen content (79.98%) of 1*H*-tetrazole ranks the highest among the common nonsubstituted five-membered azoles and six-membered azines with exception of the unstable 1*H*-pentazole. Moreover, the numerous contiguous N–N bonds give rise to a high heat of formation, as well as to powerful energy release upon explosion. The main decomposition product, dinitrogen gas, also meets the requirement of the green chemistry concept.

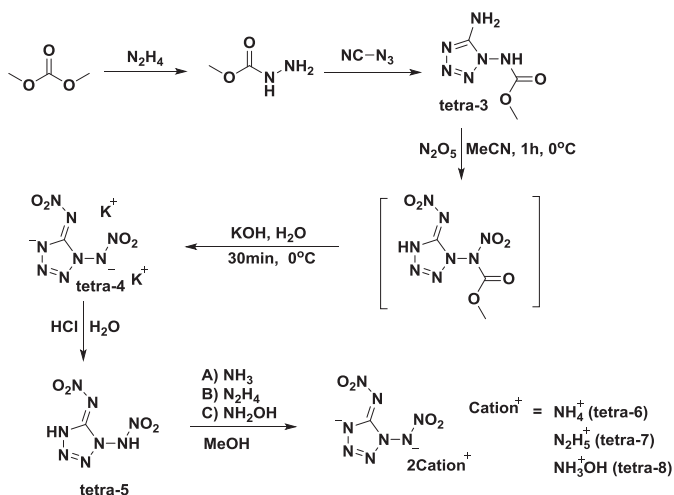
*N,N'*-Ether linkages could be readily introduced to some nitrogen-rich tetrazole compounds, such as 5-trinitromethyltetrazole and 5-nitrotetrazole (Scheme 40) (2015JMCA15576). Compared to their precursors, the resulting bis(tetrazoles) (**tetra-1** and **tetra-2**) show low acidity and better thermal behavior. More significantly, they have high density and excellent detonation properties (**tetra-1**, *d*, 1.825 g/cm<sup>3</sup>; *P*, 35.1 GPa; *v*<sub>D</sub>, 8909 m/s; **tetra-2**, *d*, 1.846 g/cm<sup>3</sup>; *P*, 34.6 GPa; *v*<sub>D</sub>, 8892 m/s).



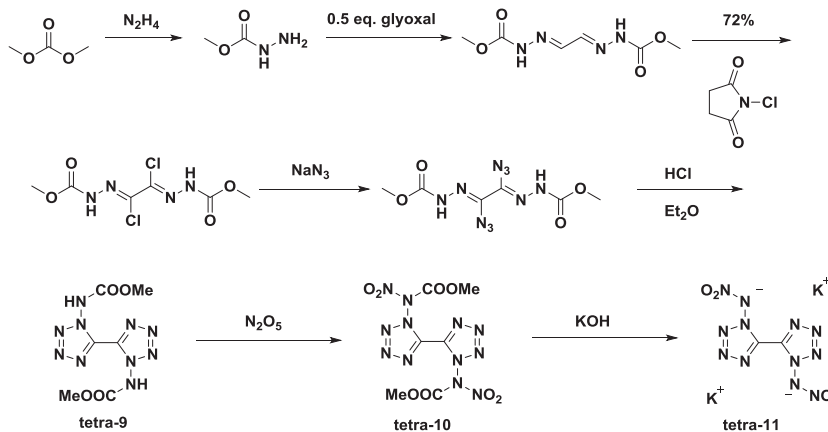
**Scheme 40** Synthesis of energetic *N,N'*-ether-bridged tetrazoles.

Although some *C*-nitramino or *N*-nitramino tetrazoles were reported in early studies, the fully *C*- and *N*-nitramino functionalized tetrazoles were still a long-term challenging high-energy molecules. Using cyanogen azide as the key reagent, *N*-protected 1,5-diamino tetrazole was formed. The following  $N_2O_5$ -induced nitration and KOH-induced alkali hydrolysis resulted in the dipotassium salt **tetra-4** (Scheme 41) (2015AN10299). 1,5-Di(nitramino)tetrazole (**tetra-5**) was obtained from **tetra-4** by the treatment with dilute aqueous HCl. Compounds **tetra-4**, **tetra-5**, and the energetic salts (**tetra-6**–**tetra-8**) showed strikingly excellent detonation properties, acceptable thermal stabilities, and extreme sensitivities ( $P$ , 31.5–52.2 GPa;  $v_D$ , 9078–10,011 m/s;  $T_d$ , 110–240 °C; IS, 1–1.5 J; FS, 5–30 N).

In spite of the highly sensitive feature of the *N*-nitramino tetrazoles, their potential application as primary explosives has been studied (2014AN8172). The most currently used primary explosives, e.g., lead azide and lead picrate are very toxic to the environment. A similar synthetic strategy was employed for *N,N'*-ditramino bis(tetrazole). Using bis(carbamates) as the intermediate, the tetrazole ring is effectively constructed in the presence of HCl in ether solution. Then *N*-methoxycarbonyl-protected **tetra-9** can be smoothly nitrated with  $N_2O_5$  (Scheme 42). The final deprotection was carried out in aqueous potassium hydroxide to give the potassium 1,1'-dinitramino-5,5'-bistetrazolate (**tetra-11**). Combining the high nitrogen content and high density, potassium salt **tetra-11** is an ideal replacement for most toxic heavy metal-based primary explosives.



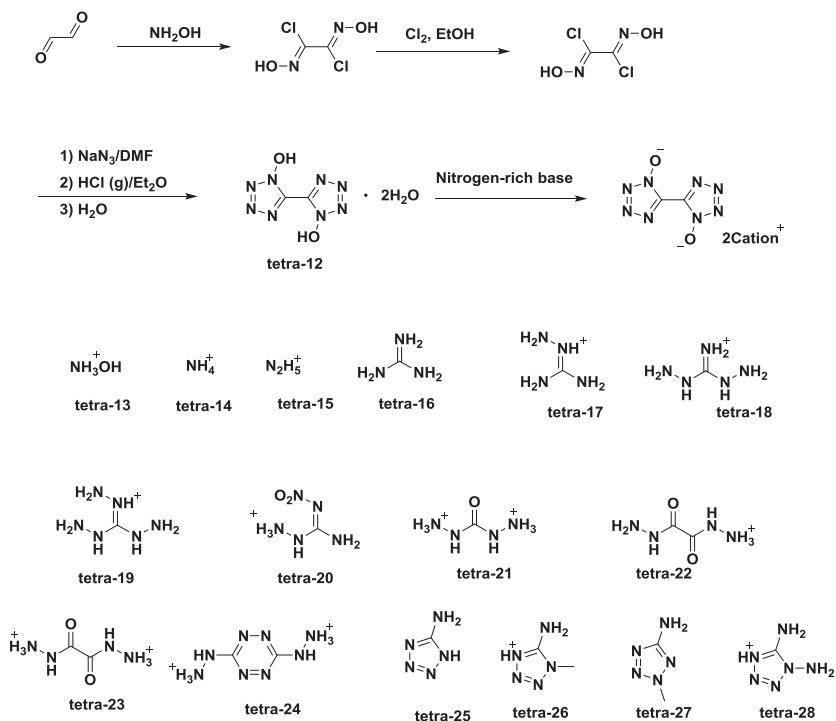
**Scheme 41** Synthesis of 1,5-di(nitramino)tetrazole and its energetic salts.



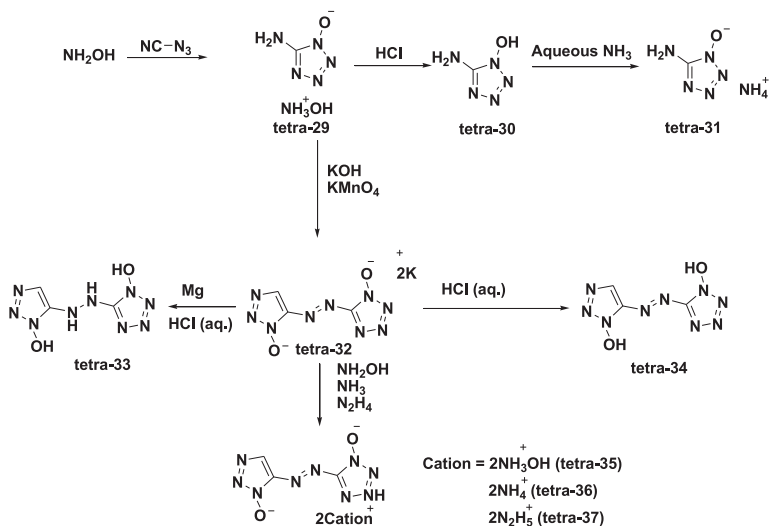
**Scheme 42** Synthesis of potassium 1,1'-dinitramino-5,5'-bistetrazolate.

The introduction of an N–N functionality, e.g., *N*-amino, *N*-nitramino, or *N,N'*-azo groups, enhances the detonation performance greatly; however, their high sensitivity restricts them to primary explosives. In comparison, introducing an N–O functionality is a more favorable strategy to produce low sensitive secondary explosives. *N*-Hydroxyl-substituted tetrazoles have become the hottest area of research in nitrogen-rich HEMDs. 5,5'-Bistetrazole-1,1'-diol dihydrate (**tetra-12**) was synthesized and characterized by Tselinskii in 2001 (Scheme 43) (2001RJOC430). Later, the preparation method was modified and a series of energetic salts (**tetra-13**–**tetra-28**) were obtained by the treatment of **tetra-12** with nitrogen-rich bases (2012JMC20418). Among these new energetic salts, dihydroxylammonium 5,5'-bistetrazole-1,1'-diolate (**tetra-13**) exhibits great density, good thermal stability, excellent detonation properties with low impact and friction sensitivities (**tetra-13**,  $d$ , 1.877 g/cm<sup>3</sup>;  $T_d$ , 221 °C;  $P$ , 42.4 GPa;  $\nu_D$ , 9698 m/s; IS, 20 J; FS, 120 N). Based on low production cost, super energetic performance, and good stability, the overall properties of **tetra-13** are superior to most known high explosives, e.g., RDX, HMX, and CL-20.

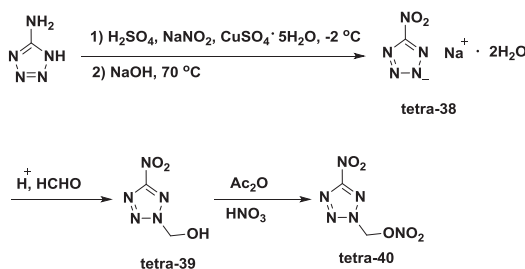
As the great potential of tetrazol-1-olate was demonstrated by **tetra-13**, an extensive study of amino- and azo-substituted tetrazole-1-olates was carried out. The cyclization of cyanogen azide and hydroxylamine resulted in hydroxylammonium 5-aminotetrazole-1-olate (**tetra-29**) in excellent yield (Scheme 44) (2013CEJ4602). Treated with dilute aqueous hydrochloric acid, the salt **tetra-29** was converted to molecular form 5-aminotetrazole-1-ol (**tetra-30**), which could be reacted with aqueous ammonia to give



Scheme 43 Synthesis of 5,5'-bistetrazole-1,1'-diol dihydrate and its energetic salts.



Scheme 44 Synthesis of 5-aminotetrazole-1-ol and its energetic derivatives.



**Scheme 45** Synthesis of 5-nitro-2-nitratomethyl-tetrazole.

ammonium 5-aminotetrazole-1-olate (**tetra-31**). Using potassium permanganate in alkaline solution, azo-bridged potassium bis(5-aminotetrazole-1-olate) (**tetra-32**) was obtained. The reduction and acidification gave rise to **tetra-33** and **tetra-34**, respectively.

While *N*-NHNO<sub>2</sub> and *N*-OH groups play pivotal roles in the tetrazole-based HEDMs, another functionalized strategy using an *N*-CH<sub>2</sub>ONO<sub>2</sub> group extends the chemistry of energetic tetrazoles (2012M5040). Using sulfuric acid, sodium nitrite, copper (II) sulfate pentahydrate, and sodium hydroxide, 5-aminotetrazole was converted to sodium 5-nitro-tetrazolate via a diazonium salt. Further introduction of the (nitrooxy)methyl group was carried out using dilute sulfuric acid and aqueous formaldehyde. This was then treated with acetic anhydride and fuming nitric acid. The resulting product, **tetra-40**, has a good density, positive heat of formation, and high detonation performance (*d*, 1.801 g/cm<sup>3</sup>; Δ*H*<sub>f</sub>, 228.07 kJ/mol; *P*, 37.92 GPa; *v*<sub>D</sub>, 9260 m/s) (Scheme 45).

## 6. SUMMARY

Versatile family members of five-membered azole backbones promote better understanding of structure–property of HEDMs and provide diversified choices for the future design of HEDMs. The rational utilization of energetic functionalized groups with azole backbones is the key factor to balance energetic performance and molecular stability.

From the standpoint of nitrogen-rich requirement, tetrazole is the most favorable backbone to match the topic of green chemistry. There are few functionalized positions on the tetrazole ring which may restrict designing strategy. In comparison, although pyrazole and imidazole rings have less nitrogen content than tetrazole, the three CH moieties in the pyrazole or

imidazole ring enable more opportunities to introduce diverse functionalities.

In the recent progress of pyrazole-based energetic materials, TNP (**pyr-1**) is the most representative compound which exhibits more advanced overall properties than other fully nitrated azoles. Some nitramino functionalized pyrazoles and their ionic derivatives, such as **pyr-37**, **pyr-54**, and **pyr-71**, have high density and excellent detonation properties. With amino-nitro functionalities, **pyr-17**, **pyr-18**, **pyr-82**, and **pyr-84** are potential candidates for insensitive energetic materials arising from enhanced hydrogen-bonding interaction. The *N*-hydroxyl compounds **pyr-10** and **pyr-78** could be used for energetic oxidizers because of the high density and positive oxygen balance. In addition, the high density and highly thermal stability of **pyr-75** highlight the application potential of fused pyrazole-based HEDMs.

As an isomer of pyrazole, imidazole has received relatively less attention. However, in some comparative studies *N*-trinitroethylamino imidazoles showed better overall performance than those of the pyrazole analogs. *C*-/*N*-fully functionalized bis(imidazole), i.e., **imi-21**, has a strikingly high density (2.007 g/cm<sup>3</sup> at 100 K; 1.94 g/cm<sup>3</sup> at 298 K), which is higher than any known imidazole-based CHNO compound.

Among triazole-based energetic salts, **tri-31** and **tri-70** are as highly energetic as HMX, and more importantly, their mechanical sensitivities are as low as TATB. The trinitromethyl triazole, **tri-1**, and dinitromethyl triazole, **tri-29**, have positive oxygen balance and high densities of 1.94 and 1.95 g/cm<sup>3</sup>, respectively, and may be applied as oxygen carriers in energetic ingredients. The 1,2,3-triazole-based compound, **tri-110**, is a very promising molecular compound with overall properties superior to RDX.

Both *N*-nitroamino and *N*-hydroxyl functionalities have been investigated for tetrazole backbones. With high nitrogen content, good detonation properties and extremely high sensitivity, *N*-nitroamino tetrazoles and their energetic salts are favorable candidates for the next generation of primary explosives. By introducing the *N*-hydroxyl group, the performance and stability tetrazole-based HEDMs are enhanced. The advantage of the *N*-O functionality is exemplified by the energetic salt **tetra-13**, which based on its excellent detonation performance and low impact and friction sensitivities is superior to most known energetic materials.

With the rapid development of heterocyclic chemistry, we believe that azole-based energetic materials will continue to be the hot spot in the

framework of material science. From the standpoint of synthetic methodology, exploring new transformations of various functionalized energetic groups is highly appealing for searching for the next generation of HEDMs. Meanwhile, considering industry interests, modification of reaction conditions are also highly appealing to reduce production costs and to limit environment pollution. With the growing database of physicochemical properties for energetic compounds, computer-aided design will provide a shortcut toward new HEDMs. Hence, more collaboration between synthetic chemists and computer scientists is required for further development of future energetic materials.

## ACKNOWLEDGMENTS

Financial support from the Office of Naval Research (N00014-12-1-0536) and the Defense Threat Reduction Agency (HDTRA 1-11-1-0034) are gratefully acknowledged.

## REFERENCES

- 1863ACP178 J. Wilbrand, *Ann. Chem. Pharm.*, **128**, 178 (1863).  
1873JCS796 H. Sprengel, *J. Chem. Soc.*, **26**, 796 (1873).  
1943CPE396 T.L. Davis, In *The Chemistry of Powder and Explosives II*, John Wiley & Sons Inc.: New York (1943), p 396.  
1959JA6461 N. A. Milas and A. Golubović, *J. Am. Chem. Soc.*, **81**, 6461 (1959).  
1965AX485 H.H. Cady and A.C. Larson, *Acta Crystallogr.*, **18**, 485 (1965).  
1970SKGS259 L.I. Bagal, M.S. Pevzner, A.N. Frolov, and N.I. Sheludyakova, *Khim. Geterotsikl. Soedin*, **6**, 259 (1970).  
1972AX(B)193 C.S. Choi and J.E. Abel, *Acta Crystallogr.*, **B28**, 193 (1972).  
1986JOC3261 R.L. Atkins, R.A. Hollins, and W.S. Wilson, *J. Org. Chem.*, **51**, 3261 (1986).  
1989PCE|7| A.T. Nielsen, M.L. Chan, K.J. Kraeutle, C.K. Lowe-Ma, R.A. Hollins, M.P. Nadler, R.A. Nissan, W.P. Norris, D.J. Vanderah, and R.Y. Yee, *Polynitropolyaza Caged Explosives*, Report NWC TP 7020 (Part 7), Naval Weapons Center (1989).  
1992BR751 T. Baryshnikov, V.I. Erashko, N.I. Zubanova, B.I. Ugrak, S.A. Shevelev, A.A. Fainzil'berg, A.L. Laikhter, L.G. Mel'nikova, and V. Semenov, *Bull. Russ. Acad. Sci. Div. Chem. Sci.*, **41**, 751 (1992).  
1992JHC1721 J.C. Hinshaw, W.W. Edwards, C. George, and R. Gilardi, *J. Heterocycl. Chem.*, **29**, 1721 (1992).  
1996EE P.W. Cooper, In *Explosives Engineering*, Wiley-VCH: New York (1996).  
1997RJOC1771 G.I. Koldobskii, D.S. Soldatenko, E.S. Gerasimova, N.R. Khokhryakova, M.B. Shcherbinin, V.P. Lebedev, and V.A. Ostrovskii, *Russ. J. Org. Chem.*, **33**, 1771 (1997).  
1998T11525 N.V. Latypov, J. Bergman, A. Langlet, U. Wellmar, and U. Bemm, *Tetrahedron*, **54**, 11525 (1998).  
2000AG401 M. Zhang, P.E. Eaton, and R. Gilardi, *Angew. Chem. Int. Ed.*, **39**, 401 (2000).  
2001RJOC430 I.V. Tselinskii, S.F. Mel'nikova, and T.V. Romanova, *Russ. J. Org. Chem.*, **37**, 430 (2001).

- 2004JHM35 N. Sikder, A.K. Sikder, N.R. Bulakh, and B.R. Gandhe, *J. Hazard. Mater.*, **113**, 35 (2004).
- 2009AFM347 M. Gobel and T.M. Klapötke, *Adv. Funct. Mater.*, **19**, 347 (2009).
- 2009JA7490 W.G. Liu, S.V. Zybin, S. Dasgupta, T.M. Klapotke, and W.A. Goddard, *J. Am. Chem. Soc.*, **131**, 7490 (2009).
- 2010AG3177 G. Hervé, C. Roussel, and H. Graindorge, *Angew. Chem. Int. Ed.*, **49**, 3177 (2010).
- 2010CEJ10778 Y. Zhang, Y. Guo, Y.-H. Joo, D.A. Parrish, and J.M. Shreeve, *Chem. Eur. J.*, **16**, 10778 (2010).
- 2010JHM1 V.M. Boddu, D.S. Viswanath, T.K. Ghosh, and R. Damavarapu, *J. Hazard. Mater.*, **181**, 1 (2010).
- 2010JPCA2727 C.M. Tarver, *J. Phys. Chem. A*, **114**, 2727 (2010).
- 2010MC355 I.L. Dalinger, I.A. Vatsadze, T.K. Shkineva, G.P. Popova, and S.A. Shevelev, *Mendeleev Commun.*, **20**, 355 (2010).
- 2010PEP15 D.M. Hoffman and A.T. Fontes, *Propellants Explos. Pyrotech.*, **35**, 15 (2010).
- 2011CRV7377 H. Gao and J.M. Shreeve, *Chem. Rev.*, **111**, 7377 (2011).
- 2011JA6464 V. Thottampudi, H.X. Gao, and J.M. Shreeve, *J. Am. Chem. Soc.*, **133**, 6464 (2011).
- 2011JMC6891 Y. Zhang, Y.G. Huang, D.A. Parrish, and J.M. Shreeve, *J. Mater. Chem.*, **21**, 6891 (2011).
- 2012CEJ987 Y. Zhang, D.A. Parrish, and J.M. Shreeve, *Chem. Eur. J.*, **18**, 987 (2012).
- 2012CEJ16562 C. Qi, S.H. Li, Y.C. Li, Y. Wang, X.X. Zhao, and S.P. Pang, *Chem. Eur. J.*, **18**, 16562 (2012).
- 2012CEJ16742 A.A. Dippold and T.M. Klapotke, *Chem. Eur. J.*, **18**, 16742 (2012).
- 2012EJ12429 A.A. Dippold, T.M. Klapotke, F.A. Martin, and S. Wiedbrauk, *Eur. J. Inorg. Chem.*, 2429 (2012).
- 2012JMC12659 Y. Zhang, D.A. Parrish, and J.M. Shreeve, *J. Mater. Chem.*, **22**, 12659 (2012).
- 2012JMC20418 N. Fischer, D. Fischer, T.M. Klapötke, D.G. Piercey, and J. Stierstorfer, *J. Mater. Chem.*, **22**, 20418 (2012).
- 2012M5040 Y.C. Li, W. Liu, and S.P. Pang, *Molecules*, **17**, 5040 (2012).
- 2012ZAAC1278 T.M. Klapötke, A. Preimesser, J. Stierstorfer, and Z. Anorg, *Allg. Chem.*, **638**, 1278 (2012).
- 2013CEJ4602 D. Fischer, T.M. Klapotke, D.G. Piercey, and J. Stierstorfer, *Chem. Eur. J.*, **19**, 4602 (2013).
- 2013CEJ8929 J. Zhang, C. He, D.A. Parrish, and J.M. Shreeve, *Chem. Eur. J.*, **19**, 8929 (2013).
- 2013EJ14667 T.M. Klapötke, A. Penger, C. Pfluger, J. Stierstorfer, and M. Suceška, *Eur. J. Inorg. Chem.*, 4667 (2013).
- 2013JA9931 A.A. Dippold and T.M. Klapotke, *J. Am. Chem. Soc.*, **135**, 9931 (2013).
- 2013JMCA585 Y. Zhang, D.A. Parrish, and J.M. Shreeve, *J. Mater. Chem. A*, **1**, 585 (2013).
- 2013JMCA2863 C. He, J.H. Zhang, D.A. Parrish, and J.M. Shreeve, *J. Mater. Chem. A*, **1**, 2863 (2013).
- 2013JMCA7500 P. Yin, Q. Zhang, J. Zhang, D.A. Parrish, and J.M. Shreeve, *J. Mater. Chem. A*, **1**, 7500 (2013).
- 2013NJC2837 K. Hou, C. Ma, and Z. Liu, *New J. Chem.*, **37**, 2837 (2013).
- 2013RA10859 J.H. Song, K. Wang, L.X. Liang, C.M. Bian, and Z.M. Zhou, *RSC Adv.*, **3**, 10859 (2013).
- 2014AG8172 D. Fischer, T.M. Klapotke, and J. Stierstorfer, *Angew. Chem. Int. Ed.*, **53**, 8172 (2014).



- 2014CEJ6707 P. Yin, D.A. Parrish, and J.M. Shreeve, *Chem. Eur. J.*, **20**, 6707 (2014).  
2014CEJ16529 P. Yin, J. Zhang, D.A. Parrish, and J.M. Shreeve, *Chem. Eur. J.*, **20**, 16529 (2014).
- 2014JMCA18907 Liang, K. Wang, C.M. Bian, J. Zhang, and Z.M. Zhou, *J. Mater. Chem. A*, **2**, 18097 (2014).
- 2014JA16102 T.T. Vo, D.A. Parrish, and J.M. Shreeve, *J. Am. Chem. Soc.*, **136**, 16102 (2014).
- 2014JMCA3200 P. Yin, J.H. Zhang, C.L. He, D.A. Parrish, and J.M. Shreeve, *J. Mater. Chem. A*, **2**, 3200 (2014).
- 2014JMCA15978 W. Liu, S.H. Li, Y.C. Li, Y.Z. Yang, Y. Yu, and S.P. Pang, *J. Mater. Chem. A*, **2**, 15978 (2014).
- 2015AG6260 C. He and J.M. Shreeve, *Angew. Chem. Int. Ed.*, **54**, 6260 (2015).  
2015AG10299 D. Fischer, T.M. Klapotke, and J. Stierstorfer, *Angew. Chem. Int. Ed.*, **54**, 10299 (2015).
- 2015AG14721 P. Yin and J.M. Shreeve, *Angew. Chem. Int. Ed.*, **54**, 14721 (2015).  
2015CAJ1987 I.L. Dalinger, I.A. Vatsadze, T.K. Shkineva, A.V. Kormanov, M.I. Struchkova, K.Y. Suponitsky, A.A. Bragin, K.A. Monogarov, V.P. Sinditskii, and A.B. Sheremetev, *Chem. Asian J.*, **10**, 1987 (2015).
- 2015CEJ9219 T.M. Klapotke, P.C. Schmid, S. Schnell, and J. Stierstorfer, *Chem. Eur. J.*, **21**, 9219 (2015).
- 2015JA1697 J. Zhang, Q. Zhang, T.T. Vo, D.A. Parrish, and J.M. Shreeve, *J. Am. Chem. Soc.*, **137**, 1697 (2015).
- 2015JA4778 P. Yin, D.A. Parrish, and J.M. Shreeve, *J. Am. Chem. Soc.*, **137**, 4778 (2015).
- 2015JMCA163 C.M. Bian, M. Zhang, C. Li, and Z.M. Zhou, *J. Mater. Chem. A*, **3**, 163 (2015).
- 2015JMCA2685 T.M. Klapotke, P.C. Schmid, S. Schnell, and J. Stierstorfer, *J. Mater. Chem. A*, **3**, 2658 (2015).
- 2015JMCA8606 P. Yin, J.H. Zhang, D.A. Parrish, and J.M. Shreeve, *J. Mater. Chem. A*, **3**, 8606 (2015).
- 2015JMCA15576 Y. Tang, C. He, H. Gao, and J.M. Shreeve, *J. Mater. Chem. A*, **3**, 15576 (2015).
- 2015JMCA17693 M.C. Schulze, B.L. Scott, and D.E. Chavez, *J. Mater. Chem. A*, **3**, 17963 (2015).
- 2016CAJ844 T.M. Klapotke, M. Leroux, P.C. Schmid, and J. Stierstorfer, *Chem. Asian J.*, **11**, 844 (2016).
- 2016CEJ2108 P. Yin, C. He, and J.M. Shreeve, *Chem. Eur. J.*, **22**, 2108 (2016).  
2016JMCA1514 P. Yin and J.M. Shreeve, *J. Mater. Chem. A*, **4**, 1514 (2016).  
2015PEP491 D.G. Piercey, D.E. Chavez, S. Heimsch, C. Kirst, T.M. Klapotke, and J. Stierstorfer, *Propellants Explos. Pyrotech.*, **40**, 491 (2015).



# Heterocyclic Building Blocks for Organic Semiconductors

Xikang Zhao, Saadia T. Chaudhry, Jianguo Mei\*

Department of Chemistry, Purdue University, West Lafayette, IN, USA

\*Corresponding author: E-mail: jgmei@purdue.edu

## Contents

1. Introduction	134
2. Thiophene-Related Building Blocks	135
2.1 Thiophenes, Selenophenes, and Tellurophenes	135
2.2 Fused Thiophenes	138
2.2.1 Isothianaphthene	138
2.2.2 Thienothiophenes	139
2.2.3 Dibenzothiophene	140
2.2.4 Cyclopenta[1,2-b:5,4-b']dithiophen-4-one and Cyclopenta[1,2-b:5,4-b'] dithiophene	141
2.2.5 Benzodithiophenes	142
2.2.6 Naphthodithiophenes	143
3. Nitrogen-Containing Building Blocks	145
3.1 Quinoxalines and Thienopyrazines	146
3.2 Benzothiadiazoles and Benzoselenodiazoles	146
3.3 Benzotriazole	148
3.4 Carbazoles	148
3.5 Dithieno[3,2-b:2',3'-d]pyrrole	149
3.6 Imide-Based Building Blocks	150
4. Other Building Blocks	157
4.1 Silole Derivatives	157
4.2 Phosphole Derivatives	159
4.3 BODIPY	160
References	162

## Abstract

Organic semiconductors are an important class of functional materials. Numerous molecular and polymeric organic semiconductors have been developed for their great potentials in next generation flexible and printed electronics. In this chapter, the authors review some of the most popular heterocyclic building blocks and their chemistry.

These building blocks are organized based on the heteroatom(s) that are present in their structures, including sulfur-, nitrogen-, silicon-, phosphorus-, and boron-containing heterocycles.

**Keywords:** Heterocycles; Organic semiconductor; Semiconducting polymer



## 1. INTRODUCTION

Organic semiconductors (OSCs) are a class of carbon-based materials that exhibit optical and electronic properties ([2001AGE2591](#), [2010CSR2354](#)). They have been a focus of inquiry in the development of potential low-cost, large-area, flexible, and lightweight optoelectronic devices, such as light-emitting diodes, solar cells, field-effect transistors, organic lasers, and electrochromics ([2006MI1](#), [2007CRV1272](#), [2007CRV1324](#), [2009CRV897](#), [2009CRV5868](#), [2010CRV3](#), [2010CRV268](#), [2011CM733](#), [2012CRV2208](#), [2014AM1319](#)). Compared with their widely known inorganic counterparts (mainly silicon, germanium, and metal oxide semiconductors), organic semiconductors offer some intrinsic advantages. For instance, materials properties can be fine-tuned via structural modifications that can be easily achieved through intelligent molecular design ([2013AM6158](#)). Solution-processing can be realized for low-cost and large-area devices via numerous techniques (spin coating, spray coating, inkjet printing, roll-to-roll printing, and Langmuir layer-by-layer assembly, etc.) ([2009MI5](#), [2011NAT364](#), [2012MI4](#), [2014MI2](#), [2014MI4](#)). The low processing temperature, combined with the mechanical flexibility of organic materials, provides great opportunities to access flexible integrated circuits, electronic paper (or fabric), and foldable organic electronics ([2010MI2](#)). To date, numerous molecular and polymeric semiconductors have been designed and synthesized for their technological relevance and potential advantages as mentioned for next generation flexible and printed electronics. These developments are nicely summarized in many excellent reviews ([2010ACR1396](#), [2011ACR501](#), [2011JA20009](#), [2013AM5372](#), [2013JA6724](#), [2014CM604](#), [2014CM647](#)), whose focus mostly lies in establishing the relationship between molecular structures and their semiconducting properties. There is a need to summarize organic semiconductors from the perspective of chemical synthesis. This is a daunting task, if we think about the vast number of organic semiconductors available. We decided to take a different approach and focus on the chemistry and synthesis of heterocyclic building blocks, because the majority of the organic semiconductors come from the combinations of these

building blocks. We cover some of the most popular heterocyclic building blocks and their chemistry. They are organized based on the heteroatom they contain, including chalcogen-, nitrogen-, silicon-, phosphorous-, and boron-containing heterocycles.

## 2. THIOPHENE-RELATED BUILDING BLOCKS

### 2.1 Thiophenes, Selenophenes, and Tellurophenes

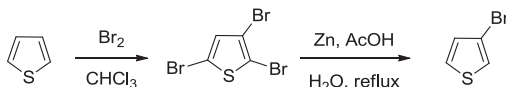
Among the most common donor units used in the field of semiconducting, thiophenes have been the most popular one since the 1980s (1986APPLAB1210, 1988APPLAB195, 1992CRV711, 1996APPLAB4108, 1998AM93, 1998SCI1741, 2012MI2, 2014MI1). In particular, polythiophenes (PTs) have been extensively studied since the 1980s. Oligothiophenes have been widely implemented for the generation of OSC building blocks.

Based on the commercial availability and low cost of thiophene, a number of related building blocks and polymers can be synthesized. Oxidation of thiophenes under certain conditions, such as with ferric chloride, gives PTs with high yields (1984MI1, 1986MI1). An alternative way is to introduce functional groups to the  $\alpha$ -positions of the thiophene rings. As an electronic rich heterocycle, these positions are readily activated by direct lithiation or bromination (Scheme 1).

PTs are among the most important and commercially successful semiconducting polymers. Extensive effort has been made to improve the performance of the devices based on such materials in a variety of chemical and processing aspects (1992CRV711, 1998AM93, 2009AM1091, 2014MI1). One successful modification is side-chain engineering (2014CM604). By introducing side chains to the polymer backbone, the solubility of the polymer can be improved. Moreover, side chains are beneficial for the packing between the  $\pi$ -systems, and the orientation of the polymer molecules can be changed to an “edge-on” mode. As a result, solution-processable materials with outstanding performance can be designed and synthesized. As to PTs, side chains are introduced to the  $\beta$ -positions.



**Scheme 1** Direct lithiation and bromination of thiophene.

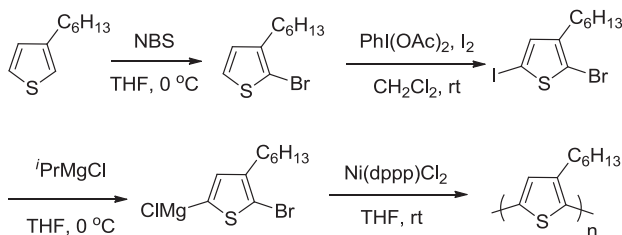


**Scheme 2** Synthesis of 3-bromothiophene.

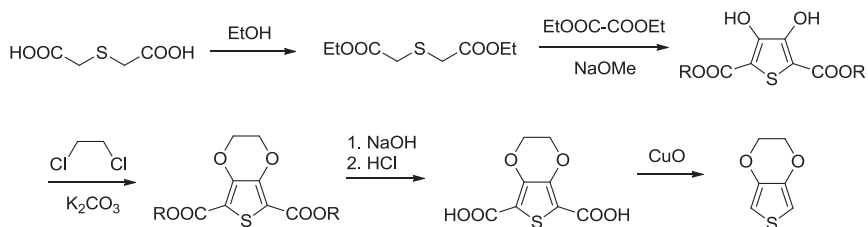
Due to their lower reactivity, modification at these positions is indirect compared to the  $\alpha$ -positions. For example, 3-bromothiophene, the starting material of a number of 3-substituted thiophenes, can be synthesized in two steps, involving tribromination followed by  $\alpha$ -debromination (Scheme 2) (1955BSF424, 1959ACSA1045, 1964OS9, 2005JA13281).

$\beta$ -Alkylation is a successful method to improve the performance of PT-based materials. The pioneering work by Sugimoto et al. used PT as the semiconducting layer of an organic field-effect transistor (OFET) and obtained a low mobility of around  $10^{-5}$   $\text{cm}^2/\text{Vs}$  (1986APPLAB1210). As a comparison, by introducing hexyl side chains to the polymer backbone, the mobility of regioregular poly(3-hexylthiophene) (*rr*-P3HT) can be improved to  $0.1$   $\text{cm}^2/\text{Vs}$  (1996APPLAB4108, 1998SCI1741). Regioregular P3HT has been synthesized by various methods including metal-catalyzed cross-coupling (1992JA10087, 1992JCS(CC)70, 1998JMC25, 2004MI1, 2004MM1169, 2006TL5143) and oxidative coupling polymerization reactions (1986MI1). The Yokozawa's route for the synthesis of regioregular P3HT is shown in Scheme 3 (2004MI1, 2004MM1169).

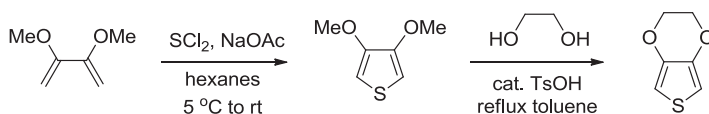
Another approach is to chemically construct the desired substituted thiophenes. For instance, 3,4-dialkoxylated thiophenes are obtained from ring closure reactions. The most important example is 3,4-ethylenedioxythiophene (EDOT). The homopolymer of EDOT, PEDOT, is currently among the most commercially available and successful conducting polymers (2000AM481, 2011MI2). A number of synthetic strategies have been reported, most of which were not started from thiophene or substituted thiophenes. A notable approach for the synthesis of EDOT was developed by



**Scheme 3** Synthesis of *rr*-P3HT based on Yokozawa's method.



**Scheme 4** Synthesis of 3,4-ethylenedioxythiophene from thiodiglycolic acid and diethyl oxalate.



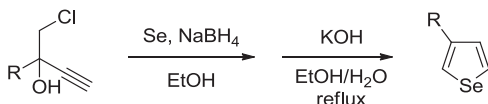
**Scheme 5** Synthesis of 3,4-ethylenedioxythiophene from 2,3-dimethoxy-1,3-butadiene and sulfur dichloride.

Jonas et al., through which EDOT could be obtained from thiodiglycolic acid in five steps (Scheme 4) (1989EUP).

Another approach was reported by Hellberg et al., in which sulfur dichloride was used as the sulfur source and reacted with 2,3-dimethoxy-1,3-butadiene. In this method, EDOT is obtained in two steps (Scheme 5) (2004TL6049).

Another strategy to improve the performance of the semiconducting polymer is by atomic substitution. As for thiophene derivatives, research on the selenium and tellurium analogs of thiophenes, namely selenophenes and tellurophenes, has witnessed a significant growth in the past decade due to developments in synthetic techniques. Heavy-atom substitution changes the property of the polymers in a number of aspects. First, the band gaps of the selenophene- and tellurophene-containing polymers are smaller than those of the thiophene homologues. Second, the C–C bond length between the heterocycles shrinks from PTs to polytellurophenes, and the rings are also becoming more coplanar. Third, the strong interaction between the heavy atoms has large impact on the interaction between the polymer chains and the crystallinity of the polymer (2010JMC422, 2014IJ440, 2014IJ621, 2015MM297).

Selenophene was first synthesized in 1885 (1885CB2255) and the synthesis of selenophenes has been reviewed extensively (2002MI1, 2005MI1). The study of polyselenophenes as semiconducting polymers started in the mid-1980s, and several review articles have been published (2010JMC422,



**Scheme 6** Synthesis of 3-substituted selenophenes from 1-chlorobut-3-yn-2-ol derivatives.

2014IJ621). Recently, a number of reports on the application of selenophene building blocks instead of thiophenes in D–A type polymers have also been published (2012JA20713, 2012MM1303, 2015JA1314).

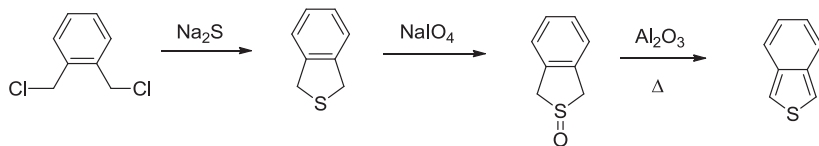
Although somewhat expensive, selenophene is a commercially available substance produced from the gas-phase reaction between selenium and acetylene (1983JOC3544). The chemical properties of selenophenes are rather similar to thiophenes. The  $\alpha$ -positions of selenophenes are more reactive compared to the  $\beta$ -positions. 3-alkylated selenophenes can be synthesized from selenophene with 2,3,4,5-tetraiodoselenophene as intermediate (1997JMC1731). Although this process is similar to thiophene, the use of highly toxic mercury reagents forbids this route for massive production. One alternative route is the reaction between 2-substituted 1-chlorobut-3-yn-2-ol with selenium with the presence of base (Scheme 6) (1990PS35, 2012MM1303). For 3,4-disubstituted species, such as 3,4-ethylenedioxyseleophene, the synthesis is similar to EDOT (2008JA6734, 2014ACR1465). Compared to the sulfur and selenium congeners, the examples of tellurophene-containing polymer are rare due to the poor stability, different reactivity, and higher toxicity (2015MM297).

## 2.2 Fused Thiophenes

The chemical and electronic characteristics of the building blocks and the polymer can also be tuned by expanding the conjugated system. Based on thiophene, a number of fused systems can be constructed and applied to the field of semiconducting polymers. Their high degree of diversity leads to different electronic and structural features, which allows us to build high-performance semiconducting polymers that meet specific needs. The synthesis of selected fused thiophene system is reviewed in the following part.

### 2.2.1 Isothianaphthene

Isothianaphthene (ITN), or benzo[*c*]thiophene, is a bicyclic system with thiophene fused with a benzene ring at the  $\beta$ -positions. Similar to thiophenes, ITNs are introduced into the polymer chains at the  $\alpha$ -positions.



**Scheme 7** Synthesis of isothianaphthene from sodium sulfide and 1,2-dichloromethylbenzene.

The first report of poly(isothianaphthene) (PITN) was published by Wudl et al. in 1984 (1984JOC3382), and the application of ITN as a unit in D-A polymer was published by Qin et al. in 2008 (2008MM5563). ITN received some interest in the 2000s due to the low band gap of the homopolymer, PITN (2001MM1810).

The synthesis and reactivity of ITN was previously reviewed (2001MI1). As a 3,4-disubstituted thiophene, this building block is constructed similarly with EDOT. Sodium sulfide is used as the sulfur source, which is reacted with 1,2-dichloromethylbenzene to construct the dihydroisothianaphthene backbone followed by oxidation and dehydration over aluminum oxide to form ITN (1971JOC3932, 1989MI1) (Scheme 7).

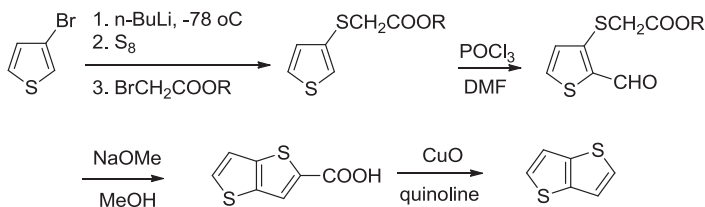
### 2.2.2 Thienothiophenes

Thienothiophenes (TTs) are bicyclic aromatics with two thiophene rings fused to each other. Two isomers, thieno[3;2-*b*]thiophene and thieno[3;4-*b*]thiophene, are commonly used as building blocks for semiconducting polymers. The synthesis of TTs and some related aromatics has been reviewed (2015CRV3036). Here we highlight some applications of these units to semiconducting polymers.

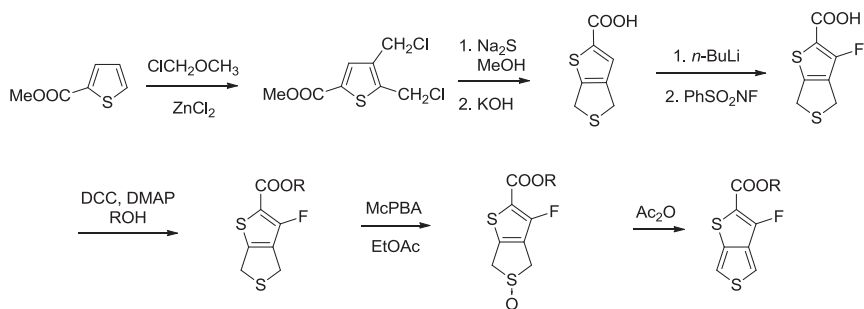
Thieno[3;2-*b*]thiophene is a commonly used electron-rich unit in semiconducting polymers. In this unit, the  $\alpha$ -positions of both thiophene rings are fused with the  $\beta$ -positions of the other ring, giving rise to C<sub>2h</sub> point group symmetry of this unit. The remaining  $\alpha$ -positions, or the 2,5-positions, are the reactive sites for polymerization. Currently, thieno[3;2-*b*]thiophene is synthesized by ring closure of 2-formylthiophen-3-ylthioacetates (1963IZV2183, 1965IZV510, 1968ACSA63, 1992MM2294, 2005JA13281) (Scheme 8).

In contrast to thieno[3;2-*b*]thiophene and most of the other thiophene-based units, thieno[3;4-*b*]thiophene is utilized as an electron-deficient unit. Without the stabilization of the electron withdrawing group at the 2- and 3-positions, the HOMO level would be too high for the molecule to be stable





**Scheme 8** Synthesis of thienothiophene from 3-bromothiophene in four steps.



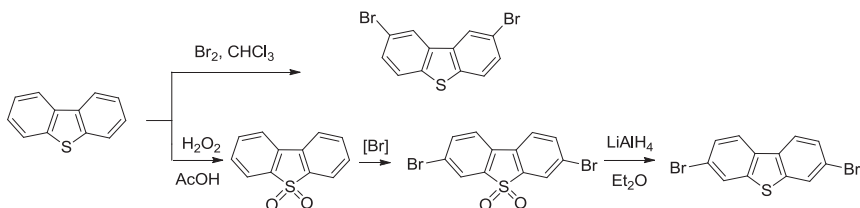
**Scheme 9** Synthesis of 3-TT in six steps.

in air. The first air-stable polymer containing thieno[3;4-*b*]thiophene was reported in 2007, and the building block is stabilized by an ester group at the 2-position (1966JOC3363, 2007AM3979). Additionally, the more exciting 3-fluorinated species, 3-TT, was reported in 2009 (2009JA7792). The synthesis of 3-TT is shown in Scheme 9.

### 2.2.3 Dibenzothiophene

Dibenzothiophene (DBT) is a tricyclic thiophene derivative with two benzene rings fused at both 2,3- and 4,5-positions. DBT is a natural occurring compound found in petroleum. In industry, DBT is currently produced from biphenyl and hydrogen sulfide under catalytic oxidizing conditions (1950USP, 1978JHC561).

DBTs and DBT dioxides have been copolymerized with fluorenes to tune the chain arrangement and aggregation of fluorene-based organic light-emitting diodes (OLEDs). With less aromatic DBT present in the main chain, the dihedral angles between aromatic systems increases, leading to less aggregation between the polymer chains and stable blue emissions (2003JMC1351, 2008CM4499, 2009MI1, 2009MI3, 2010MM4481). Yang et al. studied the random copolymer of 9,9-dioctylfluorene and 2,8-dibromodibenzothiophene with various ratios. They found that with the



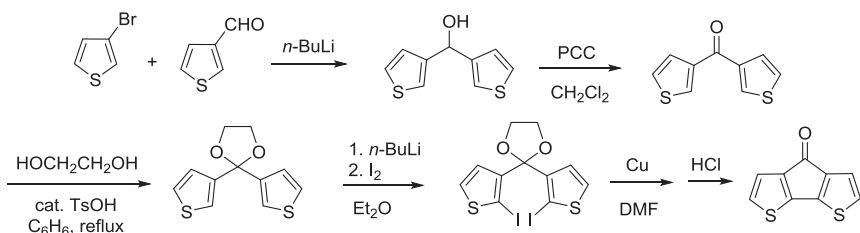
**Scheme 10** Bromination of dibenzothiophene under different conditions.

addition of DBT into the polymer, the fluorescence peak of the polymer witnessed a slight hypochromic shift, indicating disturbed interactions between the polymer molecules. With lower DBT portions (0–30%), the efficiency of the material dropped from 0.52% to 0.10%. However, with more DBT (50%), the quantum yield grew back to 0.42% (2003JMC1351).

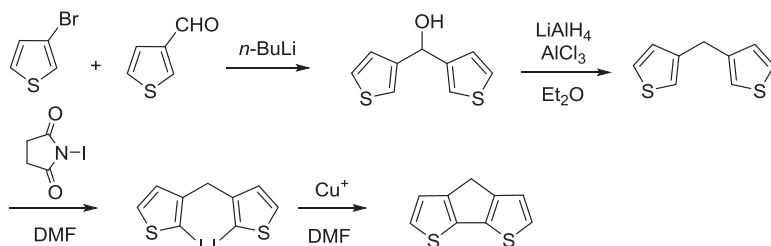
Unsubstituted DBT is a commercially available and inexpensive precursor, where both 3,7- and 2,8-positions can be substituted under different conditions (1985JHC215, 2007JMC1421). Direct bromination of DBT yields the 2,8-substituted species (1997JPS(A)2813). To obtain the 3,7-substituted derivative, the electron-donating sulfur atom has to be oxidized into an electron-withdrawing sulfone group prior to bromination (1999JMC2095) (Scheme 10).

### 2.2.4 Cyclopenta[1,2-*b*:5,4-*b'*]dithiophen-4-one and Cyclopenta[1,2-*b*:5,4-*b'*]dithiophene

Cyclopenta[1,2-*b*:5,4-*b'*]dithiophen-4-one (CDT) can be considered as an electron-deficient dithiophene with fixed syn-conformation. Due to their electron-poor nature, they have attracted interest in the potential capability to construct n-type materials. The synthesis of CDT exploits 2,2'-coupling of di-3-thienyl ketone as the key intermediate (Scheme 11) (1963AK335, 1967AK99, 1970JCS(C)273, 1995SM147, 1998SM25). A number of other



**Scheme 11** Synthesis of cyclopenta[1,2-*b*:5,4-*b'*]dithiophen-4-one from 3-bromothiophene and 3-thiophenecarboxaldehyde in five steps.



**Scheme 12** Synthesis of cyclopenta[1,2-*b*:5,4-*b'*]dithiophenes from 3-bromothiophene and 3-thiophenecarboxaldehyde in four steps.

electron-deficient building blocks based on CDT, such as 4-dicyanomethylene-4*H*-cyclopenta[1,2-*b*:5,4-*b'*]dithiophene (1991JCS(CC)1268, 1993USP, 1997SM973) and 4-(1,3-dithiol-2-ylidene)-4*H*-cyclopenta[1,2-*b*:5,4-*b'*]dithiophene (1992JCS(CC)1137, 1994JOC442), can also be obtained.

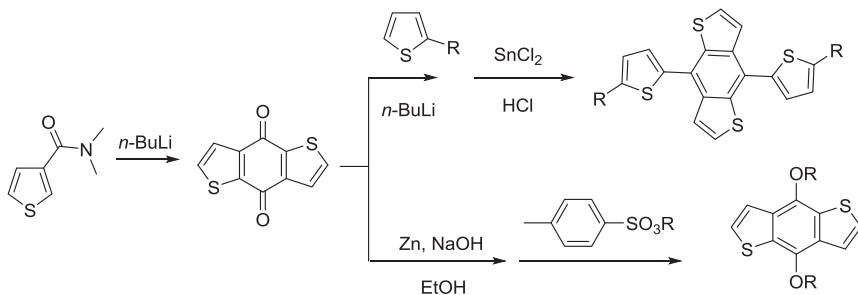
Cyclopenta[1,2-*b*:5,4-*b'*]dithiophenes (CPDT) are reduced CDT species and thiophene-fused analogs of fluorene. Similar to fluorene, side chains can be introduced to the 4-position of CPDT. The synthesis of CPDT was first reported in 1964 (1964JOC2455). The first example of a polymer bearing alkyl-substituted CPDT was reported in 1994 (1994MM1938). CPDT can be obtained from the reduction of CDT. Some recent reports on the modification of this route are also available (2009MI2, 2010MM697, 2012JA539). One example utilizes the 2,2'-coupling of bis(3-thienyl) methane (Scheme 12).

### 2.2.5 Benzodithiophenes

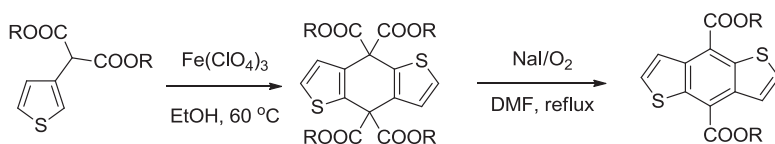
Benzo[1,2-*b*:4,5-*b'*]dithiophene and benzo[1,2-*b*:6,5-*b'*]dithiophene are the two benzodithiophene (BDT) species applied in semiconducting polymers. The former can be considered as a benzene ring fused by two thiophene rings, whereas the latter is a syn-dithiophene moiety locked by a benzene ring, which is similar to CPDT. The point group symmetry of the isomers is different to each other: benzo[1,2-*b*:4,5-*b'*]dithiophene is in  $C_{2h}$  whereas benzo[1,2-*b*:6,5-*b'*]dithiophene is in  $C_{2v}$ .

The synthesis of benzo[1,2-*b*:4,5-*b'*]dithiophenes exploits the dimerization of 3-substituted thiophenes. For the dialkylxyl- and dithienyl-substituted derivatives, the dione species serves as the key intermediate (Scheme 13) (1986CB3198, 2011AGE9697).

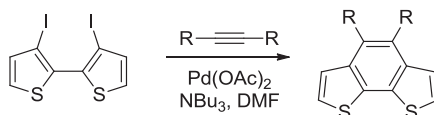
As to the dicarboxylate-substituted species, oxidative dimerization of 2-(thiophen-3-yl) malonic ester followed by removal of two ester



**Scheme 13** Synthesis of dithieno- or dialkyloxy-substituted benzo[1,2-*b*:4,5-*b'*]dithiophene derivatives.



**Scheme 14** Synthesis of dicarboxylate-substituted benzo[1,2-*b*:4,5-*b'*]dithiophene derivatives.



**Scheme 15** Synthesis of benzo[1,2-*b*:6,5-*b'*]dithiophenes from palladium-catalyzed coupling.

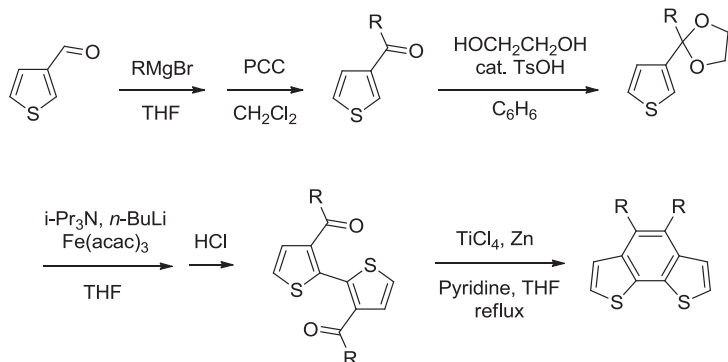
groups is applied to build the benzene ring (1996T13227, 2014MM4987) (Scheme 14).

For the synthesis of benzo[1,2-*b*:6,5-*b'*]dithiophenes, two routes have been reported. The first one utilizes palladium-catalyzed coupling between 3,3'-diiodobisthiophene and an alkyne (Scheme 15) (2008MM5688).

The second route utilizes the reductive coupling of [(2,2'-bithiophene)-3,3'-diyl]diketone (Scheme 16) (2010AM83).

## 2.2.6 Naphthodithiophenes

Naphthodithiophenes (NDTs) are tetracyclic conjugated systems with two thiophene rings fused to the naphthalene skeleton. With an additional benzene ring, NDT has more isomers than BDT. Based on the difference in connection between the thiophene rings and the naphthalene ring, the isomers can be classified into two categories, and the synthesis of these isomers is discussed separately.



**Scheme 16** Synthesis of benzo[1,2-*b*:6,5-*b'*]dithiophenes from reductive coupling.

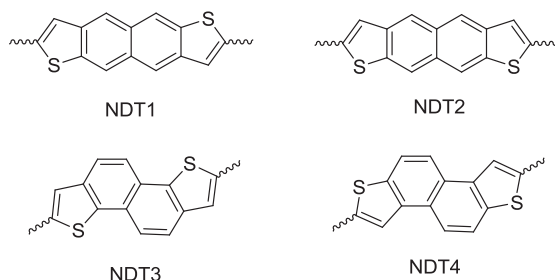
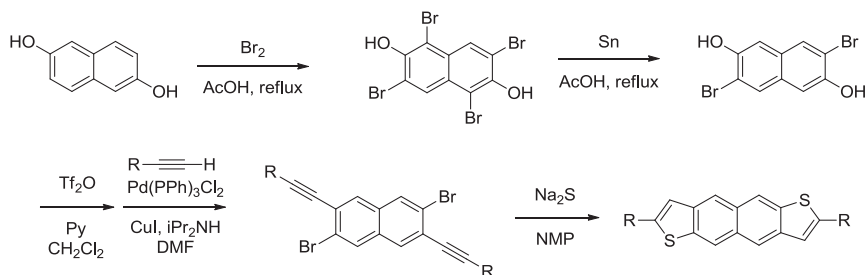


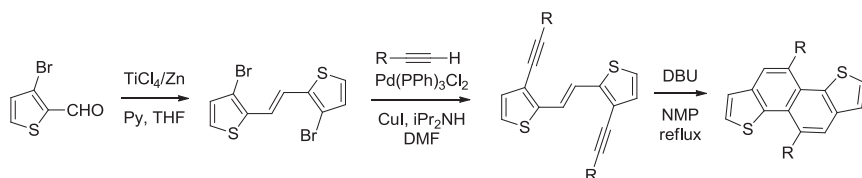
**Figure 1** Structures of naphthodithiophene building blocks with thiophene rings fused to each benzene ring.

In the first category, the two thiophene rings are fused to the both ends of the naphthalene skeleton (Figure 1). NDT1 and NDT2, namely linear-shaped NDTs, have thiophene rings fused to the  $\beta, \beta'$ -positions of naphthalene. As a comparison, the  $\alpha, \beta$ -fused derivative, NDT3 and NDT4, are described as angular-shaped NDTs. Research on the application of these units on OSCs traces back to 2011 (2011JA5024, 2011JA6852, 2011MI1, 2013JMC(C)1297, 2014MM616, 2014MM3502, 2015MI2). Two strategies are available to synthesize these building blocks. The first strategy was reported by Takimiya and coworkers for NDT3 in 2010 (2010JOC1228) and other monomers in 2011 (2011JA5024). In this strategy, NDTs are synthesized based on the naphthalene skeletons. The synthesis of NDT1 is shown in Scheme 17.

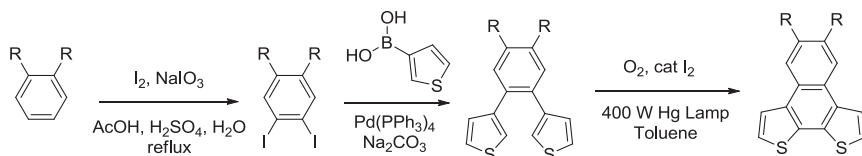
The second strategy was recently reported by Cheng et al., which did the reverse by constructing the naphthalene skeleton based on bis(thiophen-2-yl)ethylene. The synthesis of NDT3 is provided in Scheme 18 as an



**Scheme 17** Synthesis of NDT1 from 2,6-dihydroxynaphthalene.



**Scheme 18** Synthesis of NDT1 from 3-bromo-2-thiophenecarboxaldehyde.



**Scheme 19** Synthesis of naphtho[2,1-*b*;3,4-*b'*]dithiophene derivatives from oxidative ring-closing reaction.

example. Based on this strategy, side chains can be introduced into the 5- and 10-positions ([2013OL5338](#), [2015MI2](#)).

The two thiophene rings can also be fused to the same benzene ring, which gives naphtho[2,1-*b*;3,4-*b'*]dithiophene. This monomer can be synthesized from the oxidative ring-closing of bis(thiophene-3-yl)benzene, which was first reported in 2001 ([2001AM1775](#)) and a recent modification was published in 2008 ([2008MM5688](#)) ([Scheme 19](#)). Naphtho[2,1-*b*;3,4-*b'*]dithiophenes are typically applied as a weak donor unit to build organic photovoltaics (OPVs) ([2008MM5688](#), [2010MI1](#), [2010JPC\(C\)16793](#)).

### 3. NITROGEN-CONTAINING BUILDING BLOCKS

Nitrogen-containing building blocks are typically electron poor and are applied as acceptor units in semiconducting polymers. By choosing

the suitable building block, n-type materials with high performance can be designed and synthesized (2007JA1805).

### 3.1 Quinoxalines and Thienopyrazines

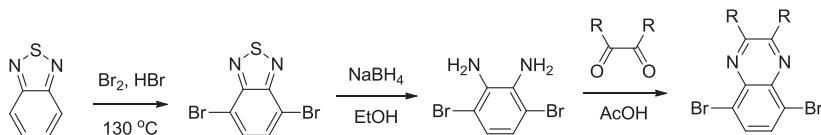
Quinoxaline is a bicyclic aromatic system with a benzene ring fused to a pyrazine ring. The first example of quinoxaline as a unit in conductive polymers was reported in 1993 (1993MM3464). Quinoxalines are popular acceptor units applied in both OPVs and OLEDs. For example, Chen et al. reported the application of a copolymer of a fluorinated quinoxaline and BDT as the donor material in bulk-heterojunction organic photovoltaics (BHJ-OPVs), which showed high power conversion efficiency (PCE) of 8% (2012CM4766). Wu et al. reported an alternating copolymer of fluorene and quinoxaline, which presented electroluminescent peak at 480 nm with an external quantum efficiency of 0.20% (2006PLM527).

Although quinoxaline is commercially available and inexpensive, the electron-deficient nature prevents the phenyl ring to be substituted under common conditions. As an alternative, 5,8-dibromoquinoxalines are alternatively synthesized with 4,5-dibromo-1,2-phenylenediamine as the key intermediate. For example, 2,1,3-benzothiadiazole (BT) can be utilized as the starting material (Scheme 20) (2005TL6843).

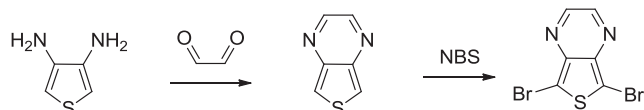
Thieno[3,4-*b*]pyrazines (TPZs), the thiophene-containing analog of quinoxalines, are also popular acceptor units in polymer semiconductors. Due to a larger quinoidal character, the band gap of TPZ-containing polymers is smaller than that of the quinoxaline-containing derivatives (2008MM6012). TPZs are synthesized from glyoxal and 3,4-diaminothiophene (1983BSF159). Due to the relatively electron-rich nature of the thiophene ring, electrophilic substitution at TPZs occurs more readily compared to quinoxalines (2008MM6012) (Scheme 21).

### 3.2 Benzothiadiazoles and Benzoselenodiazoles

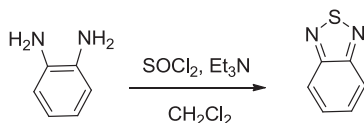
BTs and 2,1,3-benzoselenodiazoles are among the most popular and acceptor units in the field of polymer semiconductors. The synthesis and



**Scheme 20** Synthesis of 5,8-dibromoquinoxalines from benzothiadiazole.



**Scheme 21** Synthesis of dibromothieno[3,4-*b*]pyrazines from 3,4-diaminothiophene in two steps.



**Scheme 22** Synthesis of 2,1,3-benzothiadiazole from *o*-phenylenediamine and sulfonyl dichloride.

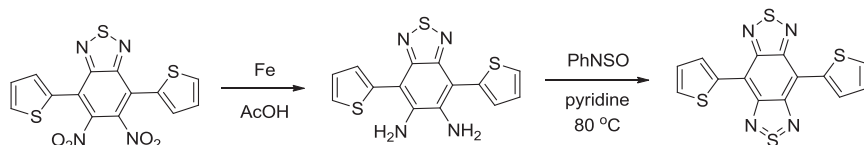
application of these units have been extensively studied and a number of reviews are available (2013EJO228, 2014MI6, 2015MI5). The synthetic routes of these units are similar to each other with *o*-phenylenediamine reacting with a chalcogen-atom source.

As to the synthesis of BT, thionyl chloride is chosen as the sulfur source and the reaction is completed with the presence of base (1889CB2895, 1956DOK88, 1967JOC2823, 1984JCS(P1)2591), which produces gram scale of product with high yield (Scheme 22).

More complicated aromatics can be constructed from BTs. Benzobis-thiadiazole (2015MI4), for example, can be synthesized with *o*-phenylenediamines as the key intermediate, which is obtained from the reduction of the corresponding nitrile species (Scheme 23) (1995JA6791, 2015MI5).

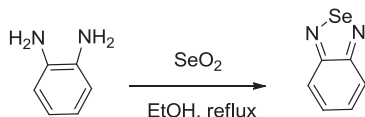
Similar to BTs, 2,1,3-benzoselenodiazoles can be synthesized with selenium dioxide as selenium source (Scheme 24) (1963JCS4767).

Recently, several examples have also been published for the application of the tellurium derivative, 2,1,3-benzotellurodiazole, in polymer semiconductors. However, 2,1,3-benzotellurodiazoles are not suitable for polymerization due to the thermal decomposition over 50 °C. Polymers bearing such units are synthesized instead from the 2,1,3-benzoselenodiazole derivatives followed by a two-step atomic exchange (Scheme 25) (2012JA539).

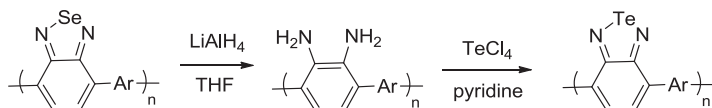


**Scheme 23** Synthesis of benzobisthiadiazole from dinitrobenzothiadiazole derivative in two steps.





**Scheme 24** Synthesis of 2,1,3-selenoselenodiazole from *o*-phenylenediamine and selenium dioxide.



**Scheme 25** Synthesis of 2,1,3-benzotellurodiazole-containing polymer from the 2,1,3-benzoselenodiazole-containing analogs.

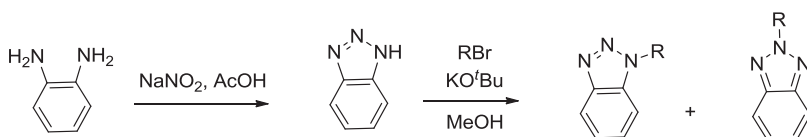
### 3.3 Benzotriazole

2-Substituted benzotriazoles are electron-poor heterocycles made by the reaction between *o*-phenylenediamine and nitrous acid (1940OS16), which act as acceptor units in semiconducting polymers. The alkylation of benzotriazoles can occur at either 1- or 2-position, and the products can be separated by column chromatography (2004ASC1818) (Scheme 26).

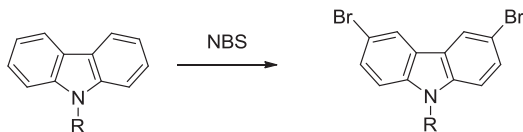
### 3.4 Carbazoles

Carbazole is a tricyclic aromatic with a benzene ring fused to the 2,3-positions of an indole ring. Carbazole is among the most popular donor units in the field of semiconducting polymers owing to its low price and ease of modification (2003MI1, 2008MI1, 2010CSR2399, 2010MI3).

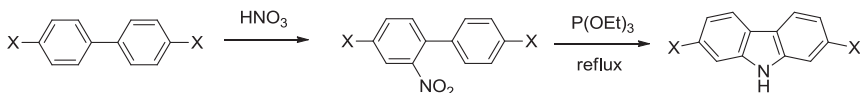
Similarity to CBT, carbazoles can be incorporated to the polymer chain at both the 3,6-positions and the 2,7-positions. Direct electrophilic substitution on carbazoles occurs at the 3,6-positions. For example, the reaction between carbazoles and *N*-bromosuccinamide yields the 3,6-dibromocarbazole (Scheme 27) (1957CCC64, 1967KKZ63, 1974M1306, 2002MM6080, 2004CM2165).



**Scheme 26** Synthesis of benzotriazoles from *o*-phenylenediamine and sodium nitrite.



**Scheme 27** Direct bromination of N-alkylated carbazole.



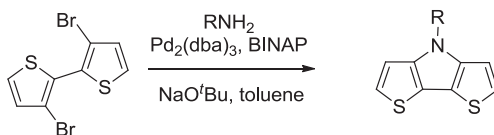
**Scheme 28** Synthesis of 2,7-disubstituted carbazole from 4,4'-disubstituted biphenyl.

2,7-Dibromocarbazoles, on the other hand, cannot be synthesized directly from carbazoles. As an alternative, diphenyl derivatives are typically used as the starting materials. For example, 2,7-disubstituted carbazoles can be synthesized from 4,4'-disubstituted biphenyl derivatives in two steps, including nitration and reductive ring closure (Scheme 28) (2001MM4680, 2003S2470). A review article is available for the synthesis and applications of related polymers (2008ACR1110).

### 3.5 Dithieno[3,2-*b*:2',3'-*d*]pyrrole

Dithieno[3,2-*b*:2',3'-*d*]pyrrole (DTP) is the thiophene-fused analog of carbazole. Due to the presence of the electron-rich thiophene rings, the HOMO levels of the DTP-containing polymers are expected to be higher than the carbazole-containing derivatives (2009CM4055). A number of examples on the application of DTP in OSCs (2008MM8302, 2009CM4055, 2009JMC2199, 2009JMC5794, 2010JMC123, 2010MM821, 2011AGE2799) and OFETs (2008JA13167, 2009JMC5794, 2010AM4617, 2010JMC123) have been published.

DTP can be constructed from 3,3'-dibromo-2,2'-dithiophene via Buchwald–Hartwig ring closure with the corresponding alkylamine (Scheme 29) (2005T687, 2009JPS(A)6514, 2010OL4054, 2011JPC(C)23149).



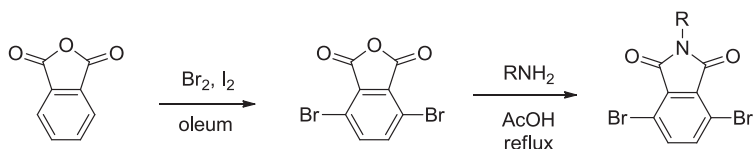
**Scheme 29** Synthesis of dithieno[3,2-*b*:2',3'-*d*]pyrrole from 3,3'-dibromo-2,2'-dithiophene.

### 3.6 Imide-Based Building Blocks

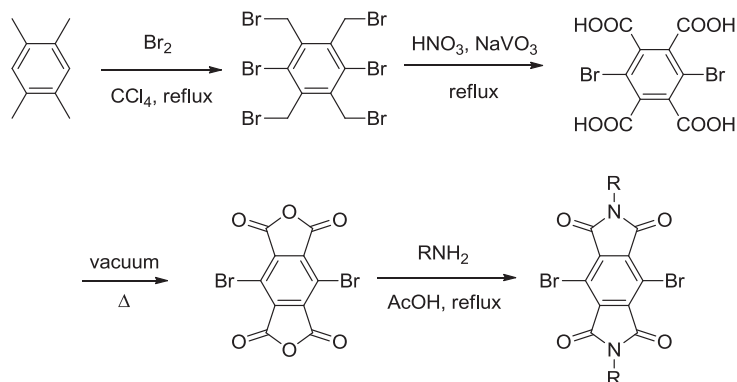
Owing to the electron-deficient nature and easy modification at the N-position, imide-based building blocks have been extensively studied in the recent years as a candidate to construct high-performance n-type semiconducting polymers (2014CRV8943). In this part, a brief overview on the structure and synthesis of a number of representative units is provided.

Phthalimide, which represents one lactam ring fused to a benzene ring, is the simplest species among all the units in this category. The synthesis of a phthalimide-based polymer was reported in 2009, which utilizes commercially available phthalic anhydride as starting material (Scheme 30) (2009JA7206). Synthesis of a number of other related units is similar to this strategy.

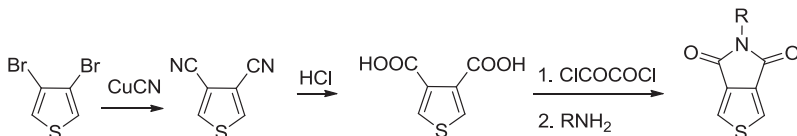
With one more lactam ring fused to the benzene ring, pyromellitic diimide (PMDI) can be constructed. Despite the similarity between PMDI and phthalimide, the benzene ring of PMDI becomes less reactive owing to the presence of an additional electron-deficient ring, which prevents direct bromination. A detoured route with four steps from durene has been developed (Scheme 31) (1961HCA1231, 2011MM6711).



**Scheme 30** Synthesis of N-alkylated phthalimides from phthalic anhydride in two steps.



**Scheme 31** Synthesis of N-alkylated pyromellitic diimides from durene in four steps.



**Scheme 32** Synthesis of thieno[3,4-*c*]pyrrole-4,6-diones from 3,4-dibromothiophene in three steps.

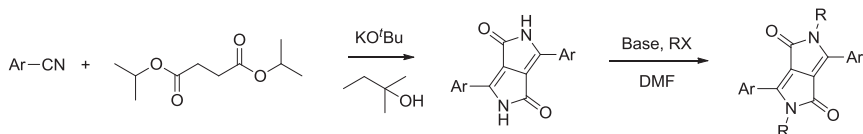
Thieno[3,4-*c*]pyrrole-4,6-dione (TPD) is the analog of phthalimide with thiophene ring substituting the benzene ring (2013MI2). This exchange leads to more quinoidal character of the polymer backbone and lower band gaps for TPD-based semiconducting polymers compared to the phthalimide analogs. The synthesis of TPD is similar to phthalimide, which involves the formation of thiophene-3,4-dicarboxylic acid or anhydride as the key intermediate (Scheme 32) (1977GEP, 1997JA5065). Due to the electron-rich character of the thiophene ring, electrophilic substitution at the  $\alpha$ -position of TPD occurs more readily than at phthalimides.

TPD is a popular acceptor unit particularly in OPVs (2010CM2696, 2010JA5330, 2010JA7595, 2011AM3315, 2011JA4250, 2011JA10062, 2012JA18427, 2012MI5, 2013JA4656, 2013MI3). Guo et al. reported a TPD-oligothiophene copolymer which presented an enhanced fill factor of 76–80% and an average PCE of 7.7% (2013MI3). They also studied the FET properties of these polymers. Interestingly, the polymers with shorter oligothiophene chain showed ambipolar mobilities, whereas the polymers with longer oligothiophene chains showed only hole mobilities as high as 0.6 cm<sup>2</sup>/V s.

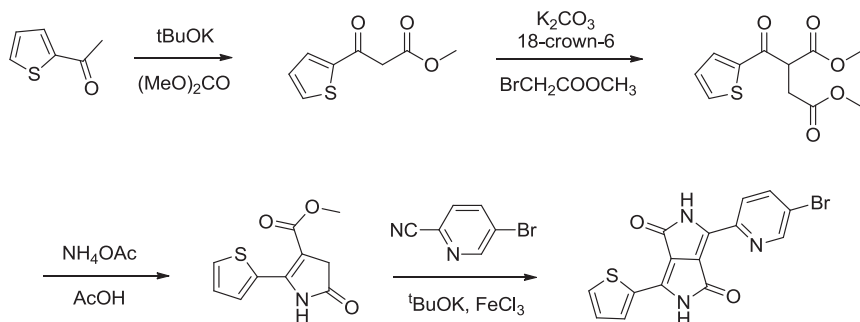
Another important bicyclic system is diketopyrrolopyrrole (DPP), which consists of two fused unsaturated lactam rings. DPP derivatives are among the most popular acceptor units for decades (2012JCS(CC)3039, 2013AM1859, 2013MI1, 2014MI3, 2015AM3589).

The synthesis of DPPs has been reviewed recently (2015MI3). The most widely studied DPP building blocks are those with identical aryl rings on both wings. These monomers are synthesized from the condensation between arylcyanides and succinates, established by Rochat et al. in 1986 (1983EUP). The last alkylation step could also occur on the O-position (2011TL5769, 2012CM2364) (Scheme 33).

Research on DPP building blocks with asymmetrical wings has just received attention due to the unique properties from the lack of symmetry of the acceptor unit (2016AM943). The synthesis of these DPP monomers with different wings is tedious compared to the symmetrical derivative. The



**Scheme 33** Construction of diketopyrrolopyrrole building blocks from arylcyanides and succinate derivatives.



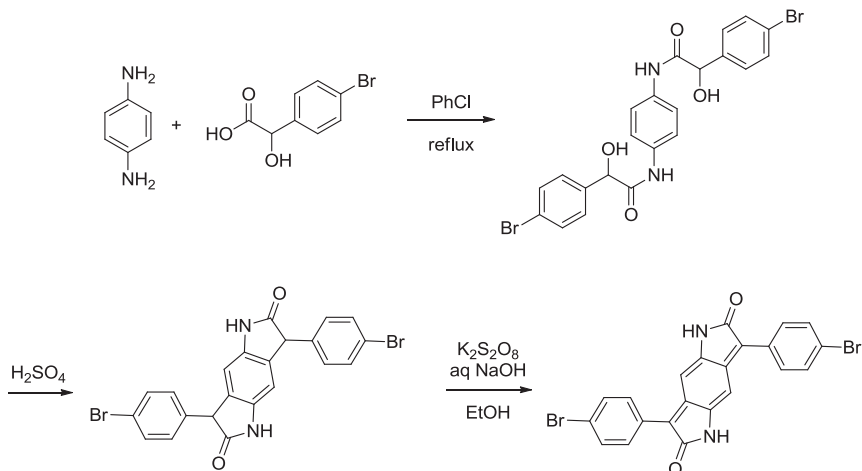
**Scheme 34** Construction of diketopyrrolopyrrole with thiophene and pyridine wings in four steps.

unsaturated ketopyrrole derivatives (2013DP530) with one aromatic ring is constructed first, followed by condensation with the carbonitrile to give another aromatic ring (Scheme 34) (2011USP, 2012MI1, 2016AM943).

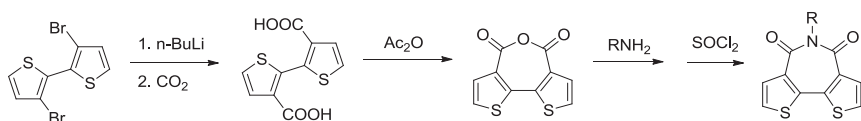
An extended analog of DPP, namely benzodipyrroledione (BPD), is tricyclic aromatic with a cyclohexadiene ring fused between two lactam rings. The synthesis of BPD was first reported in 1980 (1980DP103) and the application of BPD in semiconducting polymers in 2011 (2011MM7869). Synthesis of *p*-bromophenyl-flanked BPD is shown in Scheme 35 (2011MM7869). In the first step, *p*-phenylenediamine and 4-bromomandelic acid gives the diimide. Dehydration builds up the tricyclic backbone, which is followed by oxidation to form the BPD.

Another important tricycle is bithiophene imide (BTI). In BTI, two thiophene rings are fused to a seven-membered lactam ring. BTI was first synthesized and applied to semiconducting polymers in 2008 (2008JA9679). Due to the similarity between the structures of BTI and phthalimide, the synthesis of BTI also exploits the anhydride derivative as the key intermediate (Scheme 36).

Thienoisindole-dione (TID), another tricyclic acceptor, is a thiophene fused with isoindole-dione at the 3,4-positions. The synthesis of TID was first reported in 2001 (2001MM1810). A recent modification has been published



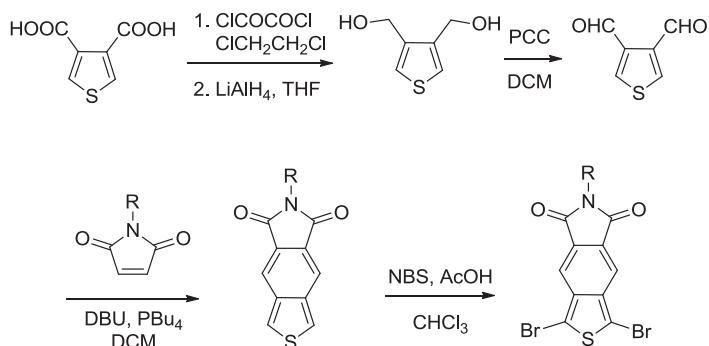
**Scheme 35** Synthesis of phenyl-winged benzodipyrroledione in three steps.



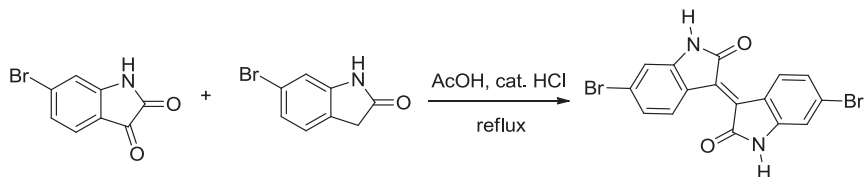
**Scheme 36** Synthesis of bithiophene imides from 3,3'-dibromo-2,2'-dithiophene in three steps.

in 2012, which involves a one-pot Wittig reaction and Knoevenagel condensation with thiophene-3,4-carboxaldehyde and maleimide ([Scheme 37](#)) ([2012CM1346](#)).

Isoindigo (IID) consists of two fused lactam rings connected with a double bond. The synthesis of IID was published in 1988 ([1988HCA1079](#)),



**Scheme 37** Synthesis of thienoisindoleidones from thiophene-3,4-dicarboxylic acid in four steps.



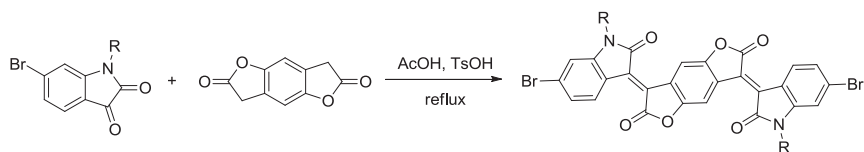
**Scheme 38** Synthesis of isoindigo from isosatin and oxindole derivatives in one step.

and the application in polymer semiconductor was reported in 2010 (2010MM8348, 2010OL660). The synthesis of IID can be achieved in one step from aldol condensation between commercially available 6-bromoisatin and 6-bromooxindole (Scheme 38) (2010OL660). The inexpensive starting material and the ease of synthesis and purification make IIDs a promising building block for semiconducting polymers for industrial and commercial devices. Extensive effort has been made on pursuing high-performance IID-based semiconducting polymer materials (2014ACR1117, 2014AM1801, 2014CM664, 2014MI5).

Based on the structure of IID, a number of related units, such as thienoisindigo (2012JCS(CC)3939) and 3,7-bis(2-oxoindolin-3-ylidene)benzo[1,2-*b*:4,5-*b'*]difuran-2,6(3*H*,7*H*)-dione (IBDF) (2013JCS(CC)3790), can be constructed. The highly fused IBDF is more electron deficient than IID, giving rise to examples of ambipolar and n-type semiconducting polymers (2013JA12168). The synthesis of IBDF monomer utilizes the similar strategy of IID (Scheme 39).

The last category of imide-based building blocks to be discussed here is rylene diimides (2011AM268). They are highly electron-deficient units, often leading to deep LUMO levels and air-stable n-type semiconducting polymers. The size of the  $\pi$ -system is variable, from four fused rings in naphthalene diimide (NDI), seven rings in perylene diimide (PDI) to eleven rings in dithienocoronene diimide (DTCDI), etc. (Figure 2).

Although the structure of NDI is the simplest among this series, the first report of an NDI-containing semiconducting polymer was published in



**Scheme 39** Synthesis of 3,7-bis(2-oxoindolin-3-ylidene)benzo[1,2-*b*:4,5-*b'*]difuran-2,6(3*H*,7*H*)-dione from isosatin derivatives in one step.

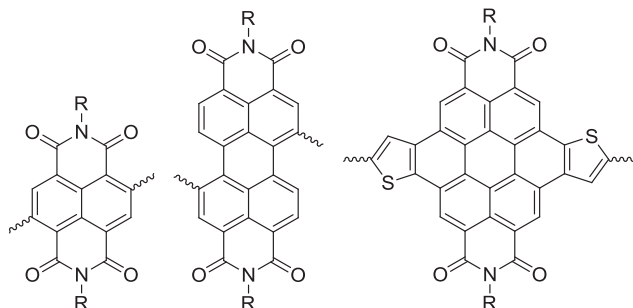
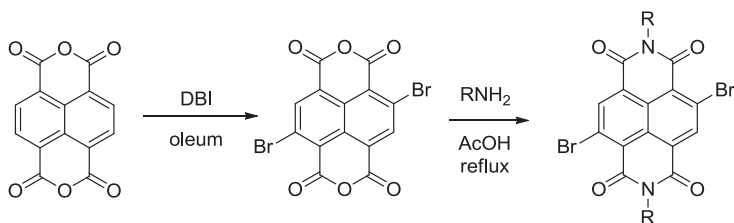


**Figure 2** Structures of naphthalene diimide (left), perylene diimide (center), and dithienopyrene diimide (right).

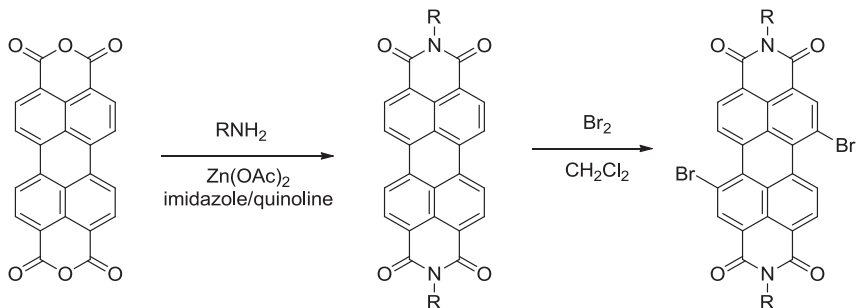
2008 (2008CSR331, 2008OL5333, 2009JA8, 2014AGE7428). However, the better solubility and planar backbone of NDI polymers, together with the ease to purify the monomer, often lead to better performance of the NDI-containing polymers compared to the PDI-containing congeners. The synthesis of NDI monomers starts from bromination of naphthalene dianhydride under strong conditions. The intermediate mixture, which contains a number of isomers, is reacted with the corresponding amine and the desired pure product can be obtained from column chromatography (1937LA1, 2006JOC8098) (Scheme 40).

The higher extended analog, PDIs are the first diimide family applied to semiconducting polymers and are currently the most studied unit to build n-type semiconductors (2011JOC2386, 2013DP160). The synthesis of PDI is similar to NDI with commercially available pyrene dianhydride as the starting material. The desired 1,7-dibrominated species can be obtained from tedious crystallization (1997GEP, 2003JOC10058, 2004JOC7933, 2007JOC5973).



**Scheme 40** Synthesis of naphthalene diimide derivatives from naphthalene dianhydride in two step.

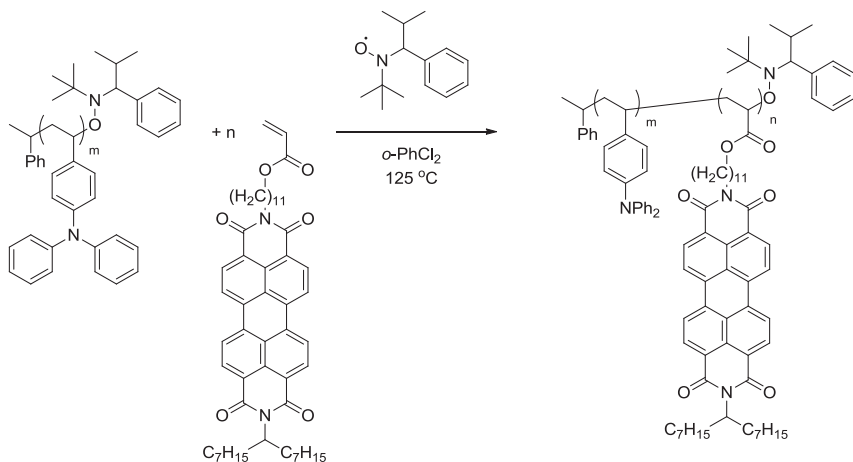




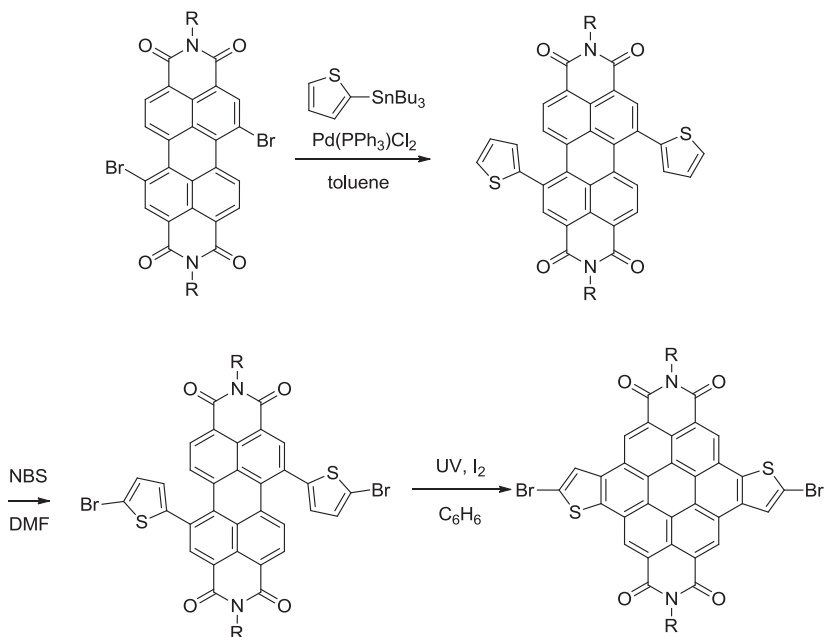
**Scheme 41** Synthesis of pyrene diimide derivatives from pyrene dianhydride in two steps.

Besides acting as acceptor units in conjugated polymers, PDIs can also be introduced into the polymer chain via N-positions or serve as side chains. An early example of PDI side chains was reported in 2004 and the synthesis of the polymer (Scheme 41) (2004MM8832).

Although PDI-based semiconducting polymers have proven to have high performances, the steric hindrance of the PDI backbone serves as a major limitation for further improvements. As an alternate, DTCDI, the thiophene-fused derivative, is also applied as an acceptor in n-type semiconducting polymers. DTCDI is synthesized from the dibrominated PDI (Scheme 42) (2012AM3678) (Scheme 43).



**Scheme 42** Synthesis of semiconducting polymer with pyrene diimide moiety in the side chain.



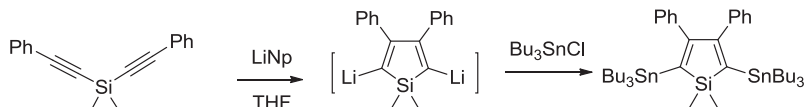
**Scheme 43** Synthesis of dithienocoronene diimide from 1,7-bromopyrene diimide in three steps.

## 4. OTHER BUILDING BLOCKS

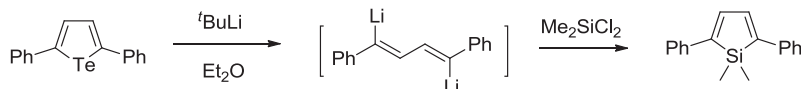
### 4.1 Silole Derivatives

Siloles, or silacyclopenta-2,4-dienes, are the silicon congeners of cyclopentadiene-based units. By substituting the carbon atom with silicon, the LUMO orbitals significantly drop as a result of the mixing between the  $\sigma^*$  orbital of the silylene scaffold and the  $\pi^*$  orbital of the butadiene moiety (1998JCS(D)3693). As a consequence, siloles and other fused relatives are popular acceptor building blocks for semiconducting polymers (2007MI1).

An early example of the synthesis of a silole was reported in 1961 from tetrachlorosilacyclopentanes (1961JA3716). However, direct functionalization at the 2,5-positions of siloles is very challenging. As a result, alternative routes are required for the synthesis of silole building blocks for polymerization. The first strategy is based on the reductive cyclization of diethynylsilanes, which produces the lithiated 3,4-diarylated silole intermediate (1994JA11715) (Scheme 44).



**Scheme 44** Synthesis of silole monomer from reductive cyclization of diethynylsilane derivatives.



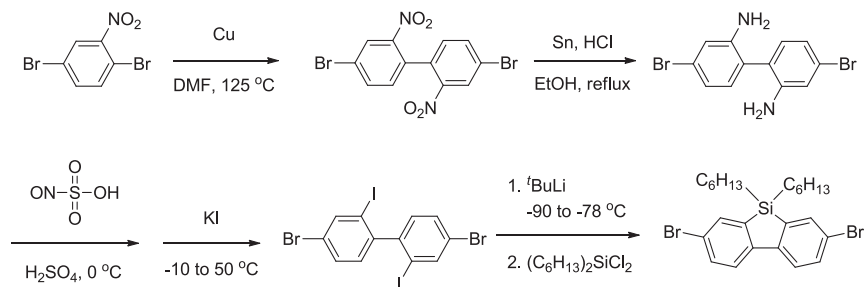
**Scheme 45** Synthesis of phenyl-winged silole from transmetalation of tellurophene.

The second strategy is based on the transmetalation of other heterocyclopentadienes (Scheme 45). This pathway is able to produce 3,4-unsubstituted siloles. However, the 2,5-positions are often linked to other aryl groups (1987AGE1187, 1989JA2870, 1989JA3336, 1995JOMC7, 1996JA10457, 1998OM5796). This method was also successful in the synthesis of the germanium derivative, namely germole (1996JA10457).

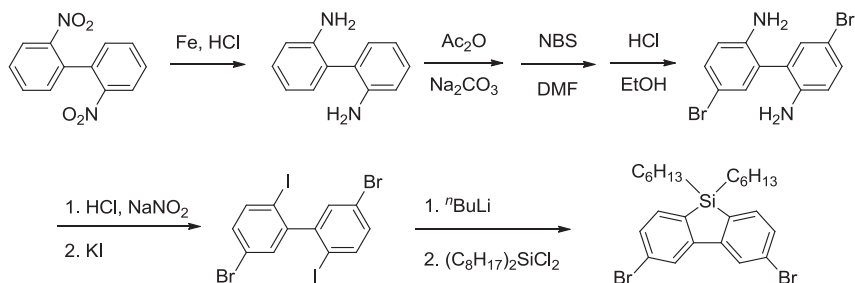
Dibenzosilole, which is a silole fused with two benzene rings, is the silicon-containing analog to DBT and carbazole. A number of dibenzosilole-containing polymers have been synthesized and studied due to their potential applications in blue light-emitting materials (2005JCS(CC)4925, 2005JCS(CC)5766, 2005JA7662, 2006JMC4133). Polymerization can occur at both 2,7- and 3,6-positions of dibenzosiloles. Due to the electron-poor nature of silole, direct bromination on the benzene ring is difficult. As an alternative, dibromodibenzosiloles are synthesized from dibromodiiodobiphenyl derivatives. This route relies on the higher reactivity of the iodine atoms at the 2,2'-positions compared to the bromine atoms. One of the monomers, 2,7-dibromodibenzosilole, can be synthesized with 4,4'-dibromo-2,2'-diiodobiphenyl as the key intermediate (Scheme 46) (2005JA7662).

Similarly, 3,6-dibromodibenzosilole can be synthesized with 5,5'-dibromo-2,2'-diiodobiphenyl as intermediate (2005JCS(CC)4925, 2005JCS(CC)5766, 2006JMC4133) (Scheme 47).

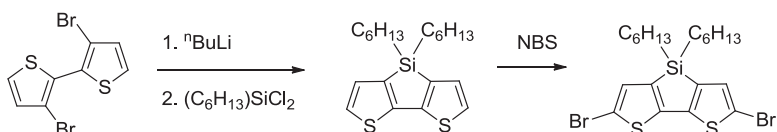
For the thiophene-fused derivative, dithienosilole, on the other hand, bromination occurs readily at the electron-rich thiophene rings. The synthesis of dithienosiloles is similar to DTP, which utilizes 3,3'-dibromo-2,2'-dithiophene as starting material. The dithienosilole skeleton is constructed from lithiation followed by salt metathesis with silyl dichloride, and the bromination is accomplished with common bromination reagents (Scheme 48) (1999OM1453, 2006JA9034).



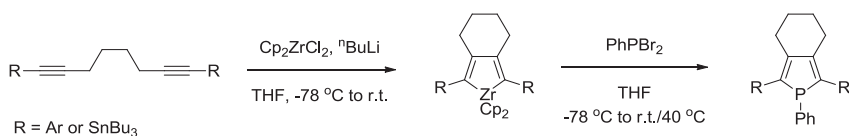
**Scheme 46** Synthesis of 2,7-dibromodibenzosilole in four steps.



**Scheme 47** Synthesis of 3,6-dibromodibenzosilole in four steps.



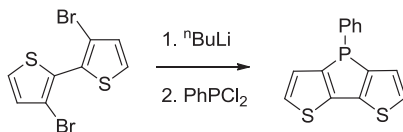
**Scheme 48** Synthesis of dithienosilole from 3,3'-dibromo-2,2'-dithiophene.



**Scheme 49** Synthesis of phosphole from transmetalation of zirconocene.

## 4.2 Phosphole Derivatives

Phospholes, or phosphacyclopentadienes, are a series of electron-poor heterocycles with either P<sup>III</sup> or P<sup>V</sup> substituting one carbon atom of cyclopentadiene. Theoretical studies have shown that the phosphorous atom is highly pyramidalized with the lone pair exhibiting highly *s* character. As a consequence, phosphole rings exhibited a low degree of aromaticity and the pseudoaromaticity is a result of the hyperconjugation between the



**Scheme 50** Synthesis of dithieno[3,2-*b*:2',3'-*d*]phosphole derivatives from 3,3'-dibromo-2,2'-dithiophene.

$\pi$ -orbital of butadiene and the  $\sigma$ -orbital of the P–C bond, giving rise to a low-lying LUMO level (1988CRV429, 2001CRV1229). Therefore, the electronic structure of phospholes is similar to siloles rather than to pyrroles, and phospholes are applied as strong acceptor building blocks and a candidate to construct n-type semiconducting polymers (2008TH).

The synthesis of phosphole building blocks utilizes the transmetalation of zirconocene, which involves ring formation between diynes and zirconocene dichloride followed by substitution with the corresponding dibromophosphine species (1997MM5566, 2001CEJ4222).

Ladder-type phosphole derivatives, dithieno[3,2-*b*:2',3'-*d*]phosphole, can be synthesized from 3,3'-dibromo-2,2'-dithiophene, which is similar to dithienosilole (2004AGE6197) (Scheme 50).

Owing to the reducing nature of phospholes, the electron-withdrawing character can be further improved by oxidizing the trivalent species to form a series of pentavalent species (2007EJI3611, 2010OL2675, 2013MI4). For instance, the phosphole *P*-imides can be synthesized from the Staudinger reaction between phospholes and corresponding organic azides (Scheme 49) (2013OL932). The high-polarized P–O bond promotes the charge transport from the polymer to an external acceptor, which is beneficial to OPVs. A recent example by Park et al. demonstrated the application of dithieno[3,2-*b*:2',3'-*d*]phosphole oxide as a building block in high-performance solar cells, which showed PCE as high as 7.08% (2015MI1) (Scheme 51).

### 4.3 BODIPLY

The boron-containing heterocyclic building blocks have attracted increasing interest due to their rich luminescent properties (2010CL430, 2012MI3,



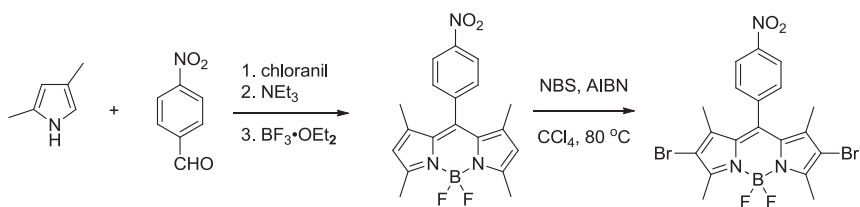
**Scheme 51** Oxidation of phosphole to generate phosphole *P*-imide.

2015MI6). Currently, building blocks with tetracoordinated boron atoms are more studied than the tricoordinated derivatives due to their improved stability.

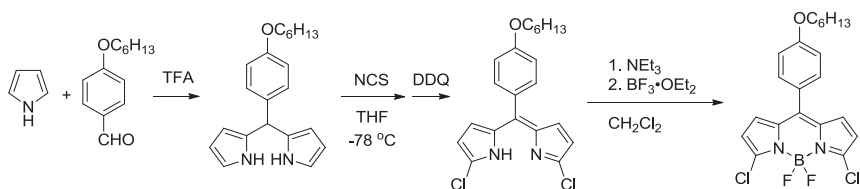
The most important category of boron-containing building block as a polymer semiconductor is boron dipyrromethanes, or (4-bora-3a,4a-diaza-s-indacenes) (BODIPY). As a famous and widely studied dye, the synthesis and application of BODIPYs as luminescence and light-harvesting materials have been extensively studied and reviewed (2007CRV4891, 2011T3573). The interest in BODIPY-containing semiconducting polymers is focused on the potential application in OLEDs and infrared light harvesting. A number of BHJ-OPVs based on BODIPY with narrow optic band gap (smaller than 2 eV) and promising PCE values (up to 2%) have been reported (2010JCS(CC)4148, 2012JMC14119, 2015JMC(A)16279). As to the application in transistors, the BODIPY-thiophene copolymer introduced by Usta et al. showed high hole mobility of  $0.17 \text{ cm}^2/\text{Vs}$  (2013AM4327).

BODIPY is typically constructed by condensation between aldehydes and pyrroles, followed by the addition of a boron source, sometimes with the presence of an oxidant. Both the 2,6- and 3,5-disubstituted derivatives were synthesized and applied as monomers in BODIPY-based semiconducting polymers. 2,6-Dibromo(BODIPY) species are obtained from direct bromination of BODIPY cores (Scheme 52) (2001JA100, 2009MI4).

With 3,5-dichloro(BODIPY) derivatives, the chlorine atoms are introduced to the moiety prior to the addition of borane (Scheme 53) (2012JMC14119).



**Scheme 52** Synthesis of 2,6-dibromo(BODIPY) from pyrrole and benzaldehyde derivatives in two steps.



**Scheme 53** Synthesis of 3,5-dibromo(BODIPY) from pyrrole and benzaldehyde derivatives in two steps.

## REFERENCES

- 1885CB2255 C. Paal, *Ber. Dtsch. Chem. Ges.*, **18**, 2255–2256 (1885).  
1889CB2895 O. Hinsberg, *Ber. Dtsch. Chem. Ges.*, **22**, 2895–2902 (1889).  
1937LA1 H. Vollmann, H. Becker, M. Corell, H. Streeck, and G. Langbein, *Liebigs Ann. Chem.*, **531**, 1–159 (1937).  
1940OS16 R.E. Damschroder and W.D. Peterson, *Org. Synth.*, **20**, 16–18 (1940).  
1950USP J.A. Patterson and C.H. Culnane, *Pat. US2509938A*.  
1955BSF424 C. Troyanowsky, *Bull. Soc. Chim. Fr.*, 424–426 (1955).  
1956DOK88 A.M. Khaletskii, V.G. Pesin, and C.-C. Chao, *Dokl. Akad. Nauk SSSR*, **106**, 88–91 (1956).  
1957CCC64 Z.J. Allan and F. Muzik, *Collect. Czech. Chem. Commun.*, **22**, 64–75 (1957).  
1959ACSA1045 S. Gronowitz, *Acta Chem. Scand.*, **13**, 1045–1046 (1959).  
1961HCA1231 H. Hopff, P. Doswald, and B.K. Manukian, *Helv. Chim. Acta.*, **44**, 1231–1237 (1961).  
1961JA3716 R.A. Benkeser, R.F. Grossman, and G.M. Stanton, *J. Am. Chem. Soc.*, **83**, 3716 (1961).  
1963AK335 S. Gronowitz and B. Eriksson, *Ark. Kemi*, **21**, 335–341 (1963).  
1963IZV2183 V.P. Litvinov and Y.L. Gol'dfarb, *Izv. Akad. Nauk SSSR Ser. Khim.*, 2183–2192 (1963).  
1963JCS4767 C.W. Bird, G.W. Cheeseman, and A.A. Sarsfiel, *J. Chem. Soc.*, 4767–4770 (1963).  
1964JOC2455 H. Wynberg and A. Kraak, *J. Org. Chem.*, **29**, 2455–2457 (1964).  
1964OS9 S. Gronowitz and T. Raznikiewicz, *Org. Synth.*, **44**, 9–11 (1964).  
1965IZV510 Y.L. Gol'dfarb, V.P. Litvinov, and S.A. Ozolin, *Izv. Akad. Nauk SSSR Ser. Khim.*, 510–515 (1965).  
1966JOC3363 D.J. Zwanenburg, H. de Haan, and H. Wynberg, *J. Org. Chem.*, **31**, 3363–3365 (1966).  
1967AK99 S. Gronowitz, J.E. Skramstad, and B. Eriksson, *Ark. Kemi*, **28**, 99–107 (1967).  
1967JOC2823 L.M. Weinstock, P. Davis, B. Handelsman, and R.J. Tull, *J. Org. Chem.*, **32**, 2823–2828 (1967).  
1967KKZ63 M. Kuroki, *Kogyo Kagaku Zasshi*, **70**, 63–66 (1967).  
1968ACSA63 A. Bugge, *Acta Chem. Scand.*, **22**, 63–69 (1968).  
1970JCS(C)273 P. Jordens, G. Rawson, and H. Wynberg, *J. Chem. Soc. C*, 273–277 (1970).  
1971JOC3932 M.P. Cava, N.M. Pollack, O.A. Mamer, and M.J. Mitchell, *J. Org. Chem.*, **36**, 3932–3937 (1971).  
1974M1306 J. Pielichowski and J. Kyziol, *Monatsh. Chem.*, **105**, 1306–1312 (1974).  
1977GEP M. Dimmler and H. Eilingsfeld, *Pat. DE2538951A1*.  
1978JHC561 L.H. Klemm and J.J. Karchesy, *J. Heterocyclic Chem.*, **15**, 561–563 (1978).  
1980DP103 C.W. Greenhalgh, J.L. Carey, and D.F. Newton, *Dyes Pigm.*, **1**, 103–120 (1980).  
1983EUP A.C. Rochat, L. Cassar, and A. Iqbal, *Pat. EP0094911A2*.  
1983BSF159 F. Outurquin and C. Paulmier, *Bull. Soc. Chim. Fr.*, 159–163 (1983).  
1983JOC3544 S. Mohmand, J. Bargon, and R.J. Waltman, *J. Org. Chem.*, **48**, 3544–3545 (1983).  
1984JCS(P)2591 M.R. Bryce, *J. Chem. Soc. Perkin Trans.*, **1**, 2591–2593 (1984).  
1984MI1 Y. Katsumi, H. Shigenori, and S. Ryu-ichi, *Jpn. J. Appl. Phys.*, **23**, L899 (1984).

- 1984JOC3382 F. Wudl, M. Kobayashi, and A.J. Heeger, *J. Org. Chem.*, **49**, 3382–3384 (1984).
- 1985JHC215 H. Kudo, R.N. Castle, and M.L. Lee, *J. Heterocyclic Chem.*, **22**, 215–218 (1985).
- 1986APPLAB1210 A. Tsumura, H. Koezuka, and T. Ando, *Appl. Phys. Lett.*, **49**, 1210–1212 (1986).
- 1986CB3198 P. Beimling and G. Kobmehl, *Chem. Ber.*, **119**, 3198–3203 (1986).
- 1986MI1 R. Sugimoto, S. Takeda, H.B. Gu, and K. Yoshino, *Chem. Express*, **1**, 635–638 (1986).
- 1987AGE1187 T. Hiroy, N. Kambe, A. Ogawa, N. Miyoshi, S. Murai, and N. Sonoda, *Angew. Chem. Int. Ed.*, **26**, 1187–1188 (1987).
- 1988APPLAB195 A. Assadi, C. Svensson, M. Willander, and O. Inganäs, *Appl. Phys. Lett.*, **53**, 195–197 (1988).
- 1988CRV429 F. Mathey, *Chem. Rev.*, **88**, 429–453 (1988).
- 1988HCA1079 C. Papageorgiou and X. Borer, *Helv. Chim. Acta.*, **71**, 1079–1083 (1988).
- 1989EUP F.D. Jonas, G.D. Heywang, W. Schmidtberg, J.P.D. Heinze, and M. Dietrich, *Pat. EP0339340A2*.
- 1989MI1 P.A. Christensen, J.C.H. Kerr, S.J. Higgins, and A. Hamnett, *Faraday Discuss. Chem. Soc.*, **88**, 261–275 (1989).
- 1989JA2870 S.L. Buchwald and R.B. Nielsen, *J. Am. Chem. Soc.*, **111**, 2870–2874 (1989).
- 1989JA3336 E. Negishi, S.J. Holmes, J.M. Tour, J.A. Miller, F.E. Cederbaum, D.R. Swanson, and T. Takahashi, *J. Am. Chem. Soc.*, **111**, 3336–3346 (1989).
- 1990PS35 C. Mahatsekake, J.M. Catel, C.G. Andrieu, M. Ebel, Y. Mollier, and G. Tourillon, *Phosphorus, Sulfur Silicon Relat. Elem.*, **47**, 35–41 (1990).
- 1991JCS(CC)1268 J.P. Ferraris and T.L. Lambert, *J. Chem. Soc. Chem. Commun.*, 1268–1270 (1991).
- 1992CRV711 J. Roncali, *Chem. Rev.*, **92**, 711–738 (1992).
- 1992JA10087 T.A. Chen and R.D. Rieke, *J. Am. Chem. Soc.*, **114**, 10087–10088 (1992).
- 1992JCS(CC)70 R.D. McCullough and R.D. Lowe, *J. Chem. Soc. Chem. Commun.*, 70–72 (1992).
- 1992JCS(CC)1137 M. Kozaki, S. Tanaka, and Y. Yamashita, *J. Chem. Soc. Chem. Commun.*, 1137–1138 (1992).
- 1992MM2294 D.R. Rutherford, J.K. Stille, C.M. Elliott, and V.R. Reichert, *Macromolecules*, **25**, 2294–2306 (1992).
- 1993USP J.P. Ferraris, T.L. Lambert, and S. Rodriguez, *Pat. US5274058A*.
- 1993MM3464 T. Kanbara and T. Yamamoto, *Macromolecules*, **26**, 3464–3466 (1993).
- 1994JA11715 K. Tamao, S. Yamaguchi, and M. Shiro, *J. Am. Chem. Soc.*, **116**, 11715–11722 (1994).
- 1994JOC442 M. Kozaki, S. Tanaka, and Y. Yamashita, *J. Org. Chem.*, **59**, 442–450 (1994).
- 1994MM1938 G. Zotti, G. Schiavon, A. Berlin, G. Fontana, and G. Pagani, *Macromolecules*, **27**, 1938–1942 (1994).
- 1995JA6791 M. Karikomi, C. Kitamura, S. Tanaka, and Y. Yamashita, *J. Am. Chem. Soc.*, **117**, 6791–6792 (1995).
- 1995JOMC7 U. Bankwitz, H. Sohn, D.R. Powell, and R. West, *J. Organomet. Chem.*, **499**, C7–C9 (1995).
- 1995SM147 J.P. Ferraris, C. Henderson, D. Torres, and D. Meeker, *Synth. Met.*, **72**, 147–152 (1995).



- 1996APPLAB4108 Z. Bao, A. Dodabalapur, and A.J. Lovinger, *Appl. Phys. Lett.*, **69**, 4108–4110 (1996).
- 1996JA10457 W.P. Freeman, T.D. Tilley, L.M. LiableSands, and A.L. Rheingold, *J. Am. Chem. Soc.*, **118**, 10457–10468 (1996).
- 1996T13227 A. Citterio, R. Sebastiano, A. Maronati, F. Viola, and A. Farina, *Tetrahedron*, **52**, 13227–13242 (1996).
- 1997GEP A. Boehm, H. Arms, G. Henning, and P. Blaschka, *Pat. DE19547209A1*.
- 1997JA5065 Q. Zhang and J.M. Tour, *J. Am. Chem. Soc.*, **119**, 5065–5066 (1997).
- 1997JMC1731 P. Franchetti, L. Cappellacci, G.A. Sheikha, H.N. Jayaram, V.V. Gurudutt, T. Sint, B.P. Schneider, W.D. Jones, B.M. Goldstein, G. Perra, A. De Montis, A.G. Loi, P. La Colla, and M. Grifantini, *J. Med. Chem.*, **40**, 1731–1737 (1997).
- 1997JPS(A)2813 O. Shimomura, T. Sato, I. Tomita, M. Suzuki, and T. Endo, *J. Polym. Sci. A Polym. Chem.*, **35**, 2813–2819 (1997).
- 1997MM5566 S.S.H. Mao and T.D. Tilley, *Macromolecules*, **30**, 5566–5569 (1997).
- 1997SM973 S.R. Gunatunga, G.W. Jones, M. Kalaji, P.J. Murphy, D.M. Taylor, and G.O. Williams, *Synth. Met.*, **84**, 973–974 (1997).
- 1998AM93 R.D. McCullough, *Adv. Mater.*, **10**, 93–116 (1998).
- 1998JCS(D)3693 S. Yamaguchi and K. Tamao, *J. Chem. Soc. Dalton. Trans.*, 3693–3702 (1998).
- 1998JMC25 A. Iraqi and G.W. Barker, *J. Mater. Chem.*, **8**, 25–29 (1998).
- 1998OM5796 M. Katkevics, S. Yamaguchi, A. Toshimitsu, and K. Tamao, *Organometallics*, **17**, 5796–5800 (1998).
- 1998SCI1741 H.N.R.H. Siringhaus, *Science*, **280**, 1741–1744 (1998).
- 1998SM25 R. Beyer, M. Kalaji, G. Kingscote-Burton, P.J. Murphy, V.M.S.C. Pereira, D.M. Taylor, and G.O. Williams, *Synth. Met.*, **92**, 25–31 (1998).
- 1999JMC2095 H. Siringhaus, R.H. Friend, C. Wang, J. Leuninger, and K. Mullen, *J. Mater. Chem.*, **9**, 2095–2101 (1999).
- 1999OM1453 J. Ohshita, M. Nodono, H. Kai, T. Watanabe, A. Kunai, K. Komaguchi, M. Shiotani, A. Adachi, K. Okita, Y. Harima, K. Yamashita, and M. Ishikawa, *Organometallics*, **18**, 1453–1459 (1999).
- 2000AM481 B.L. Groenendaal, F. Jonas, D. Freitag, H. Pielartzik, and J.R. Reynolds, *Adv. Mater.*, **12**, 481–494 (2000).
- 2001AM1775 J.D. Tovar and T.M. Swager, *Adv. Mater.*, **13**, 1775–1780 (2001).
- 2001AGE2591 A.J. Heeger, *Angew. Chem. Int. Ed.*, **40**, 2591–2611 (2001).
- 2001CRV1229 L. Nyulaszi, *Chem. Rev.*, **101**, 1229–1246 (2001).
- 2001CEJ4222 C. Hay, M. Hissler, C. Fischmeister, J. Rault-Berthelot, L. Toupet, L. Nyulaszi, and R. Reau, *Chem. Eur. J.*, **7**, 4222–4236 (2001).
- 2001JA100 H. Imahori, H. Norieda, H. Yamada, Y. Nishimura, I. Yamazaki, Y. Sakata, and S. Fukuzumi, *J. Am. Chem. Soc.*, **123**, 100–110 (2001).
- 2001MM1810 H. Meng and F. Wudl, *Macromolecules*, **34**, 1810–1816 (2001).
- 2001MM4680 J.F. Morin and M. Leclerc, *Macromolecules*, **34**, 4680–4682 (2001).
- 2001MI1 T.L. Gilchrist and S.J. Higgins, *Sci. Synth.*, **10**, 185–210 (2001).
- 2002MM6080 J. Huang, Y. Niu, W. Yang, Y. Mo, M. Yuan, and Y. Cao, *Macromolecules*, **35**, 6080–6082 (2002).
- 2002MI1 J. Schatz, *Sci. Synth.*, **9**, 423–432 (2002).
- 2003JOC10058 L.D. Wescott and D.L. Mattern, *J. Org. Chem.*, **68**, 10058–10066 (2003).
- 2003JMC1351 W. Yang, Q. Hou, C.Z. Liu, Y.H. Niu, J. Huang, R.Q. Yang, and Y. Cao, *J. Mater. Chem.*, **13**, 1351–1355 (2003).

- 2003MI1 J.V. Grazulevicius, P. Strohrriegl, J. Pielichowski, and K. Pielichowski, *Prog. Polym. Sci.*, **28**, 1297–1353 (2003).
- 2003S2470 F. Dierschke, A.C. Grimsdale, and K. Mullen, *Synthesis*, 2470–2472 (2003).
- 2004ASC1818 A. Tanimoto and T. Yamamoto, *Adv. Synth. Catal.*, **346**, 1818–1823 (2004).
- 2004AGE6197 T. Baumgartner, T. Neumann, and B. Wirges, *Angew. Chem. Int. Ed.*, **43**, 6197–6201 (2004).
- 2004CM2165 Y. Li, J. Ding, M. Day, Y. Tao, J. Lu, and M. D'Iorio, *Chem. Mater.*, **16**, 2165–2173 (2004).
- 2004JOC7933 F. Wuerthner, V. Stepanenko, Z. Chen, C.R. Saha-Moeller, N. Kocher, and D. Stalke, *J. Org. Chem.*, **69**, 7933–7939 (2004).
- 2004MI1 R. Miyakoshi, A. Yokoyama, and T. Yokozawa, *Macromol. Rapid Commun.*, **25**, 1663–1666 (2004).
- 2004MM1169 A. Yokoyama, R. Miyakoshi, and T. Yokozawa, *Macromolecules*, **37**, 1169–1171 (2004).
- 2004MM8832 S.M. Lindner and M. Thelakkat, *Macromolecules*, **37**, 8832–8835 (2004).
- 2004TL6049 F. von Kieseritzky, F. Allared, E. Dahstedt, and J. Hellberg, *Tetrahedron Lett.*, **45**, 6049–6050 (2004).
- 2005JCS(CC)4925 Y.Q. Mo, R.Y. Tian, W. Shi, and Y. Cao, *Chem. Commun.*, 4925–4926 (2005).
- 2005JCS(CC)5766 K.L. Chan, S.E. Watkins, C.S.K. Mak, M.J. McKiernan, C.R. Towns, S.I. Pascu, and A.B. Holmes, *Chem. Commun.*, 5766–5768 (2005).
- 2005JA7662 K.L. Chan, M.J. McKiernan, C.R. Towns, and A.B. Holmes, *J. Am. Chem. Soc.*, **127**, 7662–7663 (2005).
- 2005JA13281 K. Xiao, Y. Liu, T. Qi, W. Zhang, F. Wang, J. Gao, W. Qiu, Y. Ma, G. Cui, S. Chen, X. Zhan, G. Yu, J. Qin, W. Hu, and D. Zhu, *J. Am. Chem. Soc.*, **127**, 13281–13286 (2005).
- 2005MI1 G.L. Sommen, *Mini Rev. Org. Chem.*, **2**, 373–388 (2005).
- 2005T687 G. Koeckelberghs, L. De Cremer, W. Vanormelingen, W. Dehaen, T. Verbiest, A. Persoons, and C. Samyn, *Tetrahedron*, **61**, 687–691 (2005).
- 2005TL6843 B.A.D. Neto, A.S. Lopes, M. Wust, V.E.U. Costa, G. Ebeling, and J. Dupont, *Tetrahedron Lett.*, **46**, 6843–6846 (2005).
- 2006MI1 R.J. Mortimer, A.L. Dyer, and J.R. Reynolds, *Displays*, **27**, 2–18 (2006).
- 2006JOC8098 C. Thalacker, C. Roeger, and F. Wuerthner, *J. Org. Chem.*, **71**, 8098–8105 (2006).
- 2006JMC4133 E.G. Wang, C. Li, Y.Q. Mo, Y. Zhang, G. Ma, W. Shi, J.B. Peng, W. Yang, and Y. Cao, *J. Mater. Chem.*, **16**, 4133–4140 (2006).
- 2006JA9034 H. Usta, G. Lu, A. Facchetti, and T.J. Marks, *J. Am. Chem. Soc.*, **128**, 9034–9035 (2006).
- 2006PLM527 W.C. Wu, C.L. Liu, and W.C. Chen, *Polymer*, **47**, 527–538 (2006).
- 2006TL5143 I.A. Liversedge, S.J. Higgins, M. Giles, M. Heeney, and I. McCulloch, *Tetrahedron Lett.*, **47**, 5143–5146 (2006).
- 2007AM3979 Y. Yao, Y. Liang, V. Shrotriya, S. Xiao, L. Yu, and Y. Yang, *Adv. Mater.*, **19**, 3979–3983 (2007).
- 2007CRV1272 I.D.W. Samuel and G.A. Turnbull, *Chem. Rev.*, **107**, 1272–1295 (2007).
- 2007CRV1324 S. Gunes, H. Neugebauer, and N.S. Sariciftci, *Chem. Rev.*, **107**, 1324–1338 (2007).
- 2007CRV4891 A. Loudet and K. Burgess, *Chem. Rev.*, **107**, 4891–4932 (2007).

- 2007EJI3611 M.G. Hobbs and T. Baumgartner, *Eur. J. Inorg. Chem.*, 3611–3628 (2007).
- 2007JOC5973 P. Rajasingh, R. Cohen, E. Shirman, L.J.W. Shimon, and B. Rybtchinski, *J. Org. Chem.*, **72**, 5973–5979 (2007).
- 2007JMC1421 J. Gao, L. Li, Q. Meng, R. Li, H. Jiang, H. Li, and W. Hu, *J. Mater. Chem.*, **17**, 1421–1426 (2007).
- 2007JA1805 M. Winkler and K.N. Houk, *J. Am. Chem. Soc.*, **129**, 1805–1815 (2007).
- 2007MI1 J. Chen and Y. Cao, *Macromol. Rapid Commun.*, **28**, 1714–1742 (2007).
- 2008TH Y. Dienes, *RWTH Aachen University*.
- 2008ACR1110 N. Blouin and M. Leclerc, *Acc. Chem. Res.*, **41**, 1110–1119 (2008).
- 2008CSR331 S.V. Bhosale, C.H. Jani, and S.J. Langford, *Chem. Soc. Rev.*, **37**, 331–342 (2008).
- 2008CM4499 H. Liu, J.H. Zou, W. Yang, H.B. Wu, C. Li, B. Zhang, J.B. Peng, and Y. Cao, *Chem. Mater.*, **20**, 4499–4506 (2008).
- 2008JA6734 A. Patra, Y.H. Wijsboom, S.S. Zade, M. Li, Y. Sheynin, G. Leitus, and M. Bendikov, *J. Am. Chem. Soc.*, **130**, 6734–6736 (2008).
- 2008JA9679 J.A. Letizia, M.R. Salata, C.M. Tribout, A. Facchetti, M.A. Ratner, and T.J. Marks, *J. Am. Chem. Soc.*, **130**, 9679–9694 (2008).
- 2008JA13167 J. Liu, R. Zhang, G. Sauve, T. Kowalewski, and R.D. McCullough, *J. Am. Chem. Soc.*, **130**, 13167–13176 (2008).
- 2008MM5563 Y. Qin, J.Y. Kim, C.D. Frisbie, and M.A. Hillmyer, *Macromolecules*, **41**, 5563–5570 (2008).
- 2008MM5688 S. Xiao, H. Zhou, and W. You, *Macromolecules*, **41**, 5688–5696 (2008).
- 2008MM6012 J.H. Hou, M.H. Park, S.Q. Zhang, Y. Yao, L.M. Chen, J.H. Li, and Y. Yang, *Macromolecules*, **41**, 6012–6018 (2008).
- 2008MM8302 E. Zhou, M. Nakamura, T. Nishizawa, Y. Zhang, Q. Wei, K. Tajima, C. Yang, and K. Hashimoto, *Macromolecules*, **41**, 8302–8305 (2008).
- 2008OL5333 X.G. Guo and M.D. Watson, *Org. Lett.*, **10**, 5333–5336 (2008).
- 2008MI1 S. Wakim, B.-R. Aïch, T. Ye, and M. Leclerc, *Polym. Rev.*, **48**, 432–462 (2008).
- 2009MI1 S.M. King, I.I. Perepichka, I.F. Perepichka, F.B. Dias, M.R. Bryce, and A.P. Monkman, *Adv. Funct. Mater.*, **19**, 586–591 (2009).
- 2009MI2 J.C. Bijleveld, M. Shahid, J. Gilot, M.M. Wienk, and R.A.J. Janssen, *Adv. Funct. Mater.*, **19**, 3262–3270 (2009).
- 2009AM1091 I. McCulloch, M. Heeney, M.L. Chabinyc, D. DeLongchamp, R.J. Kline, M. Coelle, W. Duffy, D. Fischer, D. Gundlach, B. Hamadani, R. Hamilton, L. Richter, A. Salleo, M. Shkunov, D. Sporrowe, S. Tierney, and W. Zhong, *Adv. Mater.*, **21**, 1091–1109 (2009).
- 2009CM4055 E. Zhou, S. Yamakawa, K. Tajima, C. Yang, and K. Hashimoto, *Chem. Mater.*, **21**, 4055–4061 (2009).
- 2009CRV897 A.C. Grimsdale, K.L. Chan, R.E. Martin, P.G. Jokisz, and A.B. Holmes, *Chem. Rev.*, **109**, 897–1091 (2009).
- 2009CRV5868 Y.J. Cheng, S.H. Yang, and C.S. Hsu, *Chem. Rev.*, **109**, 5868–5923 (2009).
- 2009JMC2199 W. Yue, Y. Zhao, S. Shao, H. Tian, Z. Xie, Y. Geng, and F. Wang, *J. Mater. Chem.*, **19**, 2199–2206 (2009).
- 2009JMC5794 X. Zhan, Z.A. Tan, E. Zhou, Y. Li, R. Misra, A. Grant, B. Domercq, X.-H. Zhang, Z. An, X. Zhang, S. Barlow, B. Kippelen, and S.R. Marder, *J. Mater. Chem.*, **19**, 5794–5803 (2009).
- 2009JPS(A)6514 S.P. Mishra, A.K. Palai, R. Srivastava, M.N. Kamalasanan, and M. Patri, *J. Polym. Sci. A Polym. Chem.*, **47**, 6514–6525 (2009).

- 2009JA8 Z.H. Chen, Y. Zheng, H. Yan, and A. Facchetti, *J. Am. Chem. Soc.*, **131**, 8–9 (2009).
- 2009JA7206 X. Guo, F.S. Kim, S.A. Jenekhe, and M.D. Watson, *J. Am. Chem. Soc.*, **131**, 7206–7207 (2009).
- 2009JA7792 Y. Liang, D. Feng, Y. Wu, S.-T. Tsai, G. Li, C. Ray, and L. Yu, *J. Am. Chem. Soc.*, **131**, 7792–7799 (2009).
- 2009MI3 Y. Li, H. Wu, J. Zou, L. Ying, W. Yang, and Y. Cao, *Org. Electron.*, **10**, 901–909 (2009).
- 2009MI4 A. Cihaner and F. Algi, *React. Funct. Polym.*, **69**, 62–67 (2009).
- 2009MI5 F.C. Krebs, *Sol. Energ. Mat. Sol. C.*, **93**, 394–412 (2009).
- 2010ACR1396 P.M. Beaujuge, C.M. Amb, and J.R. Reynolds, *Acc. Chem. Res.*, **43**, 1396–1407 (2010).
- 2010MI1 H. Zhou, L. Yang, S. Stoneking, and W. You, *ACS Appl. Mater. Interfaces*, **2**, 1377–1383 (2010).
- 2010MI2 A.C. Siegel, S.T. Phillips, M.D. Dickey, N.S. Lu, Z.G. Suo, and G.M. Whitesides, *Adv. Funct. Mater.*, **20**, 28–35 (2010).
- 2010AM83 R. Rieger, D. Beckmann, W. Pisula, W. Steffen, M. Kastler, and K. Müllen, *Adv. Mater.*, **22**, 83–86 (2010).
- 2010AM4617 T.L. Nelson, T.M. Young, J. Liu, S.P. Mishra, J.A. Belot, C.L. Balliet, A.E. Javier, T. Kowalewski, and R.D. McCullough, *Adv. Mater.*, **22**, 4617–4621 (2010).
- 2010JCS(CC)4148 B. Kim, B. Ma, V.R. Donuru, H. Liu, and J.M.J. Frechet, *Chem. Commun.*, **46**, 4148–4150 (2010).
- 2010CRV3 A.C. Arias, J.D. MacKenzie, I. McCulloch, J. Rivnay, and A. Salleo, *Chem. Rev.*, **110**, 3–24 (2010).
- 2010CRV268 P.M. Beaujuge and J.R. Reynolds, *Chem. Rev.*, **110**, 268–320 (2010).
- 2010CSR2354 A.J. Heeger, *Chem. Soc. Rev.*, **39**, 2354–2371 (2010).
- 2010CSR2399 J. Li and A.C. Grimsdale, *Chem. Soc. Rev.*, **39**, 2399–2410 (2010).
- 2010CL430 A. Nagai and Y. Chujo, *Chem. Lett.*, **39**, 430–435 (2010).
- 2010CM2696 Y. Zhang, S.K. Hau, H.-L. Yip, Y. Sun, O. Acton, and A.K.Y. Jen, *Chem. Mater.*, **22**, 2696–2698 (2010).
- 2010JMC123 X. Zhang, T.T. Steckler, R.R. Dasari, S. Ohira, W.J. Potscavage Jr., S.P. Tiwari, S. Coppee, S. Ellinger, S. Barlow, J.-L. Bredas, B. Kippelen, J.R. Reynolds, and S.R. Marder, *J. Mater. Chem.*, **20**, 123–134 (2010).
- 2010JMC422 A. Patra and M. Bendikov, *J. Mater. Chem.*, **20**, 422–433 (2010).
- 2010JOC1228 S. Shinamura, E. Miyazaki, and K. Takimiya, *J. Org. Chem.*, **75**, 1228–1234 (2010).
- 2010JPC(C)16793 L. Yang, H. Zhou, and W. You, *J. Phys. Chem. C*, **114**, 16793–16800 (2010).
- 2010JA5330 Y. Zou, A. Najari, P. Berrouard, S. Beaupre, B. Reda Aich, Y. Tao, and M. Leclerc, *J. Am. Chem. Soc.*, **132**, 5330–5331 (2010).
- 2010JA7595 C. Piliago, T.W. Holcombe, J.D. Douglas, C.H. Woo, P.M. Beaujuge, and J.M.J. Frechet, *J. Am. Chem. Soc.*, **132**, 7595–7597 (2010).
- 2010MM697 C.H. Chen, C.H. Hsieh, M. Dubosc, Y.J. Cheng, and C.S. Su, *Macromolecules*, **43**, 697–708 (2010).
- 2010MM821 E. Zhou, Q. Wei, S. Yamakawa, Y. Zhang, K. Tajima, C. Yang, and K. Hashimoto, *Macromolecules*, **43**, 821–826 (2010).
- 2010MM4481 K.T. Kamtekar, H.L. Vaughan, B.P. Lyons, A.P. Monkman, S.U. Pandya, and M.R. Bryce, *Macromolecules*, **43**, 4481–4488 (2010).
- 2010MM8348 R. Stalder, J. Mei, and J.R. Reynolds, *Macromolecules*, **43**, 8348–8352 (2010).

- 2010OL660 J. Mei, K.R. Graham, R. Stalder, and J.R. Reynolds, *Org. Lett.*, **12**, 660–663 (2010).
- 2010OL2675 A. Saito, Y. Matano, and H. Imahori, *Org. Lett.*, **12**, 2675–2677 (2010).
- 2010OL4054 S.J. Evenson and S.C. Rasmussen, *Org. Lett.*, **12**, 4054–4057 (2010).
- 2010MI3 P.-L.T. Boudreault, S. Beaupre, and M. Leclerc, *Polym. Chem.*, **1**, 127–136 (2010).
- 2011USP P. Hayoz, M. Dueggeli, N. Chebotareva, and O.F. Aebischer, *Pat. US20110284826A1*.
- 2011ACR501 H. Usta, A. Facchetti, and T.J. Marks, *Acc. Chem. Res.*, **44**, 501–510 (2011).
- 2011AM268 X. Zhan, A. Facchetti, S. Barlow, T.J. Marks, M.A. Ratner, M.R. Wasielewski, and S.R. Marder, *Adv. Mater.*, **23**, 268–284 (2011).
- 2011AM3315 M.-S. Su, C.-Y. Kuo, M.-C. Yuan, U.S. Jeng, C.-J. Su, and K.-H. Wei, *Adv. Mater.*, **23**, 3315–3319 (2011).
- 2011AGE2799 E. Zhou, J. Cong, Q. Wei, K. Tajima, C. Yang, and K. Hashimoto, *Angew. Chem. Int. Ed.*, **50**, 2799–2803 (2011).
- 2011AGE9697 L. Huo, S. Zhang, X. Guo, F. Xu, Y. Li, and J. Hou, *Angew. Chem. Int. Ed.*, **50**, 9697–9702 (2011).
- 2011CM733 A. Facchetti, *Chem. Mater.*, **23**, 733–758 (2011).
- 2011JOC2386 C. Huang, S. Barlow, and S.R. Marder, *J. Org. Chem.*, **76**, 2386–2407 (2011).
- 2011JPC(C)23149 L.E. Polander, L. Pandey, S. Barlow, P. Tiwari, C. Risko, B. Kippelen, J.L. Bredas, and S.R. Marder, *J. Phys. Chem. C*, **115**, 23149–23163 (2011).
- 2011JA4250 T.-Y. Chu, J. Lu, S. Beaupre, Y. Zhang, J.-R. Pouliot, S. Wakim, J. Zhou, M. Leclerc, Z. Li, J. Ding, and Y. Tao, *J. Am. Chem. Soc.*, **133**, 4250–4253 (2011).
- 2011JA5024 S. Shinamura, I. Osaka, E. Miyazaki, A. Nakao, M. Yamagishi, J. Takeya, and K. Takimiya, *J. Am. Chem. Soc.*, **133**, 5024–5035 (2011).
- 2011JA6852 I. Osaka, T. Abe, S. Shinamura, and K. Takimiya, *J. Am. Chem. Soc.*, **133**, 6852–6860 (2011).
- 2011JA10062 C.M. Amb, S. Chen, K.R. Graham, J. Subbiah, C.E. Small, F. So, and J.R. Reynolds, *J. Am. Chem. Soc.*, **133**, 10062–10065 (2011).
- 2011JA20009 P.M. Beaujuge and J.M.J. Frechet, *J. Am. Chem. Soc.*, **133**, 20009–20029 (2011).
- 2011MM6711 X. Guo and M.D. Watson, *Macromolecules*, **44**, 6711–6716 (2011).
- 2011MM7869 W.B. Cui, J. Yuen, and F. Wudl, *Macromolecules*, **44**, 7869–7873 (2011).
- 2011NAT364 H. Minemawari, T. Yamada, H. Matsui, J. Tsutsumi, S. Haas, R. Chiba, R. Kumai, and T. Hasegawa, *Nature*, **475**, 364–367 (2011).
- 2011MI1 K. Takimiya, I. Osaka, S. Shinamura, and E. Miyazaki, *Proc. SPIE*, **8117**, 811702 (2011).
- 2011MI2 M.J. Mancheno, A. de la Pena, and J.L. Segura, *Targ. Heterocycl. Syst.*, **15**, 263–293 (2011).
- 2011T3573 M. Benstead, G.H. Mehl, and R.W. Boyle, *Tetrahedron*, **67**, 3573–3601 (2011).
- 2011TL5769 S. Frebort, Z. Elias, A. Lycka, S. Lunak, J. Vynuchal, L. Kubac, R. Hrdina, and L. Burgert, *Tetrahedron Lett.*, **52**, 5769–5773 (2011).
- 2012MI1 P. Hayoz, O.F. Aebischer, M. Dueggeli, M.G.R. Turbiez, M. Fonrodona Turon, and N. Chebotareva, *Pat. WO2010115767A1*.

- 2012AM3678 H. Usta, C. Newman, Z.H. Chen, and A. Facchetti, *Adv. Mater.*, **24**, 3678–3684 (2012).
- 2012JCS(CC)3039 S. Qu and H. Tian, *Chem. Commun.*, **48**, 3039–3051 (2012).
- 2012JCS(CC)3939 R.S. Ashraf, A.J. Kronemeijer, D.I. James, H. Sirringhaus, and I. McCulloch, *Chem. Commun.*, **48**, 3939–3941 (2012).
- 2012CRV2208 C.L. Wang, H.L. Dong, W.P. Hu, Y.Q. Liu, and D.B. Zhu, *Chem. Rev.*, **112**, 2208–2267 (2012).
- 2012CM1346 W.A. Braunecker, Z.R. Owczarczyk, A. Garcia, N. Kopidakis, R.E. Larsen, S.R. Hammond, D.S. Ginley, and D.C. Olson, *Chem. Mater.*, **24**, 1346–1356 (2012).
- 2012CM2364 G. Qian, J. Qi, J.A. Davey, J.S. Wright, and Z.Y. Wang, *Chem. Mater.*, **24**, 2364–2372 (2012).
- 2012CM4766 H.C. Chen, Y.H. Chen, C.C. Liu, Y.C. Chien, S.W. Chou, and P.T. Chou, *Chem. Mater.*, **24**, 4766–4772 (2012).
- 2012MI2 A. Marocchi, D. Lanari, A. Facchetti, and L. Vaccaro, *Energy Environ. Sci.*, **5**, 8457–8474 (2012).
- 2012JMC14119 D. Cortizo-Lacalle, C.T. Howells, S. Gambino, F. Vilela, Z. Vobecka, N.J. Findlay, A.R. Inigo, S.A.J. Thomson, P.J. Skabara, and I.D.W. Samuel, *J. Mater. Chem.*, **22**, 14119–14126 (2012).
- 2012JA539 G.L. Gibson, T.M. McCormick, and D.S. Seferos, *J. Am. Chem. Soc.*, **134**, 539–547 (2012).
- 2012JA18427 X. Guo, N. Zhou, S.J. Lou, J.W. Hennek, R. Ponce Ortiz, M.R. Butler, P.-L.T. Boudreault, J. Strzalka, P.-O. Morin, M. Leclerc, J.T. Lopez Navarrete, M.A. Ratner, L.X. Chen, R.P.H. Chang, A. Facchetti, and T.J. Marks, *J. Am. Chem. Soc.*, **134**, 18427–18439 (2012).
- 2012JA20713 J. Lee, A.R. Han, J. Kim, Y. Kim, J.H. Oh, and C. Yang, *J. Am. Chem. Soc.*, **134**, 20713–20721 (2012).
- 2012MI3 K. Tanaka and Y. Chujo, *Macromol. Rapid Commun.*, **33**, 1235–1255 (2012).
- 2012MM1303 W.-H. Lee, S.K. Son, K. Kim, S.K. Lee, W.S. Shin, S.-J. Moon, and I.-N. Kang, *Macromolecules*, **45**, 1303–1312 (2012).
- 2012MI4 R. Sondergaard, M. Hosel, D. Angmo, T.T. Larsen-Olsen, and F.C. Krebs, *Mater. Today*, **15**, 36–49 (2012).
- 2012MI5 C.E. Small, S. Chen, J. Subbiah, C.M. Amb, S.-W. Tsang, T.-H. Lai, J.R. Reynolds, and F. So, *Nat. Photonics*, **6**, 115–120 (2012).
- 2013AM1859 C.B. Nielsen, M. Turbiez, and I. McCulloch, *Adv. Mater.*, **25**, 1859–1880 (2013).
- 2013AM4327 H. Usta, M.D. Yilmaz, A.-J. Avestro, D. Boudinet, M. Denti, W. Zhao, J.F. Stoddart, and A. Facchetti, *Adv. Mater.*, **25**, 4327–4334 (2013).
- 2013AM5372 Y. Zhao, Y.L. Guo, and Y.Q. Liu, *Adv. Mater.*, **25**, 5372–5391 (2013).
- 2013AM6158 H.L. Dong, X.L. Fu, J. Liu, Z.R. Wang, and W.P. Hu, *Adv. Mater.*, **25**, 6158–6182 (2013).
- 2013JCS(CC)3790 Z. Yan, B. Sun, and Y. Li, *Chem. Commun.*, **49**, 3790–3792 (2013).
- 2013DP160 E. Kozma and M. Catellani, *Dyes Pigm.*, **98**, 160–179 (2013).
- 2013DP530 T. Aysha, S. Lunak, A. Lycka, J. Vynuchal, Z. Elias, A. Ruzicka, Z. Padelkova, and R. Hrdina, *Dyes Pigm.*, **98**, 530–539 (2013).
- 2013MI1 Y. Li, P. Sonar, L. Murphy, and W. Hong, *Energy Environ. Sci.*, **6**, 1684–1710 (2013).
- 2013EJO228 B.A.D. Neto, A.A.M. Lapis, E.N. da Silva Júnior, and J. Dupont, *Eur. J. Org. Chem.*, **2013**, 228–255 (2013).
- 2013JMC(C)1297 I. Osaka, S. Shinamura, T. Abe, and K. Takimiya, *J. Mater. Chem. C*, **1**, 1297–1304 (2013).

- 2013JA4656 C. Cabanetos, A. El Labban, J.A. Bartelt, J.D. Douglas, W.R. Mateker, J.M.J. Frechet, M.D. McGehee, and P.M. Beaujuge, *J. Am. Chem. Soc.*, **135**, 4656–4659 (2013).
- 2013JA6724 J. Mei, Y. Diao, A.L. Appleton, L. Fang, and Z. Bao, *J. Am. Chem. Soc.*, **135**, 6724–6746 (2013).
- 2013JA12168 T. Lei, J.-H. Dou, X.-Y. Cao, J.-Y. Wang, and J. Pei, *J. Am. Chem. Soc.*, **135**, 12168–12171 (2013).
- 2013MI2 A. Pron, P. Berrouard, and M. Leclerc, *Macromol. Chem. Phys.*, **214**, 7–16 (2013).
- 2013MI3 X. Guo, N. Zhou, S.J. Lou, J. Smith, D.B. Tice, J.W. Hennek, R.P. Ortiz, J.T.L. Navarrete, S. Li, J. Strzalka, L.X. Chen, R.P.H. Chang, A. Facchetti, and T.J. Marks, *Nat. Photonics*, **7**, 825–833 (2013).
- 2013OL932 Y. Matano, H. Ohkubo, Y. Honsho, A. Saito, S. Seki, and H. Imahori, *Org. Lett.*, **15**, 932–935 (2013).
- 2013OL5338 S.-W. Cheng, D.-Y. Chiou, Y.-Y. Lai, R.-H. Yu, C.-H. Lee, and Y.-J. Cheng, *Org. Lett.*, **15**, 5338–5341 (2013).
- 2013MI4 X.M. He and T. Baumgartner, *RSC Adv.*, **3**, 11334–11350 (2013).
- 2014ACR1117 T. Lei, J.Y. Wang, and J. Pei, *Acc. Chem. Res.*, **47**, 1117–1126 (2014).
- 2014ACR1465 A. Patra, M. Bendikov, and S. Chand, *Acc. Chem. Res.*, **47**, 1465–1474 (2014).
- 2014AM1319 H. Sirringhaus, *Adv. Mater.*, **26**, 1319–1335 (2014).
- 2014AM1801 E. Wang, W. Mammo, and M.R. Andersson, *Adv. Mater.*, **26**, 1801–1826 (2014).
- 2014MI1 J. Zaumseil, *Adv. Polym. Sci.*, **265**, 107–137 (2014).
- 2014AGE7428 S.-L. Suraru and F. Wuerthner, *Angew. Chem. Int. Ed.*, **53**, 7428–7448 (2014).
- 2014CRV8943 X.G. Guo, A. Facchetti, and T.J. Marks, *Chem. Rev.*, **114**, 8943–9021 (2014).
- 2014CM604 J.G. Mei and Z.N. Bao, *Chem. Mater.*, **26**, 604–615 (2014).
- 2014CM647 S. Holliday, J.E. Donaghey, and I. McCulloch, *Chem. Mater.*, **26**, 647–663 (2014).
- 2014CM664 R. Stalder, J. Mei, K.R. Graham, L.A. Estrada, and J.R. Reynolds, *Chem. Mater.*, **26**, 664–678 (2014).
- 2014MI2 Y. Diao, L. Shaw, Z.A. Bao, and S.C.B. Mannsfeld, *Energy Environ. Sci.*, **7**, 2145–2159 (2014).
- 2014MI3 L. Wang, J.-P. Sun, Z.-Y. Li, X.-B. Zhou, X. Wang, L.-Y. Luo, and Q.-D. Ling, *Gaofenzi Tongbao*, 24–34 (2014).
- 2014IJ440 J. Hollinger, D. Gao, and D.S. Seferos, *Isr. J. Chem.*, **54**, 440–453 (2014).
- 2014IJ621 A. Patra, R. Kumar, and S. Chand, *Isr. J. Chem.*, **54**, 621–641 (2014).
- 2014MM616 S. Shi, X. Xie, C. Gao, K. Shi, S. Chen, G. Yu, L. Guo, X. Li, and H. Wang, *Macromolecules*, **47**, 616–625 (2014).
- 2014MM3502 I. Osaka, Y. Houchin, M. Yamashita, T. Kakara, N. Takemura, T. Koganezawa, and K. Takimiya, *Macromolecules*, **47**, 3502–3510 (2014).
- 2014MM4987 K. Shibasaki, K. Tabata, Y. Yamamoto, T. Yasuda, and M. Kijima, *Macromolecules*, **47**, 4987–4993 (2014).
- 2014MI4 Y. Yuan, G. Giri, A.L. Ayzner, A.P. Zoombelt, S.C. Mannsfeld, J. Chen, D. Nordlund, M.F. Toney, J. Huang, and Z. Bao, *Nat. Commun.*, **5**, 3005 (2014).
- 2014MI5 P. Deng and Q. Zhang, *Polym. Chem.*, **5**, 3298–3305 (2014).
- 2014MI6 A.V. Akkuratov and P.A. Troshin, *Polym. Sci. Ser. B*, **56**, 414–442 (2014).
- 2015MI1 K.H. Park, Y.J. Kim, G.B. Lee, T.K. An, C.E. Park, S.K. Kwon, and Y.H. Kim, *Adv. Funct. Mater.*, **25**, 3991–3997 (2015).

- 2015MI2 S.-W. Cheng, D.-Y. Chiou, C.-E. Tsai, W.-W. Liang, Y.-Y. Lai, J.-Y. Hsu, C.-S. Hsu, I. Osaka, K. Takimiya, and Y.-J. Cheng, *Adv. Funct. Mater.*, **25**, 6131–6143 (2015).
- 2015AM3589 Z. Yi, S. Wang, and Y. Liu, *Adv. Mater.*, **27**, 3589–3606 (2015).
- 2015MI3 M. Grzybowski and D.T. Gryko, *Adv. Opt. Mater.*, **3**, 280–320 (2015).
- 2015CRV3036 M.E. Cinar and T. Ozturk, *Chem. Rev.*, **115**, 3036–3140 (2015).
- 2015JMC(A)16279 B.M. Squeo, N. Gasparini, T. Ameri, A. Palma-Cando, S. Allard, V.G. Gregoriou, C.J. Brabec, U. Scherf, and C.L. Chochos, *J. Mater. Chem. A*, **3**, 16279–16286 (2015).
- 2015MI4 T.L.D. Tam and J. Wu, *J. Mol. Eng. Mater.*, **3**, 1540003 (2015).
- 2015JA1314 R.S. Ashraf, I. Meager, M. Nikolka, M. Kirkus, M. Planells, B.C. Schroeder, S. Holliday, M. Hurhangee, C.B. Nielsen, H. Sirringhaus, and I. McCulloch, *J. Am. Chem. Soc.*, **137**, 1314–1321 (2015).
- 2015MM297 E.I. Carrera and D.S. Seferos, *Macromolecules*, **48**, 297–308 (2015).
- 2015MI5 T.C. Parker, D.G. Patel, K. Moudgil, S. Barlow, C. Risko, J.L. Bredas, J.R. Reynolds, and S.R. Marder, *Mater. Horizons*, **2**, 22–36 (2015).
- 2015MI6 K. Tanaka and Y. Chujo, *NPG Asia Mater.*, **7**, e223 (2015).
- 2016AM943 Y. Ji, C. Xiao, Q. Wang, J. Zhang, C. Li, Y. Wu, Z. Wei, X. Zhan, W. Hu, Z. Wang, R.A.J. Janssen, and W. Li, *Adv. Mater.*, **28**, 943–950 (2016).





# Heterogeneously Catalyzed Synthesis of Heterocyclic Compounds

Colin H. McAteer\*, Ramiah Murugan, Yarlagadda V. Subba Rao

Vertellus Specialties Inc., Indianapolis, IN, USA

\*Corresponding author: E-mail: cmcateer@vertellus.com

## Contents

1. Tribute	174
2. Introduction	174
3. Catalyst Choice	175
4. Zeolites, Metallosilicates, and Clays	176
5. Classification of Reaction Chemistry	178
6. Three-Membered Heterocycles	178
7. Four-Membered Heterocycles	182
8. Five-Membered Heterocycles	183
9. Six-Membered Heterocycles	192
10. Seven-Membered Heterocycles	199
11. Process and Economic Considerations	201
12. Final Comments	202
References	202

## Abstract

This chapter covers the synthesis of heterocyclic compounds using heterogeneous catalysts from the perspective of practicing industrial chemists. Before discussing the synthesis of various heterocycles using heterogeneous catalysts a brief discussion on catalyst choice and classification of reaction chemistry is provided. Next, the synthesis of commercially important heterocycles from acyclic precursors is provided starting with the three-membered aziridines and epoxides. For the four-membered heterocycles, propiolactone synthesis is discussed followed by the five-membered pyrroles, furans, and thiophenes. Within the five-membered ring category of heterocycles, the benz-fused pyrrole, indole and rings with more than one heteroatom such as pyrazoles, imidazoles, thiazoles, oxa- and thio-diazoles synthesis are also discussed. Similar to the five-membered ring heterocycles, the six-membered heterocycle syntheses discussed are pyridines, picolines, quinolines, acridines, pyrimidines, pyrazines, triazines, coumarins, etc. Finally a small section on process and economics consideration is provided along with final comments.

**Keywords:** 1,3,4-Oxadiazole; 1,3,4-Thiadiazole; 1,5-Benzodiazepines; Aluminosilicates; Amberlyst-15; Aza Diels–Alder reaction; Aziridines; Butyrolactone; Caprolactam; Catalytic oxidation; Clays; Cyanuric chloride; Epoxides; Gold catalysts; Heterocycles synthesis; Heterogeneous catalyst; Hydrotalcite; Hydroxymethylfurfural; Imidazole; Indole; Maleic anhydride; Metallophosphates; Metallosilicates; Montmorillonite; Nafion; Nicotine; Phthalic anhydride; Piperidine; Propiolactones; Pyrazines; Pyrazoles; Pyridine; Pyrimidines; Pyrroles; Pyrrolidine; Quinolines; Thiazole; Thiophene; Titanosilicates; Triazines; Zeolites



---

## 1. TRIBUTE

One of the authors had the great fortune to study heterocyclic chemistry first as a graduate student and then as a postdoctoral fellow with Professor Alan Katritzky while at the University of Florida. Later, all of the authors, as industrial chemists at Reilly Industries (now Vertellus Specialties Inc.), were privileged to have Alan as our chief academic consultant. Always appreciative of learning heterocyclic chemistry from the greatest practitioner of the age, we also gained much insight from Alan into our own areas of expertise that cover inorganic chemistry and heterogeneous catalysis. It is a great honor for us to contribute this chapter in this Alan Katritzky tribute volume.



---

## 2. INTRODUCTION

Heterogeneous catalysts have been used commercially to make heterocyclic compounds for over 80 years (1991MI1). This chapter reviews selected literature from the past 25 years covering the time period of our collaboration with Alan Katritzky. It is written from the perspective of industrial chemists who practise heterogeneous catalysis applied to the formation of heterocyclic compounds. The discussion is restricted to reactions that form a new heterocyclic ring from either acyclic compounds or the noncyclic fragment of ring-containing compounds. We do not include reactions that either add or modify existing ring substituents of a heterocyclic compound. Where possible, emphasis is placed on commercialized chemistry, including features of the heterogeneous catalysts employed and conditions.

Heterocyclic compounds produced directly from heterogeneously catalyzed processes span commodities through specialties to fine chemicals. Examples of the former include ethylene oxide (EO), propylene oxide (PO), phthalic anhydride (PA), and maleic anhydride (MA) whose 2013

global production was in the region of 26, 8.1, 4.3, and 1.9 million tonnes, respectively. Significant annual production of 1.2 and 0.2 million tonnes for melamine and cyanuric chloride, respectively, places these triazine compounds in the commodity category. The combined global demand for pyridine, picolines, and lutidines is in the region of 200,000 tonnes per year of which certain products would constitute a true fine chemical (e.g., 2,6-lutidine, ca. 100 tonne/year).



### 3. CATALYST CHOICE

That a catalyst provides an alternative lower activation energy pathway from reactants to products is of course well known. Incentives to use a catalyst are primarily economic and include increased yield, savings in time, improved product quality, minimization of waste, or a combination of these factors. The choice of catalyst to use for a potentially new chemical process is usually guided by literature precedent followed by experimentation. Key advantages touted for heterogeneous over homogeneous catalysis is the ease of separation of catalyst from products and the subsequent regeneration of the recovered catalyst for reuse. This is especially true where heterogeneous catalysts are employed for liquid-phase reactions involving complex high-molecular weight reagents that cannot be vaporized for gas-phase conversions. The type of reaction in which solid heterogeneous catalysts find most use in organic synthesis have been classified into five main categories, including acid catalysis, base catalysis, catalytic hydrogenation and dehydrogenation, catalytic oxidation, and catalytic C–C bond formation (2007M11). The classes also apply in the synthesis of heterocyclic compounds while some unique reaction types (e.g., isomerization via the Benzamine rearrangement) are also found.

The families of heterogeneous catalytic materials commercially available are diverse and growing. Their classification is not straightforward and a simple list would include pure elements (e.g., bulk metals, carbon), inorganic compounds (e.g., oxides, nitrides, carbides, and phosphates), supported metal/metal oxides (e.g.,  $M/M'O_x$ ,  $MO_x/M'O_y$ ,  $M/M'$  alloys), organic compounds (e.g., polymer resins), inorganic–organic hybrids (e.g., silica-tethered amines, metal-organic frameworks or MOFs), and biochemical related materials (e.g., immobilized whole cells, cross-linked enzymes). Depending on the reactor type and operating conditions, solid catalysts are usually formed into a required shape (e.g., monolith, tablet, extrudate,

spheres, microspheres, etc.) although powders and suspended nanoparticles can be used in the slurry phase. In order to maximize contact with the reactants, a heterogeneous catalyst typically requires the greatest surface density of the catalytic entity (whose identity is often unknown) dispersed on a high surface area support. Most heterogeneously catalyzed reactions can be considered to take place on a two-dimensional surface in an unconstrained fashion. Constrained reactions at active sites within pockets/folds of naturally occurring enzymes provide high reaction specificity and this behavior is mimicked to some degree in inorganic catalysts. The application of shape-selective zeolite catalysts containing a well-defined micropore channel structure (i.e., diameters  $\leq 20$  Å) has become commonplace. The use of zeolites and zeotype materials (e.g., metallosilicates) features heavily in this review and are described briefly.



## 4. ZEOLITES, METALLOSILICATES, AND CLAYS

The International Zeolite Association (IZA) website provides an excellent means to visualize the channel arrangements in over 200 microporous zeolite structures (both synthetic and naturally occurring minerals)—this includes aluminosilicates and their all-silica variants plus metallosilicates and metallophosphates (2016MI1). A small minority of these structures (ca. 20 or less) have found significant commercial application as catalysts and adsorbents. Microporous zeolites are subdivided into small ( $\leq 5$  Å), medium (5–6 Å), and large ( $\geq 6$  Å) pore channels for those containing  $\leq 8$ , 10, and  $\geq 12$  T-atom rings, respectively (T-atom refers to tetrahedral atoms—either Si or Al—each connected via O atoms). Replacing a framework Si<sup>IV</sup> atom by Al<sup>III</sup> formally introduces an anionic site on the structure that must be counterbalanced by a cationic species (e.g., H<sup>+</sup>, NH<sub>4</sub><sup>+</sup>, Na<sup>+</sup>, Ni<sup>2+</sup>, etc.) within the zeolite channel. Many zeolite structures can be prepared with a range of Si/Al molar ratio that can lead either to variable Brønsted acid site (BAS) density (in the case of the H<sup>+</sup> form) or Lewis acid site (LAS) density (in the case of metal ion exchanged forms). The IZA assigns three-letter codes for each zeolite structure and Table 1 presents key physical properties for selected structures including FAU, MOR, BEA, and MFI—these large and medium pore zeolites have proven to be useful catalysts in the synthesis of heterocyclic compounds.

Metallosilicates are formally derived from the all-silica zeolite structure by substitution of a framework Si<sup>IV</sup> atom by a metal ion (M<sup>n+</sup>, typically

**Table 1** Selected microporous zeolites used as catalysts and adsorbents

Ring size [T-atoms]	Zeolite International Association code	Mineral/ commercial name(s)	Largest channel (Å)	Effective channel dimensions	Comments/ applications
Small [8]	LTA	Linde type-A (molecular sieves)	4.1 × 4.1	3D	K-A (3A sieve), NaA (4A), CaA (5A)
	CHA	Chabazite, SAPO- 34, SSZ-13	3.8 × 3.8	3D	Methanol to olefins
Medium [10]	MFI	ZSM-5, silicalite (S-1), TS-1 (TiMFI)	5.6 × 5.3	3D	Aromatics ( <i>p</i> -xylene, cumene, ethylbenzene)
Large [12]	FER	Ferrierite, ZSM-35	5.4 × 4.2	2D	
	BEA	Zeolite Beta	6.7 × 6.6	3D	
	MOR	Mordenite	7.0 × 6.7	1D	Lube oil dewaxing, cumene
	FAU	Faujasite, zeolite X and Y, USY, CSY	7.4 × 7.4	3D	Petroleum cracking catalysts
	LTL	Linde type-L or zeolite L	7.1 × 7.1	1D	

$n = 2-4$ ) that can lead to either a negatively charged structure ( $n = 2$  and  $3$ ) with charge balancing cations or a neutral structure ( $n = 4$ ) of which titanosilicates have proven to be useful catalysts. Most prominent of the titanosilicates is TS-1, derived from the medium-pore MFI structure, which is used commercially to produce catechol/hydroquinone and cyclohexanone oxime.

Sulfuric acid-treated montmorillonite clays (e.g., K-10) have been used as solid-acid catalysts before synthetic zeolites became available. The 2D layered structure of montmorillonite can be expanded by incorporation of large cations (e.g.,  $[\text{Al}_{13}\text{O}_4(\text{OH})_{24}(\text{H}_2\text{O})_{12}]^{7+}$ ) leading to pillared clays whose channel openings (interlamellar region) are 12–18 Å. Ordered mesoporous materials (i.e., diameters 20–500 Å) include silicas and zeolites with structures ranging from stacked tubes/honeycomb arrays (e.g., SBA-15, MCM-41) to 2D layered sheets (e.g., MCM-22P). As with clays, whole molecular entities can be anchored within the mesopore channels to enable a range of catalyzed conversions of large and more complex feeds into high-value fine chemical products. In general, mesoporous silicas, zeolites, and clays are useful in liquid-phase reactions but are less hydrothermally stable than microporous zeolites leading to more rapid loss of activity following repeated oxidative regeneration cycles.

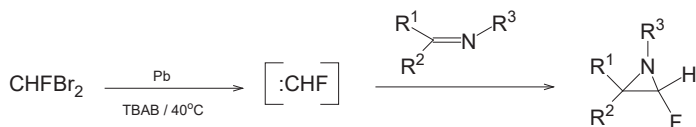
A range of solid-base materials (e.g., quaternary ammonium resins, hydrotalcite, and hydroxyapatite) have found use as catalysts where acidity is detrimental. As with clays, the layered double hydroxide (LDH) structure of hydrotalcite can be modified by replacing interlamellar carbonate by hydroxide/alkoxide and polyoxometallate anions to catalyze nucleophilic and redox processes, respectively.

## 5. CLASSIFICATION OF REACTION CHEMISTRY

Most of the literature describing the formation of heterocyclic compounds using heterogeneous catalysts originates broadly from two directions: first, organic chemists making either a specific target molecule or series of desired compounds and will use any catalyst for that goal; second, chemists and materials engineers who seek any organic reaction to demonstrate utility of their chosen catalyst system. The latter approach has seen a significant growth in publications in the last 10–15 years particularly in the area of biomass conversion into fuels and oxygenate chemicals. For simplicity, the examples described below are presented in sequence by increasing ring number. Within each ring size group, single heteroatom compounds are discussed before those containing two or more heteroatoms. In all cases, the atom prioritization is N-, O-, and then S-containing compounds.

## 6. THREE-MEMBERED HETEROCYCLES

Aziridines substituted with fluorine were synthesized from N-alkyl-N-benzhydrylideneamines with fluorocarbene, generated in situ from dibromofluoromethane, in the presence of metallic lead powder and tetrabutylammonium bromide under ultrasonic irradiation (Scheme 1). The reaction readily occurs at 40 °C and an azomethine ylide intermediate has been proposed before cyclization to the final aziridine product (2005TL8337).



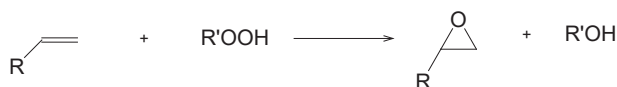
Scheme 1

Epoxides are the most important group of three-membered heterocycles because of their great versatility as intermediates. Epoxides are typically prepared on a commercial scale via organic hydroperoxides (i.e., ROOH) with a catalyst under liquid-phase conditions (Scheme 2) but there are key exceptions.

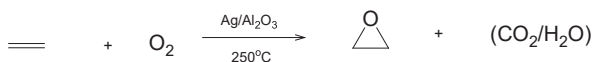
Vapor-phase EO production from ethylene and oxygen (Scheme 3) is an exothermic process and uses an Ag-based catalyst in a multitubular fixed-bed reactor (ca. 250 °C, 15 psig). Incremental improvements to both catalyst and process conditions suggest EO selectivity has improved from 65% to 70% in the 1970s to a 3-year 90% average in current plants (2016MI2). Shell Oil patents from the mid-1990s would suggest an Ag-Cs/ $\alpha$ -Al<sub>2</sub>O<sub>3</sub> catalyst is used together with 1,2-dichloroethane in the feed that reduces EO and ethylene combustion to CO<sub>2</sub> and H<sub>2</sub>O (1988USP4761394).

Eastman Chemical developed a vapor-phase process to oxidize butadiene to 3,4-epoxy-1-butene (EpB) (Scheme 4) and operated a demonstration unit (ca. 4 tonnes/day). This fixed-bed process (250 °C, C<sub>4</sub>H<sub>6</sub>/O<sub>2</sub> = 1, GHSV = 1200 h<sup>-1</sup>) probably uses low conversion conditions with butane as inert diluent to achieve optimum EpB selectivity (ca. 91%). Like the EO process, the EpB catalyst is believed to be Ag-Cs/ $\alpha$ -Al<sub>2</sub>O<sub>3</sub> but of a different composition. A highly versatile platform chemical, EpB can be converted into range of C<sub>4</sub> derivatives such as THF (for Spandex), 1,4-butanediol (for polybutylene terephthalate), and cyclopropanecarboxaldehyde.

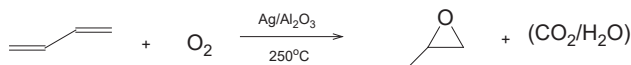
Other nonallylic alkenes that undergo vapor-phase epoxidation with the EpB catalyst include styrene (95% selectivity), 4-vinylpyridine (86%), and norbornene (92%) (Scheme 5).



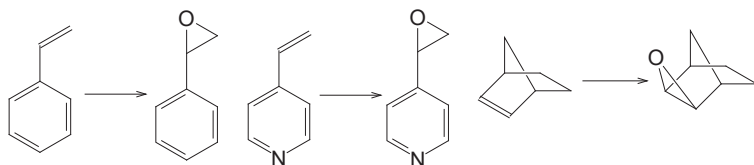
Scheme 2



Scheme 3



Scheme 4

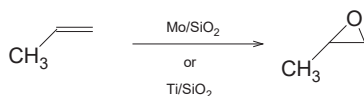


Scheme 5

The Ag-catalyzed vapor-phase processes used to make EO and EpB are not viable for PO production. The challenge to directly oxidize propene selectively to PO has to address methyl group reactivity and the competing acrolein formation in route to acrylic acid (MoO<sub>3</sub>-based mixed-oxide catalysts are used in acrolein and acrylic acid production). Alternative catalysts have been evaluated for the propene-to-PO reaction with Ti- and Mo-loaded silica catalysts showing some promise (Scheme 6, PO selectivity ca. 35%). The mechanism has been described as a combination of surface radical generation and a homogeneous chain reaction (2007SSSC389, 2006EJSSN74).

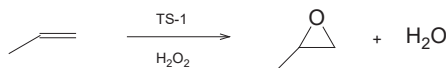
Commercial production of PO uses liquid-phase chemistry, including the original hypochlorous acid route that suffers from high electricity costs, poor chlorine utilization, and waste salt by-product formation (NaCl or CaCl<sub>2</sub>). More cost-effective routes were introduced from the early 1970s that employed either *t*-butyl hydroperoxide (TBHP) or ethylbenzene hydroperoxide leading to PO formation (87–94% selectivity) with coproduct *t*-BuOH and phenylmethylcarbinol (PhMeCHOH), respectively. Both homogeneous (e.g., molybdenum naphthenate) and heterogeneous (e.g., silylated Ti/SiO<sub>2</sub>) catalysts are used commercially. Dehydration of the coproduced alcohols *t*-BuOH and PhMeCHOH leads to isobutene (for MTBE production) and styrene monomer, respectively. Because alcohol is produced in both the organic hydroperoxide and PO forming steps, the overall tonnage output of coproduct:PO is typically greater than 2:1.

In the last decade, new propene-to-PO plants have come on stream that use hydrogen peroxide (H<sub>2</sub>O<sub>2</sub>) and TS-1 catalyst suspended in aqueous



Scheme 6



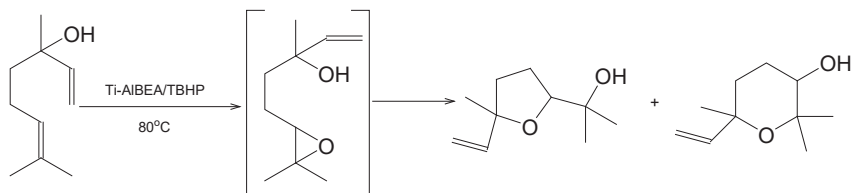


Scheme 7

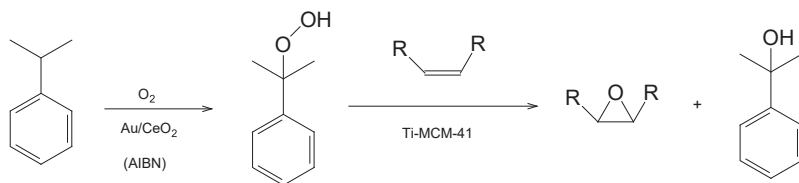
methanol (Scheme 7). Advantages of using TS-1 include high PO selectivity (>95%), water as the only significant by-product, and no coproduct chemistry to manage. The TS-1-catalyzed reaction was known for some time but the breakthrough leading to adoption of this technology was significant cost reductions for H<sub>2</sub>O<sub>2</sub> production arising from a combination of yield improvement and larger capacity plants. The additional capital required for the H<sub>2</sub>O<sub>2</sub> production line is more than offset by eliminating equipment for making the organic hydroperoxide and separating/recovering the coproduct.

Spectroscopic and kinetic studies of TS-1 suggest H<sub>2</sub>O<sub>2</sub> incorporates to form Ti( $\eta^2$ -OOH) and silanol (SiOH) entities (2004JPCB3573) while oxygen transfers directly to propene forming PO without prior coordination of propene to titanium (i.e., Eley-Rideal mechanism) (2013CEngJ306). The tetrahedrally coordinated Ti atom in the MFI framework is not unique and other larger pore zeolite structures (e.g., BEA, MCM-41) can also incorporate titanium to catalyze epoxidation reactions—using H<sub>2</sub>O<sub>2</sub> and TBHP—although they are less effective for PO but can show yield benefits over TS-1 with larger alkenes.

Synthesis of zeolites containing framework Ti<sup>4+</sup> and Al<sup>3+</sup> leads to LAS and BAS, respectively, and can provide novel bifunctional epoxidation catalysts such as Ti-AlBEA and Ti-AlMCM-41. An example of their use is the one-pot synthesis of furan and pyran—via an in situ formed epoxide—from linalool and TBHP (Scheme 8) (2000JCSCC1789). The pyran-to-furan product ratio remains the same throughout the reaction indicating initial epoxidation at titanium sites is followed by proton-catalyzed rearrangement/cyclization at aluminum sites.



Scheme 8



Scheme 9

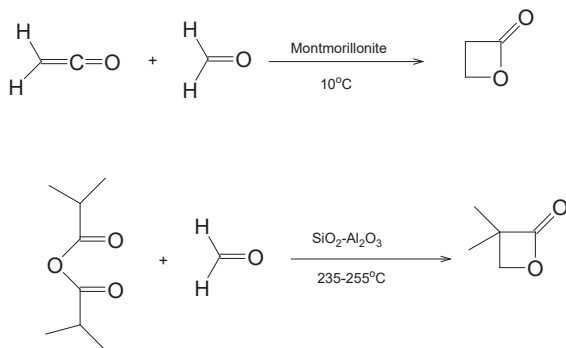
Two types of heterogeneous catalyst have been employed in a cascade-type reaction in the liquid-phase formation of epoxides starting from alkene, oxygen, and a hydrocarbon having a tertiary hydrogen (e.g., cumene). Use of Au/CeO<sub>2</sub> nanoparticles and AIBN promoter generated cumene hydroperoxide that subsequently transferred oxygen to an alkene within silylated Ti-MCM41 (Scheme 9) (2009JCAT44).

The Sharpless epoxidation is a named reaction that involves conversion of an asymmetric allylic alcohol to enantiomerically pure epoxide using a titanium alkoxide, an optically active tartrate ester, and an alkyl hydroperoxide. Although best known in homogeneously catalyzed reactions, the heterogeneously catalyzed Sharpless epoxidation has been demonstrated with a wide range of supported titanium materials (e.g., silicas, zeolites, resins) (2005CRV1603).

## 7. FOUR-MEMBERED HETEROCYCLES

The strained nature of four-membered heterocycles make them interesting intermediates in organic synthesis. Oxetanes are such examples finding use in the synthesis of various heterocyclic compounds via ring expansion, ring opening, and C-2 functionalization reactions (2015JOC8489).

Use of heterogeneous catalysis in the synthesis of four-membered heterocycles is an area worthy of further research based upon the scarcity of its literature. A rare example is the formation of propiolactones using solid-acid catalysts based on montmorillonite and amorphous SiO<sub>2</sub>-Al<sub>2</sub>O<sub>3</sub> (Scheme 10). Propiolactone has been produced from ketene and formaldehyde at 10 °C using mineral acid-activated montmorillonite clay (1952USP2580714). Pivalolactone (3,3-dimethyloxetan-2-one) has been produced from isobutyric anhydride and formaldehyde in up to 74% yield using SiO<sub>2</sub>-Al<sub>2</sub>O<sub>3</sub> at 235–255 °C (1975USP3915995).



Scheme 10

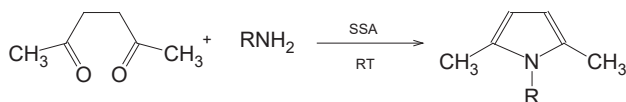
## 8. FIVE-MEMBERED HETEROCYCLES

Paal–Knorr synthesis of pyrroles from 1,4-diones and a primary amine (Scheme 11) is catalyzed by silica-supported sulfuric acid (SSA). Hexane-2,5-dione and a primary amine readily form *N*-substituted-2,5-dimethylpyrroles in excellent yields of 70–98% at room temperature and solvent-free conditions (2010TL2109).

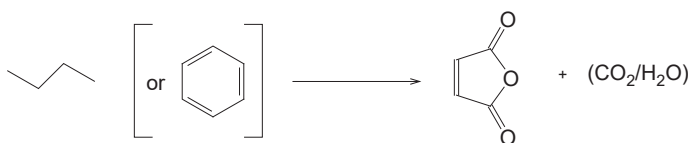
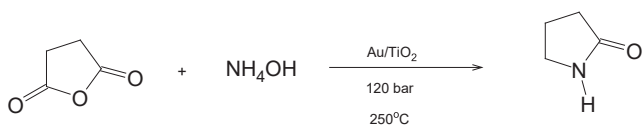
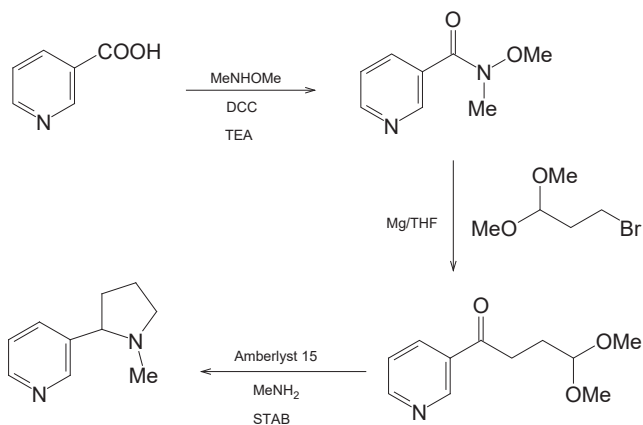
Amberlyst-15, a macroreticular styrene-based sulfonic acid resin with an average pore size of 300 Å, is a versatile strong acid catalyst (2012ARK570). An example of its use is in the final step for the synthesis of a pyrrolidine ring of the natural product nicotine (Scheme 12) (2002JCSPT143). The nicotine forming step involves hydrolysis of an acetal followed by cyclization with methylamine and reduction with sodium triacetoxy borohydride.

Gold catalysts can be highly selective in hydrogenation reactions. Hydrogenation (250 °C, 120 bar, 10 h) of succinic anhydride in the presence of ammonium hydroxide solution and Au/TiO<sub>2</sub> gave 2-pyrrolidone in 80% yield (99% selectivity) essentially free of pyrrolidine (Scheme 13) (2008JCAT403).

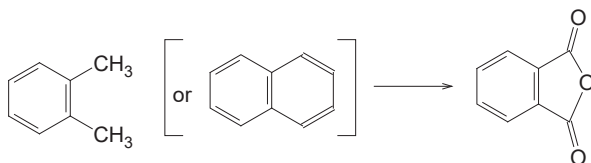
MA is mostly produced by the partial oxidation (400–440 °C) of either butane or benzene using vanadium-based catalysts (Scheme 14). The original benzene route is still in use with supported V<sub>2</sub>O<sub>5</sub> catalysts giving an



Scheme 11



MA selectivity of 70–73% in either fixed- or fluid-bed reactors. The butane-based routes, introduced during the 1980s, uses VPO catalyst (i.e.,  $[(VO)_2P_2O_7]$  derived from  $VOHPO_4 \cdot \frac{1}{2}H_2O$ ) and gives an MA selectivity of ca. 55%. Butane routes are dominant in North America and Europe where the lower feedstock price outweighs the selectivity shortfall—the benzene route remains dominant in China. In the 1990s, DuPont operated a circulating fluidized bed (CFB) process in which butane and a  $SiO_2$ -coated attrition-resistant VPO catalyst are fed to a riser reactor. Transfer of oxygen from the catalyst forms MA and oxygen-depleted VPO that moves into a second fluidized vessel where air regeneration occurs to complete the cycle. The CFB process gave an MA selectivity of ca. 65% together with higher butane conversion; however, operational difficulties led to the unit being

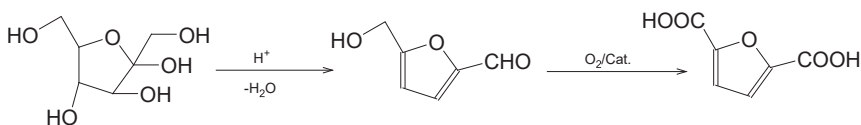


Scheme 15

idled (2010ACAG4). A sizeable amount of MA is consumed in 1,4-butanediol (BDO) production and the butane-to-MA route competes with other BDO-production chemistries (e.g., acetylene- $\text{CH}_2\text{O}$ , PO- $\text{C}_1$ , and butadiene routes).

PA is produced by the partial oxidation (350–450 °C) of either *o*-xylene or naphthalene over supported vanadia ( $\text{V}_2\text{O}_5$ ) catalysts using either fixed- or fluid-bed reactors (Scheme 15). The PA selectivity is reported to be ca. 80% (2013MI1) although a value of closer to 70% is thought more likely (1991MI1). The majority of PA plants use *o*-xylene but the naphthalene-based process, which dates back to the 1920s, is still used and actually gives a slightly higher selectivity. A beneficial byproduct of the PA processes is MA that can be recovered. A majority of the PA produced is consumed for making plasticizers especially bis(2-ethylhexyl) phthalate.

Five-membered oxygen-containing ring compounds, especially furan derivatives, feature heavily in chemistry of biomass-derived fuels and chemicals. Key C-6 platform chemicals include 5-hydroxymethylfurfural (HMF) (2013CRV1499, 2014GC2015) and furan-2,5-dicarboxylic acid (FDCA) (Scheme 16) (2015ACSC6529). An efficient route from C-6 sugars to HMF is essential in order for bio-derived specialty chemicals to compete with their petrochemical derived counterparts. Isomerization of glucose to fructose is a prerequisite to achieve higher yields of HMF whether homogeneous or heterogeneous catalysts are used in aqueous or organic solvent media. Lewis acidity of the M-BEA (M = Sn, Ti) catalyst systems make them particularly effective for the isomerization of glucose to fructose in water (2012PNA9727). Using  $\text{H}^+$ -USY (ultrastabilized zeolite Y, FAU structure) in methanol in a 2-step conversion leads to improved fructose yields



Scheme 16

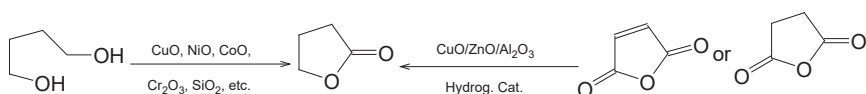
(2013JA5246). Dehydration of fructose to HMF can be accomplished in >70% yield in water with an acid resin (e.g., Dowex type). Higher HMF yields (>90%) can be obtained in nonaqueous solvents (e.g., DMF, DMSO) with a range of acid catalysts (e.g., Amberlyst-15, Nafion, and  $H^+$ -BEA).

Catalytic oxidation of HMF can form diformylfuran and FDCA but most attention has been devoted to the latter as it is a potential intermediate for polymer production such as bio-PET (via terephthalic acid) and polyethylenefuranoate (PEF). A range of supported Pt, Pd, and Au catalysts (e.g., Pt/ $Al_2O_3$ , Pt/ $ZrO_2$ , Pd/C, Au/LDH) have led to FDCA yields over 75% (2013CRV1499).

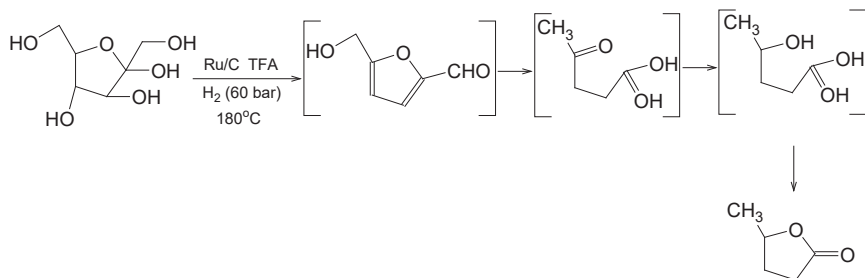
The vapor-phase reaction of BDO at 250–450 °C in the presence of oxide catalysts (e.g., CuO, NiO, CoO,  $Cr_2O_3$ ,  $SiO_2$ ,  $WO_3$ ,  $B_2O_3$ ,  $H_7CoB(W_2O_7)_6$ , and  $H_7P(Mo_2O_7)_6$ ) forms  $\gamma$ -butyrolactone (GBL) along with THF and 2,3-dihydrofuran as coproducts (Scheme 17) (1978NKKTF122, 1996IJCT237). GBL has also been made starting from butane-derived MA or succinic anhydride (1997WO9743234A1), under vapor-phase conditions (250–270 °C, 0.1–0.5 MPa) using a CuO/ $ZnO/Al_2O_3$  hydrogenation catalyst (1992PL157851B1). The conversion of diols to lactones also occurs using Au supported on Al-Mg hydrotalcite (Au/LDH). For example, using Au/LDH catalyst, excellent yields (88–99%) of lactones have been obtained in one step starting from diols under atmospheric pressure of oxygen in toluene solvent at 80 °C (2009GC793).

$\gamma$ -Valerolactone has been directly synthesized (52% yield) from C-6 sugars (glucose, fructose) without isolation of the intermediate levulinic acid (Scheme 18). The cascade catalyst system used for this conversion was a homogeneous dehydration catalyst (trifluoroacetic acid) combined with a heterogeneous hydrogenation catalyst (Ru/C, 180 °C, 16 h) with hydrogen gas or an H-donor such as formic acid (2009GC1247).

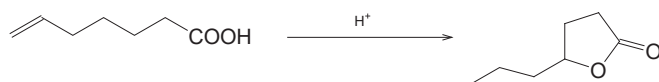
Olefinic acids have been converted into  $\gamma$ -lactones catalyzed by solid Brønsted-acid resins, instead of conventional liquid acids, in a tandem isomerization and then cyclization reaction (Scheme 19). Amberlyst-15 and Nafion SAC-13 were found to be the most active catalysts in refluxing



Scheme 17



Scheme 18



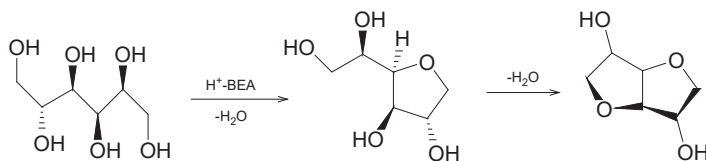
Scheme 19

chlorobenzene. With double bonds at the three- and four-chain positions, there was no isomerization necessary and the  $\gamma$ -lactone formed in 95–100% yield (2007ACAG238).

The current sulfuric acid catalyzed process to convert sorbitol to isosorbide ( $127^\circ\text{C}$ ) gives a yield of 70–77%. Product separation is difficult due to large amounts of sulfuric acid pitch. Promising isosorbide yields of 72–76% have been achieved using  $\text{H}^+$ -BEA that were superior to other large pore zeolites (USY, MOR) that gave yields below 30% (Scheme 20) (2015GC2732).

The solid-acid SSA has been used as a recyclable catalyst in the synthesis of pyrazoles. For example, a regio- and chemo-selective condensation occurs between hydrazines and various 1,3-dicarbonyl compounds to give pyrazoles under solvent-free conditions (Scheme 21) (2009SC947).

Pyrazole synthesis from a chalcone and a hydrazine involves two consecutive steps that are regioselective cyclization and oxidation. A bifunctional catalyst comprised of Pd- or Pt-supported on carbon and acidic K-10



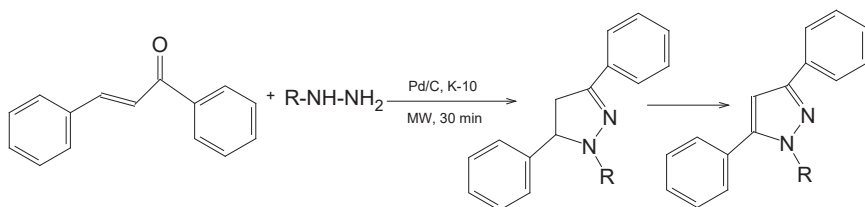
Scheme 20



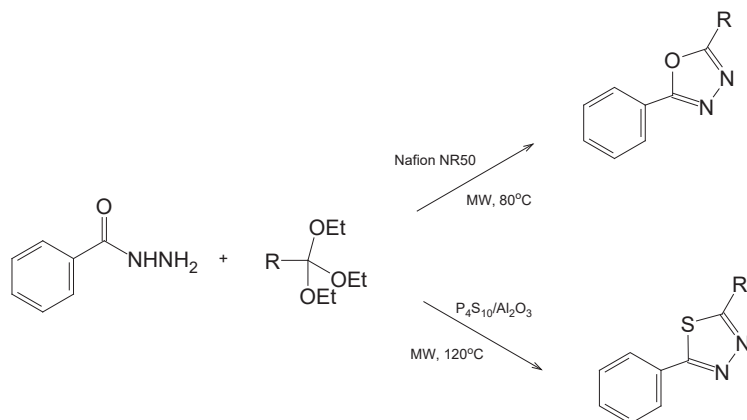
Scheme 21

montmorillonite is effective under microwave irradiation (30 min) without any solvent (Scheme 22) (2007SL1600). The K-10 promotes condensation and cyclization while the PGM facilitates dehydrogenation/oxidation to form the aromatic product. Supported Pd was more selective than Pt giving pyrazole yields between 86% and 96%.

The bioactive heterocycles 1,3,4-oxadiazole and 1,3,4-thiadiazole are usually synthesized in multistep processes. These compounds, however, can be formed in one step using an ortho-ester and an acid hydrazide using the solid Brønsted acid catalyst Nafion NR50 under microwave irradiation (10 min) without needing a solvent (Scheme 23). When the reaction was



Scheme 22



Scheme 23



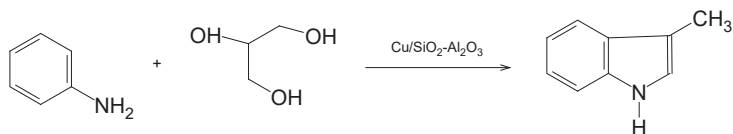
conducted in presence of phosphorus pentasulfide on  $\text{Al}_2\text{O}_3$  as the sulfur source, the resulting product was the 1,3,4-thiadiazole (2008TL879).

Copper on amorphous  $\text{SiO}_2\text{-Al}_2\text{O}_3$  was found to be a good catalyst for the vapor-phase synthesis of 3-methylindole from aniline and glycerol (Scheme 24). Zinc and potassium oxides have a promoting effect on the catalyst performance (2012CX1055). Silver on silica has been found to catalyze an efficient vapor-phase reaction of aniline with 1,2-propanediol to form 3-methylindole at atmospheric pressures (2008CX1199).

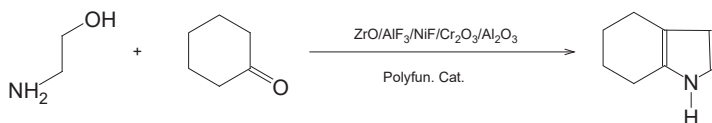
The heterogeneously catalyzed cyclocondensation of cyclohexanone with monoethanolamine leads to 4,5,6,7-tetrahydroindole under liquid- and vapor-phase conditions (Scheme 25). In the vapor phase (320–400 °C) with a reactant 1:1 ratio, use of a polyfunctional catalyst containing  $\text{ZnO}$ ,  $\text{AlF}_3$ ,  $\text{NiF}_2$ ,  $\text{Cr}_2\text{O}_3$ , and  $\text{Al}_2\text{O}_3$  gave the product tetrahydroindole in 30% yield. The same reaction under liquid-phase conditions (250 °C in presence of a strong base) gave the product in 40% yield (1992DANRU57).

Generally, N-acylindoles are prepared in two steps but a novel one-pot synthesis is possible using 2,5-dimethoxytetrahydrofuran (a succindialdehyde synthon) and an amide in presence of the solid-acid K-10 montmorillonite catalyst under microwave irradiation (Scheme 26) (2008SL410). The reaction requires two equivalents of 2,5-dimethoxytetrahydrofuran with 1 mole reacting with the amide to form the N-acyl pyrrole followed by the second mole that forms the N-acylindole derivative. The K-10 generates succindialdehyde (or 1,4-butanedial) from 2,5-dimethoxytetrahydrofuran.

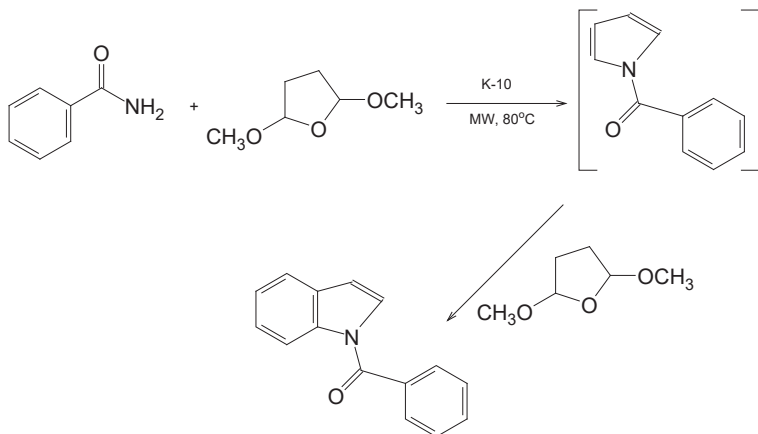
A Sonogashira coupling followed by cyclization has been used in the synthesis of 2-phenylindole utilizing a  $\text{Pd}^{\text{II}}/\text{C}$  catalyst and  $\text{CuI}$  as cocatalyst (Scheme 27). 2-Iodoaniline reacts with phenylacetylene in presence of the catalyst at 120 °C in  $\text{DMF}/\text{H}_2\text{O}$  (1:1) solvent to give 2-phenylindole



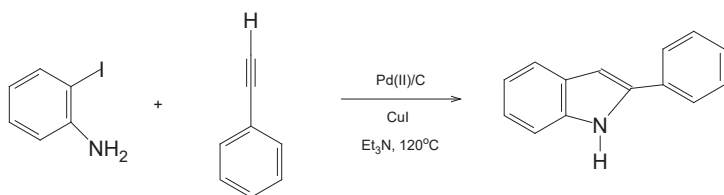
Scheme 24



Scheme 25



Scheme 26

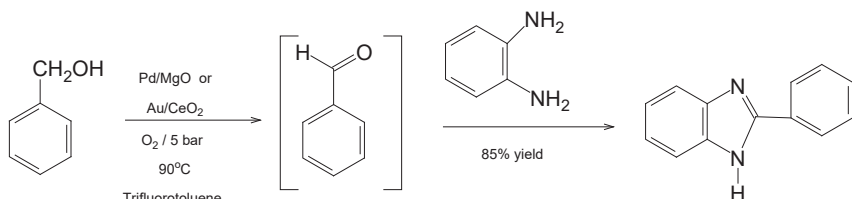


Scheme 27

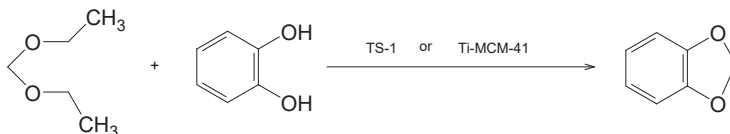
(2004ACAG161). The catalyst on recycle showed some deactivation; however, the selectivity towards 2-phenylindole was retained.

Imidazole is prepared in 84% yield using a Pd/C catalyst in an aqueous solution of glyoxal-formaldehyde-NH<sub>3</sub> (1:1:3 M) (1988USP4719309). 2-Methylimidazole can be made in a similar way by using acetaldehyde in place of formaldehyde.

Benzimidazoles are synthesized starting from a 1,2-phenylenediamine with either an aldehyde or an acid (Scheme 28). With aldehydes, two steps occur which is condensation to form the cyclic intermediate followed by



Scheme 28

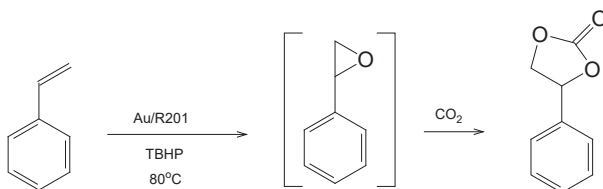


Scheme 29

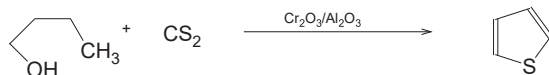
oxidation to form the aromatic imidazole. A one-pot two-step process for making 2-phenylbenzimidazole (2010T730) is reported starting from 1,2-phenylenediamine and benzyl alcohol using Au- and Pd-based catalysts in trifluorotoluene solvent at 90 °C in the presence of air at elevated pressure. The benzyl alcohol is first oxidized to form benzaldehyde which in turn reacts with 1,2-phenylenediamine to form a dihydrobenzimidazole that oxidizes to form the final product 2-phenylbenzimidazole in 85% yield.

The vapor-phase synthesis of 1,2-methylenedioxybenzene is possible starting from catechol and diethoxymethane, a formaldehyde acetal derivative, using either TS-1 or M-MCM-41 (M = Ti, Sn, Zr) catalysts (Scheme 29). This approach is claimed to be environmentally friendly as no dihalomethane is used to introduce the methylene group. The initial adduct, 2-(ethoxymethoxy)phenol, was proposed as an intermediate to the final product 1,2-methylenedioxybenzene (2010ACBE72).

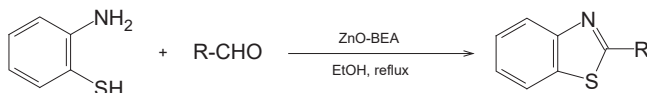
Cyclic carbonates are important fine chemical intermediates and readily form from epoxides and carbon dioxide. Various catalysts have been evaluated for the one-step synthesis of cyclic carbonates that combines the epoxidation and carbonation steps. Gold supported on a basic resin R201, whose functional group is a quaternary ammonium hydroxide (polystyryl-methyl-trimethyl ammonium), was found to catalyze both steps in the conversion of styrene to styrene carbonate using TBHP (Scheme 30) (2009CATT383). The overall selectivity to styrene carbonate was 51% at 100% styrene conversion. The Au/R201 catalyst was reused in a second run without any loss of reactivity.



Scheme 30



Scheme 31



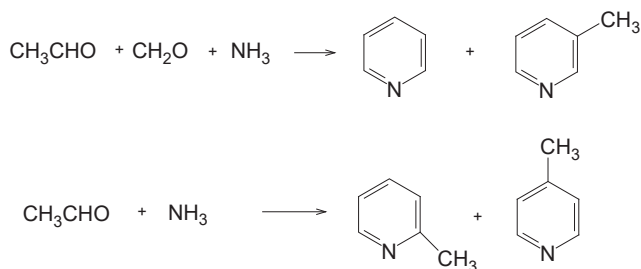
Scheme 32

An investigation into the synthesis of thiophene from butanol and  $\text{CS}_2$  under vapor-phase conditions made use of a  $\text{Cr}_2\text{O}_3/\text{Al}_2\text{O}_3$  heterogeneous catalyst (Scheme 31). The reaction pathway for the formation of thiophene from butanol involves successive dehydrogenations, oxygen–sulfur exchange, and the final dehydroheterocyclization (1998CATL207).

Benzothiazole derivatives containing a substituent at the 2-position are generally prepared in a coupling reaction using 2-bromobenzothiazole and the required R-bearing reagent. A simpler method is reported that uses cyclization of 2-aminobenzenethiol with various aldehydes to form 2-substituted benzothiazole derivatives catalyzed by ZnO-BEA (Scheme 32) (2010CCL421). The aldehyde and 2-aminobenzenethiol in the presence of ZnO-BEA was refluxed in ethanol for 1–2 h to give benzothiazole in ca. 90% yield. The catalyst aids both the condensation and oxidation steps to form the product and was recycled successfully without significant loss of activity.

## 9. SIX-MEMBERED HETEROCYCLES

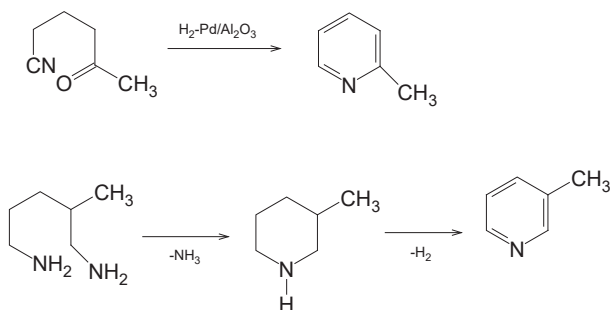
The commercial synthesis of pyridine bases began in 1953 and quickly replaced the coal tar-derived compounds. The vapor-phase production of pyridine and  $\beta$ -picoline from acetaldehyde, formaldehyde, and  $\text{NH}_3$  (400–500 °C) is accomplished using either fixed- or fluid-bed reactors (Scheme 33) (2012KC274). Use of acetaldehyde and  $\text{NH}_3$  under similar process conditions leads to the formation of  $\alpha$ - and  $\gamma$ -picoline. Catalysts described in the patent literature for the formation of pyridine and picolines include amorphous  $\text{SiO}_2\text{-Al}_2\text{O}_3$  and zeolites with and without metal promotion. Useful zeolite structures reported in patents include FAU, MOR, MEL, TON, MEL, MFI, BEA, and MCM-22 (2001MI1) as well as MEL-FER (2009CN1011485995A) and MFI-MCM-22 (2009CN101485996A)



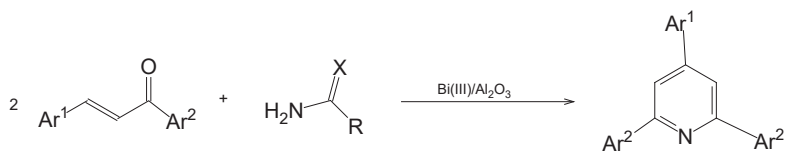
Scheme 33

intergrowths. The most effective metal promoters include Cd, Tl, and Pb such as Pb/TS-1 (2008USP7365204). A Tl-Pd-MFI catalyst is reported to give pyridine and picoline yields of 65% and 19%, respectively (1993USP5237068). Other carbonyl-containing feeds can be used to produce alkylpyridines with different substitution patterns such as 2,6-lutidine that is made from acetone, formaldehyde, and  $\text{NH}_3$ .

In addition to the vapor-phase processes that produce picolines as a coproduct, certain picolines are selectively produced in other heterogeneously catalyzed reactions (Scheme 34). The conversion of 5-oxohexanenitrile, derived from acetone and acrylonitrile, over a fixed-bed Pd/ $\text{Al}_2\text{O}_3$  catalyst produces  $\alpha$ -picoline (1986CIL129). Since 1990,  $\beta$ -picoline is also been produced from 2-methyl-1,5-pentanediamine (MPDA) originally in a one-step fluid-bed process (1992USP5149816) and more recently in a 2-step process, via 3-methylpiperidine, using fixed-beds of MFI and Pd/ $\text{Al}_2\text{O}_3$  in series (2005ACAG75). Vanadia-based catalysts have been shown to convert MPDA under ammoxidation conditions directly to 3-cyanopyridine without having to isolate  $\beta$ -picoline (2000USP6118003).



Scheme 34

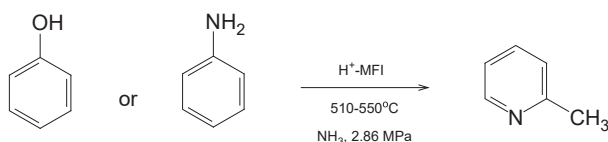


Scheme 35

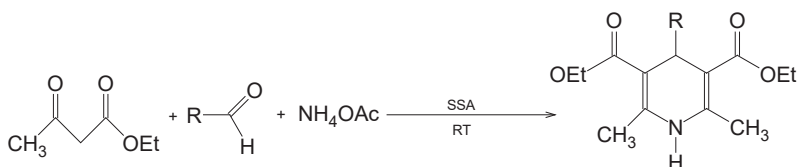
Polyarylpyridines, specifically 2,4,6-triarylpyridines, are an important class of compounds due to their application as therapeutic agents. They are typically prepared by multistep synthetic procedures. The one-step synthesis of 2,4,6-triarylpyridines can be achieved by reaction of chalcones with urea, or its derivatives, in presence of a solid Lewis acid catalyst such as bismuth(III) nitrate immobilized on  $\text{Al}_2\text{O}_3$  at  $130^\circ\text{C}$  (Scheme 35). The yield of 2,4,6-triarylpyridines are reported to be in the range of 65–85% (2006TL837).

Aniline and phenol in the presence of ammonia and  $\text{H}^+$ -MFI ( $510^\circ\text{C}$ , 30–50 barg) undergo the Benzamine rearrangement to form  $\alpha$ -picoline (Scheme 36) (1983USP4395554, 1983USP4388461). This rearrangement occurs with reasonable selectivity but has not been commercialized owing to low conversions. Use of  $\text{H}^+$ -MFI also catalyzes the Benzamine rearrangement of 1,3-phenylenediamines to form 2-amino-alkylpyridines (1986USP4628097).

Hantzsch's dihydropyridine synthesis, a condensation–cyclization reaction of aldehydes, 1,3-dicarbonyl compounds, and ammonium acetate, has been achieved under mild and solvent-free conditions using the SSA catalyst (Scheme 37). The advantages of this approach are that it is



Scheme 36



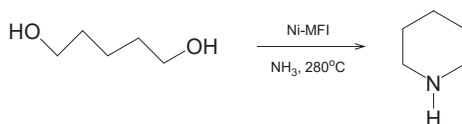
Scheme 37

environmentally benign, gives high yield, and is achieved with short reaction times (2011CNJC1180). Other heterogeneous catalysts such as silica-supported 12-tungstophosphoric acid (2009ICA3555), perchloric acid supported on silica (2006JMCAC179), and nanoparticles of zinc oxide (2012IJC101) have also been successfully used in the synthesis of Hantzsch dihydropyridines.

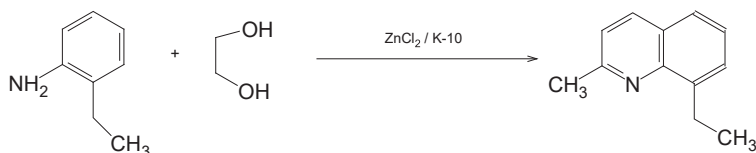
A majority of commercially produced piperidine is made via the catalytic hydrogenation of pyridine while a lesser amount is made by the catalyzed aminocyclization of 1,5-pentanediol (Scheme 38). A Ni-MFI catalyst is claimed to convert aqueous pentanediol (280 °C) in the presence of NH<sub>3</sub> to piperidine in 90% yield (2003USP6528647).

The vapor-phase reaction of one or more aldehydes with arylamines provides a route to quinoline and a range of alkylquinoline derivatives without forming large amount of waste salts that are associated with liquid-phase Doebner–Von Miller–Skraup reactions (1997USP5700942, 2006JCAT362). Evaluation of a range of zeolite structures (e.g., FAU, MOR, BEA, LTL, MFI) with formaldehyde-acetaldehyde and *o*-toluidine feed gave 8-methylquinoline with yields up to 55%. The vapor-phase reaction 2-ethylaniline and ethylene glycol in presence of K-10 montmorillonite, with or without zinc chloride, gave 2-methyl-8-ethylquinoline (Scheme 39). The same starting materials in the presence of a different catalyst, copper chromite, gave 7-ethylindole as the product (2000CATT289).

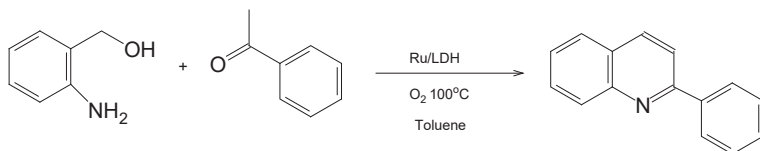
A modification of Friedlander quinoline synthesis involves the reaction of 2-aminobenzyl alcohol and a ketone in the presence of Ru/LDH (Ru/hydrotalcite) catalyst and oxygen (Scheme 40) (2001JCSCC2576, 2003T7997). The initial reaction step on the catalyst is the oxidation of



Scheme 38



Scheme 39

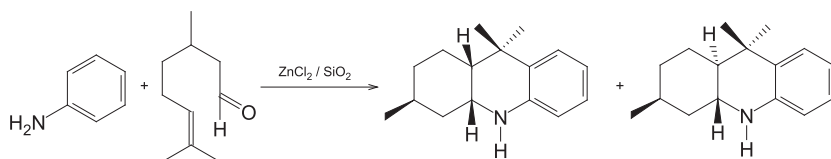


Scheme 40

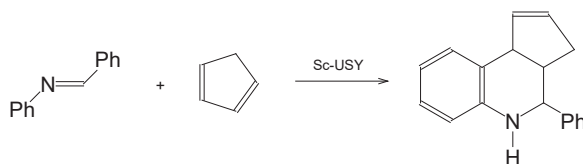
2-aminobenzyl alcohol to 2-aminobenzaldehyde, followed by the condensation of the added ketone with the formed aldehyde to give a chalcone derivative which immediately cyclizes with the amine group to form the 2-substituted quinoline. The Ru/LDH catalyst can be reused without any loss of activity and yields of the product quinolines are good to moderate (74–90%).

Octahydroacridines yields of 75–92% have been produced from (+)-citronellal and arylamines using the solid Lewis acid catalyst ZnCl<sub>2</sub>/SiO<sub>2</sub> combined with microwave heating (Scheme 41). The initial aniline condensation step to form imine is followed by a hetero-Diels–Alder reaction involving the imine and the alkene citronellal group to form 1,2,3,4,4a,9,9a,10-octahydroacridines (2003TL6809).

An aza-Diels–Alder reaction between *N*-benzylideneaniline and cyclopentadiene is catalyzed by a Sc-USY catalyst at room temperature in acetonitrile (Scheme 42) (2012JPCC13661). The resulting tetrahydroquinoline is formed quantitatively when the scandium content of Sc-USY is optimized (ca. 2–5 mol% of Sc<sup>3+</sup>). Higher loadings of Sc<sup>3+</sup> led to lower product yield while the parent H<sup>+</sup>-USY produced very little tetrahydroquinoline. These



Scheme 41



Scheme 42



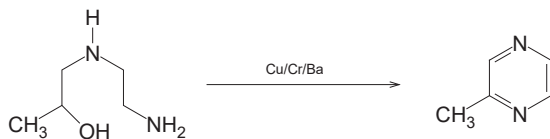
observations suggest that well-dispersed  $\text{Sc}^{3+}$  ions provide the highest LAS concentration and are essential for the aza-Diels–Alder reaction.

Pyrazine is a minor by-product formed during the catalyzed vapor-phase production of pyridine. The most important member of the pyrazine family is 2-methylpyrazine that is manufactured (up to 1000 tonnes/year) as a precursor for the production of the anti-TB drug pyrazinamide. The vapor-phase conversion of ethylenediamine and propylene glycol over  $\text{Cu}/\text{Cr}_2\text{O}_3$  and related dehydrogenation catalysts produces 2-methylpyrazine (2001ACAG197). Preparation of 2-methylpyrazine starting from *N*-(2-hydroxypropyl)-ethylenediamine (a PO-ethylenediamine adduct) was achieved under vapor-phase conditions at 360 °C using heterogeneous catalysts prepared from copper, chromium, and barium oxides (Scheme 43). The best yield achieved for 2-methylpyrazine was 78% (2000XXH1).

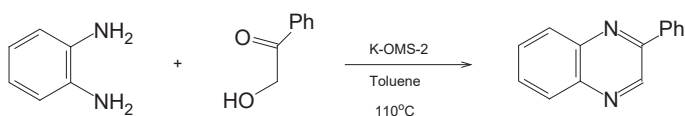
A combined oxidation and condensation sequence occurs in a one-pot synthesis of quinoxalines from  $\alpha$ -hydroxyketones and 1,2-diamines catalyzed by the manganese oxide octahedral molecular sieve K-OMS-2 (Scheme 44) (2008GC1029). The K-OMS-2 catalyst was easily recovered and reused without loss of any activity.

The high temperatures (350–400 °C) that form 2-methylpyrazine and related alkylpyrazines in the catalyzed conversion of diamine-diol feeds must rapidly dehydrogenate any piperazine intermediate. Piperazine heterocycles can form in a double N-alkylation reaction of 1,2-diamines by 1,2-diols using a  $\text{Pd}/\text{MgO}$  catalyst at 160 °C (Scheme 45) (1995CRV661).

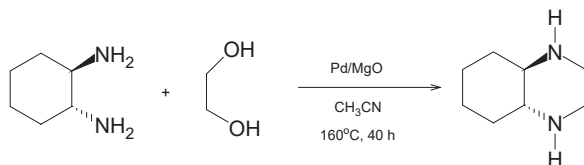
Related to the Hantzsch dihydropyridine synthesis is the Biginelli reaction that uses urea or a derivative (in place of ammonium acetate) along with aldehydes and 1,3-dicarbonyl compounds to form a dihydropyrimidines. The solid SSA catalyst is effective in the Biginelli reaction which is



Scheme 43



Scheme 44



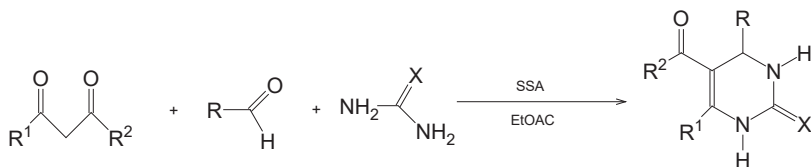
Scheme 45

performed under mild conditions (refluxing ethanol) to provide high yields of the product dihydropyrimidine with a bonus of easy workup and effective catalyst recycle (Scheme 46) (2003TL2889).

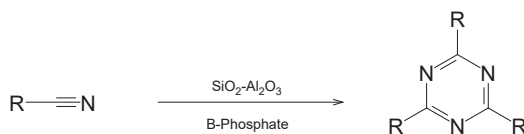
The most important S-triazines are melamine and cyanuric chloride that serve resin and herbicide markets, respectively. Melamine is produced in over 95% yield by cyclocondensation of urea mostly by a noncatalytic melt process (90–150 bar, 380–450 °C) but a significant amount is produced in a catalyzed process (350–450 °C) using modified SiO<sub>2</sub>-Al<sub>2</sub>O<sub>3</sub> catalysts in fixed- or fluid-bed reactors (1983USP4408046). Cyanuric chloride is produced by the gas-phase trimerization of cyanogen chloride (Cl-CN) over a bed of activated charcoal at 350–450 °C.

Alkyl or aryl s-triazines are also made by treating aliphatic or aromatic nitriles, along with urea in presence of ammonia, under vapor-phase conditions using heterogeneous catalysts such as Al<sub>2</sub>O<sub>3</sub>, amorphous SiO<sub>2</sub>-Al<sub>2</sub>O<sub>3</sub>, SiO<sub>2</sub>, and boron phosphate (Scheme 47) (1969RO51482).

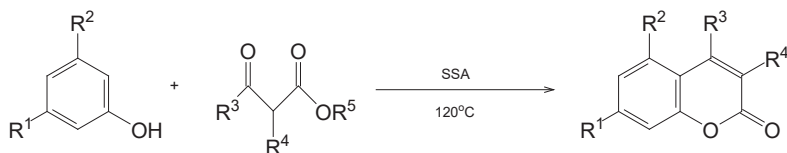
The Pechmann condensation involves the synthesis of coumarins from phenols with β-ketoesters in the presence of a Lewis acid catalyst. The same reaction can be catalyzed by SSA which is predominantly a



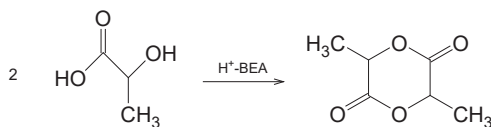
Scheme 46



Scheme 47



Scheme 48



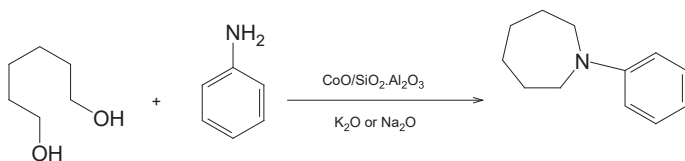
Scheme 49

solid-Brønsted acid catalyst (Scheme 48). The approach of using SSA is cleaner, with high yield, short reaction time, and easy workup (2009OCJ33).

The current polylactic acid process uses ring opening polymerization of lactide intermediate which is the cyclic dimer of lactic acid (LA). Lactide intermediate is formed in a 2-step process involving LA oligomerization followed by its high-temperature (150–220 °C) vacuum pyrolysis. A potential 1-step process to convert LA to lactide (ca. 80% yield) using  $H^+$ -BEA has been proposed (Scheme 49) (2015SCI6243). Compared to  $H^+$ -BEA, mineral acids and solid-acid resins (e.g., Amberlyst-15, nafion) gave inferior lactide yields (<25%).

## 10. SEVEN-MEMBERED HETEROCYCLES

The vapor-phase synthesis of 1-phenylazepane from aniline and 1,6-hexanediol is accomplished using a cobalt oxide on  $SiO_2-Al_2O_3$  catalyst doped with sodium or potassium oxide (Scheme 50). Characterization of the catalyst revealed the sodium oxide reduced the number of medium and strong acid sites while actually increasing the number of weak acid sites, thus improving the selectivity towards 1-phenylazepane (2012FC340).

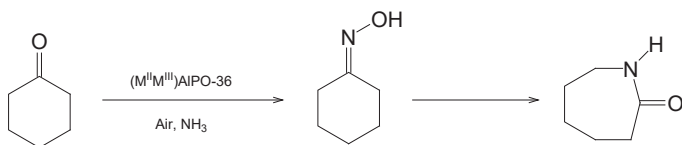


Scheme 50

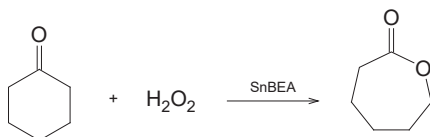
$\epsilon$ -Caprolactam (CPL) is an important industrial intermediate in the manufacture of Nylon-6 and is produced from cyclohexanone via Beckmann rearrangement of cyclohexanone oxime. The CPL process that uses hydroxylamine sulfate to form the oxime and sulfuric acid for the rearrangement produces the greatest amount of waste ammonium sulfate; the ammonium sulfate-to-CPL weight ratio is ca. 4. In 2003, Sumitomo introduced a new process that avoids waste salt formation using two heterogeneous catalysts (2007BCJ1280). The first step is a liquid-phase ammoximation using TS-1 that reacts cyclohexanone with  $\text{NH}_3$  and  $\text{H}_2\text{O}_2$  to form the oxime and water. The second step uses a high-silica MFI catalyst in a fluid-bed reactor (350–400 °C) to isomerize the oxime to CPL. Co-feeding methanol with the oxime increases the CPL selectivity from ca. 80% to 95%. The CPL capacity of the Sumitomo plant in Japan was expanded from 65,000 to 85,000 tonnes/year.

Research aimed at using air rather than  $\text{H}_2\text{O}_2$  in a one-step process to convert cyclohexanone through to CPL could provide a significant advantage over the Sumitomo process. One such study reported the solvent-free liquid-phase transformation of cyclohexanone to CPL using the bifunctional transition-metal catalyst ( $\text{M}^{\text{II}}\text{M}^{\text{III}}$ )AlPO-36 ( $\text{M} = \text{Co}, \text{Mn}$ ) (Scheme 51) (2001JA8153). Hydroxylamine is formed in situ from  $\text{NH}_3$  and oxygen which reacts with cyclohexanone to form the oxime in route to CPL.

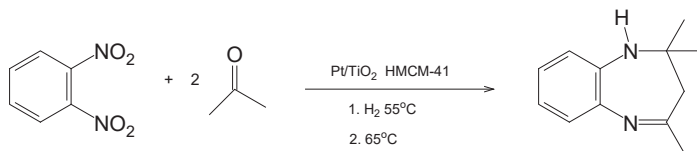
The Baeyer–Villiger (BV) oxidation uses peracids in the stoichiometric conversion of ketones to esters or lactones. Use of  $\text{H}_2\text{O}_2$  combined with SnBEA is a particularly effective catalytic system for BV oxidations (Scheme 52) (2001NAT423). The SnBEA catalyst is able to convert cyclohexanone to caprolactone with greater than 98% selectivity.



Scheme 51



Scheme 52

**Scheme 53**

Another class of seven-membered heterocycles important for their bioactivity are 1,5-benzodiazepines which are usually synthesized from 1,2-diaminobenzene and  $\alpha,\beta$ -unsaturated carbonyl compounds. A new synthetic approach replaces 1,2-phenylenediamine with less expensive precursor 1,2-dinitrobenzene. Reaction of 1,2-dinitrobenzene and acetone in the presence of the bifunctional catalyst Pt/TiO<sub>2</sub>-HMCM-41 is performed in two stages; initial hydrogenation at 55 °C that reduces the nitro groups followed by acid catalyzed acetone cyclocondensation at 65 °C in the absence of hydrogen to form the 1,5-benzodiazepine product (Scheme 53) (2009CEJ8834).

## 11. PROCESS AND ECONOMIC CONSIDERATIONS

Most research activity on the use of heterogeneous catalysts for making heterocyclic compounds is focused on existing larger volume products. Incremental process improvements through the introduction of new catalysts that give higher yield and productivity, while using existing equipment and feedstock, usually lead to better financial return in the short term. Process improvements that involve new chemistry routes (i.e., different feedstock) and new types of catalyst/reactor entail greater risk and capital outlay, but in the longer term may derive greater rewards in terms of competitive advantage through lowest cost. This has been demonstrated with examples of by-product (e.g., waste salts) and coproduct elimination.

The decision to commercially introduce a new heterocyclic compound made using a heterogeneous catalyst is not straightforward and is associated with the risk that market projections are overly optimistic. Risk can be minimized if the new compound is a derivative of a current product and can be made in existing process equipment (e.g., by changing one feed component to a higher homolog). Large capital outlays to build new plant to use unproven technology for a new product introduction carry the greatest risks (and rewards).

A catalyst vendor will be keen to derive maximum benefit when supplying a new generation of heterogeneous catalyst to an existing customer. The resulting catalyst price increase can substantially offset any cost savings for the customer's new/improved chemical process. This is especially true if operational difficulties are encountered that can include excessive sintering, rapid coke buildup/slow regeneration, high attrition rates (fluid-bed reactors), and catalyst leaching/dissolution (liquid-phase reactors). Ideally the operational experience meets or exceeds expectations (in terms of yield, productivity, and catalyst life) to the mutual benefit of customer and catalyst vendor.

Green chemistry principles frequently underpin innovation in heterogeneous catalysis and have typically led to lower-cost chemical processes. This is not always the case in all regions of the world and older chemistries, now abandoned in the West, are reemerging elsewhere to displace cleaner technologies; a notable example being the use of calcium carbide-derived acetylene routes to produce PVC, BDO, and other commodity chemicals.



## 12. FINAL COMMENTS

This short review on the use of heterogeneous catalysts for making heterocyclic compounds is by no means comprehensive. It is hoped that it will encourage synthetic organic chemists to consider reading further on the topic of catalytic materials and even to pursue their own research in the area.

## REFERENCES

- 1952USP2580714 F.G. Young, J.T. Fitzpatrick, US patent 2,580,714, assigned to Union Carbide, (January 1, 1952).
- 1969RO51482 C. Matasa, A. Cocan, E. Tonca, Romanian Patent 51482, (January 25, 1969).
- 1975USP3915995 J.D. Holmes, H.J. Hagemeyer, Jr., US patent 3,915,995, assigned to Eastman Kodak Company, (October 28, 1975).
- 1978NKKTFS122 J. Osis, A. Andersons, and M.V. Shimanskaya, *Vses Nauchn Konf Khim Tekhnol Furanovykh Soedin, Tezisy Dokl*, 3rd ed., 122-3.
- 1983USP4388461 C.D. Chang, P.D. Perkins, US patent 4,388,461, assigned to Mobil Oil Corp., (June 14, 1983).
- 1983USP4395554 C.D. Chang, P.D. Perkins, US patent 4,395,554, assigned to Mobil Oil Corp., (July 26, 1983).
- 1983USP4408046 R. van Hardevald, US patent 4,408,046, assigned to DSM, (October 4, 1983).
- 1986CIL129 C.G.M. van de Moesdijk, *Chemistry Industry*, 4, 129 (1986).
- 1986USP4628097 H. Le Blanc, L. Puppe, K. Wedemeyer, US patent 4,628,097, assigned to Bayer, (December 9, 1986).

- 1988USP4719309 W. Mesch, US patent 4,719,309, assigned to BASF, (January 12, 1988).
- 1988USP4761394 A.M. Lauritzen, US patent 4,761,394, assigned to Shell Oil Company, (August 2, 1988).
- 1991MI1 C.N. Satterfield, *Heterogeneous Catalysis in Industrial Practice*, 2nd ed., McGraw-Hill (1991), p 298.
- 1992DANRU57 M.Ch. Kudratova, D. Yusupov, M.G. Ismatullaeva, and R.I. Israilov, *Doklady Akademii Nauk Respubliki Uzbekistan (1992–2001)*, p 57.
- 1992PL157851B1 I. Szelejewska, S. Ciborowski, A. Kur, W. Biernacki, B. Wieckiewicz, Chmielewski, K.; Panachida, J. Pol., PL 157851 B1, (July 31, 1992).
- 1992USP5149816 G.L. Goe, R.D. Davis, US patent 5,149,816, assigned to Vertellus Specialties Inc., (September 22, 1992).
- 1993USP5237068 S. Shimizu, N. Abe, M. Doba, A. Iguchi, US patent 5,237,068, assigned to Koei Chemical Co. Ltd, (August 17, 1993).
- 1995CRV661 M. Boudart, *Chem. Rev.*, **95**, 661 (1995).
- 1996IJCT237 B. Srinivas, M. Subramanyam, S.J. Kulkarni, Y.V. Subba Rao, and A.V. Rama Rao, *Ind. J. Chem. Tech.*, **3**, 237 (1996).
- 1997USP5700942 C.H. McAteer, R.D. Davis, J.R. Calvin, US patent 5,700,942, assigned to Vertellus Specialties Inc., (December 23, 1997).
- 1997WO9743234A1 M.W.M. Tuck, M.A. Wood, A.G. Hiles, PCT Int. Appl. WO 9743234 A1, (November 20, 1997).
- 1998CATL207 B.W.L. Southward, L.S. Fuller, G.J. Hutchings, R.W. Joyner, and R.A. Stewart, *Catal. Lett.*, **55**, 207 (1998).
- 2000CATT289 M. Campanati, A. Vaccari, and O. Piccolo, *Catal. Today*, **60**, 289 (2000).
- 2000JCSCC1789 M.G.M. Guidotti, R. Psaro, and N. Ravasio, *Chem. Commun.*, **1789** (2000).
- 2000USP6118003 C.H. McAteer, J.R. Calvin, R.D. Davis, US patent 6,118,003, assigned to Vertellus Specialties Inc., (September 12, 2000).
- 2000XXH1 L. Zhou, Y. Feng, H. Song, H. Qu, and H. Chen, *Xiangliao Xiangjing Huazhuangpin*, 1 (2000).
- 2001ACAG197 Y.S. Higasio and T. Shoji, *Appl. Catal. A: General*, **221**, 197 (2001).
- 2001JA8153 R. Raja, S. Gopinathan, and J.M. Thomas, *J. Am. Chem. Soc.*, **123**, 8153 (2001).
- 2001JCSCC2576 C.S. Cho, B.T. Kim, T.J. Kim, and S.C. Shim, *Chem. Commun.*, **2576** (2001).
- 2001MI1 C.H. McAteer and E.F.V. Scriven, *Heterocyclic Synthesis*, In R.A. Sheldon and R.A. van Bekkum, editors: *Fine Chemicals Through Heterogeneous Catalysis*, Wiley-VCH: Weinheim (2001), 6.3, 285.
- 2001NAT423 A. Corma, L.T. Nemeth, M. Renz, and S. Valencia, *Nature*, **412**, 423 (2001).
- 2002JCSPT143 I.R. Baxendale, G. Brusotti, M. Matsuoka, and S.V. Ley, *J. Chem. Soc. Perkin Trans.*, **1**, 143 (2002).
- 2003T7997 C.S. Cho, B.T. Kim, H.J. Choi, T.J. Kim, and S.C. Shim, *Tetrahedron*, **59**, 7997 (2003).
- 2003TL2889 P. Salehi, M. Dabiri, M.A. Zolfigol, and M.A.B. Fardb, *Tetrahedron Lett.*, **44**, 2889 (2003).
- 2003TL6809 R.G. Jacob, G. Perin, G.V. Botteselle, and E.J. Lenardao, *Tetrahedron Lett.*, **44**, 6809 (2003).

- 2003USP6528647 S.J. Kulkarni, K.V. Raghavan, R.R. Vippagunta, S. Nagabandi, US patent 6,528,647 B2 assigned to CSIR, (March 4, 2003).
- 2004ACAG161 M. Gruber, S. Choouzier, K. Koehler, and L. Djakovitch, *Appl. Catal. A: General*, **265**, 161 (2004).
- 2004JPCB3573 F. Bonino, A. Damin, G. Ricchiardi, M. Ricci, G. Spano, R. D'Aloisio, A. Zecchinna, C. Lamberti, C. Prestipino, and S. Bordiga, *J. Phys. Chem. B.*, **108**, 3573 (2004).
- 2005ACAG75 R. Chuck, *Appl. Catal. A: General*, **280**, 75 (2005).
- 2005CRV1603 Q.H. Xia, H.Q. Ge, C.P. Ye, Z.M. Liu, and K.X. Su, *Chem. Rev.*, **105**, 1603 (2005).
- 2005TL8337 A.S. Konev, M.S. Novikov, and A.F. Khlebnikov, *Tetrahedron Lett.*, **46**, 8337 (2005).
- 2006EJSSN74 N. Mimura, Z. Song, S. Tsubota, H. Yamashita, and S.T. Oyama, *e-J. Surf. Sci. Nanotechnol.*, **4**, 74 (2006).
- 2006JCAT362 R. Brosius, D. Gammon, F. van Laar, E. van Steen, B. Sels, and P. Jacobs, *J. Catal.*, **239**, 362 (2006).
- 2006JMCAC179 M. Maheswara, V. Siddaiah, Y.K. Rao, Y.M. Tzeng, and C. Sridhar, *J. Mol. Cat. A Chem.*, **260**, 179 (2006).
- 2006TL837 A. Kumar, S. Koul, T.K. Razdan, and K.K. Kapoor, *Tetrahedron Lett.*, **47**, 837 (2006).
- 2007ACAG238 Y. Zhou, L.K. Woo, and R. Angelici, *Appl. Catal. A: General*, **333**, 238 (2007).
- 2007BCJ1280 Y. Izumi, H. Ichihashi, Y. Shimazu, M. Kitamura, and H. Sato, *Bull. Chem. Soc. Jpn.*, **80**, 1280 (2007).
- 2007MI1 R.A. Sheldon, I. Arends, and U. Hanefeld, *Green Chemistry and Catalysis*, Wiley-VCH: Weinheim (2007).
- 2007SL1600 S.M. Landge, A. Schmidt, V. Outerbridge, and B. Torok, *SynLett*, **1600** (2007).
- 2007SSSC389 N. Mimura, Z. Song, T. Akita, H. Yamashita, S. Tsubota, and S.T. Oyama, *Stud. Surf. Sci. Catal.*, **172**, 389 (2007).
- 2008CX1199 J. Zheng, J. Liu, W. Tan, L. Shi, and Q. Sun, *Cuihua Xuebao*, **29**, 1199 (2008).
- 2008GC1029 S. Sithambaram, W.G. Ding, W. Li, X. Shen, F. Gaenzler, and S.L. Suib, *Green Chem.*, **10**, 1029 (2008).
- 2008JCAT403 G. Budroni and A. Corma, *J. Catal.*, **257**, 403 (2008).
- 2008SL410 M. Abid, O. De Paolis, and B. Torok, *SynLett*, **410** (2008).
- 2008TL879 V. Polshettiwar and R.S. Varma, *Tetrahedron Lett.*, **49**, 879 (2008).
- 2008USP7365204 R. Kumar, P.N. Joshi, G.M. Chaphekar, P.S. Niphadkar, A. Agarwal, P.K. Verma, K.S. Singh, US patent 7,365,204 B2, assigned to CSIR-Jubilant Organosys Ltd, (April 29, 2008).
- 2009CATT383 D. Xiang, X. Liu, J. Sun, and F.S. Xiao, *J. Sun., Catal. Today*, **148**, 383 (2009).
- 2009CEJ8834 M.J. Climent, A. Corma, S. Iborra, and L.L. Santos, *Chem. Eur. J.*, **15**, 8834 (2009).
- 2009CN1011485995A L. Xu, S.L. Liu, S. Yang, J. Tao, S. Xie, Y. Yi, Q. Wang, Chinese Patent CN101485995A, assigned to DICP, (July 22, 2009).
- 2009CN101485996A L. Xu, S.L. Liu, S. Yang, J. Tao, S. Xie, Y. Yi, Q. Wang, Chinese Patent CN101485996A, assigned to DICP, (July 22, 2009).
- 2009GC793 T. Mitsudome, A. Noujima, T. Mizugaki, K. Jitsukawa, and K. Kaneda, *Green Chem.*, **11**, 793 (2009).
- 2009GC1247 H. Heeres, R. Handana, D. Chunai, C.B. Rasrendra, B. Girisuta, and H. Heeres, *Green Chem.*, **11**, 1247 (2009).



- 2009ICA3555 E. Rafiee, S. Eavani, S. Rashidzadeh, and M. Joshaghani, *Inorg. Chim. Acta*, **362**, 3555 (2009).
- 2009JCAT44 C. Aprile, A. Corma, M.E. Domine, H. Garcia, and C. Mitchell, *J. Catal.*, **264**, 44 (2009).
- 2009OCJ33 B.M. Reddy, B. Thirupathi, and M.K. Patil, *Open Catal. J.*, **2**, 33 (2009).
- 2009SC947 X. Chen, J. She, Z.C. Shang, J. Wu, and P. Zhang, *Synth. Commun.*, **39**, 947 (2009).
- 2010ACAG4 G.S. Patience and R.H. Bockrath, *Appl. Catal. A: General*, **376**, 4 (2010).
- 2010ACBE72 A. Giugni, D. Impala, O. Piccolo, A. Vaccari, and A. Corma, *Appl. Catal., B: Environmental*, **98**, 72 (2010).
- 2010CCL421 S.S. Katkar, P.H. Mohite, L.S. Gadekar, K.N. Vidhate, and M.K. Lande, *Chinese Chem. Lett.*, **21**, 421 (2010).
- 2010T730 V.R. Ruiz, A. Corma, and M.J. Sabater, *Tetrahedron*, **66**, 730 (2010).
- 2010TL2109 H. Veisi, *Tetrahedron Lett.*, **51**, 2109 (2010).
- 2011CNJC1180 B. Datta and M.A. Pasha, *Chin. J. Catal.*, **32**, 1180 (2011).
- 2012ARK570 R. Pal, T. Sarkar, and S. Khasnobis, *ARKIVOC*, 570 (2012).
- 2012CX1055 Y. Zhang, W. Sun, L. Shi, and Q. Sun, *Cuihua Xuebao*, **33**, 1055 (2012).
- 2012FC340 L. Zhao, X. Li, P. Sun, X. Liu, L. Shi, and Q. Sun, *Fenzi Cuihua*, **26**, 340 (2012).
- 2012IJC101 F. Tamaddon and S. Moradi, *Iran. J. Catal.*, **2**, 101 (2012).
- 2012JPCC13661 A. Olmos, S. Rigolet, and P. Pale, *J. Phys. Chem. C.*, **116**, 13661 (2012).
- 2012KC274 K.S.K. Reddy, C. Srinivasakannan, and K.V. Raghavan, *Kinet. Catal.*, **53**, 274 (2012).
- 2012PNA9727 R. Bermejo-Deval, R.S. Assary, E. Nikolla, M. Moliner, Y. Roman-Leshkov, S.-J. Hwang, A. Palsdottir, D. Silverman, R.F. Lobo, L.A. Curtis, and M.E. Davis, *Proc. Nat. Acad. Sci. U.S.A.*, **109**, 9727 (2012).
- 2013CEngJ306 G. Wu, Y. Wang, L. Wang, W. Feng, H. Shi, Y. Lin, T. Zhang, X. Jin, S. Wang, X. Wu, and P. Yao, *Chem. Eng. J.*, **215**, 306 (2013).
- 2013CRV1499 R.-J. van Putten, J.C. van del Waal, E. de Jong, C.B. Rasrendra, H.J. Heeres, and J.G. de Vries, *Chem. Rev.*, **113**, 1499 (2013).
- 2013JA5246 S. Saravanamurugan, M. Paniagua, J.A. Melero, and A. Riisager, *J. Am. Chem. Soc.*, **135**, 5246 (2013).
- 2013MI1 H.A. Wittcoff, B. Reuben, and J.S. Plotkin, *Industrial Organic Chemicals*, 3rd ed., Wiley: Hoboken, NJ (2013).
- 2014GC2015 S.P. Teong, G. Yi, and Y. Zhang, *Green Chem.*, **16**, 2015 (2014).
- 2015ACSC6529 Z. Zhang and K. Dang, *ACS Catal.*, **5**, 6529 (2015).
- 2015GC2732 H. Kobayashi, H. Yokoyama, B. Feng, and A. Fukuoka, *Green Chem.*, **17**, 2732 (2015).
- 2015JOC8489 C.A. Malapit and A.R. Howell, *J. Org. Chem.*, **80**, 8489 (2015).
- 2015SCI6243 M. Dusselier, P. van Wouwe, A. Dewaele, P.A. Jacobs, and B.F. Sels, *Science*, **349**, 6243 (2015).
- 2016MI1 <http://izasc.fos.su.se/fmi/xsl/IZA-SC/ft.xml>, (last accessed January 12, 2016).
- 2016MI2 [www.shell.com/business-customers/global-solutions/petrochemicals-technologies-licensing/ethylene-oxide-ethylene-glycol-processes.html](http://www.shell.com/business-customers/global-solutions/petrochemicals-technologies-licensing/ethylene-oxide-ethylene-glycol-processes.html), (last accessed January 12, 2016).



# Palladium-Catalyzed Carbonylative Synthesis of Heterocycles

Jian-Bo Feng, Xiao-Feng Wu\*

Leibniz-Institut für Katalyse e.V. an der Universität Rostock, Rostock, Germany

\*Corresponding author: E-mail: xiao-feng.wu@catalysis.de

## Contents

1. Introduction	207
2. Synthesis of Five-Membered Heterocycles	208
3. Synthesis of Six-Membered Heterocycles	221
4. Synthesis of Other Heterocycles	241
References	243

## Abstract

Palladium-catalyzed carbonylative coupling reactions have been a powerful method in organic synthesis. The importance and significance have been described abundantly. Moreover, with the rapid development of palladium-catalyzed coupling reactions, various elegant methodologies for palladium-catalyzed carbonylative synthesis of heterocycles have been developed. In this chapter, the main achievements from 2013 to the middle 2015 are discussed.

**Keywords:** Carbonylation; Coupling; Heterocycles; Organic synthesis; Palladium catalyst



## 1. INTRODUCTION

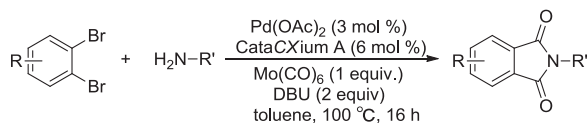
Palladium-catalyzed carbonylative transformations have experienced impressive progress during the past decades. Numerous novel methodologies have been developed and applied. Because of the importance of heterocyclic compounds, the applications of carbonylations in heterocyclic synthesis are even more interesting. At the beginning of 2013, some of us published a general review on palladium-catalyzed carbonylative synthesis of heterocycles (2013CR(113)1). Hence, in this chapter, only work that has appeared since is covered.

## 2. SYNTHESIS OF FIVE-MEMBERED HETEROCYCLES

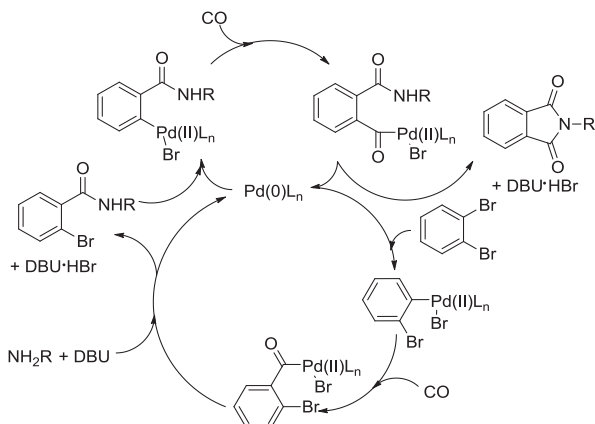
In 2013 (2013ASC(355)3581), Wu and coworkers reported a convenient and mild procedure to synthesize phthalimides from 1,2-dibromoarenes, which was conducted in the presence of a palladium catalyst and with molybdenum hexacarbonyl as the carbon monoxide source (Scheme 1). Various functional groups were tolerated and the procedure gave phthalimides in good to excellent yields. However, during the optimization process, a drastically decreased conversion was observed when the amount of  $\text{Mo}(\text{CO})_6$  was decreased or the reaction temperature was lowered below  $100\text{ }^\circ\text{C}$ . DBU was a superior base because of its ability to undergo a ligand exchange with the carbonyl complex to promote the release of CO (2012SN(23)685). In addition,  $\text{Fe}(\text{CO})_5$ ,  $\text{Co}_2(\text{CO})_8$ , and  $\text{W}(\text{CO})_6$  were also investigated, and 16%, 2%, and 56% yields of the corresponding products were obtained, respectively. Even  $\text{Cr}(\text{CO})_6$  gave the desired phthalimide in 86% yield which seemed to be applicable as an alternative CO source but its toxicity limited its application. Subsequently, primary amines were investigated and gave corresponding phthalimides in moderate to good yields. The aliphatic amines with short chains gave better yields while *t*-butylamine and unsubstituted aniline just afforded the amides, which were considered to be due to the steric hindrance of *t*-butylamine and the low nucleophilicity of the aniline derivative.

The mechanism of this domino reaction can be regarded as a Heck-type amidation. The reaction was initiated by oxidative addition to the C–Br bond which was followed by insertion of carbon monoxide into the Pd–C bond. Then, the amine acting as a nucleophile attacked the newly formed acyl species to give the corresponding amide. Finally, a second catalytic step gave the phthalimides (Scheme 2).

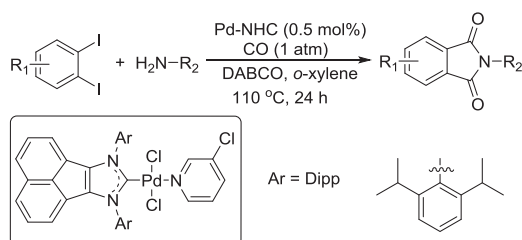
Similarly, a double aminocarbonylation of *o*-diiodobenzenes with anilines which gave the corresponding phthalimides under atmospheric CO pressure was reported by Tu and collaborators (Scheme 3) (2014OCF(1)1261). For high catalytic activity, an acenaphthoimidazolyliene palladium



**Scheme 1** Synthesis of phthalimides via Pd-catalyzed carbonylation.



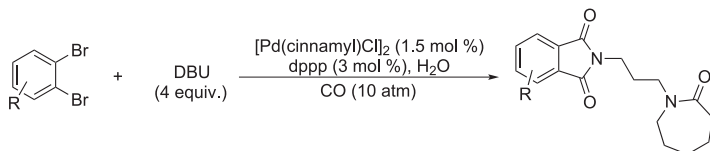
**Scheme 2** Reaction mechanism for Pd-catalyzed carbonylative phthalimide synthesis.



**Scheme 3** Pd-catalyzed aminocarbonylation of *o*-diiodobenzene.

complex was employed as the catalyst in Pd-catalyzed cross-coupling reactions, which was considered as a stronger  $\sigma$ -donor and weaker  $\pi$ -acceptor (2013OL(15)3678). Under optimal reaction conditions, full conversion and over 99% isolated yield of corresponding product was observed. However, only 47% isolated yield was obtained when it was replaced by  $\text{Pd}(\text{OAc})_2/\text{PPh}_3$ , which indicated that the reaction rejects the ligand with a strong  $\pi$ -acceptor. Then, various primary amines were tested under the standard reaction conditions. Results obtained indicated that anilines with both electron-donating groups and electron-withdrawing groups were all well tolerated. Moreover, aniline derivatives with halogen atoms, e.g., Cl and Br could be tolerated and gave the desired products in excellent yields, which offer the possibilities for further functionalization.

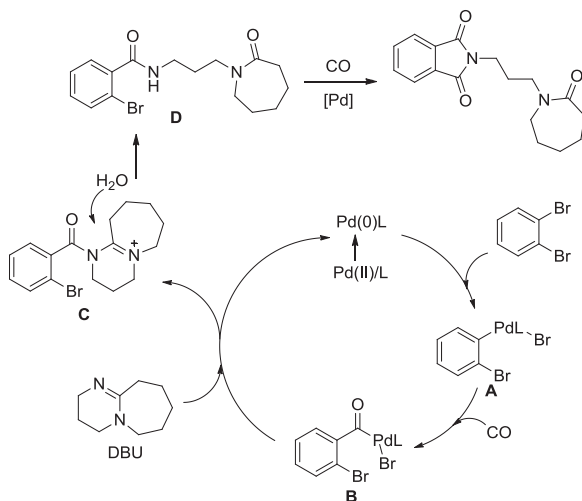
Furthermore, a novel and convenient strategy to the phthalimide and amide scaffold via Pd-catalyzed aminocarbonylation of dibromobenzenes was found by Wu and coworkers more recently (Scheme 4) (2015THL(56)342). In this protocol, DBU and DBN can be applied as



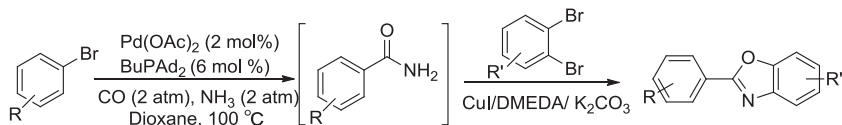
**Scheme 4** Pd-catalyzed aminocarbonylation of dibromobenzene to phthalimide.

the nitrogen source after hydrolysis and ring opening. After careful optimization, good yields can be obtained with  $[\text{Pd}(\text{cinnamyl})\text{Cl}]_2/\text{dppp}$  as the catalyst and toluene as the solvent. It should be noted that water played a crucial role in this reaction. In the presence of water, 96% of the desired product can be isolated while only 31% of the product can be obtained without addition of water. However, when the reaction was performed under lower pressure of carbon monoxide (1 bar), the yield decreased dramatically.

In the mechanism, it was considered that Pd(II) was reduced by the ligand to generate Pd(0) and then oxidative addition of dibromobenzene to Pd(0) gave the corresponding organopalladium species **A**. Then, the intermediate **B** was formed by the CO insertion into **A**. Subsequently, attack of DBU on **B** took place resulting in the formation of intermediate **C** and the regeneration of Pd(0). Finally, the intermediate **D** was formed by the hydrolysis of **C**, followed by an intramolecular aminocarbonylation in the presence of Pd(0) to generate the product (Scheme 5).



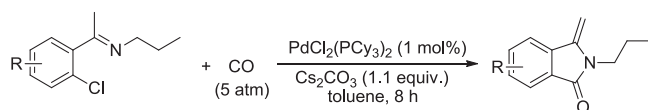
**Scheme 5** Mechanism of Pd-catalyzed aminocarbonylation of dibromobenzene to phthalimide.



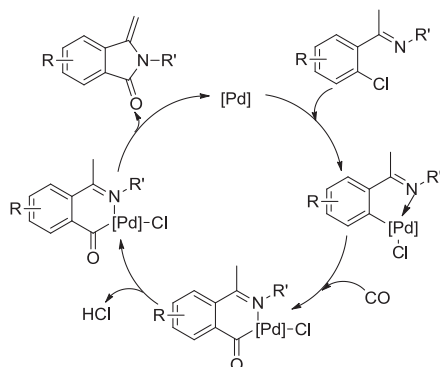
**Scheme 6** Sequential one-pot synthesis of benzoxazole from aryl bromide.

In 2013, Wu, Beller, and coworkers reported a sequential one-pot synthesis of benzoxazoles from aryl bromides employing catalytic systems of Pd and Cu (**Scheme 6**) ([2013THL\(54\)3040](#)). Initially, bromobenzene was aminocarbonylated with 2 bar of  $\text{NH}_3$  and 2 bar of  $\text{CO}$  in 1,4-dioxane in the presence of 2 mol% of  $\text{Pd}(\text{OAc})_2$  and 6 mol% of  $\text{BuPAd}_2$  at 100 °C. Next, the addition of 1,2-dibromobenzene to this reaction mixture and heating at the same temperature for another 16 h gave the desired products. Notably, no desired product was obtained with different bases like  $\text{K}_2\text{CO}_3$ ,  $\text{K}_3\text{PO}_4$ ,  $\text{NEt}_3$ , and  $\text{DBU}$  or the additional amount of palladium catalyst. Inspired by the report on copper catalysts from Glorius and coworkers ([2004ASC\(346\)1661](#)), a  $\text{CuI}/\text{DMEDA}/\text{K}_2\text{CO}_3$  system was added to the mixture, and 71% of corresponding product was isolated. Moreover, both electron-donating and electron-withdrawing functional groups on the 2-aryl-substituent were tolerated, which provided a convenient procedure for the synthesis of 2-aryl-substituted benzoxazoles from commercial aryl bromides and 1,2-dihalobenzenes.

The activation of aryl chlorides is considered an interesting and challenging topic in organic synthesis ([2002AGE\(41\)4176](#)). Recently, Hua and coworkers published several  $\text{PdCl}_2(\text{PCy}_3)_2$ -catalyzed Sonogashira and Heck cross-coupling reactions of aryl chlorides ([2006JOC\(71\)2532](#), [2007ASC\(349\)1738](#)). They also developed an alternative strategy for the synthesis of 3-methyleneisindolin-1-one derivatives via palladium-catalyzed cyclocarbonylation of *ortho*-chloroketimines (**Scheme 7**) ([2013THL\(54\)5159](#)). In this report, various catalysts and bases were tested in detail. As a result, the Pd(II) catalyst with trialkylphosphine ligand  $\text{PCy}_3$  was proven to be more efficient compared with the previous reports. With the  $\text{PdCl}_2(\text{PCy}_3)_2/\text{Cs}_2\text{CO}_3$  catalytic system under the pressure of  $\text{CO}$ , different



**Scheme 7** Pd-catalyzed cyclocarbonylation of *ortho*-chloroketimines to isindolin-1-ones.

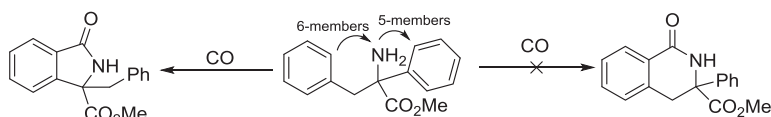


**Scheme 8** Mechanism of Pd-catalyzed carbonylation of *o*-chloroketimines to isoindolin-1-ones.

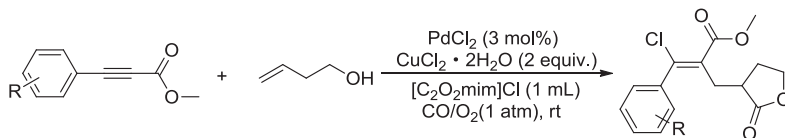
substrate-substituted ketimines were examined and gave the corresponding products in moderate to good yields. It should be noted when the chloro group was not in the *ortho* position, it was inert in the system. The selectivity was considered as the C–Cl bond activation facilitated by the coordination of N atom in the ketimine to Pd.

With regard to the mechanism, firstly, the *o*-chloroketimine undergoes an oxidative addition to the Pd catalyst and gives a five-membered intermediate. Subsequently, a six-membered palladacyclic intermediate formed after the insertion of CO. Finally, reductive elimination of the intermediate gives the desired product and regenerates the catalytic species (Scheme 8).

Use of the N atom as a directing group was also applied in the synthesis of benzolactams by cyclopalladation of amino esters was reported by Granell and coworkers (Scheme 9) (2013OM(32)649). This transformation to give five-membered rings was considered as a stoichiometric process; all the experimental results indicated that the complete substitution of the carbon in the  $\alpha$  position of the amino esters plays an important role in cyclopalladation and there was a strong bias toward six-membered lactams over the five-membered analogs. This will be discussed further in the section on synthesis of six-membered heterocycles.



**Scheme 9** Pd-catalyzed carbonylation of N-unprotected aryethylamines to five-membered benzolactams.



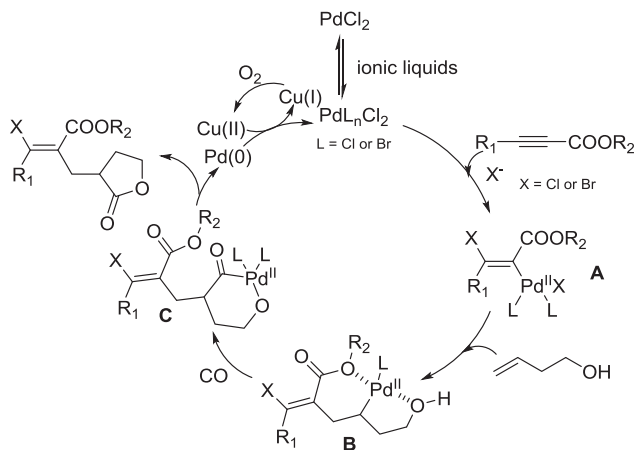
**Scheme 10** Pd-catalyzed carbonylative annulation to  $\gamma$ -lactones in ionic liquids.

In 2014, Jiang and coworkers published a novel palladium-catalyzed cascade carbonylative annulation to construct functionalized  $\gamma$ -lactones in ionic liquids with high regio- and stereoselectivity (Scheme 10) (2014CC(50)1381). Initially, ethyl 3-phenyl propiolate and homoallyl alcohol were treated with PdCl<sub>2</sub> (3 mol%) and CuCl<sub>2</sub> · 2H<sub>2</sub>O (2 equiv.) under 1 atm of CO/O<sub>2</sub> in [Bmim]Cl. However, none of the desired product was found. Subsequently, ionic liquids such as [C<sub>2</sub>O<sub>2</sub>Hmim]Cl, [C<sub>2</sub>OHmim]Cl, and [C<sub>2</sub>O<sub>2</sub>mim]Cl also were investigated. Interestingly, [C<sub>2</sub>O<sub>2</sub>mim]Cl seemed to be the most suitable medium for this reaction and the oxygen was considered to play a crucial role. It was found that ethyl, allyl, and phenyl alkynoates and substituted phenylpropionic acid can be transformed into the corresponding products in good to excellent yields, and both electron-withdrawing and electron-donating functional groups on the aromatic ring were tolerated. Unfortunately, alkynes like alkynone and alkynamide failed to undergo this reaction.

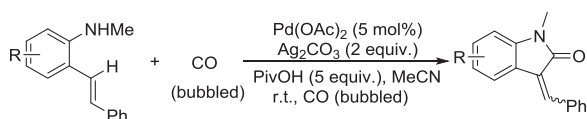
In the reaction mechanism proposed, a Pd complex was considered to be formed in situ in ionic liquids (2008TH(64)2930) and vinylpalladium intermediate **A** was formed by *trans*-chloropalladation of the alkyne in a polar solvent in the presence of excess chloride ions. Then, the insertion of alkene into **A** generated a Pd-alkyl intermediate **B**. Next, the insertion of CO into the palladium-carbon  $\sigma$  bond produced intermediate **C** (1995JACS(117)3422). Finally, reductive elimination gave the desired product and Pd(II) was regenerated in the presence of an oxidant for the next cycle (Scheme 11).

Inspired by the palladium-catalyzed intramolecular oxidative aminocarbonylation of aryl C(sp<sup>2</sup>)-H bonds with amines and CO, Li and coworkers considered that the vinylic C(sp<sup>2</sup>)-Pd<sup>II</sup> ← N complex might be readily formed under similar conditions and vinylic C(sp<sup>2</sup>)-H bond is more reactive than aryl C(sp<sup>2</sup>)-H bond (2014EJOC616). Hence, a novel oxidative aminocarbonylation of vinylic C(sp<sup>2</sup>)-H bonds via palladium-catalyzed intramolecular aminocarbonylation of alkenes with amines and CO was developed (Scheme 12). PivOH (5 equiv.) can improve the reaction, by





**Scheme 11** Mechanism of Pd-catalyzed carbonylative annulation to  $\gamma$ -lactones in ionic liquids.

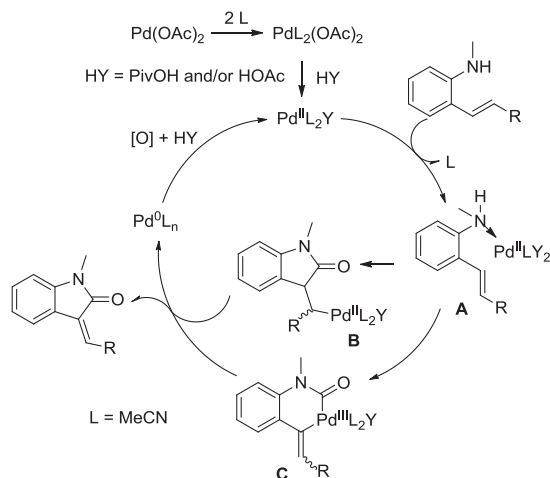


**Scheme 12** Pd-catalyzed aminocarbonylation of vinylic C(sp<sup>2</sup>)-H bond with amines.

acting as a promoter. In addition, oxidants like CuCl<sub>2</sub>, AgOAc, and Ag<sub>2</sub>CO<sub>3</sub> were tested as well. AgOAc and Ag<sub>2</sub>CO<sub>3</sub> also gave good yields. However, CuCl<sub>2</sub> just gave a trace of product, in contrast to previous reports that CuCl<sub>2</sub> proved an efficient oxidant for amination-carbonylation. Under the best conditions, a variety of 2-vinylanilines were tested and most of them gave the corresponding products in moderate to good yields except the free NH<sub>2</sub>- and N-Ac-substituted substrates.

A possible reaction mechanism was proposed: MeCN coordinated with Pd(OAc)<sub>2</sub> to form the PdL<sub>2</sub>(OAc)<sub>2</sub> complex (L = MeCN) and then exchange with the acid HY (PivOH) gives a more active species PdL<sub>2</sub>Y<sub>2</sub>. Next the nitrogen atom of the substrate can complex with the palladium species to afford the intermediate **A**. Subsequently, two pathways involving **B** and **C** may take place, respectively. Finally, by reductive elimination either **B** or **C** can form the desired product and the Pd<sup>0</sup>L species (Scheme 13).

In 2014, Wu and coworkers developed a convenient procedure for the synthesis of isoindoloquinazolinones, which employed 1,2-dibromoarenes

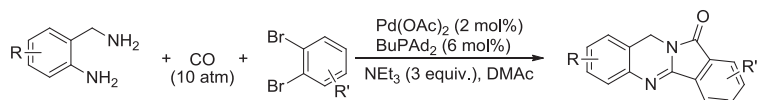


**Scheme 13** Mechanism of Pd-catalyzed intramolecular oxidative aminocarbonylation of vinylic C(sp<sup>2</sup>)-H bond with amines and CO.

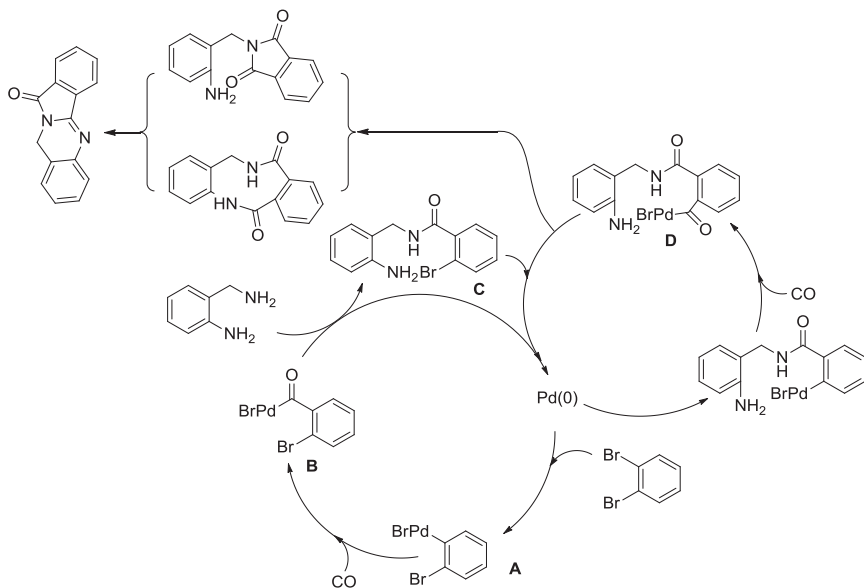
and 2-aminobenzylamines as the substrates (Scheme 14) (2014OBC(12) 5835). It was the first example of carbonylative synthesis of batracylin analogs that with two molecules of carbon monoxide installed. A variety of ligands, bases, and solvents were tested; Pd(OAc)<sub>2</sub>/BuPAD<sub>2</sub> was proven to be the best catalytic system with the NEt<sub>3</sub> as the base in DMAc. Under optimal reaction conditions, moderate to good yields can be obtained for all substrates.

Pd(0) was considered oxidized initially with 1,2-dibromobenzene to give the organopalladium species **A**, followed by the coordination and the CO insertion to afford the acylpalladium complex **B**. Subsequently, it was attacked by 2-aminobenzylamine formed intermediate **C**. After that the *N*-(2-aminobenzyl)-2-bromobenzamide undergoes an oxidative addition with Pd(0) and the installation of CO to provide the intermediate **D**. Certainly, there were two possible pathways to give the final product by an intramolecular condensation (Scheme 15).

Considering the importance of 1,2,4- and 1,3,4-oxadiazole in drug discovery research, few carbonylative approaches to them exist with aryl

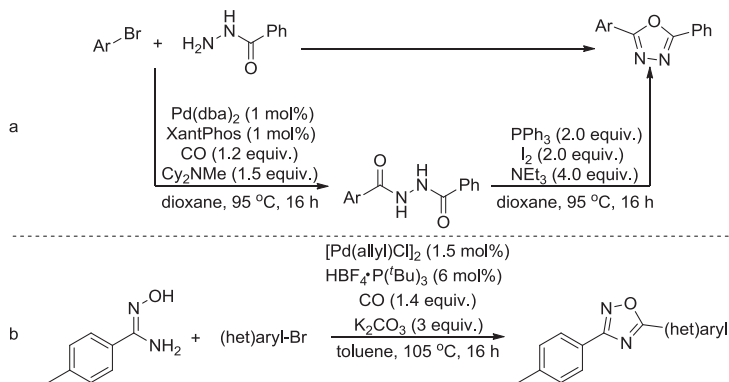


**Scheme 14** Pd-catalyzed synthesis of isoindoloquinazolinones from 1,2-dibromoarenes.



**Scheme 15** The mechanism of Pd-catalyzed synthesis of isoindoloquinazolinones.

iodides or iodonium salts as substrates. Recently, Skrydstrup and coworkers developed a procedure with aryl bromides and hydrazide as the starting materials for the production of 1,2,4- and 1,3,4-oxadiazole (Scheme 16) (2014ASC(356)3074). From the results obtained, a broad scope of substrates with various functional groups were well tolerated with good to excellent yields.

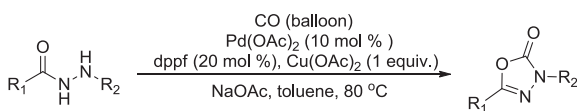


**Scheme 16** Pd-catalyzed synthesis of 1,2,4- and 1,3,4-oxadiazole from aryl and heteroaryl bromides.

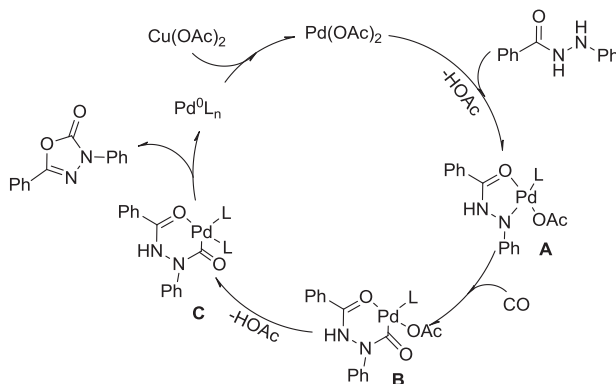
Moreover, a straightforward method to synthesize 1,3,4-oxadiazol-2(3*H*)-one via Pd-catalyzed oxidative cyclocarbonylation of hydrazide was presented by Chen and coworkers (2015CC(51)1905). In this procedure, CO insertion took place between the amine and the carbonyl group, which is different from the previous reports that employed the amino group or the carbonyl group as the sole nucleophile. Various different palladium catalysts, ligands and oxidants were tested, Pd(OAc)<sub>2</sub>/dppf/Cu(OAc)<sub>2</sub>·H<sub>2</sub>O seemed to be the most efficient catalytic system (Scheme 17). In addition, the effect of additives were investigated while only NaOAc could accelerate and improve this reaction (2010JACS(132)686). Subsequently, the range of substrates was extended. Benzoyl 2-phenylhydrazides with electron-withdrawing groups were transformed into the corresponding products in good to excellent yields. However, with hydrazides substituted by electron-donating groups, the reaction turned out to be smooth, but only 46–74% yields of the desired products could be obtained. Moreover, *N*-acetylbenzoylhydrazide and benzoyl hydrazine failed to give the desired products.

The mechanism was considered to involve assistance of the carbonyl group of the starting material, its N–H activated by Pd(OAc)<sub>2</sub> could form the intermediate **A** (2014OL(16)2342). Then the insertion of CO into the N–Pd bond gave intermediate **B** and then release of HOAc to afford **C**. Subsequently, the reductive elimination of **C** provided the desired product and the Pd<sup>(0)</sup> species. Then Pd<sup>(II)</sup> was regenerated in the presence of oxidant for the next catalytic cycle (Scheme 18).

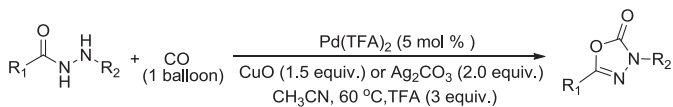
Similarly, Jiang and coworkers employed hydrazides as the starting materials and treated them with CO under the Pd(TFA)/CuO/TFA catalytic system (Scheme 19) (2015JOC(80)5713). A variety of substituted hydrazides were tested and the target products were obtained in moderate to good yields regardless of the nature of their substituents. However, when *N*'-phenylbenzohydrazide was subjected to the standard reaction conditions, only 15% of the corresponding product was obtained. Later, different oxidants were added and only Ag<sub>2</sub>CO<sub>3</sub> was found to be a suitable oxidant while others were inactive. Also, under optimal reaction conditions, various substituents were tolerated and gave the corresponding products in



**Scheme 17** Pd-catalyzed oxidative carbonylation of hydrazides.



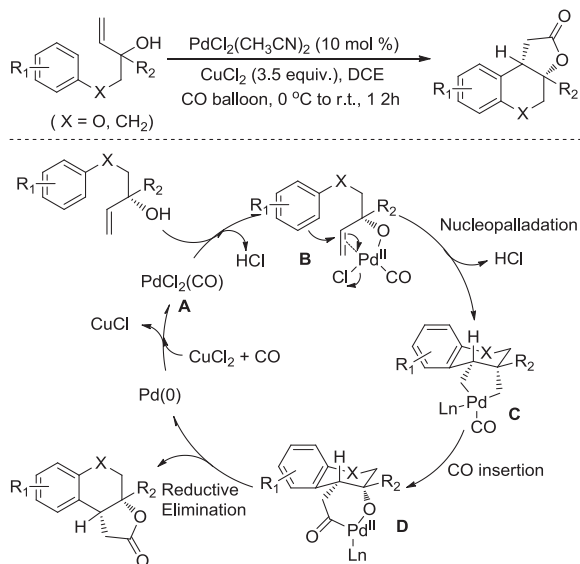
**Scheme 18** Reaction mechanism for Pd-catalyzed oxidative carbonylation of hydrazides.



**Scheme 19** Pd-catalyzed oxidative O–H/N–H carbonylation of hydrazides.

good to excellent yields. It should be noted that all the halide substituents could survive in this reaction which can provide pathways for the further functionalization.

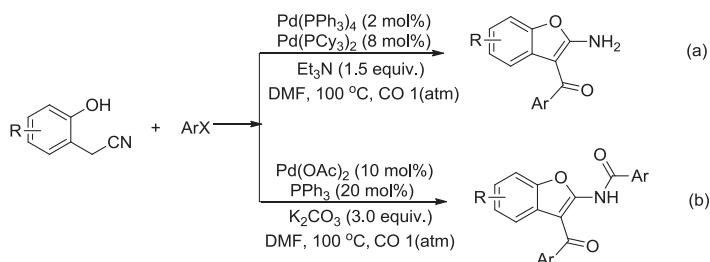
Compared to the transition metal-catalyzed Heck-type carbonylation that the insertion of CO into an aryl–palladium bond followed by the formation of an acylpalladium complex. Subsequently, various nucleophiles are employed to form the corresponding aryl carbonyl compounds (1996JACS(118)5904, 1996JACS(118)5919). Recently, Yang and co-workers considered that the direct Pd-catalyzed carbonylative cyclization of a carbon nucleophile and a carbonyl group across the C=C double bond of an unactivated olefin would be an atom economy efficient way to make functionalized polycyclic aryl derivatives from simple alkenyl arenes (2015OL(17)1240). Meanwhile, encouraged by their previous work on Pd-catalyzed alkoxy carbonylative cyclization reaction (2011AGE(50)7373), nine electron-rich aryl alkenols were prepared and annulated under optimal reaction conditions to synthesize chromane lactones (Scheme 20). The allylic alcohol was considered to react with the palladium carbonyl complex **A** and generated the complex **B** (2013AGE(52)10598), then an intramolecular nucleopalladation of **B** could afford a *cis*-configured palladocyclic



**Scheme 20** Pd-catalyzed carbonylative cyclization of aryl alkenols.

intermediate **C**. Subsequently, the migratory insertion of CO into the alkyl–Pd bond gave the resultant complex **D**, which would undergo reductive elimination to stereoselectively produce lactone and palladium(0). In the presence of CuCl<sub>2</sub>, palladium(0) would be oxidized and give palladium(II) complex **A** for the next catalytic cycle.

In 2015, Ohe and coworkers synthesized 3-acyl-2-aminobenzofurans and 3-acyl-2-(*N*-acylamino)benzofurans from 2-(cyanomethyl)phenol, aryl halides, and carbon monoxide by switching the base, which took place in the presence of Pd and via a three-component coupling (Scheme 21) (2015TH(71)4432). Initially, when the reaction was conducted under

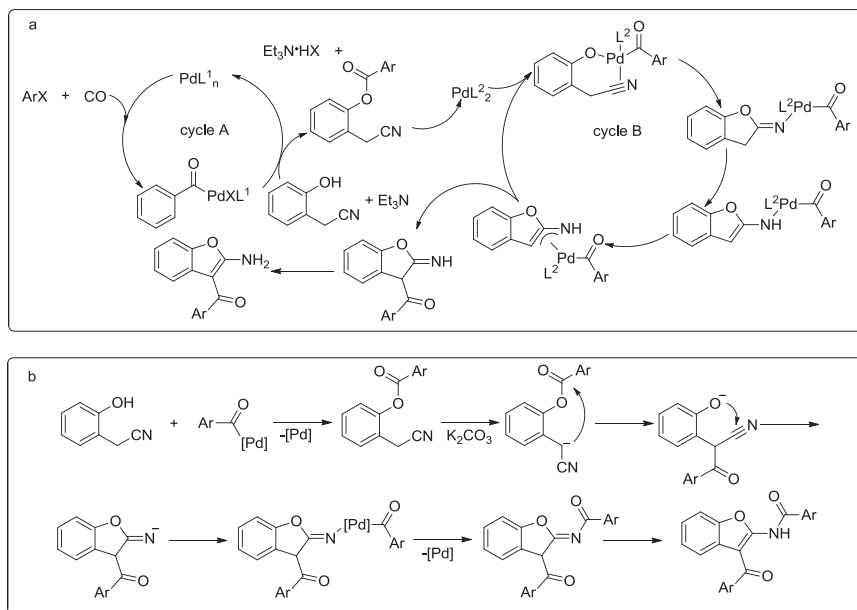


**Scheme 21** Pd-catalyzed three-component coupling reactions to 3-acyl-2-aminobenzofurans and 3-acyl-2-(*N*-acylamino)benzofurans.

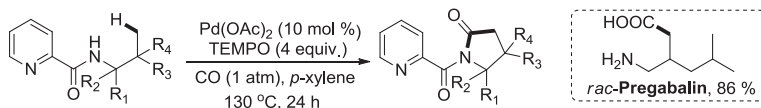
$\text{Pd}(\text{PPh}_3)_4/\text{Pd}(\text{PCy}_3)_2/\text{Et}_3\text{N}$  reaction system with 1 bar of CO in DMF, 3-acyl-2-aminobenzofuran and its derivatives were transformed in moderate to good yields. However, when the reaction was treated with  $\text{K}_2\text{CO}_3$  or  $\text{NaOEt}$  in the presence of  $\text{Pd}(\text{OAc})_2/\text{PPh}_3$ , the corresponding 3-acyl-2-(*N*-acylamino)benzofuran and derivatives can also be obtained in moderate to good yields. Interestingly, under this catalytic system, no 3-acyl-2-aminobenzofurans could be detected, which indicated these two products may be produced in different pathways.

In the control experiments, the 3-acyl-2-aminobenzofuran was treated with excess of 4-bromotoluene under (b) reaction condition. Unfortunately, no desired 2-(*N*-acylamino)benzofuran was found, which indicated that the reaction did not proceed via 3-acyl-2-aminobenzofuran as an intermediate. It was considered that these two different pathways were determined by the different nature of the base. Two corresponding plausible reaction mechanisms were proposed in detail (Scheme 22).

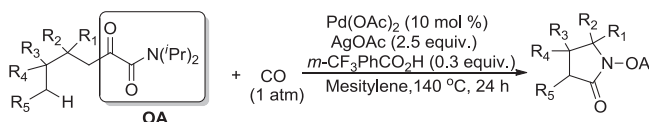
Recently, Wang and coworkers developed a direct carbonylation of alkylamides for synthesizing the  $\gamma$ -lactams and  $\gamma$ -amino acids, via Pd-catalyzed  $\text{C}(\text{sp}^3)\text{-H}$  bond activation under 1 atm of CO with TEMPO as



**Scheme 22** Mechanism of Pd-catalyzed three-component coupling reaction to 3-acyl-2-aminobenzofuran and 3-acyl-2-(*N*-acylamino)benzofuran.



**Scheme 23** Pd-catalyzed C(sp<sup>3</sup>)-H carbonylation of alkylamines.



**Scheme 24** Pd-catalyzed synthesis of pyrrolidones via carbonylation of  $\gamma$ -C(sp<sup>3</sup>)-H bonds of aliphatic amines.

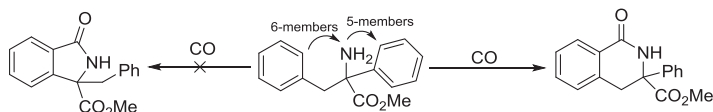
the sole oxidant (Scheme 23) (2015OL(17)3698). In the optimization process, various oxidants such as Cu(II), Ag(I), PhI(OAc)<sub>2</sub>, DDQ, NFSI, CAN, and K<sub>2</sub>S<sub>2</sub>O<sub>8</sub> were tested. Unfortunately, there was no reactivity in the transformation until TEMPO was used as the sole oxidant and gave 38% of the target product. After further optimizations, the scope of *N*-alkylpicolinamide was examined and the corresponding pyrrolidones were isolated in good to excellent yields including a number of chiral substrates. Moreover, it was applied in the total synthesis of *rac*-Pregabalin and an 86% yield was obtained after the deprotection of the corresponding pyrrolidone with 6 N HCl.

In addition, Zhao and coworkers developed a Pd-catalyzed regioselective  $\gamma$ -carbonylation of oxalyl amide-protected aliphatic amines with carbon monoxide to afford pyrrolidones as well (2015CS(6)4610). In this reaction, C–H bonds of both  $\gamma$ -methyl and cyclopropyl methylenes were activated and gave the corresponding products in moderate to excellent yields (Scheme 24). For the 3-(trifluoromethyl)benzoic acid, it was considered to make the palladium intermediate stable during the catalytic cycle. Based on the results obtained, it was shown that the substrates scope could be further extended to oxalyl amide protected benzyl amine and allyl amine derivatives.

### 3. SYNTHESIS OF SIX-MEMBERED HETEROCYCLES

As previously mentioned, Santos and coworkers reported the cyclopalladation of amino esters to benzolactams by Pd-catalyzed carbonylation of *N*-unprotected aryethylamines. It should be noted that there is a strong bias toward six-membered lactams over the five-membered analogs, which was attributed to the greater reactivity of the six-membered palladacycles



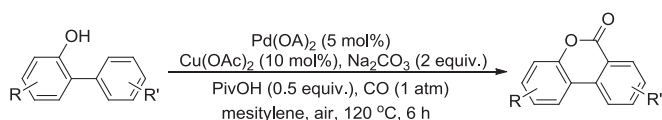


**Scheme 25** Pd-catalyzed cyclopalladation of amino esters to six-membered benzolactams.

which reacted with CO faster (Scheme 25). Under optimal reaction conditions, various phenylethylamines were transformed into the corresponding lactams. From the results obtained, it is obvious that steric hindrance plays a crucial role. Interestingly, in this reaction, the ester group is not necessary for the carbonylation which is different from the case of formation of five-membered ring product.

In 2013, a novel and efficient synthetic route to dibenzopyranones via Pd-catalyzed directed C–H activation/carbonylation of 2-arylphenols in the presence of CO was developed by Shi and collaborators (Scheme 26) (2013AGE(52)10598). It was the first example that employed a phenolic hydroxyl group as a directing group for synthesis of lactones. The challenge of this transformation is considered to be the incompatibility of phenols under the oxidative reaction conditions.

In the presence of Pd(OAc)<sub>2</sub>, various bases, solvents, and additives were tested. Subsequently, with optimal reaction conditions in hand, a variety of 2-arylphenols were converted into the corresponding products in moderate to good yields. The electron-withdrawing and electron-donating groups were tolerated, while the *ortho* position was unfavorable for the transformation of the target product which might be due to steric hindrance. Obviously, from the results obtained, the regioselectivity of this reaction favored the less sterically hindered products. Moreover, the aromatic ring of phenol seemed more sensitive to electronic effects. Generally, phenols bearing electron-donating substituents always gave higher yields than those with electron-withdrawing groups. A series of deuterium labeling experiments was conducted and based on the kinetic results; all these indicated that the C–H activation step might go through an S<sub>E</sub>Ar mechanism rather than the metalation–deprotonation (CMD) process. Moreover, it was

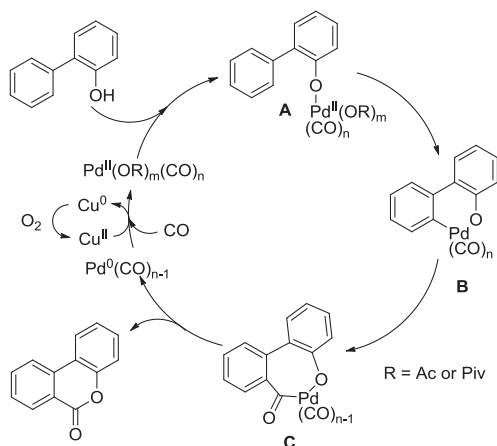


**Scheme 26** Pd-catalyzed directed C–H activation/carbonylation of 2-arylphenols.

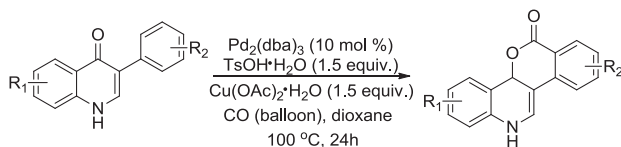
considered that the intermediate **A** was formed by the chelation of the hydroxy group with the CO-ligated palladium(II) complex. Then the C–H activation occurred through the electrophilic cyclopalladation on the non-phenol ring which generated the six-membered palladacycle **B**. The migration of coordinated CO into the aryl–Pd bond forms the seven-membered palladacycle **C**. Subsequently, the reductive elimination of **C** affords the lactone and Pd(0) species, which can be oxidized to the active Pd(II) by Cu(OAc)<sub>2</sub> together with O<sub>2</sub> (Scheme 27).

In addition, Chuang and coworkers also presented a palladium-catalyzed C–H activation and CO insertion into 2-arylphenols process to afford a one-pot synthesis of benzopyranones (2013CC(49)11797). The reaction conditions are milder here and a variety of desired products can be produced in moderate to good yields. Notably, difluoro-substituted arylphenols did not give the corresponding products, which might be due to the instability of the intermediates with electron-withdrawing groups on the ring in the catalytic process.

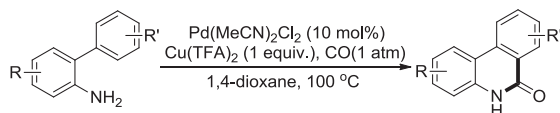
Jiang and coworkers developed a Pd-catalyzed oxidative carbonylation for the synthesis of polycyclic aromatic hydrocarbons, which occurred via a direct and facile Pd-catalyzed C–H bond oxidative carbonylation procedure (Scheme 28) (2014JOC(79)11246). 3-Phenylquinolin-4(1*H*)-one was employed as the substrate, different palladium catalysts, oxidants, and additives were screened with various solvents. Under optimal reaction conditions, the scopes of the substrates were investigated in detail. From the



**Scheme 27** Pd-catalyzed directed C–H activation/carbonylation of 2-arylphenols.



**Scheme 28** Pd-catalyzed carbonylation for the synthesis of polycyclic aromatic hydrocarbons.



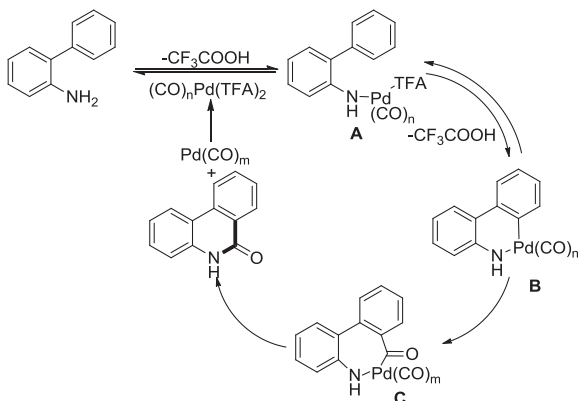
**Scheme 29** Pd-catalyzed aminocarbonylation of *o*-arylanilines to phenanthridinones.

results obtained, good functional group tolerances were exhibited and moderate to excellent yields were obtained.

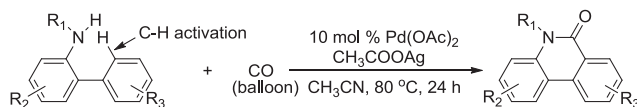
Zhu and coworkers used *o*-arylaniline as the starting material for the synthesis of phenanthridinones under an atmospheric pressure of CO in the presence of Pd(OAc)<sub>2</sub>, which occurred via a Pd-catalyzed C(sp<sup>2</sup>)-H aminocarbonylation procedure (Scheme 29) (2013CC(49)173). Under the Pd(MeCN)<sub>2</sub>Cl<sub>2</sub>/Cu(TFA)<sub>2</sub> catalytic system, with the addition of TFA, a variety of different functional groups on both phenyl rings were investigated in detail. Based on the obtained results, most of them with varied electronic substituents were well tolerated and gave the corresponding products in moderate to good yield. However, *o*-arylanilines with electron-withdrawing groups attached to the nonaniline ring gave higher yields than electron-donating groups, which indicated that there may be an S<sub>E</sub>Ar mechanism involved in C–H bond activation. Also, in this procedure, steric hindrance played an important role; the carbonylation process took place on the less sterically hindered C–H bond.

Finally, a plausible reaction mechanism was presented that the aniline NH<sub>2</sub> with CO-ligated palladium(II) complex formed the intermediate **A** firstly. Subsequently, the electrophilic cyclopalladation on the nonaniline ring resulted in intermediate **B** followed by migratory insertion of coordinated CO into the aryl–Pd bond. Next, the reductive elimination from the seven-membered palladacycle **C** leading to the aminocarbonylation product, regenerated a Pd(0) species, which would be oxidized to the Pd(II) complex by Cu(TFA)<sub>2</sub> in the presence of TFA and CO (Scheme 30).

Similarly, another access to phenanthridinone was reported by Chuang and coworkers (Scheme 31) (2013OL(15)1468). With Pd(OAc)<sub>2</sub> as the



**Scheme 30** Mechanism of Pd-catalyzed aminocarbonylation of *o*-arylanilines.

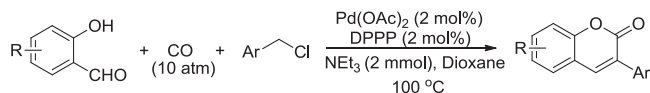


**Scheme 31** Pd-catalyzed carbonylation of *N*-sulfonyl-2-aminobiaryls to phenanthridinones.

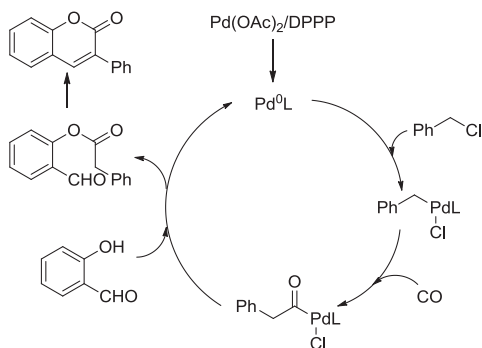
catalyst and 5 equivalents of AgOAc as oxidant in CH<sub>3</sub>CN at 80 °C for 24 h, various substrates were tested and gave the corresponding products in good to excellent yields.

Based on previous work on the synthesis of chromenones, Wu, Beller, and coworkers developed a direct strategy of the carbonylation of salicylic aldehyde and benzyl chlorides to form coumarins. Initially, the salicylic aldehyde and benzyl chloride were found to react under the Pd(OAc)<sub>2</sub>/PPh<sub>3</sub>/NEt<sub>3</sub> catalytic system in DMSO, to form 3-phenyl-2*H*-chromen-2-one in 61% yield (Scheme 32) (2013CEJ(19)12245).

When a variety of ligands, solvents, and other factors were screened, a good yield of the target product was isolated under lower pressure (5 bar) of CO at 100 °C. Good to excellent yields of the corresponding products were formed. For the reaction mechanism, initially Pd<sup>0</sup> was reduced from



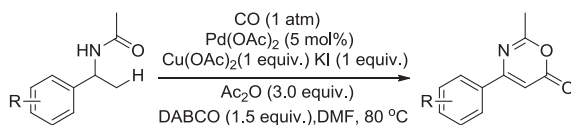
**Scheme 32** Pd-catalyzed carbonylation of salicylic aldehyde and benzyl chlorides to chromenones.



**Scheme 33** Mechanism for Pd-catalyzed carbonylation of salicylic aldehyde and benzyl chloride to chromenone.

$\text{Pd}^{\text{II}}$  by the phosphine ligand. Subsequently, oxidative addition of benzyl chloride to  $\text{Pd}^0$  to give the organopalladium species occurred; the coordination and insertion of CO then generated the acylpalladium complex. After that, elimination occurred after the nucleophilic attack to the salicylic aldehyde on the acylpalladium complex and formed 2-formylphenyl-2-phenylacetate. Finally, the terminal product was generated by intramolecular condensation (Scheme 33).

Pd-catalyzed oxidative carbonylation of the alkenyl C–H bond of enamides to synthesize 1,3-oxazin-6-ones was reported by Guan and co-workers in 2013 (2013AGE(52)14196). Initially, the enamide was reacted with CO and ethanol. However, the 1,3-oxazin-6-one was formed rather than ethoxycarbonylation taking place (Scheme 34). In the presence of the  $\text{Pd}(\text{OAc})_2/\text{Cu}(\text{OAc})_2$  catalytic system, KI seemed a good additive to improve the efficiency. Various bases were investigated and DABCO was found to be the most effective one for this carbonylation reaction. Different solvents were also tested, but DMF still remained the most effective solvent. Hence, with optimal reaction condition in hand, the scope and limitations of this reaction were tested. From the results obtained, this carbonylation reaction displayed high functional group tolerance and gave products in excellent yields.

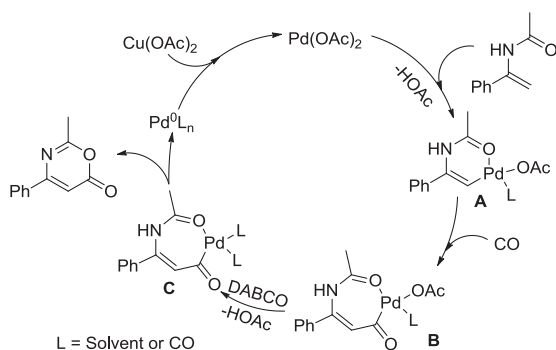


**Scheme 34** Pd-catalyzed carbonylation of alkenyl C–H bond of enamides to 1,3-oxazin-6-ones.

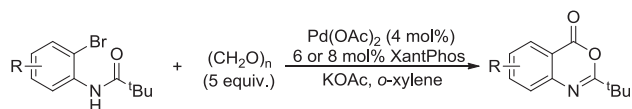
A tentative mechanism was proposed. It was considered that the alkenyl C—H bond was initially activated by Pd(OAc)<sub>2</sub> and formed the vinylpalladium intermediate **A**. Coordination and insertion of CO into **A** afforded acylpalladium intermediate **B**, which with assistance by DABCO, generated **C**. Then the reductive elimination of **C** gave the target product 1,3-oxazin-6-one and Pd<sup>0</sup>. Subsequently, Pd<sup>0</sup> was oxidized by Cu(OAc)<sub>2</sub> and gave Pd(OAc)<sub>2</sub>, which entered the next catalytic cycle (Scheme 35).

In 2014, Wu's group developed a Pd-catalyzed carbonylative synthesis of oxazinones from *N*-(*o*-bromoaryl)amides with paraformaldehyde as the carbonyl source (Scheme 36) (2014JOC(79)10410). Under optimal reaction conditions, various *N*-(*o*-bromoaryl)amides were tested and gave the corresponding products in moderate to good yields. However, it should be noted is that the acyl groups played an important role in the selectivity of the reaction. When R = *t*-butyl instead of methyl, the corresponding product was decreased drastically. Otherwise, a longer alkyl chain gave the target product in much higher yield. Generally, the substrates with electron-withdrawing groups increased the level of debromination and then gave low yields of the desired products.

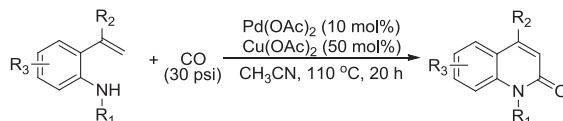
Cyclocarbonylation of 2-vinylanilines by a Pd-catalyzed oxidative process to 2(1*H*)-quinolinones was reported by Alper and coworkers



**Scheme 35** Mechanism of Pd-catalyzed carbonylation of enamides to 1,3-oxazin-6-ones.



**Scheme 36** Pd-catalyzed carbonylation of *N*-(*o*-bromoaryl)amides to benzoxazinones.

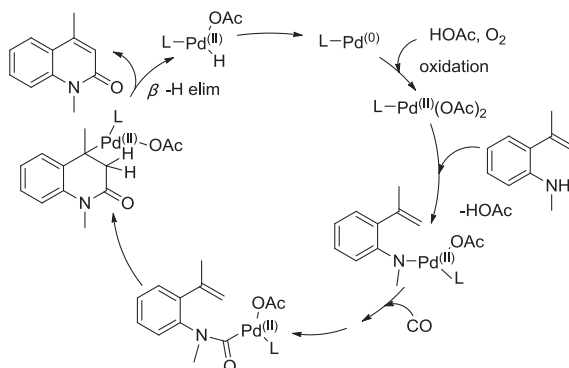


**Scheme 37** Pd-catalyzed oxidative cyclocarbonylation of 2-vinylanilines to 2(1*H*)-quinolinones.

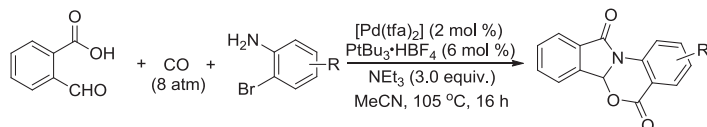
(Scheme 37) (2013OL(15)1998). It turned out to be more attractive from an environmental point of view and operational simplicity. In this report, different ligands, co-oxidants, and bases were tested. The simple combination of Pd(OAc)<sub>2</sub>/Cu(OAc)<sub>2</sub> in CH<sub>3</sub>CN was found to be the best catalytic system. With further optimization, a variety of 2-vinylanilines were tested and the corresponding products could be obtained in good to excellent yields.

Notably, a multinuclear cluster of Cu<sub>m</sub>Pd<sub>n</sub>(OAc)<sub>2(m+n)</sub> with acetate bridges between Cu and Pd was considered (2006ICA(359)2072). Hence, Cu(OAc)<sub>2</sub> could act as both an oxidant and a ligand. Thus, the aniline nitrogen was added to the active Pd<sup>II</sup> species and formed a Pd–N bond with elimination of acetic acid. Then the coordination and insertion of CO generated a Pd-carbamoyl species. Alkene insertion of the vinyl into the Pd–CO bond gave an alkylpalladium intermediate. Subsequently, 2(1*H*)-quinolinone and Pd<sup>(II)</sup> hydride were formed by the β-hydride elimination while the Pd<sup>(II)</sup> hydride species may be reduced to a Pd<sup>0</sup> species through the loss of acetic acid. At the end, Pd<sup>0</sup> was oxidized by Cu<sup>II</sup> or O<sub>2</sub> to Pd<sup>II</sup> and entered the next catalytic cycle (Scheme 38).

In 2014, Wu and collaborators developed a concise and highly versatile method of the synthesis of functionalized isoindolinones via Pd-catalyzed



**Scheme 38** Mechanism of Pd-catalyzed oxidative cyclocarbonylation of 2-vinylanilines.



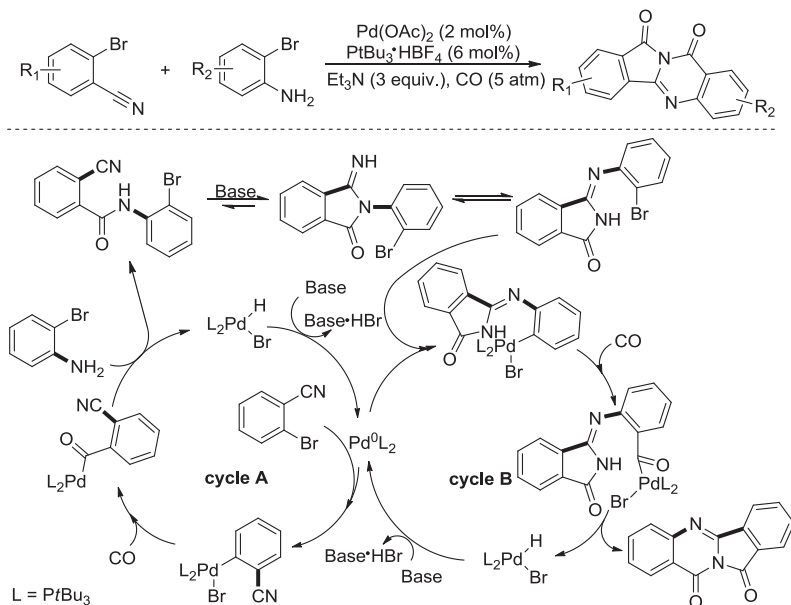
**Scheme 39** Pd-catalyzed carbonylation of 2-bromoanilines with 2-formylbenzoic acid and 2-halobenzaldehydes to isoindolinones.

carbonylation of 2-bromoanilines with 2-formylbenzoic acid or 2-halobenzaldehydes (Scheme 39) (2014CEJ(20)14184). Initially, the target isoindolinones were transformed from corresponding 2-bromoanilines and 2-formylbenzoic acids in a convenient and mild procedure in good to excellent yields. Additionally, 2-halobenzaldehydes were used as substrates under the same conditions and gave identical compounds in moderate to good yields. However, when 2-chloroaniline was treated under optimal reaction conditions, a low yield of the target product was formed while iodo/bromoanilines gave 88% and 86% yields, respectively. In general, 2-bromoanilines with electron-withdrawing substituents gave better yields.

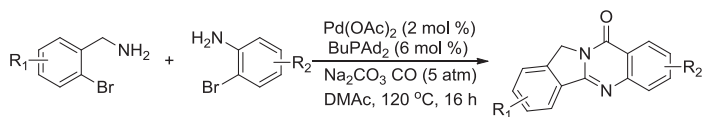
They also developed a Pd-catalyzed carbonylative synthesis of quinazolinone from 2-bromoanilines and 2-bromobenzonitriles (2014CEJ(20)8541). In this reaction, more than five different C–C and/or C–N bonds were selectively formed. The reaction proceeded through sequential carbonylation–cyclization–isomerization–carbonylation steps. Each individual reaction step occurred with high selectivity and excellent yield. The first aminocarbonylation formed amide from 2-bromoaniline and 2-bromobenzonitrile (cycle A). It should be noted that the oxidative insertion of the active palladium species favored 2-bromobenzonitrile due to the higher activity. Then the base-catalyzed isomerization–cyclization gave iminoisoindolinone. Interestingly, it did not undergo another carbonylation reaction but formed the unexpected isomerization product, which was considered for the reason of steric effects. Subsequently, an intramolecular carbonylative coupling gave the target product (Scheme 40).

Another procedure to synthesize tetracyclic heterocycles was also presented by Wu and coworkers, via a Pd-catalyzed dicarbonylation of 2-bromobenzyl amine and 2-bromoaniline with CO in DMAc (Scheme 41) (2015OBC(13)4422). Various bases and solvents were tested in the presence of Pd(OAc)<sub>2</sub>/BuPAD<sub>2</sub>; Na<sub>2</sub>CO<sub>3</sub> gave the best yield. Under optimal reaction conditions, a variety of substituents was tested and gave the corresponding products in good yields. Unfortunately, 2-bromopyridin-3-amine failed to give the corresponding product with 2-bromoaniline. It should be noted





**Scheme 40** Pd-catalyzed double carbonylative synthesis of quinazolinodiones.

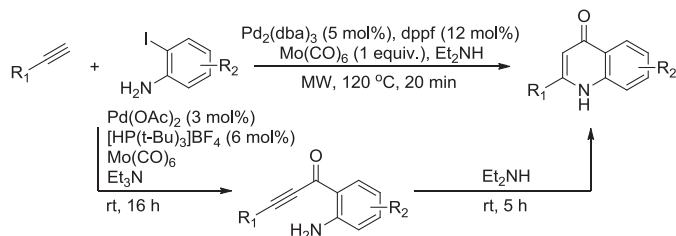


**Scheme 41** Pd-catalyzed dicarbonylative synthesis of tetracyclic quinazolinones.

that when 2-bromobenzylamine reacted with 2-iodoaniline, an excellent yield of the identical product was obtained as well.

Very recently, a carbonylative Sonogashira cross-coupling process that afforded 4-quinolone and its derivatives was reported by Larhed and collaborators. There were two different protocols used to study the reaction of 2-iodoaniline and alkyne under  $\text{CO}$  gas-free conditions (2015JOC(80) 1464). The first one was conducted under microwave heating at  $120^\circ\text{C}$  for 20 min. The second was a gas-free one-pot and two-steps sequence at room temperature (Scheme 42). Both of these methods have a broad scope; corresponding quinolones can be obtained in moderate to good yields from various 2-iodoanilines and alkynes with varying electronic substituents.

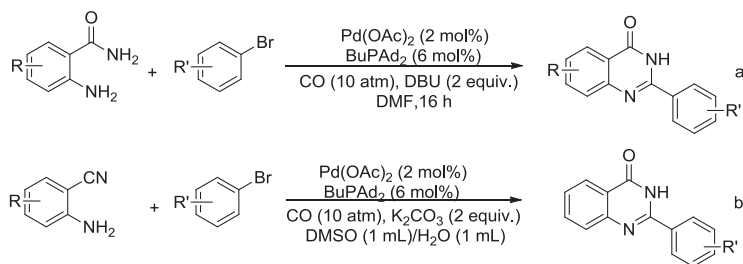
During the past years, Wu and coworkers developed several methods to synthesize quinazolinone and its derivatives via Pd-catalyzed carbonylation. Initially, 2-aminobenzamide and aryl bromides were employed in the



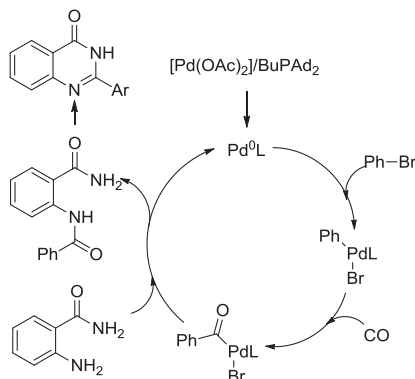
**Scheme 42** Pd-catalyzed carbonylative Sonogashira cross-coupling to 4-quinolones.

presence of  $\text{Pd}(\text{OAc})_2/\text{BuPAD}_2$  with CO in DMF at  $120\text{ }^\circ\text{C}$  (Scheme 43(a)) (2013CEJ(19)12635). Generally, the corresponding quinazolinones were formed in good to excellent yields. However, the yields of corresponding products were decreased dramatically when the aryl bromides had electron-withdrawing substituents. It was similar to a later report for the synthesis of the quinazolinones from 2-aminobenzonitrile and aryl bromide with the addition of  $\text{K}_2\text{CO}_3$  while the solvent used above was replaced by DMSO/ $\text{H}_2\text{O}$  (Scheme 43(b)) (2014GC(16)1336). The addition of the base was considered to assist by promoting the nitrile hydration.

A possible reaction mechanism was also given (Scheme 44). It started with the reduction of  $\text{Pd}^{\text{II}}$  to  $\text{Pd}^0$  and followed by the oxidative addition of bromobenzene to  $\text{Pd}^0$  and generated the organopalladium species. Then the coordination and insertion of CO formed the acylpalladium complex; subsequently, the nucleophilic attack of 2-aminobenzamide on the acylpalladium complex followed by elimination to *N*-(2-carbamoylphenyl) benzamide. Finally, the target product was obtained after the intramolecular condensation.  $\text{Pd}^0$  was regenerated with the assistance of the base and returned to the next catalytic cycle. The 2-aminobenzonitrile can be easily turned into 2-aminobenzamide in the presence of base and water while the intramolecular condensation is responsible for the relatively high temperature.



**Scheme 43** Pd-catalyzed carbonylation of aryl bromides to quinazolinones. (a) From 2-aminobenzamides. (b) From 2-aminobenzonitriles.

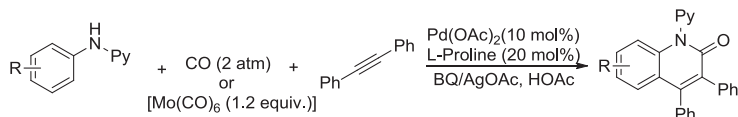


**Scheme 44** Mechanism of Pd-catalyzed carbonylation of aryl bromide to quinazoline.

At the same time, they also presented a Pd-catalyzed carbonylative synthesis of *N*-(2-cyanoaryl)benzamide from 2-aminobenzonitrile and bromobenzene. Later, the intramolecular condensation generated quinazolinones in the presence of water by a sequential process (2014TH(70)23).

Another facile synthesis of quinolinones was presented by Wu and collaborators in 2014, which involves a procedure of Pd-catalyzed carbonylative [3 + 2 + 1] annulation of *N*-arylpyridine-2-amines with internal alkynes by C–H activation (Scheme 45) (2014CEJ(20)14189). In this approach,  $[\text{Mo}(\text{CO})_6]$  was employed as a solid CO source that avoided the particular equipment demand for CO gas and decreased the limitation of the application of the carbonylation reaction. Moreover, the C–H activation was also considered as an atom economic process.

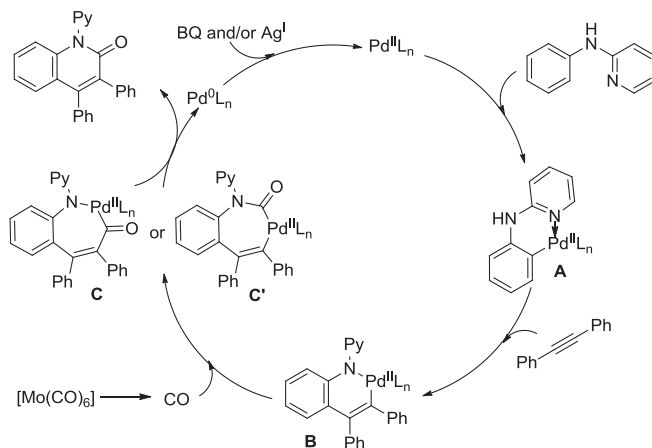
Initially, *N*-phenylpyridine-2-amine was reacted with diphenylacetylene in the presence of  $\text{Pd}(\text{OAc})_2$  and  $[\text{Cu}(\text{tfa})_2] \cdot x\text{H}_2\text{O}$ . With various oxidants and CO sources tested, BQ/AgOAc were considered as the best oxidative combination and  $[\text{Mo}(\text{CO})_6]$  were showed to be more efficient than  $[\text{Co}_2(\text{CO})_8]$  or  $[\text{Fe}_3(\text{CO})_{12}]$ . Different substituents were tested that gave the corresponding products in moderate to good yields. Electron-withdrawing groups, such as fluoro, bromo, acetyl, and trifluoromethyl



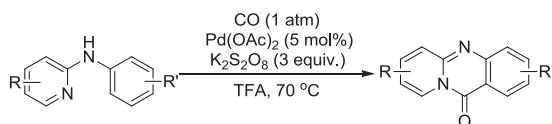
**Scheme 45** Pd-catalyzed carbonylation of *N*-arylpyridine-2-amines with internal alkynes to 2-quinolinones.

were tolerated well. In addition, the kinetic isotope effect experiment indicated that the C–H activation step was reversible and might not be the rate-determining step. Hence, initially the coordination of Pd<sup>II</sup> with pyridine followed by C–H activation formed the intermediate **A**. The insertion of alkyne to **A** generated intermediate **B** and then the insertion of CO released from [Mo(CO)<sub>6</sub>] to **B** generated intermediate **C** or **C'**. Finally, the reductive elimination of **C** or **C'** gave the target product and Pd<sup>0</sup>, which was re-oxidized by BQ and/or AgOAc to Pd<sup>II</sup> and closed the catalytic cycle (Scheme 46).

Apart from these, Zhu and coworkers disclosed an efficient method to synthesize 11*H*-pyrido[2,1-*b*]quinazolin-11-one via Pd-catalyzed C(sp<sup>2</sup>)-H carbonylation of *N*-phenylpyridine-2-amines (Scheme 47) (2014OL(16)2748). In this report the difference is the pyridyl group which acted as an intramolecular nucleophile and also a coordinating group. Under optimal reaction conditions, various functional groups with varied electronic properties were well tolerated and gave the corresponding products in



**Scheme 46** Pd-catalyzed carbonylation of *N*-arylpyridine-2-amine with internal alkyne to 2-quinolinone.

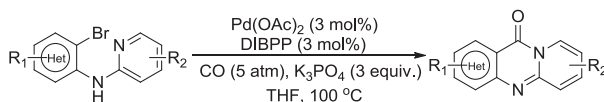


**Scheme 47** Pd-catalyzed carbonylation of *N*-phenylpyridine-2-amine to 11*H*-pyrido[2,1-*b*]quinazolin-11-one.

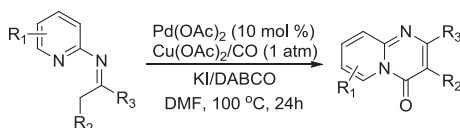
moderate to good yields. Generally, when the substrates are in the *ortho* position, it is usually unfavorable, owing to steric hindrance. For the *m*-substituted *N*-phenylpyridine-2-amine, the regioselectivity between the two C–H bonds was based on the size of the substituent.

Recently, Alper's group reported the synthesis of pyrido[2,1-*b*]quinazolin-11-ones and dipyrido[1,2-*a*:2',3'-*d*]pyrimidin-5-ones by Pd/DIBPP-catalyzed dearomatizing carbonylation of *N*-(2-bromophenyl)pyridine-2-amines (Scheme 48) (2015OL(17)1569). Under optimal reaction conditions, pyrido[2,1-*b*]quinazolin-11-one and its derivatives were transformed in nearly quantitative yields. However, from the results obtained, it was found that when there was an electron-withdrawing group on the pyridyl moiety, the corresponding product was given smoothly. Additionally, the desired dipyrido[1,2-*a*:2',3'-*d*]pyrimidin-5-ones were also obtained in up to 84% yield.

At the same year, Zeng and coworkers reported a novel Pd-catalyzed pyridine-directed carbonylation for rapid assembly of pyrido[1,2-*a*]pyrimidin-4-ones (PPO) (Scheme 49) (2015CC(51)9377). A variety of bases, Pd catalysts, and oxidants were screened. It should be noted that when the reaction was conducted in the absence of KI, the yield of desired product was decreased significantly. Both electron-withdrawing and electron-donating groups were tolerated in this catalytic system and gave the corresponding products in moderate to excellent yields. However, *meta*- and *ortho*-substituted benzene rings afforded lower yields, which was considered to be due to the steric hindrance around the ketoimine (1997JMCAC(122)103). Considering the pyridine ring, electron-rich ketoimines gave higher yields than electron-deficient groups. Unfortunately, under these conditions, bromine-containing substrates were sensitive and removed.



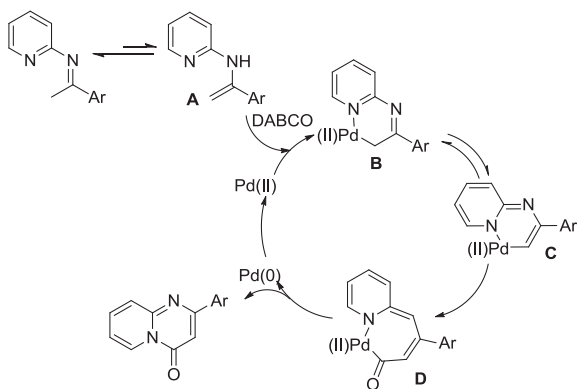
**Scheme 48** Pd/DIBPP-catalyzed carbonylation of *N*-(2-bromophenyl)pyridine-2-amines.



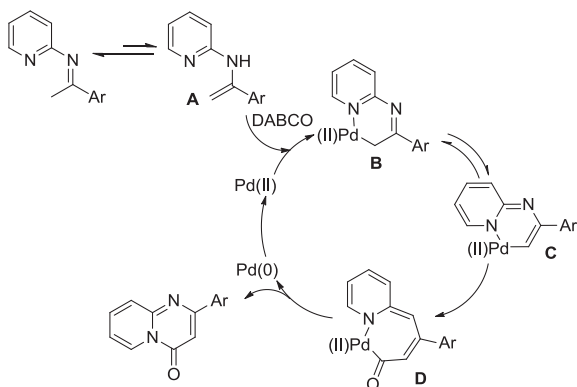
**Scheme 49** Pd-catalyzed carbonylative cycloamidation of ketoimines.

Finally, based on several controlled experiments, a Pd(II)/Pd(0) redox process was found. Firstly, the enamine **A** derived from imine–enamine isomerization can be electrophilically attacked by Pd(II) to generate a palladacycle intermediate **B**, which could be isomerized to form a palladacycle intermediate **C**. Then, the coordination and the migration of CO into the N–Pd bond afforded a seven-membered palladacycle **D**. Subsequently, the reductive elimination of **D** gave the target product and the Pd(0) species which can be oxidized to Pd(II) species by Cu(II) and enter the next catalytic recycle (Scheme 50).

Wu and coworkers reported a base-controlled synthesis of linear and angular fused quinazolinones via Pd-catalyzed carbonylation and a nucleophilic substitution process (Scheme 51) (2014AGE(53)7579).



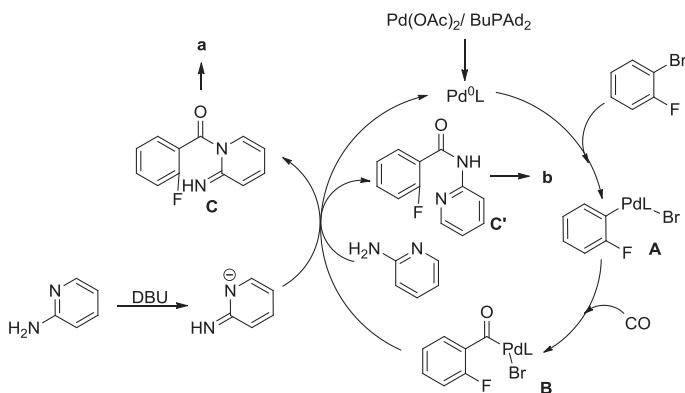
**Scheme 50** Pd-catalyzed carbonylative cycloamidation of ketoimines.



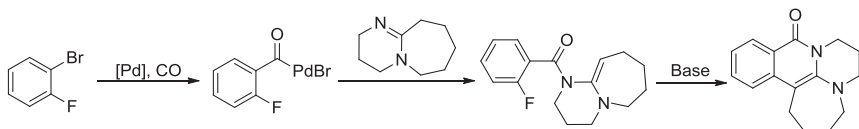
**Scheme 51** Pd-catalyzed carbonylation of 2-aminopyridine and 2-fluorobromobenzene to quinazolinone.

As described in the proposed mechanism, the base served as a key modulator, whereas DBU gave rise to the linear isomers and  $\text{Et}_3\text{N}$  afforded the angular products. The reaction starts with the reduction of  $\text{Pd}^{\text{II}}$  to  $\text{Pd}^0$ . Then, the oxidative addition of 2-fluorobromobenzene to  $\text{Pd}^0$  led to the corresponding organopalladium species **A**. The coordination and insertion of CO generated the intermediate palladium complex **B**. In the presence of DBU, 2-imino-2*H*-pyridin-1-ide attacked the acylpalladium complex with the elimination gave **C**. Similar to the  $\text{NEt}_3$ , the nucleophilic reaction gave **C'**. At the end, intramolecular nucleophilic substitution of intermediate **C** and **C'** afforded the linear and angular products, respectively. The  $\text{Pd}^0$  catalyst was regenerated with the assistance of the base as well and entered the next catalytic cycle (Scheme 52). All the target products were produced in moderate to good yields and various functional groups were well tolerated.

Meanwhile, they found that when the DBU was used as the base, an unexpected product isoquinolinone was formed too (2014CEJ(20)16107). In this case, DBU acted as both reagent and base. Firstly, the nucleophilic attack of the less hindered nitrogen atom of DBU to the acylpalladium complex and rearrangement of the  $\text{C}=\text{N}$  bond to a  $\text{C}=\text{C}$  bond, and then nucleophilic substitution of  $\text{C}-\text{F}$  with  $\text{RHC}=\text{C}$  to give the product (Scheme 53). Under optimal reaction condition, 68% of it was isolated and its derivatives were transformed in moderate to good yields. At the same time, they extended this concept to synthesize quinazolinones that 2-fluorobromobenzene reacted with amidines under the Pd-catalytic system.



**Scheme 52** Mechanism of Pd-catalyzed carbonylation to linear and angular fused quinazolinones.

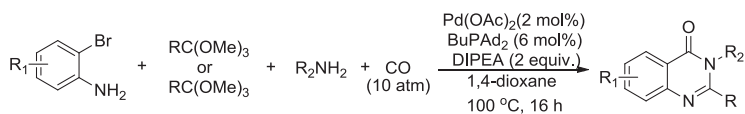


**Scheme 53** Mechanism of Pd-catalyzed carbonylation of 2-fluorobromobenzene with DBU.

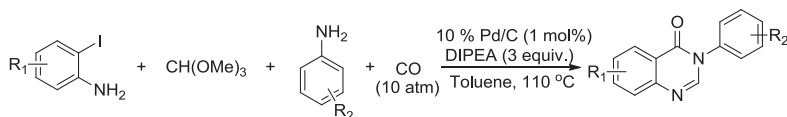
Moderate to excellent yields of the corresponding quinazolinones were formed with high selectivity and various functional groups were tolerated.

Another convenient method to quinazolinones was also presented by Wu and coworkers. With 2-bromoaniline, aniline, CO, and triethyl orthoformate as the substrates in the presence of Pd(OAc)<sub>2</sub>/BuPAd<sub>2</sub> at 120 °C for 16 h, desired products were formed with high selectivity (Scheme 54) (2014AGE(53)1420). Both anilines and 2-bromoanilines with electron-withdrawing and electron-donating groups were well tolerated and gave the corresponding products in good to excellent yields.

Under a heterogeneous catalytic system, Wu and collaborators reported another four-component carbonylative reaction in which various amines, 2-iodoanilines, trimethylorthoformate and CO in the presence of Pd/C as an efficient catalytic system gave quinazolinone and its derivatives (Scheme 55) (2015CST(5)4474). When 2-bromoaniline was applied as the substrate, unfortunately, there was no corresponding product transformed. Both electron-withdrawing and electron-donating groups were tolerated, and gave the corresponding quinazolinones in excellent yields. It should be noted is that this heterogeneous catalyst can be recycled efficiently for four consecutive cycles, which was considered as a relatively mild,



**Scheme 54** Pd-catalyzed carbonylative coupling of 2-bromoaniline with trimethylorthoformate, aniline, and CO.



**Scheme 55** Pd-catalyzed carbonylative coupling of 2-iodoaniline with trimethylorthoformate, aniline, and CO.

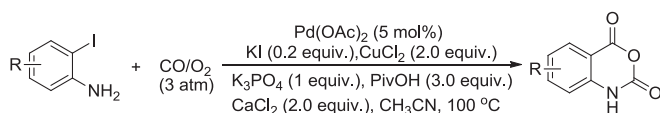


operationally simple, phosphine-free and recyclable catalytic system for the carbonylative synthesis of quinazolinones.

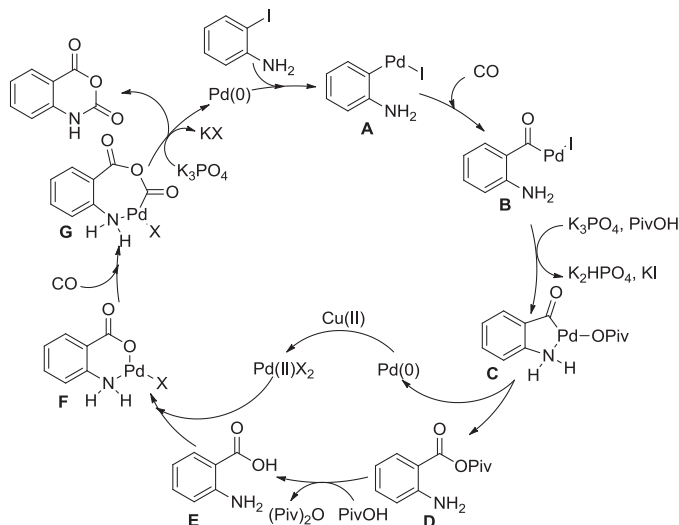
The double carbonylation of *o*-iodoanilines for direct synthesis of isatoic anhydrides was presented by Guan and coworkers, which was considered as a class of valuable chemicals and versatile blocks (Scheme 56) (2014JOC(79) 4196). In the presence of Pd(OAc)<sub>2</sub>, various oxidants, bases, and additives were tested. As a result, Pd(OAc)<sub>2</sub>/CuCl<sub>2</sub> was considered as an efficient catalytic system with K<sub>3</sub>PO<sub>4</sub> as the base in CH<sub>3</sub>CN. Moreover, the addition of the combination of KI/CaCl<sub>2</sub>/PivOH increased the effect drastically. Subsequently, a series of *o*-iodoanilines were investigated and high functional groups were well tolerated with moderate to good yields. However, electron-withdrawing group substituted *o*-iodoanilines were less active and gave low yields compared to electron-donating group.

Isatoic anhydride was formed in nearly quantitative yield. Hence, a tentative reaction mechanism was proposed. Firstly, the oxidative addition of *o*-iodoaniline to Pd(0) followed by insertion of CO gave intermediate **B**. In the presence of K<sub>3</sub>PO<sub>4</sub> and PivOH, it was transformed into intermediate **C**. The reductive elimination of **C** generated Pd(0) species and intermediate **D**. Then the reaction of **D** with PivOH provided anthranilic acid **E** by the expulsion of (Piv)<sub>2</sub>O. Meanwhile, Pd(0) was oxidized by Cu(II) to generate Pd(II)X<sub>2</sub>. After that, the reaction of Pd(II)X<sub>2</sub> and **E** gave the intermediate **F**, which with CO insertion afforded intermediate **G**. Finally, in the presence of K<sub>3</sub>PO<sub>4</sub>, the reductive elimination of **G** gave the desired product and the Pd(0) species (Scheme 57).

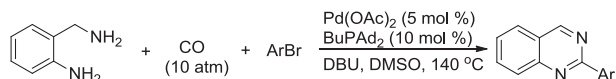
As previously mentioned, Wu and coworkers developed a Pd-catalyzed synthesis of isoindoloquinazolinones by dicarbonylation of 1,2-dibromoarenes with 2-aminobenzylamines. Various quinazolines were obtained when 2-aminobenzylamines and bromobenzene were used under the Pd(OAc)<sub>2</sub>/BuPAD<sub>2</sub> catalytic system (Scheme 58). With a variety of bases and solvents tested, DBU seemed to be more efficient among all the bases and DMSO as solvent gave the best result. DMSO also acted as an oxidant in this catalytic system. Subsequently, different substituents were tested; most of them were well tolerated and gave products in moderate to good



**Scheme 56** Pd-catalyzed carbonylation of *o*-iodoanilines to isatoic anhydrides.



**Scheme 57** Mechanism of Pd-catalyzed carbonylation of *o*-iodoanilines to isatoic anhydrides.

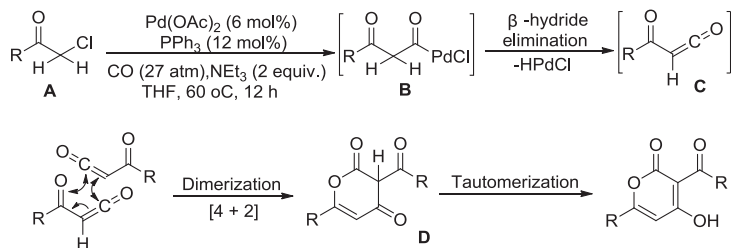


**Scheme 58** Pd-catalyzed carbonylative synthesis of quinazolines from 2-aminobenzylamine and aryl bromides.

yields. Unfortunately, it was unfavorable for multifluoro-substituted bromobenzene and more sterically hindered substrates.

Recently, Troisi and coworkers reported a Pd-catalyzed carbonylation of  $\alpha$ -chloroketones to synthesize 3-acyl-4-hydroxy-2-pyranone and its derivatives (2015THL(56)2773). From the results obtained, it was found that the methodology can be applied to a variety of aromatic and aliphatic substrates. For the mechanism, it was considered that the first step should be the carbonylation of the  $\alpha$ -chloroketones to form a dicarbonylpalladium intermediate **B**. Obviously, **B** has a couple of hydrogens in the  $\beta$ -position with respect to the palladium atom. Therefore, it should spontaneously lead to the acylketene **C** through  $\alpha$ ,  $\beta$ -hydride elimination, and subsequently, a [4 + 2] cycloaddition of **C** leading to the heterocycle **D** followed by tautomerization to give a 2-pyranone (Scheme 59).

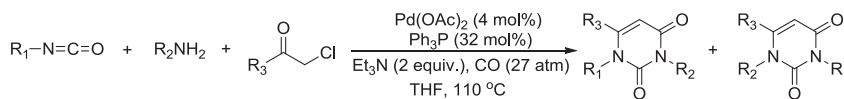
Later, Troisi and coworkers reported a multicomponent synthesis of uracil analogs by Pd-catalyzed carbonylation of  $\alpha$ -chloroketones in the



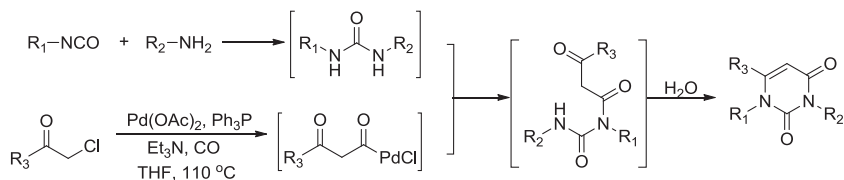
**Scheme 59** Pd-catalyzed carbonylation of  $\alpha$ -chloroketones to 3-acyl-4-hydroxy-2-pyranone.

presence of isocyanates and amines (Scheme 60) (2015JOC(80)8189). Under optimal reaction conditions, various aliphatic groups and aromatic functional groups substituted  $\alpha$ -chloroketones, isocyanates, and amines were tested, and moderate to excellent yields of corresponding products were generated. Moreover, functional groups like hydroxyl were also well tolerated in this reaction. It is noteworthy that the carbonylative coupling occurred smoothly with both a bulky aliphatic group and aromatic ring on the  $\alpha$ -chloroketones.

It was hypothesized that the unsymmetrical urea formed in situ from  $\alpha$ -chloroketone and amine. Due to the differences in nucleophilicity, the acylation only occurred at alkyl-substituted nitrogen reacted with the Pd complex gave the intermediate. Subsequently, intramolecular nucleophilic attack of the aryl-substituted nitrogen followed by the elimination of water and gave the product (Scheme 61).



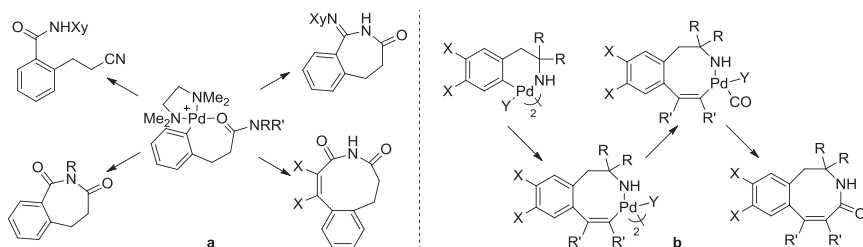
**Scheme 60** Pd-catalyzed multicomponent synthesis of uracil analogs.



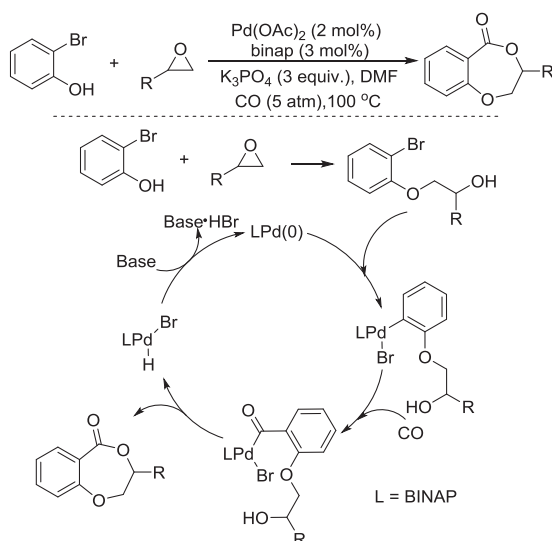
**Scheme 61** Mechanism of Pd-catalyzed carbonylation of  $\alpha$ -chloroketones with isocyanates and amines.

## 4. SYNTHESIS OF OTHER HETEROCYCLES

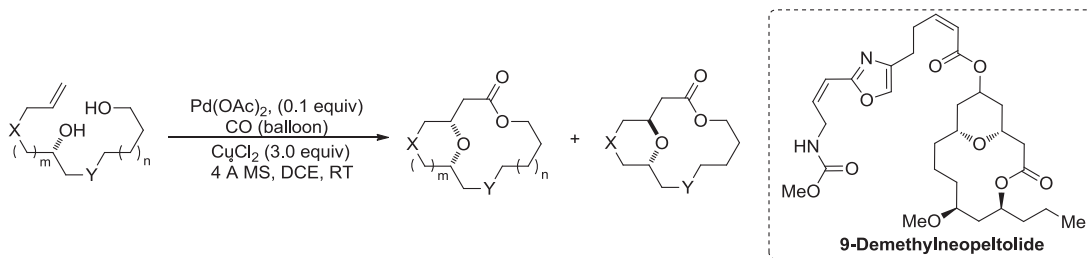
Seven-, eight- or more than nine-membered heterocycles were also obtained excellently by Pd-catalyzed carbonylation. In 2013, Vicente et al. synthesized different Pd complexes to synthesize seven- and nine-membered palladacycles, and benzazepine- and benzazonine-based heterocycles (Scheme 62(a)) (2013OM(32)1892). Also, they developed a palladium organocarbonyl intermediate to synthesize eight-membered lactams with alkyne/CO sequential insertion (Scheme 62(b)) (2013OM(32)1094). All of these have attracted increasing interest for their pharmacological properties.



**Scheme 62** Pd complex mediate in the synthesis of heterocycles. (a) 7-membered palladacycle. (b) 8-membered palladacycle.



**Scheme 63** Pd-catalyzed carbonylative synthesis of 2,3-dihydrobenzodioxepinones.



**Scheme 64** Pd-catalyzed alkoxy carbonylative macrolactonization.

In 2014, Beller, Wu, and coworkers developed a Pd-catalyzed carbonylative synthesis of 2,3-dihydrobenzodioxepinones from epoxides and 2-bromophenols. The epoxide underwent nucleophilic ring-opening and subsequent Pd-catalyzed intramolecular alkoxycarbonylation (Scheme 63) (2014CC(50)2114). Under optimal reaction conditions, different epoxides and various 2-bromophenols were tested and highly regioselective products were formed in good to excellent yields.

A Pd-catalyzed cascade alkoxycarbonylative macrolactonization from alkenediols to tetrahydropyran/tetrahydrofuran-containing macrolactones bridge in one step was presented by Dai and collaborators (Scheme 64) (2014AGE(126)6637). Various ring sizes of the corresponding products were obtained in moderate to good yields. Subsequently, it was applied to the synthesis of the potent anticancer compound 9-demethylneopeltolide which was obtained in 56% yield in three steps. It should be noted that tertiary alcohols were also well tolerated and the corresponding tertiary macrolactones were produced in good yields with diastereoselectivity.

In summary, there are numerous of elegant works on the Pd-catalyzed carbonylative synthesis of heterocycles that have been developed. Based on the existing reviews, the main achievements from 2013 to the middle of 2015 have been summarized and discussed here.

## REFERENCES

- 1995JACS(117)3422 C. Coperet, T. Sugihara, G.Z. Wu, I. Shimoyama, and E. Negishi, *J. Am. Chem. Soc.*, **117**, 3422–3431 (1995).
- 1996JACS(118)5904 E. Negishi, C. Copéret, S.M. Ma, T. Mita, T. Sugihara, and J.M. Tour, *J. Am. Chem. Soc.*, **118**, 5904–5918 (1996).
- 1996JACS(118)5919 E. Negishi, S.M. Ma, J. Amanfu, C. Copéret, J.A. Miller, and J.M. Tour, *J. Am. Chem. Soc.*, **118**, 5919–5931 (1996).
- 1997JMCAC(122)103 S.A.R. Mulla, C.V. Rode, A.A. Kelkar, and S.P. Gupte, *J. Mol. Catal. A Chem.*, **122**, 103–109 (1997).
- 2002AGE(41)4176 A.F. Littke and G.C. Fu, *Angew. Chem. Int. Ed.*, **41**, 4176–4211 (2002).
- 2004ASC(346)1661 G. Altenhoff and F. Glorius, *Adv. Synth. Catal.*, **346**, 1661–1664 (2004).
- 2006ICA(359)2072 N.Y. Kozitsyna, S.E. Nefedov, F.M. Dolgushin, N.Y. Cherkashina, M.N. Vargaftik, and I.I. Moiseev, *Inorg. Chim. Acta.*, **359**, 2072–2086 (2006).
- 2006JOC(71)2532 C. Yi and R. Hua, *J. Org. Chem.*, **71**, 2532–2537 (2006).
- 2007ASC(349)1738 C. Yi, R. Hua, H. Zeng, and Q. Huang, *Adv. Synth. Catal.*, **349**, 1738–1742 (2007).
- 2008TH(64)2930 S.R. Yanga, H.F. Jiang, Y.Q. Li, H.J. Chen, W. Luo, and Y.B. Xua, *Tetrahedron*, **64**, 2930–2937 (2008).

- 2010JACS(132)686 R. Giri, J.K. Lam, and J.Q. Yu, *J. Am. Chem. Soc.*, **132**, 686–693 (2010).
- 2011AGE(50)7373 Q. Xiao, W.W. Ren, Z.X. Chen, T.W. Sun, Y. Li, Q.D. Ye, J.X. Gong, F.K. Meng, L. You, Y.F. Liu, M.Z. Zhao, L.M. Xu, Z.H. Shan, Y. Shi, Y.F. Tang, J.H. Chen, and Z. Yang, *Angew. Chem. Int. Ed.*, **50**, 7373–7377 (2011).
- 2012SN(23)685 L.R. Odell, F. Russo, and M. Larhed, *Synlett*, **23**, 685–698 (2012).
- 2013ASC(355)3581 X.-F. Wu, S. Oschatz, M. Sharif, A. Flader, L. Krey, M. Beller, and P. Langer, *Adv. Synth. Catal.*, **355**, 3581–3585 (2013).
- 2013AGE(52)10598 S. Luo, F.X. Luo, X.S. Zhang, and Z.J. Shi, *Angew. Chem. Int. Ed.*, **52**, 10598–10601 (2013).
- 2013AGE(52)14196 M. Chen, Z.H. Ren, Y.Y. Wang, and Z.H. Guang, *Angew. Chem. Int. Ed.*, **52**, 14196–14199 (2013).
- 2013CR(113)1 X.-F. Wu, H. Neumann, and M. Beller, *Chem. Rev.*, **113**, 1–35 (2013).
- 2013CC(49)173 D.D. Liang, Z.W. Hu, J.L. Peng, J.B. Huang, and Q. Zhu, *Chem. Commun.*, **49**, 173–175 (2013).
- 2013CC(49)11797 T.H. Lee, J. Jayakumar, C.H. Cheng, and S.C. Chuang, *Chem. Commun.*, **49**, 11797–11799 (2013).
- 2013CEJ(19)12245 X.F. Wu, L.P. Wu, R. Jackstell, H. Neumann, and M. Beller, *Chem. Eur. J.*, **19**, 12245–12248 (2013).
- 2013CEJ(19)12635 X.F. Wu, L. He, H. Neumann, and M. Beller, *Chem. Eur. J.*, **19**, 12635–12638 (2013).
- 2013OM(32)649 J. Albert, X. Ariza, T. Calvet, M. Font-Bardia, J. Garcia, J. Granell, A. Lamela, B. López, M. Martínez, L. Ortega, A. Rodríguez, and D. Santos, *Organometallics*, **32**, 649–659 (2013).
- 2013OM(32)1094 J. García-López, M. Oliva-Madrid, I. Saura-Llamas, D. Bautista, and J. Vicente, *Organometallics*, **32**, 1094–1105 (2013).
- 2013OL(15)1468 V. Rajeshkumar, T.H. Lee, and S.C. Chuang, *Org. Lett.*, **15**, 1468–1471 (2013).
- 2013OM(32)1892 R. Frutos-Pedreño, P. González-Herrero, and J. Vicente, *Organometallics*, **32**, 1892–1904 (2013).
- 2013OL(15)1998 J. Ferguson, F.L. Zeng, N. Alwis, and H. Alper, *Org. Lett.*, **15**, 1998–2001 (2013).
- 2013OL(15)3678 W. Fang, Q. Deng, M. Xu, and T. Tu, *Org. Lett.*, **15**, 3678–3681 (2013).
- 2013THL(54)3040 X.-F. Wu, H. Neumann, S. Neumann, and M. Beller, *Tetrahedron Lett.*, **54**, 3040–3042 (2013).
- 2013THL(54)5159 J. Ju, C.M. Qi, L.Y. Zheng, and R.M. Hua, *Tetrahedron Lett.*, **54**, 5159–5161 (2013).
- 2014AGE(53)1420 L. He, H.Q. Li, H. Neumann, M. Beller, and X.F. Wu, *Angew. Chem. Int. Ed.*, **53**, 1420–1424 (2014).
- 2014ASC(356)3074 T.L. Andersen, W. Caneschi, A. Ayoub, A.T. Lindhardt, M.R.C. Couri, and T. Skrydstrup, *Adv. Synth. Catal.*, **356**, 3074–3082 (2014).
- 2014AGE(126)6637 Y. Bai, D.C. Davis, and M.J. Dai, *Angew. Chem. Int. Ed.*, **126**, 6637–6640 (2014).
- 2014AGE(53)7579 J.B. Chen, K. Natta, A. Spannenberg, H. Neumann, P. Langer, M. Beller, and X.F. Wu, *Angew. Chem. Int. Ed.*, **53**, 7579–7583 (2014).
- 2014CC(50)1381 J.X. Li, S.R. Yang, W.Q. Wu, and H.F. Jiang, *Chem. Commun.*, **50**, 1381–1383 (2014).

- 2014CC(50)2114 H.Q. Li, A. Spannenberg, H. Neumann, M. Beller, and X.F. Wu, *Chem. Commun.*, **50**, 2114–2116 (2014).
- 2014CEJ(20)8541 H.Q. Li, W.F. Li, A. Spannenberg, W. Baumann, H. Neumann, M. Beller, and X.F. Wu, *Chem. Eur. J.*, **20**, 8541–8544 (2014).
- 2014CEJ(20)14184 K. Natte, J.B. Chen, H.Q. Li, H. Neumann, M. Beller, and X.F. Wu, *Chem. Eur. J.*, **20**, 14184–14188 (2014).
- 2014CEJ(20)14189 J.B. Chen, K. Natte, A. Spannenberg, H. Neumann, M. Beller, and X.F. Wu, *Chem. Eur. J.*, **20**, 14189–14193 (2014).
- 2014CEJ(20)16107 J.B. Chen, K. Natte, H. Neumann, and X.F. Wu, *Chem. Eur. J.*, **20**, 16107–16110 (2014).
- 2014EJOC616 X.H. Yang, K. Li, R.J. Song, and J.H. Li, *Eur. J. Org. Chem.*, 616–623 (2014).
- 2014GC(16)1336 H.Q. Li, L. He, H. Neumann, M. Beller, and X.F. Wu, *Green. Chem.*, **16**, 1336–1343 (2014).
- 2014JOC(79)4196 S. Gao, M. Chen, M.N. Zhao, Z.H. Ren, Y.Y. Wang, and Z.H. Guan, *J. Org. Chem.*, **79**, 4196–4200 (2014).
- 2014JOC(79)10410 W.F. Li and X.F. Wu, *J. Org. Chem.*, **79**, 10410–10416 (2014).
- 2014JOC(79)11246 F.H. Ji, X.W. Li, W.Q. Wu, and H.F. Jiang, *J. Org. Chem.*, **79**, 11246–11253 (2014).
- 2014OCF(1)1261 S.L. Liu, Q.Y. Deng, W.W. Fang, J.F. Gong, M.P. Song, M.Z. Xu, and T. Tao, *Org. Chem. Front.*, **1**, 1261–1265 (2014).
- 2014OL(16)2342 T. Fang, Q.T. Tan, Z.W. Ding, B.X. Liu, and B. Xu, *Org. Lett.*, **16**, 2342–2345 (2014).
- 2014OL(16)2748 D.D. Liang, Y.M. He, and Q. Zhu, *Org. Lett.*, **16**, 2748–2751 (2014).
- 2014OBC(12)5835 J. Chen, H. Neumann, M. Beller, and X.F. Wu, *Org. Biomol. Chem.*, **12**, 5835–5838 (2014).
- 2014TH(70)23 X.F. Wu, S. Oschatz, M. Sharif, M. Beller, and P. Langer, *Tetrahedron*, **70**, 23–29 (2014).
- 2015CC(51)1905 Y. Wang, X. Meng, Y.T. Yang, L.T. Zhang, S.B. Guo, D. Tang, Y.X. Li, and B.H. Chen, *Chem. Commun.*, **51**, 1905–1907 (2015).
- 2015CST(5)4474 K. Natte, H. Neumann, and X.F. Wu, *Catal. Sci. Technol.*, **5**, 4474–4480 (2015).
- 2015CS(6)4610 C. Wang, L. Zhang, C.P. Chen, J. Han, Y.M. Yao, and Y.S. Zhao, *Chem. Sci.*, **6**, 4610–4614 (2015).
- 2015CC(51)9377 Y. Xie, T.F. Chen, S.M. Fu, H.F. Jiang, and W. Zeng, *Chem. Commun.*, **51**, 9377–9380 (2015).
- 2015JOC(80)1464 L. Åkerbladh, P. Nordeman, M. Wejdemar, L.R. Odell, and M. Larhed, *J. Org. Chem.*, **80**, 1464–1471 (2015).
- 2015JOC(80)5713 F.H. Ji, X.W. Li, W. Guo, W.Q. Wu, and H.F. Jiang, *J. Org. Chem.*, **80**, 5713–5718 (2015).
- 2015JOC(80)8189 S. Perrone, M. Capua, A. Salomone, and L. Troisi, *J. Org. Chem.*, **80**, 8189–8197 (2015).
- 2015OL(17)1240 S. Li, F.Z. Li, J.X. Gong, and Z. Yan, *Org. Lett.*, **17**, 1240–1243 (2015).
- 2015OL(17)1569 T.Y. Xu and H. Alper, *Org. Lett.*, **17**, 1569–1572 (2015).
- 2015OL(17)3698 P.L. Wang, Y. Li, Y. Wu, C. Li, Q. Lan, and X.S. Wang, *Org. Lett.*, **17**, 3698–3701 (2015).
- 2015OBC(13)4422 C.R. Shen, N.Y.T. Man, S. Stewart, and X.F. Wu, *Org. Biomol. Chem.*, **13**, 4422–4425 (2015).
- 2015THL(56)342 J.B. Chen, K. Natte, and X.F. Wu, *Tetrahedron Lett.*, **56**, 342–345 (2015).



- 2015THL(56)2773 S. Perrone, A. Caroli, G. Cannazza, C. Granito, A. Salomone, and L. Troisi, *Tetrahedron Lett.*, **56**, 2773–2776 (2015).
- 2015TH(71)4432 M. Murai, K. Okamoto, K. Miki, and K. Ohe, *Tetrahedron*, **71**, 4432–4437 (2015).



# Green Syntheses of Heterocycles of Industrial Importance. 5-Hydroxymethylfurfural as a Platform Chemical

**Johannes G. de Vries**

Leibniz-Institut für Katalyse e.V. an der Universität Rostock, Rostock, Germany

E-mail: johannes.devries@catalysis.de

## Contents

1. Introduction	248
2. Monomers for Polymers	252
2.1 Oxidation Products	252
2.1.1 2,5-Furandicarboxylic Acid	252
2.1.2 5-Hydroxymethyl-2-Furanoic Acid	260
2.1.3 2,5-Diformylfuran	260
2.2 Hydrogenation Products	262
2.2.1 Diols and Triols	262
2.2.2 1-Hydroxy-2,6-Hexanedione	267
2.2.3 Diamines and Aminoalcohols Made From 5-Hydroxymethylfurfural	270
2.2.4 Nylon Intermediates Via Hydrogenation of 5-Hydroxymethylfurfural	272
3. 5-Hydroxymethylfurfural to Carbocycles	276
4. C–C Bond Formation to 5-Hydroxymethylfurfural	277
5. 5-Hydroxymethylfurfural to Dimethylfuran	281
6. Oxidations of 5-Hydroxymethylfurfural	284
7. Various Transformations of 5-Hydroxymethylfurfural	285
8. Conclusions	286
References	287

## Abstract

The dwindling supply of fossil resources makes it interesting to find renewable resources for our everyday chemicals. 5-Hydroxymethylfurfural (HMF) is easily produced from fructose, although its isolation is not easy in view of its poor stability. More stable equivalents are its ethers or esters or 5-chloromethylfurfural. In this review, we discuss all products that have been made from HMF in the period 2013–2016. Practically in all transformations, catalysis played a major role. One major product obtained by catalyzed oxidation of HMF is 2,5-furandicarboxylic acid, that is touted as a replacement of

phthalic acid in polymers. Other compounds that have been made from HMF via hydrogenation and that could find use as monomers are 2,5-furandimethanol, 2,5-tetrahydrofurandimethanol, 1,2,6-hexanetriol, 1,6-hexanediol, 5-hydroxymethyl-2-furanoic acid, and 2,5-diaminomethylfuran. Another interesting oxidation product is 2,5-diformylfuran. Also the nylon intermediates caprolactam, adipic acid, and hexamethylenediamine have been made from HMF. Hydrogenation of HMF in water under slightly acidic conditions gives 1-hydroxy-2,5-hexanedione, which can be cyclized to a cyclopentanone derivative. Acyloin condensation gives the dimeric product, which can be hydrogenated to a diesel fuel substitute. Carbon–carbon bond formation has been performed both by Diels–Alder reaction on the furan as well as by condensation on the aldehyde and/or alcohol functionalities. Hydrogenolysis of the side chains leads to formation of 2,5-dimethylfuran, which has been proposed as fuel additive. Oxidation of HMF to butenolides, maleic acid, and anhydride as well as succinic acid has been reported. Various other transformations are also described. It is expected that HMF will be increasingly important in the direct future and, indeed, commercial production of HMF and some of its derivatives has already commenced.

**Keywords:** Alcohol; Aldehyde; Amine; Biomass; Building blocks; Carboxylic acid; Catalysis; Dehydration; Fructose; Furan; Glucose; Monomers; Renewable; Sugar

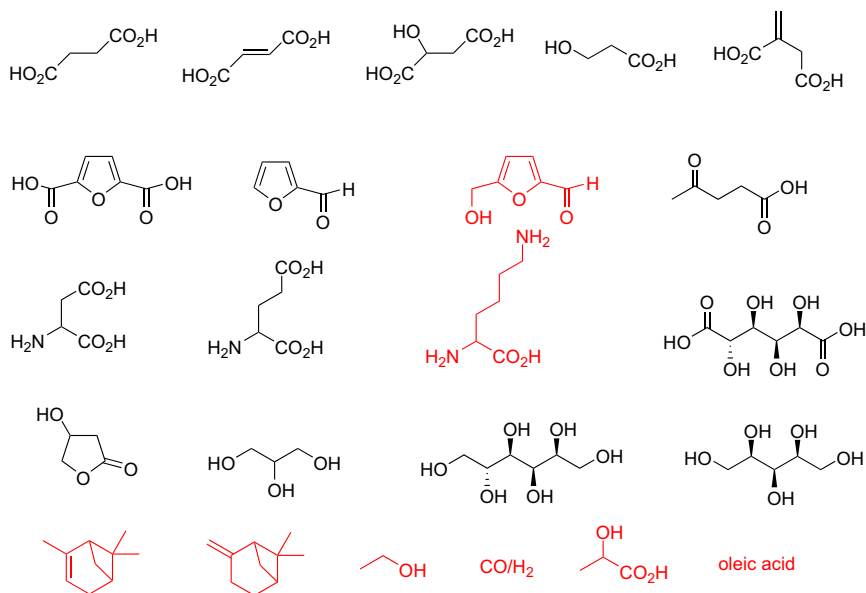


## 1. INTRODUCTION

In view of the dwindling supply of fossil resources and the growing use of energy and chemicals, there is an increasing need to tap into renewable resources. Of the available resources, lignocellulose is by far the most abundant, and thus much effort is currently aimed at converting lignocellulose or its constituents, cellulose, hemicellulose, and lignin into useful chemicals. A number of different strategies have been developed. One particular attractive strategy is to focus on the so-called platform chemicals. These are chemicals that are easily produced in high yield from renewable resources and that are sufficiently versatile to allow their conversion into a variety of useful chemicals. A report made for the US Department of Energy discusses 12 groups of platform chemicals. In the meantime some more compounds can be added to this list (Scheme 1) (2004MI01).

The next challenge is to invent short and economic synthetic routes to existing or novel chemicals. Here catalysis plays a very large role (2014CST1174) (2009EES68).

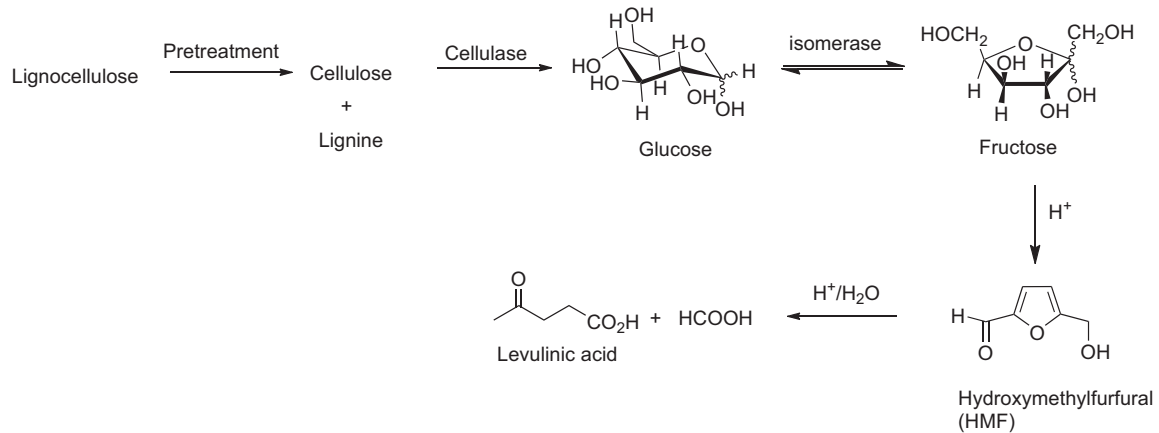
One of the more interesting platform chemicals is 5-hydroxymethylfurfural (HMF) (2013CRV1499). HMF can be obtained via acid-catalyzed dehydration of fructose at elevated temperatures (Scheme 2). However, if this reaction is performed in water a rapid rehydration of HMF takes



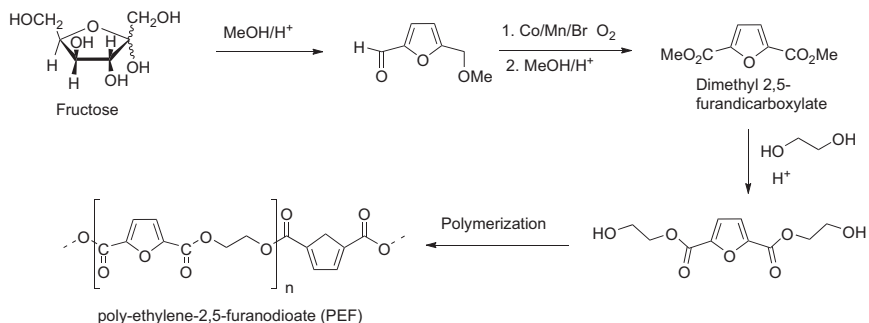
**Scheme 1** Platform chemicals [additions in red from the author].

place, leading to formation of levulinic acid and formic acid. If the dehydration is performed in a dipolar nonprotic solvent such as dimethyl sulfoxide (DMSO), very high yields of HMF up to 97% can be obtained. Unfortunately, it is very hard to separate HMF from this solution as it decomposes upon distillation. In addition, DMSO is not entirely stable under the reaction conditions. For its large-scale production, different solutions have been developed. The most advanced of these is Avantium's process, which performs the dehydration in the presence of methanol to form the HMF methyl ether (Scheme 3) (2012MI02). This compound is much more stable than HMF, and, indeed, recent research has confirmed that the initial instability of HMF is linked to the presence of the free hydroxyl group (2016AGE8338). Recently, it was announced that BASF and Avantium will build the first large-scale plant for the production of 2,5-furandicarboxylic acid (FDCA) presumably via the intermediate ether.

Dumesic and coworkers, on the other hand, have developed a two-phase process (2006SCI(312)1933). Here, HMF is protected from further rehydration through its extraction into the organic phase (MIBK). A yield of HMF of up to 72% (80% HMF selectivity at 90% fructose conversion) has been obtained in this way. However, even from this solution it has not been



**Scheme 2** Production of 5-Hydroxymethylfurfural from renewable resources.

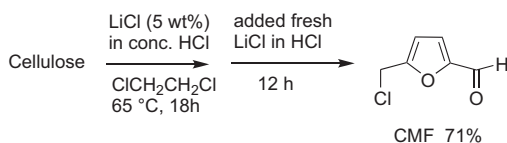


**Scheme 3** Avantium's Process to polyethylene furandioate via 5-methoxymethylfurfural.

possible to isolate HMF in good yields and usually a further transformation is performed on the crude solution to obtain a stable product. In addition the solvent system used is complicated and not easily recycled.

An entirely different approach has been developed by Mascall and coworkers (2008AGE7924). They dehydrate fructose, glucose, and even cellulose in a mixture of concentrated HCl containing a high concentration of LiCl and a chlorinated solvent (Scheme 4). Here, the product they obtain in good yield is 5-chloromethylfurfural (CMF), another very interesting platform chemical. CMF can be hydrolyzed in high yield to HMF.

Fructose is a relatively expensive raw material as it is made by enzymatic isomerization from glucose. This results in a 55:45 equilibrium mixture and for this reason simulated moving bed is used for the separation of fructose from glucose. The main product is high fructose corn syrup, which contains about 95% of fructose. It would indeed be highly interesting to be able to produce HMF from glucose and eventually also from cellulose or lignocellulose. Yields of HMF obtained from these raw materials are rather low. The bottleneck in these processes is the isomerization of glucose to fructose. Thus, much research has been performed on the isomerization of glucose to fructose using chemical catalysts that can survive the conditions of the thermal dehydration process. Thus far best results have been obtained



**Scheme 4** Preparation of 5-chloromethylfurfural (CMF) from cellulose.

with  $\text{CrCl}_2$  or  $\text{CrCl}_3$  (2007SCI(316)1597). However, these reactions work best in ionic liquids that in addition contain a high amount of halide salt.

In this chapter the recent uses of HMF as raw material for the production of several classes of products will be reviewed. In our recent review (2013CRV1499), all reactions up to 2012 were described and thus, here only the results reported in 2013–2016 will be described. Nevertheless, this field has exploded recently and over 150 publications were covered.



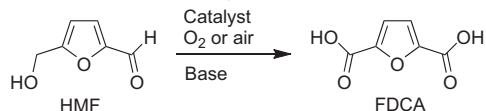
## 2. MONOMERS FOR POLYMERS

### 2.1 Oxidation Products

#### 2.1.1 2,5-Furandicarboxylic Acid

HMF can be oxidized to 2,5-diformylfuran (DFF), 5-hydroxymethyl-2-furanoic acid, but first and foremost to FDCA. This latter compound has attracted a lot of attention in view of its similarity to terephthalic acid. Terephthalic acid is one of the largest bulk chemical products and finds application in polyesters, such as polyethylene terephthalate, which is the raw material for soda bottles. A similar polyester, based on FDCA and ethylene glycol, is polyethylene furandioate (PEF) that has been developed by Avantium (Scheme 3). This material can be used to make bottles, sheets, and fibers. Other potential applications of FDCA are in the polyamide and plasticizer fields. Several groups and companies have patented and/or published methods to oxidize HMF to FDCA. In our previous review best results in terms of selectivity to FDCA (95–99%) were obtained with platinum-based heterogeneous catalysts and oxygen. However, this system needs the presence of stoichiometric amounts of base. Such a process would be impossible to scale up. Avantium has patented the use of the catalyst system that was developed for the oxidation of xylene to phthalic acid: a mixture of cobalt, manganese, and bromide salts. With this catalyst the reported selectivity is lower, but no base is needed.

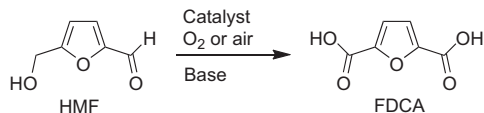
In the reported period, many more metal-catalyzed oxidations of HMF in the presence of base were reported (Table 1). Indeed, very high selectivities were obtained using air or oxygen as oxidant. Most reactions were carried out at relatively low concentrations of HMF (10–100 mmol/l) in water using a mineral base. Metals used are platinum, often promoted with Bi (Entries 1, 20). The assumption is that addition of bismuth prevents the poisoning of the surface with oxygen. The carrier material is also important since platinum on active carbon,  $\text{Al}_2\text{O}_3$ , or  $\text{ZrO}_2$  leads to

**Table 1** Oxidation of 5-hydroxymethylfurfural to 2,5-furandicarboxylic acid using base


Entry	Oxidant (pressure, bar)	Catalyst (mol%)	Base	Temperature (°C)	Time (h)	Conversion (%)	Selectivity (%)	Yield (%)	References
1.	Air (40)	5.1% Pt <sub>IMP</sub> 1% Bi/AC* (0.01)	2 eq. Na <sub>2</sub> CO <sub>3</sub>	120	6	100	98	98	2013GC2240
2.	O <sub>2</sub> (3)	Au <sub>6</sub> Pd <sub>4</sub> /AC* (0.5)	2 eq. NaOH	60	4	>99	>99	>99	2013CSC609
3.	O <sub>2</sub> (3)	Au <sub>8</sub> Pd <sub>2</sub> /AC (0.5)	2 eq. NaOH	60	2	>99	>99	>99	2013CSC609
4.	O <sub>2</sub> (3)	Au <sub>6</sub> Pt <sub>4</sub> /AC (0.5)	2 eq. NaOH	60	4	>99	94	94	2013CSC609
5.	O <sub>2</sub> (3)	Au <sub>8</sub> Pt <sub>2</sub> /AC (0.5)	2 eq. NaOH	60	4	>99	97	94	2013CSC609
6.	O <sub>2</sub> (3)	Au/HY <sup>§</sup> (Cage; 1.2 nm) (0.9)	4 eq. NaOH	60	6	>99	>99	>99	2013CEJ14215
7.	O <sub>2</sub> (6.9)	Au/CNF-N <sup>¶</sup> (HMF/Au <sub>Surface</sub> = 1400)	2 eq. NaOH	22	24	100	62	62	2014JMCA(388-389)123
8.	O <sub>2</sub> (1)	Pd-NP <sup>  </sup> (0.9 nm)/ (PVP) <sup>#</sup> (1)	8.75 eq. NaOH (dosed over 7 h)	90	7	>99	90	90	2014CL(144)498
9.	O <sub>2</sub> (1)	Au/HT <sup>**</sup> (2.5)	1 eq. Na <sub>2</sub> CO <sub>3</sub>	95	7			99	2014CSC2131
10.	O <sub>2</sub> (1)	Pt/C (10)	1.25 eq. NaOH	50	4.25			98	2014CSC2131
11.	O <sub>2</sub> (1)	Pt/Al <sub>2</sub> O <sub>3</sub> (100 wt%)	1 eq. Na <sub>2</sub> CO <sub>3</sub>	140	12	96	100	96	2014RKMC(112)173
12.	O <sub>2</sub> (1)	Pt/ZrO <sub>2</sub> (100 wt%)	1 eq. Na <sub>2</sub> CO <sub>3</sub>	140	12	100	94	94	2014RKMC(112)173
13.	O <sub>2</sub> (1)	Pt/AC (100 wt%)	1 eq. Na <sub>2</sub> CO <sub>3</sub>	140	12	100	89	89	2014RKMC(112)173
14.	O <sub>2</sub> (1)	Pt/TiO <sub>2</sub> (100 wt%)	1 eq. Na <sub>2</sub> CO <sub>3</sub>	140	12	96	2	2	2014RKMC(112)173
15.	O <sub>2</sub> (1)	Pt/CeO <sub>2</sub> (100 wt%)	1 eq. Na <sub>2</sub> CO <sub>3</sub>	140	12	100	8	8	2014RKMC(112)173

(Continued)

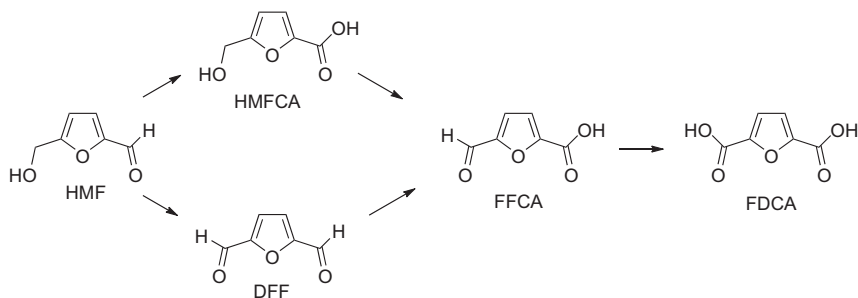


**Table 1** Oxidation of 5-hydroxymethylfurfural to 2,5-furandicarboxylic acid using base—cont'd

Entry	Oxidant (pressure, bar)	Catalyst (mol%)	Base	Temperature (°C)	Time (h)	Conversion (%)	Selectivity (%)	Yield (%)	References
16.	O <sub>2</sub> (1)	γ-Fe <sub>2</sub> O <sub>3</sub> @HAP-Pd(0) <sup>§§</sup> (80 wt%)	0.5 eq. K <sub>2</sub> CO <sub>3</sub>	100	6	97	96	93	2015GC1308
17.	O <sub>2</sub> (1)	PdBi <sub>0.35</sub> Te <sub>0.23</sub> (1)	3 eq. KOH	50	6	100	95	95	2015USP0314272
18.	O <sub>2</sub> (1)	Pd/C@Fe <sub>3</sub> O <sub>4</sub> (80 wt%) <sup>¶¶</sup>	0.5 eq. K <sub>2</sub> CO <sub>3</sub>	80	6	98	89	87	2015GC1610 2015CST3194
19.	O <sub>2</sub> (10)	Au/CeO <sub>2</sub> (1)	4 eq. NaOH	70	6	100	92	92	2015ACBE520
20.	O <sub>2</sub> (40)	PtBi <sub>0.22</sub> /TiO <sub>2</sub> (1)	2 eq. Na <sub>2</sub> CO <sub>3</sub>	100	6	100	99	99	2015CSC1206
21.	O <sub>2</sub> (10)	Pd <sub>1</sub> Au <sub>6</sub> (1)	2 eq. NaOH	70	4	100	80	80	2015ACAG(504)408
22.	O <sub>2</sub> (40)	Ru/AC (1)	4 eq. NaHCO <sub>3</sub>	100	48	100	93	93	2015ACAG(506)206
23.	O <sub>2</sub> (10)	Au/Ce <sub>0.9</sub> Bi <sub>0.1</sub> O <sub>2-δ</sub> (0.67 mol%),	4 eq. NaOH	65	2	100		>99	2015CST1314

\* AC = activated carbon.

<sup>§</sup>HY = Zeolite HY.<sup>¶</sup>CNF-N = amine-functionalized carbon nanofibers.<sup>||</sup>NP = nanoparticles.<sup>#</sup>PVP = polyvinyl pyrrolidinone.<sup>\*\*</sup>HT = Zeolite HT.<sup>§§</sup>γ-Fe<sub>2</sub>O<sub>3</sub>@HAP = hydroxyapatite-encapsulated γ-Fe<sub>2</sub>O<sub>3</sub>.<sup>¶¶</sup>C@Fe<sub>3</sub>O<sub>4</sub> core-shell microspheres (carbon-coated iron oxide particles).



**Scheme 5** Pathways for the oxidation of 5-hydroxymethylfurfural to 2,5-furandicarboxylic acid.

the formation of FDCA in good yields (Entries 10–13), whereas use of Pt on  $\text{TiO}_2$  or  $\text{CeO}_2$  resulted in the formation of only traces of FDCA (Entries 14, 15). Palladium can also be used, either as stabilized nanoparticles (Entry 8) or as heterogeneous catalyst on a support (Entries 16, 18), promoted with Bi and Te (Entry 17) or as a mixed catalyst with gold (Entries 2–5, 21). Monometallic gold catalysts have also been used. Here again the supporting material is important. A gold catalyst supported on Zeolite HY (Entry 6), hydrotalcite (HT) (Entry 9) or  $\text{CeO}_2$  (Entry 19) performed very well whereas gold supported on carbon nanofibers (Entry 7) was much slower. Use of ruthenium on carbon also allows oxidation with good selectivities, although the reaction is rather slow (Entry 22).

The pathway by which HMF is oxidized to FDCA is shown in [Scheme 5](#). In effect two different transformations take place: the oxidation of an alcohol to an aldehyde and the oxidation of both aldehyde groups to the carboxylic acids. These are fundamentally different reactions. The oxidation of an alcohol to an aldehyde often is a dehydrogenation reaction, whereas an oxidation of an aldehyde to an acid may be a radical-type reaction. Hence the success of the double metal catalysts is that they may each catalyze one of the two transformations. Pârvalescu and coworkers discovered that it is rather easy to oxidize HMF to 5-formyl-2-furancarboxylic acid (FFCA) in base without any added metal (although there may have been trace amounts of transition metals in the base). Yields up to 95% were obtained in aqueous NaOH using air as oxidant at 90 °C during 24 h. Using a Mn/Fe-mixed oxide catalyst, FFCA could be oxidized in virtually quantitative yield to FDCA at a temperature of 90 °C and a pressure of 8 bar oxygen ([2016ACBE\(180\)751](#)).

It is also possible to subject HMF to an oxidative esterification reaction. Fu and coworkers were able to obtain mixtures of monomethyl (53%) and

dimethyl 2,5-furandicarboxylate (41%) upon oxidation of HMF in the presence of methanol containing 0.2 eq. of  $K_2CO_3$  (2014CSC3334). For this they used the cobalt catalyst earlier developed by Beller and coworkers, that is, obtained via pyrolysis at 800 °C of a cobalt/1,10-phenanthroline complex in the presence of active carbon.

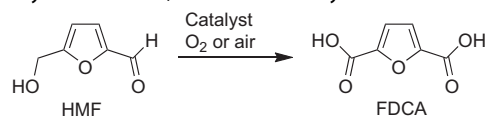
In the past few years, tremendous progress has been made with the development of oxidation reactions of HMF to FDCA that proceed without any added base. These results have been summarized in Table 2. In general, yields are lower than those obtained with base. Nevertheless, a number of catalyst systems have been reported where yields of FDCA exceeding 90% were obtained.

Signoretto and coworkers reported a base-free oxidative esterification of HMF in MeOH using a gold on sulfated zirconia catalyst (3 bar  $O_2$ , 130 °C, 5 h) (2015JC(326)1). The reaction was followed with GC only. The authors report a yield of dimethyl ester of 32%. It seems highly likely that also a large amount of the monomethyl ester was formed that escaped detection by GC. In an earlier paper on a similar reaction, the authors did report the intermediacy of the monomethyl ester (2014JC(319)61).

In addition to oxygen or air, other oxidants have been used. Although it is unlikely that these reactions will ever be used for the large-scale production of FDCA, they still may have value as synthetic methods and hence they have been summarized in Table 3 below.

Another method that can be used for the production of FDCA from HMF is enzymatic oxidation. These reactions have the advantage of very mild conditions and often high selectivity. However, serious drawbacks are the low concentrations and the very long reaction times. Often days are necessary for completion of the reaction. For these reasons, it is deemed unlikely that these methods will ever be used on industrial scale. The best reported method from our previous review is the work from Koopman and coworkers, who used whole cells to oxidize HMF to FDCA (2010BT6291). However, these cells only function well at pH 7. Thus, the pH was kept constant during the fermentation by addition of an ammonia solution. For the isolation of FDCA this solution needs to be acidified to pH 0.5 resulting in the formation of 2 moles of ammonium sulfate per mole of FDCA.

Not many enzymes are capable of oxidizing HMF all the way to FDCA. In particular, the last step from FFCA to FDCA is problematic. This is understandable for enzymes that function via a dehydrogenase mechanism. The aldehyde can only be dehydrogenated to the acid once it is hydrated.

**Table 2** Catalyzed oxidation of 5-hydroxymethylfurfural to 2,5-furandicarboxylic acid without base

Entry	Oxidant Pressure (bar)	Catalyst (solvent)	Temperature (h)	Time (h)	Conversion (%)	Selectivity (%)	Yield (%)	References
1.	Air (9)	Co(OAc) <sub>2</sub> /Mn(OAc) <sub>2</sub> , NaBr (HOAc)	110–160				89	2014USP0142326
2.	Air (10)	Immobilized Fe-porphyrin (H <sub>2</sub> O)	100	10	100	79	79	2013JC(299)316
3.	O <sub>2</sub> (5)	Au-Pd (1:1) NP on CNT (H <sub>2</sub> O)	100	12	100	94	94	2014ACSC2175
4.	O <sub>2</sub> (1)	Pt-PVP-GLY NP*	80	24	100	95	95	2014JC(315)67
5.	O <sub>2</sub> (2)	Ru-OMS-1 <sup>§</sup>	110	8			93	2015USP0336090
6.	O <sub>2</sub> (20)	CoO <sub>2</sub> /ZrO <sub>4</sub> /NaBr (HOAc)	130	24			65	2015WO155784
7.	O <sub>2</sub> (20)	CoO <sub>2</sub> /La <sub>2</sub> O <sub>3</sub> /NaBr (HOAc)	120	20			64	2015WO155784
8.	O <sub>2</sub> (20)	CoO <sub>2</sub> /MnO <sub>2</sub> /NaBr (HOAc)	130	24			57	2015WO155784
9.	O <sub>2</sub> (20)	CoO <sub>2</sub> /NiO <sub>2</sub> /NaBr (HOAc)	130	20			63	2015WO155784
10.	Air (9)	Co(OAc) <sub>2</sub> /Mn(OAc) <sub>2</sub> , NaBr/HBr (HOAc)	132	2			92	2015USP0051412
11.	O <sub>2</sub> (20)	Ru/triazine polymer (H <sub>2</sub> O)	140	1	100	78	78 <sup>¶</sup>	2015CSC3832
12.	O <sub>2</sub> (56)	Li <sub>2</sub> CoMn <sub>3</sub> O <sub>8</sub> (HOAc)	150	8	100		80 <sup>  </sup>	2015CC(58)179
13.	O <sub>2</sub> (5)	Pt-NP/CNT <sup>#</sup> (H <sub>2</sub> O)	95	14	100	98	98	2015CCC2853
14.	O <sub>2</sub> (1)	Cu <sup>2+</sup> /VO <sup>2+</sup> on SBA-15** (4-ClC <sub>6</sub> H <sub>4</sub> CH <sub>3</sub> )	130	12	100		44	2016CEJ(238)1315
15.	O <sub>2</sub> (20)	Ru/C (H <sub>2</sub> O)	120	10	100	88	88	2016GC979

\* Palladium nanoparticles prepared via reduction of Pd(II) with glycerol and stabilized with polyvinylpyrrolidone.

<sup>§</sup>OMS-1 = octahedral molecular sieves.

<sup>¶</sup>The product needs to be extracted from the catalyst using dimethyl sulfoxide.

<sup>||</sup>Isolated yield.

<sup>#</sup>Platinum nanoparticles supported on carbon nanotubes.

\*\*SBA-15 = Mesoporous silica nanoparticles.

**Table 3** Oxidation of 5-hydroxymethylfurfural to 2,5-furandicarboxylic acid using other oxidants

Entry	Oxidant	Catalyst (Solvent)	Temperature (°C)	Time (h)	Conversion (%)	Selectivity (%)	Yield (%)	References
1.	<i>t</i> -BuOOH	CuCl (CH <sub>3</sub> CN)	Room temperature	48	100	45	45	<a href="#">2013ACAG(456)44</a>
2.	Electrocatalysis	Pd <sub>1</sub> Au <sub>2</sub> /C (0.1 M KOH in H <sub>2</sub> O)	25	1	100	83	83	<a href="#">2014GC3778</a>
3.	1. Ac <sub>2</sub> O 2. NaClO <sub>2</sub> /H <sub>2</sub> O <sub>2</sub> 3. KMnO <sub>4</sub> /NaOH	(None in step 1; H <sub>2</sub> O in steps 1 and 2)					71	<a href="#">2015WO056270</a>
4.	<i>t</i> -BuOOH (70% aq. Sol)	Fe <sub>3</sub> O <sub>4</sub> -CoO <sub>x</sub> NP (dimethyl sulfoxide)	80	12	97	71	69	<a href="#">2015ACSSCE406</a>
5.	<i>t</i> -BuOOH (70% aq. Sol)	Co-porphyrin immobilized on Merrifield resin (CH <sub>3</sub> CN)	100–110	24	96	94	90	<a href="#">2015CEJ(270)444</a>

**Table 4** Enzymatic oxidation of 5-hydroxymethylfurfural (HMF) to 2,5-furandicarboxylic acid

Entry	Oxidant	Enzyme	HMF concentration	Time (h)	Yield (%)	Reference
1.	H <sub>2</sub> O <sub>2</sub>	1. TEMPO oxidation to 2,5-diformylfuran 2. Lipase/H <sub>2</sub> O <sub>2</sub>	100 mM	6	96*	2013CSC826
2.	O <sub>2</sub>	HMF oxidase/FAD (both 20 μM) (phosphate buffer pH 7)	4 mM	24	95	2014AGE6515 2014AEM1082
3.	Air	1. AAO <sup>§</sup> (5 μM) 2. UPO <sup>¶</sup> (0.65 μM)	10 mM	4 120	98 <sup>  </sup> 91 <sup>#</sup>	2014FEBSJ(282)3218
4.	Air	1. GO** + catalase + HRP <sup>§§</sup> 2. Lipase/H <sub>2</sub> O <sub>2</sub>	30 mM	96 24	92 <sup>¶¶</sup> 88*	2015GC3718
5.	Air	1. GO + catalase 2. PaoABC <sup>    </sup> + catalase	10 mM	10 5	74	2015GC3271

\* Yield of 2,5-diformylfuran to 2,5-furandicarboxylic acid.

§ Fungal aryl alcohol oxidase.

¶ Fungal unspecific heme peroxygenase.

|| HMF to 5-formyl-2-furancarboxylic acid.

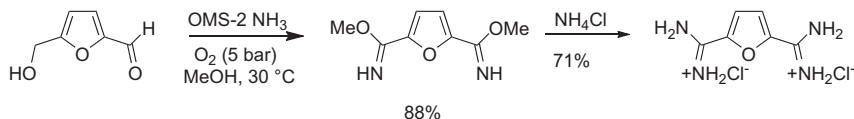
# 5-formyl-2-furancarboxylic acid to 2,5-furandicarboxylic acid.

\*\* Galactose oxidase.

§§ Horse radish peroxidase.

¶¶ Yield of HMF to 2,5-diformylfuran.

|||| *E. Coli* periplasmic aldehyde oxidase.



**Scheme 6** Bis-imidate and bis-amidinium salt from 5-hydroxymethylfurfural.

Fraaije and coworkers showed that hydration of FFCA is problematic, caused by the presence of the anionic carboxylate (2014AGE6515). A number of different solutions have been found Table 4. Oxidation of HMF using the Anelli TEMPO system yields DFF which can be oxidized to FDCA using a combination of lipase and  $\text{H}_2\text{O}_2$  (Entry 1). Fraaije and coworkers discovered an FAD-dependent oxidase enzyme, which is capable of oxidizing HMF directly to FDCA albeit at low concentrations (Entry 2). Use of an aryl alcohol oxidase allows oxidation of HMF to FFCA. In this process  $\text{H}_2\text{O}_2$  is produced, which is utilized in the next step, the oxidation of FFCA to FDCA catalyzed by an unspecific heme peroxxygenase (Entry 3). Turner and coworkers used a similar system with a galactose oxidase for the first step and an aldehyde oxidase for the second step (Entry 4).

Oxidation of HMF in the presence of ammonia and methanol, catalyzed by  $\text{MnO}_2$  or better by OMS-2 (molecular sieves based on manganese dioxide,  $\text{KMn}_8\text{O}_{16}$ ) gives good yields of the bis-imidate ester (Scheme 6). Further reaction of this with  $\text{NH}_4\text{Cl}$  gives the bisamidinium salt (2016GC974).

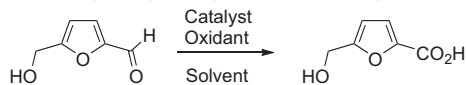
### 2.1.2 5-Hydroxymethyl-2-Furanoic Acid

5-Hydroxymethyl-2-furancarboxylic acid (HMFCFA) is an interesting monomer for polymers in its own right and a number of groups have published solutions for the direct conversion of HMF into HMFCFA. These methods have been collected in Table 5.

Another method to produce HMFCFA is via the Cannizzaro reaction (Scheme 7). Afonso and coworkers were able to achieve good yields of both HMFCFA (82% as the sodium salt) as well as 2,5-furandimethanol (FDM) (85%) by treatment of HMF with aqueous  $\text{NaOH}$  first at  $0^\circ\text{C}$  and then at room temperature (2015GC2849).

### 2.1.3 2,5-Diformylfuran

HMF can also be selectively oxidized to DFF. DFF can be used as a monomer for polymers as intermediate for drugs and agrochemicals and for ligands. The best previous result reported in our previous review was

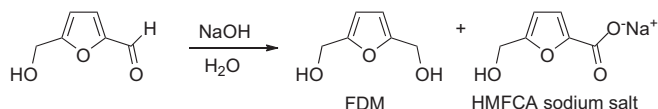
**Table 5** Conversion of 5-hydroxymethylfurfural to 5-Hydroxymethyl-2-furancarboxylic acid

Entry	Oxidant	Catalyst	Temperature (°C)	Time (h)	Conversion (%)	Selectivity (%)	Yield (%)	References
1.	O <sub>2</sub> (1)	NHC* (2 mol%), DBU (1.1 eq.), H <sub>2</sub> O (2 eq.), (MeCN)	RT	16			70 <sup>§</sup>	<a href="#">2013BJOC602</a>
2.	O <sub>2</sub> (1)	MoO <sub>2</sub> (acac) <sub>2</sub> immobilized on K-10 clay (210 wt%)	110	2	93		82	<a href="#">2014GC2762</a>
3.	O <sub>2</sub> (10)	Au/Ce <sub>0.9</sub> Bi <sub>0.1</sub> O <sub>2-δ</sub> (0.67 mol%), NaOH (4 eq.)	65	0.16	100		95	<a href="#">2015CST1314</a>
4.	Air (1)	Xanthine oxidase (buffer pH 7.5)	37	14			94	<a href="#">2015GC3718</a>

\* 1-(2,6-dimethylphenyl)-3-mesityl-4,5-dihydro-1H-imidazol-3-ium chloride.

<sup>§</sup>Yield of methyl 5-hydroxymethyl-2-furancarboxylate.





**Scheme 7** Cannizzaro reaction of 5-hydroxymethylfurfural.

obtained with the 4-acetamido variant of TEMPO and  $\text{HNO}_3$  as catalyst and was claimed to proceed in 100% yield. The reader is cautioned that many of the very high yields reported in this and other papers on the subject were measured with GC only (often without internal standard) or HPLC. In the rare cases where the product was isolated, this is marked in the tables. The reactions with DMSO as oxidant (Entries 1, 13) are Kornblum oxidations, all other ones are dehydrogenations with oxygen as terminal oxidant (Table 6).

NOTE: Many reactions of 2,5-diformylfuran have been reported. We will not discuss these here. DMSO, dimethyl sulfoxide; DMF, dimethylfuran

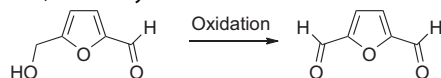
## 2.2 Hydrogenation Products

### 2.2.1 Diols and Triols

HMF can be hydrogenated and depending on the catalyst, the temperature and the pressure of different products can be formed, such as FDM, 2,5-tetrahydrofuran dimethanol, 1,2,6-hexanetriol (1,2,6-HT), 1,6-hexanediol (1,6-HD), and 1,5-hexanediol (1,5-HD) (Scheme 8). In particular, the diols are interesting as monomers for renewable polyesters. In the previous review, methods have been reported to produce all these diols and triols with good selectivity, with the exception of 1,5-hexanediol. In this period a number of new and improved methodologies have been reported. In Table 7 we summarize the recent hydrogenation processes.

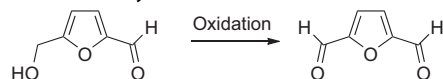
It is clear from the results displayed in the Table that hydrogenation of HMF to FDM can be achieved quite easily with excellent selectivities (Entries 1–9). The hydrogenation of HMF to THFDM requires somewhat more forcing conditions and hence, here the selectivity is somewhat lower, although still very high (Entries 10–13). The reported catalyst for the formation of 1,2,6-HT is not very selective (Entry 14). Here the two-step process reported in our earlier review is still preferred.

In addition to hydrogenation, it is also possible to reduce the functional groups in HMF via transfer hydrogenation. The recent results have been collected in Table 8.

**Table 6** Oxidation of 5-hydroxymethylfurfural to 2,5-diformylfuran

Entry	Oxidant pressure (bar)	Catalyst (Solvent)	Temperature (°C)	Time (h)	Conversion (%)	Selectivity (%)	Yield (%)	References
1.	DMSO	HBr	150	18			100	<a href="#">2013FR3008409</a>
2.	O <sub>2</sub> (3)	Ru/γ-Alumina (toluene)	130	4	99	97	96	<a href="#">2013JIEC(19)1056</a>
3.	O <sub>2</sub> (5)	TEMPO on SiO <sub>2</sub> HNO <sub>3</sub> (5 mol%) (ClCH <sub>2</sub> CH <sub>2</sub> Cl)	55	0.033	97	98		<a href="#">2013GC1975</a>
4.	O <sub>2</sub> (3)	4-CH <sub>3</sub> CONH-TEMPO (1.25 mol%), HNO <sub>3</sub> (5 mol%) (HOAc)	85	100		95		<a href="#">2013WO093322</a>
5.		V <sub>2</sub> O <sub>5</sub> /H-beta (1 mol%) (DMSO)	125	3	84	98		<a href="#">2013CCC284</a>
6.	O <sub>2</sub> (20)	Ru/C (1.25 mol%) (toluene)	110	0.5	100	96		<a href="#">2013JC(301)83</a>
7.	Air (40)	Cu <sup>2+</sup> /VO <sup>2+</sup> on sulfonated carbon (100 wt%) (CH <sub>3</sub> CN)	140	4	100		98	<a href="#">2013ACAG(464-465)305</a>
8.	O <sub>2</sub> (1)	Fe <sub>3</sub> O <sub>4</sub> @SiO <sub>2</sub> -NH <sub>2</sub> -Ru(III) (150 wt%) (toluene)	120	16	100	87	87	<a href="#">2014IECR5820</a>
9.	O <sub>2</sub> (1)	Fe <sub>3</sub> O <sub>4</sub> /Mn <sub>3</sub> O <sub>4</sub> (127 wt%) (DMF)	120	4	100	82	82	<a href="#">2014ACAG(472)64</a>

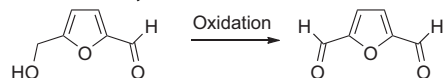
(Continued)

**Table 6** Oxidation of 5-hydroxymethylfurfural to 2,5-diformylfuran—cont'd

Entry	Oxidant pressure (bar)	Catalyst (Solvent)	Temperature (°C)	Time (h)	Conversion (%)	Selectivity (%)	Yield (%)	References
10.	O <sub>2</sub> (1)	VOSO <sub>4</sub> /Cu(NO <sub>3</sub> ) <sub>2</sub> (2 mol%) (MeCN)	80	1.5	99		99	2014ACAG(482)231
11.	Air (15)	Ag(15%)-OMS-2* (100 wt%) ( <i>i</i> -PrOH)	165	4	99		100	2014ACBE(147)293
12.	O <sub>2</sub> (5)	OMS-2* (DMF)	110	1	100		97	2014JJC(316)57
13.	DMSO	NaBr or HBr (30 mol%)	150	18			85 <sup>§</sup>	2014CCC1195
14.	O <sub>2</sub> (1)	Cu(NO <sub>3</sub> ) <sub>2</sub> /NHPI <sup>¶</sup> (2 and 10 mol%) (MeCN)	50	7			71 (53) <sup>§</sup>	2014CC(57)60.
15.	O <sub>2</sub> (1)	Mesostructured VOHPO <sub>4</sub> (81 wt%) (toluene)	110	6	99		82	2014WO122142
16.	O <sub>2</sub> (1)	Fe <sub>3</sub> O <sub>4</sub> @SiO <sub>2</sub> -TEMPO (2 mol%) <i>t</i> -BuONO (5 mol%) (toluene)	50	18	100		99	2014CCC758
17.	O <sub>2</sub> (1)	RuCo(OH) <sub>2</sub> CeO <sub>2</sub> (127 wt%) (MIBK)	120	12	97		83	2014IECR1313
18.	BAIB <sup>  </sup> (1.5 eq.)	4-Hydroxy-TEMPO (20 mol%) HOAc (10 mol%) (EtOAc)	30	0.75			66	2014KJCE1362
19.	O <sub>2</sub> (2.8)	V <sub>2</sub> O <sub>5</sub> /AC (10 mol%) (MIBK)	100	4	95	96		2014CC(57)64

20.	O <sub>2</sub> (1)	Cs <sub>m</sub> H <sub>n</sub> PMo <sub>11</sub> VO <sub>40</sub> (m + n = 4) (120 wt%) (DMSO)	120	6		99	2014CPC1448
21.	O <sub>2</sub> (1)	V-g-C <sub>3</sub> N <sub>4</sub> <sup>#</sup> (80 wt%) (DMSO)	130	6	>99	82	2014CCC3174
22.	-**	Cu(0)Cr <sub>2</sub> O <sub>3</sub> <sup>§§</sup> (12.5 wt%) (DMF)	120	6	84	93	2015AOG152.
23.	Air (20)	Ru-on triazine polymer (2.5 mol%) (MTBE)	80	3	97	73	2015CSC672
24.	BAIB <sup>  </sup> (1.5 eq.) and O <sub>2</sub> (1)	TEMPO on SBA-15 (15 mol%) AcOH 95 mol%) (EtOAc)	40	1		73	2015JMCAC(404- 405)106
25.	Air (1)	GO/catalase/HRP (H <sub>2</sub> O)	25	96		92	2015GC3718
26.	Air	Fe(NO <sub>3</sub> ) <sub>3</sub> ·9H <sub>2</sub> O/ TEMPO/NaCl (5/5/2.5 mol%) (ClCH <sub>2</sub> CH <sub>2</sub> Cl)	RT	4		92	2015CCL1265 (88) <sup>§</sup>
27.	O <sub>2</sub> (4)	TEMPO/ <i>pr</i> -GO <sup>¶¶</sup> (100 mol%/80 wt%) (CH <sub>3</sub> CN)	100	9	100	99	2015ACSC5636
28.	-	TEMPO-4-NHCOCH <sub>3</sub> (1.25 eq.)/silica (CH <sub>2</sub> Cl <sub>2</sub> )	30	3		92 <sup>§</sup> (82) <sup>   </sup>	2015RCBIE1069
29.	O <sub>2</sub> (1)	Ru-6C-1 N <sup>###</sup> (36 wt%) (MIBK)	105	8	94	89	2015CC(63)21
29.	O <sub>2</sub> (1)	Au-NP/MnO <sub>2</sub> (16 wt%)	120	8	82	99	2015CC(63)37

(Continued)

**Table 6** Oxidation of 5-hydroxymethylfurfural to 2,5-diformylfuran—cont'd

Entry	Oxidant pressure (bar)	Catalyst (Solvent)	Temperature (°C)	Time (h)	Conversion (%)	Selectivity (%)	Yield (%)	References
30.	O <sub>2</sub> (1)	Grapheneoxide (16 wt%) (DMSO)	140	24	100		90	<a href="#">2016GC2302</a>
31.	O <sub>2</sub> (1)	γ-Fe <sub>2</sub> O <sub>3</sub> @HAP-Mo (150 wt%) (4-ClC <sub>6</sub> H <sub>4</sub> CH <sub>3</sub> )	120	12	96		68	<a href="#">2016JTICE92</a>

\* OMS-2 = octahedral molecular sieve, KMn<sub>8</sub>O<sub>16</sub>.*n*H<sub>2</sub>O.

<sup>§</sup>Isolated yield.

<sup>¶</sup>NHPI = *N*-hydroxyphthalimide.

<sup>||</sup>Bis-acetoxy-iodobenzene.

<sup>#</sup>Vanadium doped graphitic carbon nitride.

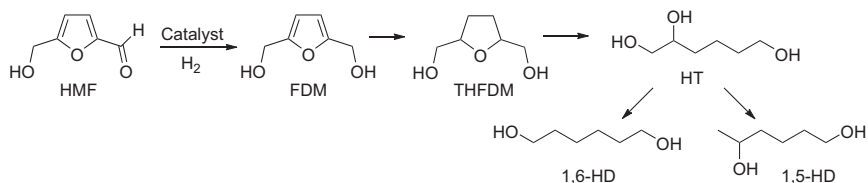
<sup>\*\*</sup>Dehydrogenation.

<sup>§§</sup>Copper nanoparticles on chromium oxide.

<sup>¶¶</sup>Partially reduced grapheneoxide.

<sup>||||</sup>Crystallized, pure product.

<sup>###</sup>Ru-NP supported on mesoporous lipophilic core-shell shuttle.



**Scheme 8** Hydrogenation of 5-hydroxymethylfurfural.

A transfer hydrogenation of HMF with formic acid catalyzed by palladium on zirconium phosphate gave a 43% yield of 1,6-hexanediol (Entry 1). This is the highest yield obtained in this conversion thus far, although a two-step hydrogenation method has been reported before that achieves much higher yields (2011AGE7083). An enzymatic reduction of HMF to FDM was also highly successful using pyruvate dehydrogenase (Entry 2). The NADH coenzyme needs to be regenerated by another dehydrogenase enzyme and glucose is the final reductant. MgO could be used as catalyst in a transfer hydrogenation with methanol to give FDM in excellent yield (Entry 3). 1,4-Butanediol has been used successfully as reductant in transfer hydrogenations. The advantage is that it forms butyrolactone (after dehydrogenation of the intermediate lactol) making this reaction irreversible. This particular reaction was performed in flow at very high temperatures making the reaction extremely fast (Entry 4).

### 2.2.2 1-Hydroxy-2,6-Hexanedione

If HMF is hydrogenated in water under slightly acidic conditions, an entirely different product may be formed. The furan ring of FDM is much more reactive toward electrophiles than the one in HMF. For this reason it is easily protonated which sets it up for attack of water, leading to formation of the ring-opened product 1-hydroxy-3-hexene-2,6-dione (the configuration of the double bond has so far not been ascertained, although it seems likely that it is *cis*) which is hydrogenated to 1-hydroxy-2,6-hexanedione (HHD) (Scheme 9).

Quite a number of papers have recently appeared on this topic. Initially, this product was mostly formed as a side product in the formation of FDM by hydrogenating HMF in water. More recently the synthesis of HHD has been more thoroughly researched and both catalysts as well as conditions for the hydrogenation leading to HHD have been optimized (Table 9). Thus now a 92% yield has been obtained using a tailored homogeneous iridium catalyst at a pH of around 2.5. Both hydrogenation as well as transfer

**Table 7** Hydrogenation of 5-hydroxymethylfurfural

Entry	Catalyst (Solvent)	H <sub>2</sub> pressure (bar)	Temperature (°C)	Time (h)	Product	Conversion (%)	Yield (%)	Selectivity (%)	References
1.	Au-NP on Al <sub>2</sub> O <sub>3</sub> (20 wt%) (H <sub>2</sub> O)	65	120	2	FDM		96		2013RSCA1033
2.	[Ru(cymene)L*(Cl)BF <sub>4</sub> , KOtBu (0.5/4 mol%) (THF)	50	70	2	FDM		99		2013CSC1737
3.	Cu-PMO <sup>§</sup> (20 wt%) (EtOH)	50	100	3	FDM	100		99	2014CSC2266
4.	Ir/TiO <sub>2</sub> (1.3 mol%) (H <sub>2</sub> O)	60	50	3	FDM	99 <sup>¶</sup>		95	2014CATO(234)59
5.	Pt/MCM-41 <sup>  </sup> (20 wt%) (H <sub>2</sub> O)	8	35	2	FDM	100		99	2014GC4734
6.	Shvo-catalyst <sup>#</sup> (0.1 mol%) (toluene)	10	90	1	FDM			99	2014JCS(D)10224
7.	Pt <sub>3</sub> Sn/SnO <sub>2</sub> /rGO <sup>**</sup> (0.15 mol%) (EtOH)	20	70	0.5	FDM	>99		>99	2015CST3108

8.	Ir-ReO <sub>x</sub> /SiO <sub>2</sub> (13 wt%) H <sub>2</sub> O	8	30	6	FDM	99	99 <sup>§§</sup>	2013JCSCC7034
9.	Ni <sub>2</sub> -Fe <sub>1</sub> /CNT <sup>¶¶</sup> (10 wt%) ( <i>n</i> -BuOH)	30	10	18	FDM	100	96	2014CCC1701
10.	Ra-Co (20 wt%) (MeOH)	40	120	4	THFDM	100	96	2014ACSSCE173
11.	Pd-Ir/SiO <sub>2</sub> (0.56 mol (%)H <sub>2</sub> O)	80	2	4	THFDM	99	95	2014ACSC2718
12.	Ni-Al HT <sup>    </sup> (450) (13 wt (%)dioxane)	60	60	6	THFDM	100	96	2015GC2504
13.	Ni-Al LDH <sup>##</sup>	20	80	12	THFDM		>99	2016CSC521
14.	Ni <sub>0.5</sub> Co <sub>2.5</sub> Al <sub>1.0</sub> (20 wt%) (MeOH)	40	120	12	1,2,6- HT	100	65	2014ACSSCE173

\*L = 1-(2-aminophenyl)-3-butyl-1*H*-imidazol-3-ium-2-ide.

§Copper = doped porous metal oxides.

¶Reaction on crude unpurified HMF.

||Mesoporous silica (Mobil Composition of Matter no 41).

#For the structure see [Figure 1](#).

\*\*Reduced grapheneoxide.

§§Isolated yield.

¶¶Carbon nanotubes.

||||Hydrotalcite.

##Layered double hydroxides. FDM, 2,5-furandimethanol, THFDM, tetrahydro-2,5-furandimethanol.



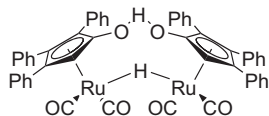


Figure 1 The Shvo catalyst (Table 7, Entry 6).

hydrogenation can be used. HHD is an interesting six-carbon building block containing three functional groups. Research on its application is expected to bloom as a result of its improved availability.

### 2.2.3 Diamines and Aminoalcohols Made From 5-Hydroxymethylfurfural

Thus far we have covered polymer building blocks containing alcohol and carboxylic acid functions, which are highly suitable to produce polyesters or polyols for polyurethanes. Renewable polyamides is another topic of great interest and for this reason monoamines and diamines based on HMF have been synthesized by various methods.

Rhodia has patented the direct reductive amination of HMF using transfer hydrogenation catalyzed by a homogeneous iridium catalyst (2014WO198057). In one example from their patent, HMF is converted into the bis *N*-benzylamino compound (Scheme 10). Note that the reaction on the alcohol is the borrowing hydrogen type, where the alcohol is first converted into the aldehyde and subsequently undergoes reductive amination.

A number of papers have appeared on the selective reductive amination of the aldehyde functionality only. Zhang and coworkers performed reductive aminations of HMF with a range of anilines and secondary amines (Scheme 11(a)) (2014RSCA59083). The amino alcohols based on the anilines were obtained in excellent yields (>90%), whereas those based on the secondary amines were obtained with yields from 67% to 87%. Surprisingly, no product was obtained with *n*-butylamine.

The reductive amination of HMF with ammonia was reported using Rh/Al<sub>2</sub>O<sub>3</sub> as catalyst; the amino alcohol was obtained in 86% yield (2016GC487).

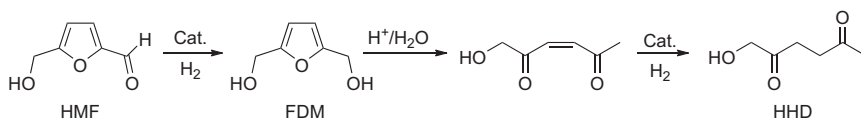
Barta and coworkers reacted DFM with 0.25 eq. of *N*-methyl-benzylamine in a borrowing hydrogen-type reaction catalyzed by the Knölker catalyst to give the monoamination product in 60% yield (Scheme 11(b)) (2016ACSC381).

**Table 8** Transfer hydrogenation of 5-hydroxymethylfurfural

Entry	Reductant	Catalyst	Temperature (°C)	Time (h)	Product	Conversion	Yield	Selectivity	References
1.	HCO <sub>2</sub> H	Pd/ZrP* (40 wt%) (EtOH)	140	21	1,6-HD	97	43		<a href="#">2014CSC96</a>
2.	Glucose	PDH/GDH <sup>§</sup> (Buffer pH 6.5)	30	7	FDM		>99		<a href="#">2014WO086702</a>
3.	MeOH	MgO (33 wt%) (MeOH)	160	3	FDM	95		>99	<a href="#">2014JC(317)206</a>
4.	1,4-Butanediol	Cu-NP on Al <sub>2</sub> O <sub>3</sub>	250	0.01	FDM		93		<a href="#">2014CST2326</a>

\* Palladium on zirconium phosphate.

<sup>§</sup>PDH = pyruvate dehydrogenase, GDH = glucose dehydrogenase, FDM = 2,5-furandimethanol.



**Scheme 9** Hydrolytic hydrogenation of 5-hydroxymethylfurfural to 1-hydroxy-2,6-hexanedione.

Interestingly, a Rhodia patent claims that direct reductive amination of DFF with ammonia and hydrogen is impossible leading to the formation of polymers. Surprisingly reductive amination with ammonia in the presence of primary amines, such as butylamines gave good yields of the primary diamine (2016WO004867). Nevertheless, Kawanami and coworkers were able to perform the direct reductive amination to form the amino alcohol in 86% yield using a Rh/Al<sub>2</sub>O<sub>3</sub> catalyst (2016GC487).

Eposito and coworkers reported the reductive amination of HMF with the sodium salt of alanine using FeNi/carbon as catalyst in excellent yield (99%) (2015CSC3590).

#### 2.2.4 Nylon Intermediates Via Hydrogenation of 5-Hydroxymethylfurfural

The number of carbon atoms in HMF is 6, which coincides nicely with the number of carbon atoms in the nylon intermediates caprolactam, adipic acid, and hexamethylenediamine. Not surprisingly this connection has been made a number of times.

Heeres, de Vries, and coworkers were capable of reducing HMF to 1,6-hexanediol in a two-step process in 86% overall yield (Scheme 12) (2011AGE7083). This diol could be converted in a highly selective Oppenauer oxidation with MIBK to caprolactone using a homogeneous ruthenium catalyst. Conversion of caprolactone to caprolactam has been an industrial process in the early years of nylon and hence, this constitutes a direct, high-yielding connection between HMF and caprolactam.

Ebitani and coworkers achieved the oxidation of 1,6-hexanediol to 6-hydroxycaproic acid by oxidation with hydrogen peroxide under basic conditions catalyzed by Au-Pd nanoparticles in 81% yield (2015CSC1862).

Beller and coworkers have converted 1,6-hexanediol into adiponitrile using their newly developed low-temperature ammoxidation process (Scheme 13) (2014NATC4123). Adiponitrile is hydrogenated to form hexamethylenediamine, one of the monomers for Nylon-6,6.

**Table 9** Conversion of 5-hydroxymethylfurfural into 1-hydroxy-2,6-hexanedione

Entry	Catalyst (solvent)	Acid	Pressure (bar)	Temperature (°C)	Time (h)	Conversion (%)	Selectivity (%)	TOF* (h <sup>-1</sup> )	References
1.	Ru/C (1 mol%)	Oxalic acid (pH 2.0)	30	100	2	100	71	50	<a href="#">1991BSF704</a>
2.	10% Pd/C (50 wt%) H <sub>2</sub> O/toluene (2:1)	HCl (pH 2.5)	1	60	6	97	68	0.27	<a href="#">2009H1037</a>
3.	Rh-Re/SiO <sub>2</sub> (10 mol%)	-	80	120	17	100	81	<1	<a href="#">2011AGE7083</a>
4.	Pd/C (THF)	Amberlyst-15	50	80	15	100	77	16	<a href="#">2014GC4110</a>
5.	Pd/C (H <sub>2</sub> O)	CO <sub>2</sub> (30 bar)	10	120	15	100	77	12	<a href="#">2014CSC2089</a>
6.	[Ru(C <sub>6</sub> H <sub>6</sub> )(H <sub>2</sub> NCH <sub>2</sub> CH <sub>2</sub> NH <sub>2</sub> )Cl]PF <sub>6</sub> (H <sub>2</sub> O)	HCOOH	-	100	8	>99	41	2	<a href="#">2015CCC4050</a>
7.	[Ru(cymene)(L)Cl]PF <sub>6</sub> § (H <sub>2</sub> O)	HCOOH	-	100	30	>99	54		<a href="#">2015GC4618</a>
8.	[Ir(Cp*)(BiPy)(OH <sub>2</sub> )] <sup>2+</sup> (OTf) <sub>2</sub> ¶ (0.26 mol%) (H <sub>2</sub> O)	-	7	120	2	>99	86	173	<a href="#">2015ACSC788</a>
9.	[Ir(Cp*)(2-HO-BiPy)(OH <sub>2</sub> )] <sup>2+</sup> (OTf) <sub>2</sub> (0.26 mol%) (H <sub>2</sub> O)	-	10	120	2	>99	81	162	<a href="#">2016ACSC3784</a>

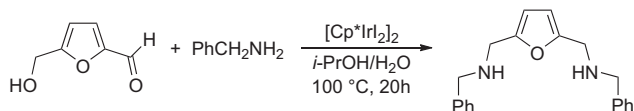
(Continued)

**Table 9** Conversion of 5-hydroxymethylfurfural into 1-hydroxy-2,6-hexanedione—cont'd

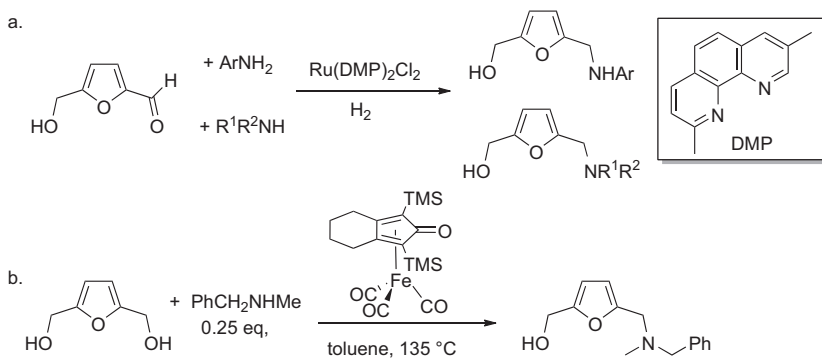
Entry	Catalyst (solvent)	Acid	Pressure (bar)	Temperature (°C)	Time (h)	Conversion (%)	Selectivity (%)	TOF* (h <sup>-1</sup> )	References
10.	[Ir(Cp <sup>★</sup> ) (2-HO-4'-Me <sub>2</sub> N-BiPy) (OH <sub>2</sub> )] <sup>2+</sup> (OTf) <sub>2</sub> (0.0025 mol%) (H <sub>2</sub> O)	-	10	120	2	43	71	6100	<a href="#">2016ACSC3784</a>
11.	[Ir(Cp <sup>★</sup> )(2-HO-4'-Me <sub>2</sub> N- BiPy)(OH <sub>2</sub> )] <sup>2+</sup> (OTf) <sub>2</sub> (0.0025 mol%) (H <sub>2</sub> O)	HCOOH	-	120	2	99	61	6140	<a href="#">2016ACSC3784</a>
12.	[Ir(Cp <sup>★</sup> )(4,4'-bishydroxy- BiPy)(OH <sub>2</sub> )] <sup>2+</sup> (OTf) <sub>2</sub> (formate buffer pH 2.5) (0.01 mol%)	HCOOH	-	130	2	100	92 (85) <sup>  </sup>	5000	<a href="#">2016CSC1209</a>

\* Turnover frequency (mol/mol h).

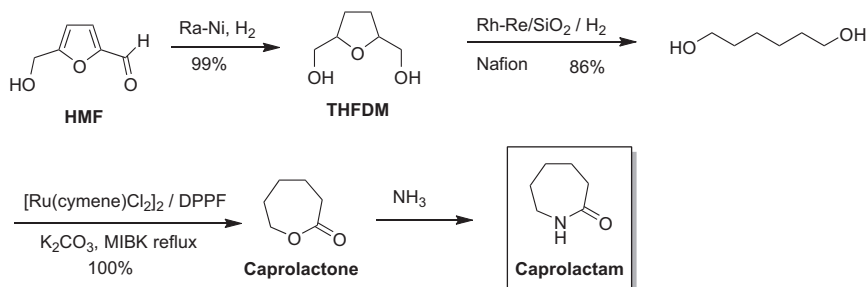
<sup>§</sup>L = 8-aminoquinoline.<sup>¶</sup>BiPy = 2,2'-Bipyridine.<sup>||</sup> Isolated yield.



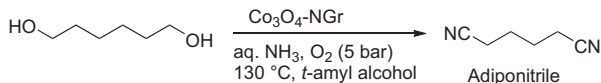
**Scheme 10** Reductive amination and borrowing hydrogen type amination of 5-hydroxymethylfurfural.



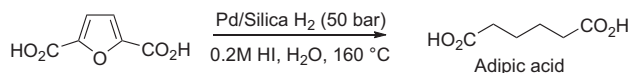
**Scheme 11** Reductive amination of 5-Hydroxymethylfurfural and dimethylfuran.



**Scheme 12** Caprolactam from 5-Hydroxymethylfurfural.



**Scheme 13** 1,6-Hexanediol to adiponitrile.



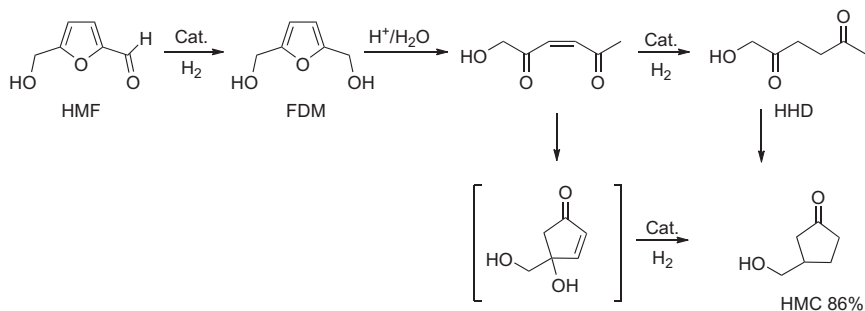
**Scheme 14** 2,5-Furandicarboxylic acid to adipic acid.

Researchers at Rennovia were able to convert FDCA to adipic acid in high yield by hydrogenation over Pd/silica in the presence of a high concentration of HI (Scheme 14) (2011WO144873).

### 3. 5-HYDROXYMETHYLFURFURAL TO CARBOCYCLES

We have previously seen that hydrogenation of HMF from an aqueous solution, particularly under mildly acidic conditions leads to formation of HDD. Surprisingly Ohyama, Satsuma, and coworkers found that another reaction can occur if HMF is hydrogenated with Au, Pt, Pd, or Ru on Nb<sub>2</sub>O<sub>5</sub> (80 bar H<sub>2</sub>, 140 °C, 12 h). They found good yields of 3-hydroxymethylcyclopentanone (HMC) in particular with the gold catalyst (86%) (Scheme 15). After hydrogenation of HMF to FDM, acid-catalyzed hydrolytic ring opening takes place to form 1-hydroxy-3-hexene-2,5-dione. From here two pathways are possible: either via aldol condensation to the unsaturated cyclopentenone, which is hydrogenated to HMC, or via hydrogenation to HDD, followed by its aldol condensation to HMC (Scheme 14) (2014JCSCC5633). The authors present evidence that the aldol reaction is the result of the Lewis acidity of the catalyst support.

In a later publication, they further investigated the role of the support by testing a range of platinum catalysts on various metal oxide carrier materials (Ta<sub>2</sub>O<sub>5</sub>, ZrO<sub>2</sub>, Nb<sub>2</sub>O<sub>5</sub>, TiO<sub>2</sub>, Al<sub>2</sub>O<sub>3</sub>, SiO<sub>2</sub>/Al<sub>2</sub>O<sub>3</sub>, CeO<sub>2</sub>, La<sub>2</sub>O<sub>3</sub>, and hydrotalcite.). Best results (82%) were obtained with Pt/Ta<sub>2</sub>O<sub>5</sub>. The authors were again able to correlate the Lewis acidity (as measured by pyridine binding) with the yield of HMC (2016GC676). Rosseinsky and coworkers were also able to convert HMF to HMC in good yields using a Ni/Al<sub>2</sub>O<sub>3</sub> catalyst



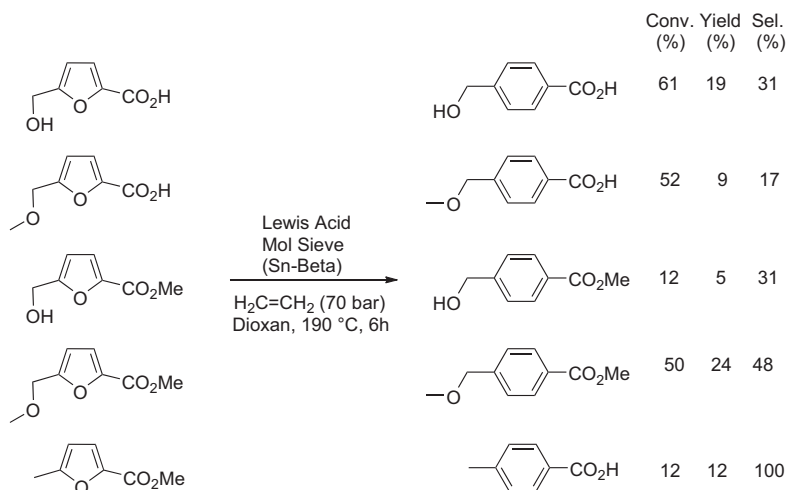
**Scheme 15** Formation of 3-hydroxymethylcyclopentanone from 5-Hydroxymethylfurfural.

that was obtained from nickel–aluminum double-layered hydroxides. At 140 °C and 20 bar of H<sub>2</sub> they obtained an 81% yield of HMC (2016CSC521).

#### 4. C–C BOND FORMATION TO 5-HYDROXYMETHYLFURFURAL

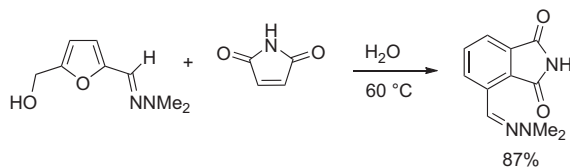
Further conversion of HMF into useful building blocks can be achieved by carbon–carbon bond formation. This has been an active field right from the start and activity is still continuing. Many groups have worked at methodology to convert HMF via a Diels–Alder approach into benzene derivatives, in particular phthalic acid. The furan ring in FDCA is deactivated for Diels–Alder reaction, but the cycloaddition is possible for 2,5-dimethylfuran (2013CRV1499). Recently, Davis and co-workers reported the Diels–Alder reaction of a number of intermediate HMF derivatives (Scheme 16) (2014PNA8363, 2015ACSC5904). Although the yields are obviously higher than with FDCA, selectivities are still too low for large-scale production in most reactions, with the exception of methyl 5-methyl-2-furancarboxylate.

Sheppard, Hailes, and coworkers were able to achieve the DA in high yield (87%) between the dimethylhydrazone of HMF and maleimide in water at 80 °C (Scheme 17) (2016GC1855).



**Scheme 16** Diels–Alder reaction of 5-Hydroxymethylfurfural derivatives with ethylene.



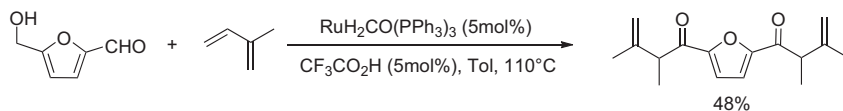


**Scheme 17** Diels–Alder reaction of 5-Hydroxymethylfurfural hydrazine with maleimide.

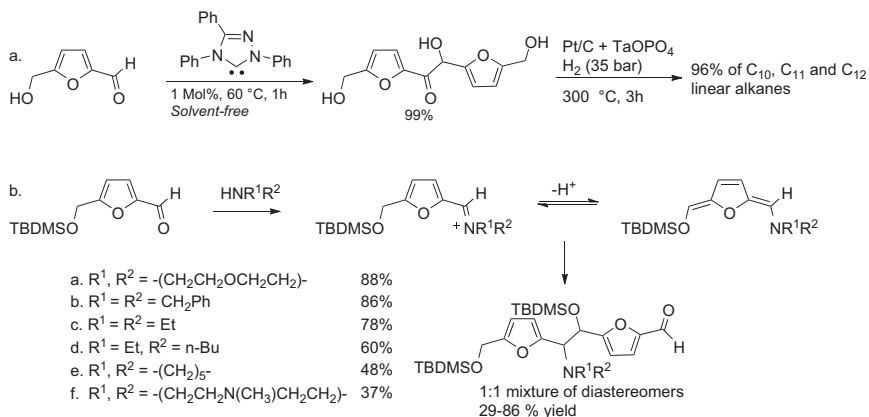
Feringa, de Vries, and coworkers used the technology developed by Krische for the double coupling of HMF with isoprene (**Scheme 18**) (2013CSC1631). In this reaction it is assumed that the ruthenium hydride complex reacts with the isoprene to form an allyl complex, which reacts with the aldehyde. The alcohol function is dehydrogenated by the same catalyst to the aldehyde under the reaction conditions.

Many researchers have developed methodology to increase the molecular weight of HMF by C–C bond formation. Hydrogenation of the product delivers a hydrocarbon with the right properties for a diesel substitute. Coupling with acetone has been a much-used method in the past. Another more recent approach is the use of the benzoin condensation reaction to create the C12 hydroxy ketone, or furoin. Chen and Liu used catalysis by an NHC (**Scheme 19(a)**) and achieved a yield of 99% (2012GC2738, 2013CSC2236). Abu-Omar screened 10 different NHC's for the same reaction and obtained a maximum 88% yield of furoin (2014CSC2742). Chen immobilized an NHC catalyst and was able to achieve a constant 96–97% yield of furoin over 10 recycles (2015ACSC6907). Chuck, Dominguez de Maria, and coworkers used a benzaldehyde lyase to effect this benzoin condensation. Although the reaction worked well, the enzyme was deactivated after 70% conversion. In addition, the majority of furoin that was formed underwent an autoxidation to the diketone (2015GC2714).

Afonso and coworkers developed a conceptually novel way to couple two alcohol-protected HMF units (**Scheme 19(b)**). Reaction with a secondary amine gives rise to the iminium compound, which can lose a proton to form the trieneamine, which is now nicely set up for a nucleophilic attack on



**Scheme 18** Coupling of 5-Hydroxymethylfurfural to isoprene.

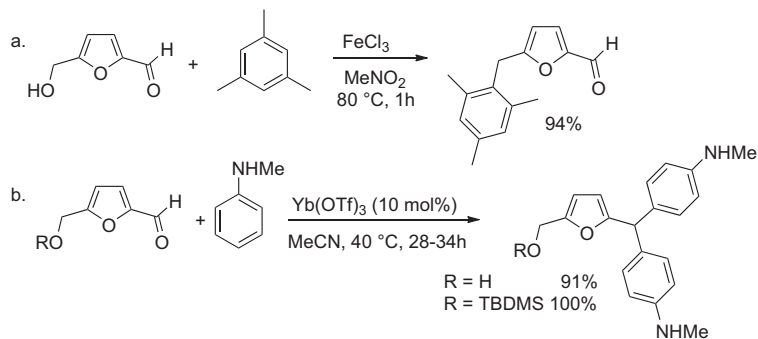


**Scheme 19** Benzoin condensation of 5-Hydroxymethylfurfural.

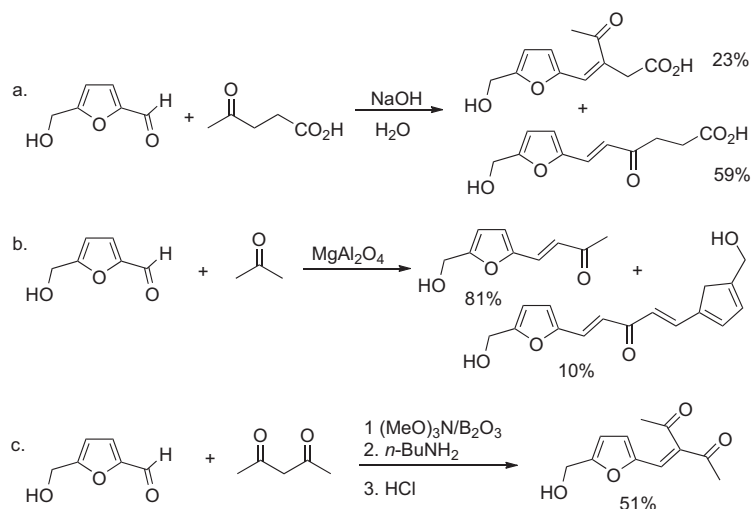
the iminium compound leading to the formation of the protected amino alcohols. A range of Lewis acids was tested as catalyst and Dy(OTf)<sub>3</sub> turned out to give the highest yields of products (2014OBC9324).

Rauchfuss and Zhou used the methodology developed by Beller for Friedel–Crafts alkylation of electron-rich arenes with the benzylic alcohol function of HMF (2013CSC383). Using FeCl<sub>3</sub> as catalyst in MeNO<sub>2</sub> or DCM as solvent, they were able to isolate good yields of the arylated products with toluene, xylene, and mesitylene (Scheme 20(a)). Interestingly, if the alcohol function of HMF is protected as its TBDMS ether, it is possible to perform a double arylation with electron-rich *N*-alkylanilines on the aldehyde, catalyzed by Yb(OTf)<sub>3</sub> in acetonitrile (Scheme 20(b)) (2015JOC10404). Surprisingly, the reaction also worked on the unprotected HMF and gave the product in 91% yield.

The aldol condensation has been used many times to effect CC bond formation to HMF. Reaction between HMF and levulinic acid in water catalyzed by NaOH gave the two expected aldol condensation products in 59% and 23% yields (Scheme 21(a)) (2015ICP546). Palkovits and co-workers performed the aldol condensation of HMF with acetone catalyzed by MgAl<sub>2</sub>O<sub>4</sub> and obtained the mono-condensation product (81%) together with a smaller amount of the bis-adduct (11%) (Scheme 21(b)). By using the same material loaded with copper, they could perform the aldol condensation and the subsequent hydrogenation in one pot with the same catalyst (2013CSC2103). The main hydrogenation product was 2-(2-hydroxybut-4-yl)-5-methylfuran. Gong, Wang, and coworkers were able to convert the acetone monoadduct into octane with excellent selectivity (96%) using

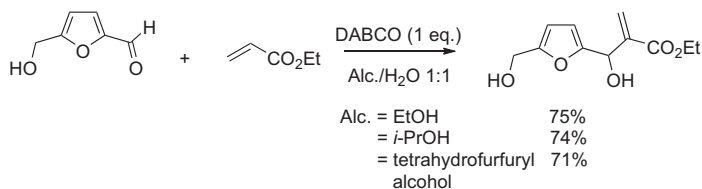


**Scheme 20** Arylations of 5-Hydroxymethylfurfural.



**Scheme 21** Aldol condensation reactions on 5-Hydroxymethylfurfural.

Pd/NbOPO<sub>4</sub> as catalyst at 170 °C and 20 bar H<sub>2</sub> (2014AGE9755). Since the formation of the double adduct necessitates an extra separation step, a more selective aldol condensation is highly desired. Román-Leshkov and coworkers found that use of Hf-beta, a Lewis acidic zeolite, was capable of catalyzing the aldol condensation between HMF and acetone to the monoadduct with >99 selectivity at 73% conversion (90 °C, 5 h) (2015AGE9837). Martichonok and coworkers found that reaction between HMF and acetylacetone catalyzed by (MeO)<sub>3</sub>B/B<sub>2</sub>O<sub>3</sub>/n-BuNH<sub>2</sub> led to the formation of the Knoevenagel product (Scheme 21(c)), whereas the same



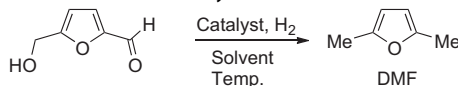
**Scheme 22** Baylis–Hillman reaction of 5-Hydroxymethylfurfural and ethyl acrylate.

reaction with benzaldehyde led to formation of the terminal aldol condensation product (2016SC1245).

The Baylis–Hillman reaction is another method to establish a carbon–carbon bond to an aldehyde. The Baylis–Hillman reaction of HMF with ethyl acrylate was catalyzed by DABCO (2015RSCA69238). The yield of the reaction was highly dependent on the solvent system used. In the end, mixtures of various alcohol solvents and water (1:1) gave the highest yield of adduct (Scheme 22).

## 5. 5-HYDROXYMETHYLFURFURAL TO DIMETHYLFURAN

One method to make fuels out of HMF is condensation with other cheap and renewable building blocks, such as acetone, followed by hydrogenation as we have seen in the preceding part. However, there is another conceptually simpler way to turn HMF into a fuel. Dumesic has developed the conversion of fructose via HMF to dimethylfuran (DMF) with the objective to develop this compound as a fuel (2007NAT(447)982). And indeed, the properties of DMF are somewhere in between gasoline and ethanol, when it comes to combustion and octane number. In addition, DMF is very stable and not hygroscopic, which simplifies its purification. For the hydrogenation step he used a Cu–Ru/C catalyst. This catalyst is not inhibited by chloride as were other copper catalysts, which is important as the yield of HMF is increased by the presence of high concentrations of chloride. Nevertheless, the yield of DMF was only 71%, so there is clearly room for improvement. Since this paper, many more hydrogenations of HMF to DMF have been published. These have been collected in Table 10. It is clear that several different heterogeneous hydrogenation catalysts, including cheap metal-based catalysts, are capable of catalyzing this reaction with high selectivity. Surprisingly, higher temperatures seem to correlate with higher yields.

**Table 10** Hydrogenation of 5-Hydroxymethylfurfural to 2,5-dimethylfuran

Entry	Catalyst (Solvent)	H <sub>2</sub> pressure (bar)	Temperature (°C)	Time (h)	Conversion (%)	Yield (%)	Selectivity (%)	References
1.	7Ni-30W <sub>2</sub> C/AC (100 wt %) (THF)	40	180	3	100	96	96	<a href="#">2014CSC1068</a>
2.	Pd/C (20 mol%) H <sub>2</sub> O/scCO <sub>2</sub> (100 bar)	10	80	2	100	100	100	<a href="#">2014GC1543</a>
3.	Pd/C-ZnCl <sub>2</sub> (10 wt%) (THF)	8	150	8	>99	85	84	<a href="#">2014CSC3095</a>
4.	Ra-Ni (33 wt%) (dioxane)	15	180	15	100	89	89	<a href="#">2014RSCA60469</a>
5.	CuZn nanoalloy (7 wt%) (CPME)*	20	200	6	100	94 <sup>§</sup>		<a href="#">2015CSC1323</a>
6.	Pt/C (10 wt%) (EtOH, PrOH, or toluene)	33	180	2	100		48–63	<a href="#">2015AICEJ590</a>
7.	Ni <sub>2</sub> -Fe <sub>1</sub> /CNT (10 wt%) ( <i>n</i> -BuOH)	30	200	3	100		91	<a href="#">2015CCCC1701</a>
8.	NiAl-850 <sup>¶</sup> (7 wt%)	12	180	4	100		92	<a href="#">2015GC2504</a>
9.	Ru-Sn/ZnO <sub>2</sub> (flow) ( <i>n</i> -BuOH)	1	240		100		99	<a href="#">2015GC3310</a>
10.	CuO/ZnO (33 wt%)	15	220	5	100		92	<a href="#">2015CST4208</a>
11.	Ni/Co <sub>3</sub> O <sub>4</sub> (40 wt%) (THF)	10	130	24	>99	76		<a href="#">2015CC(66)55</a>
12.	Pt/rGO (1 mol%) ( <i>n</i> -BuOH)	30	120	2	100	73		<a href="#">2016F(163)74</a>

\*Cyclopentyl methyl ether.

<sup>§</sup>Yield refers to mixture of DMF and DMTHF (18:1).<sup>¶</sup>Nickel on hydrotalcite calcined at 850 °C.

**Table 11** Transfer hydrogenation of 5-Hydroxymethylfurfural to 2,5-dimethylfuran

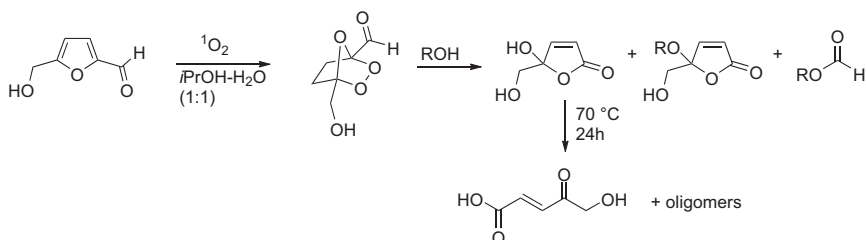
Entry	Catalyst	Reductant	Temperature (°C)	Time (h)	Conversion (%)	Yield (%)	Selectivity (%)	References
1.	Pd/Fe <sub>2</sub> O <sub>3</sub>	<i>i</i> PrOH	180	Flow (0.4 h)	100	72		<a href="#">2014CSC268</a>
2.	Cu-NP on HT	1,4-Butanediol	220	Flow (0.5 h)	100	72		<a href="#">2014CST2326</a>
3.	Ru/C (3 mol%)	<i>i</i> PrOH	190	6	100		80	<a href="#">2013CSC1158</a> <a href="#">2014CCC848</a>

In addition to a classical hydrogenation reaction, it is also possible to use transfer hydrogenation to convert HMF to DMF. This option is less desirable for large-scale production as it is more expensive and/or leads to a second product, such as acetone (from isopropanol) or butyrolactone (from 1,4-butanediol). Nevertheless, in the lab, this may be a useful reaction. The published examples have been summarized in [Table 11](#). In general, yields are lower as compared to the hydrogenation.

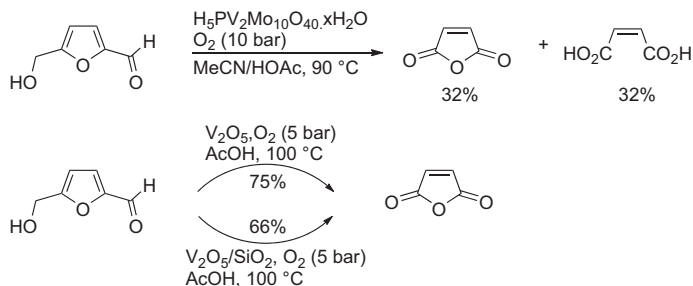
## 6. OXIDATIONS OF 5-HYDROXYMETHYLFURFURAL

In addition to the side chain oxidations of HMF, leading to DFF and FDCA, it is also possible to oxidize the furan ring. In particular, reactions with bromine and with singlet oxygen were reported in our previous review. Kappe and coworkers subjected HMF to reaction with singlet oxygen in a flow reactor ([Scheme 23](#)). The singlet oxygen was generated photochemically using Rose Bengal as photosensitizer. The products depended on the solvent system used. In this reaction, the initial Diels–Alder adduct reacts with the alcohol or water to form the butenolides and the formate. Use of dioxane/water or *i*PrOH/water gave the butenolide with  $R = H$  in >99% selectivity. Use of methanol, on the other hand led to a 14:86 mixture of butenolides ( $R = Me$  vs  $R = H$ , respectively) ([2015CSC1648](#)). The butenolide could be reacted at 70 °C to give 5-hydroxy-4-keto-2-pentenoic acid, which partially polymerized.

Another reaction on the furan ring is the metal-catalyzed oxidation to maleic anhydride and acid ([Scheme 24](#)). Using polyoxometallates as catalysts, a mixture of maleic anhydride and maleic acid was obtained ([2015ACSC2035](#)). Vanadium oxide, with or without carrier material, was an even better catalyst allowing the formation of maleic anhydride in up to 75% yield ([2016GC643](#)).



**Scheme 23** Butenolides from 5-Hydroxymethylfurfural.



**Scheme 24** Maleic acid and anhydride from 5-Hydroxymethylfurfural.

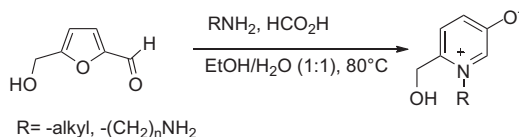
Ebitani and coworkers oxidized HMF with  $\text{H}_2\text{O}_2$  in the presence of the solid acid Amberlyst-15 and were able to achieve a 19% yield of succinic acid. Higher yields of 2-oxoglutaric acid were achieved up to 31%. The authors were able to show that 2-oxo-glutaric acid is a precursor of succinic acid (2013ACAG(458)55).

## 7. VARIOUS TRANSFORMATIONS OF 5-HYDROXYMETHYLFURFURAL

The formation of the anion of N-alkyl 2-hydroxymethyl 5-hydroxypyridinium salts from HMF via reaction with alkylamines or amino acids has been reported a number of times (2013CRV1499). Afonso and coworkers have rejuvenated this chemistry, improved the yields (30–82%), and expanded the scope to include diamines (Scheme 25) (2015OL5244). With the latter substrates the aminoalkyl pyridinium salts are formed (59–80%) and not the bis-pyridinium compounds.

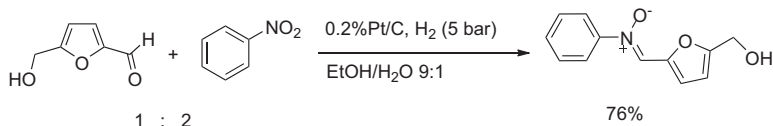
Corma and coworkers reacted nitrobenzene with HMF under catalytic hydrogenation conditions and obtained the nitrone in 76% yield (Scheme 26) (2014AGE9306).

Koh and Loh revisited the Achmatowicz rearrangement on a derivative obtained from HMF. The hemiacetal in the product could be reduced to the ether by hydrosilylation (Scheme 27) (2015GC3746).

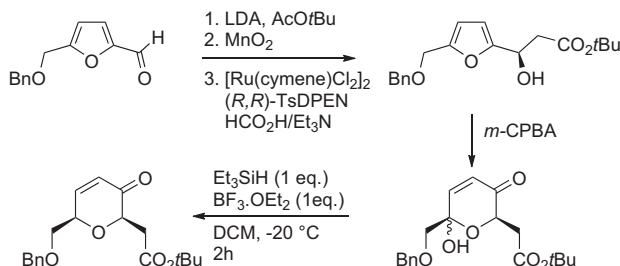


**Scheme 25** Pyridines from 5-Hydroxymethylfurfural.

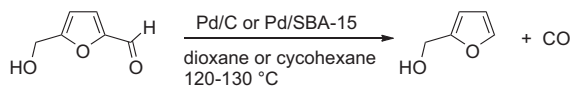




**Scheme 26** Nitron from 5-Hydroxymethylfurfural.



**Scheme 27** Achmatowicz rearrangement of a 5-Hydroxymethylfurfural derivative.



**Scheme 28** Decarbonylation of 5-Hydroxymethylfurfural to furfuryl alcohol.

The decarbonylation of HMF leads to the formation of furfuryl alcohol. This product can also be obtained via reduction of furfural, but it is expected that HMF will be cheaper than furfural in the near future and hence this reaction could make sense for a large-scale production process. Two groups have reported upon the palladium-catalyzed decarbonylation of HMF in excellent yields around 95% (Scheme 28) (2013CSC1348, 2015GC307).

Topics that have not been treated in this review for lack of space are as follows: (1) Etherification of the hydroxymethyl group, mostly catalyzed by solid acid catalysts; (2) Esterification catalyzed by lipases; (3) Acetalization of the aldehyde catalyzed by solid acids or In(OTf)<sub>3</sub>; and (4) Conversion of the alcohol group into a bromide (HBr) or chloride (HCl) in halogenated solvents.

## 8. CONCLUSIONS

It is clear from the above that HMF is a most versatile platform chemical that can be converted into a plethora of different compounds. Many of these are potential monomers for polymers, both for existing as well as for

novel polymers, such as PEF. Thus it is clear that the importance of HMF goes far beyond the bench and indeed HMF is already produced on ton scale in very high purity by AVA-Biochem in Switzerland. Avantium has run a pilot plant for the production of FDCA and PEF for many years and at the moment of writing the building of a large-scale plant for the production of FDCA in Antwerp has commenced. The largest problem in HMF chemistry is its instability. This has been combatted by the development of stable derivatives such as its ethers, esters as well as the chloro-compound. A further accelerated growth of HMF chemistry is expected to take place in the next decade.

## REFERENCES

- 1991BSF704 V. Schiavo, G. Descotes, and J. Mentech, *Bull. Soc. Chim. Fr.*, **128**, 704 (1991).
- 2004MI01 Top value-added chemicals from biomass, In T. Werpy and G. Petersen, editors: *Results of Screening for Potential Candidates From Sugars and Synthesis Gas*, **Vol. I**, U. S. Department of Energy (DOE) by the National Renewable Energy Laboratory, a DOE National Laboratory (2004).
- 2006SCI(312)1933 Y. Román-Leshkov, J.N. Chheda, and J.A. Dumesic, *Science*, **312**, 1933 (2006).
- 2007NAT(447)982 Y. Román-Leshkov, C.J. Barrett, Z.Y. Liu, and J.A. Dumesic, *Nature*, **447**, 982 (2007).
- 2007SCI(316)1597 H. Zhao, J.E. Holladay, H. Brown, and Z.C. Zhang, *Science*, **316**, 1597 (2007).
- 2008AGE7924 M. Mascal and E.B. Nitikin, *Angew. Chem. Int. Ed.*, **47**, 7924 (2008).
- 2009EES68 Y.-C. Lin and G.W. Huber, *Energy Environ. Sci.*, **2**, 68 (2009).
- 2009H1037 G.C.A. Luijkx, N.P.M. Huck, G. van Rantwijk, L. Maat, and H. Van Bekkum, *Heterocycles*, **77**, 1037 (2009).
- 2010BT6291 F. Koopman, N. Wierckx, J.H. de Winde, and H.J. Ruijsenaars, *Bioresour. Technol.*, **101**, 6291 (2010).
- 2011AGE7083 T. Buntara, S. Noel, P.H. Phua, I. Melián-Cabrera, J.G. de Vries, and H.J. Heeres, *Angew. Chem. Int. Ed.*, **50**, 7083 (2011).
- 2011WO144873 T.R. Boussie, E.L. Dias, Z.M. Fresco, and V.J. Murphy, WO2011/144873, to Rennovia, Inc. (2011).
- 2012GC2738 D.J. Liu, Y. Zhanga, and E.Y.-X. Chen, *Green Chem.*, **14**, 2738 (2012).
- 2012MI02 E. de Jong, M.A. Dam, L. Sipos, and G.-J.M. Gruter, ACS Symposium Series. 1105, In P.B. Smith and R. Gross, editors: *Biobased Monomers, Polymers and Materials*, p 1.
- 2013ACAG(456)44 T.S. Hansen, I. Sádaba, E.J. García-Suárez, and A. Riisager, *Appl. Catal. A*, **456**, 44 (2013).
- 2013ACAG(458)55 H. Choudhary, S. Nishimura, and K. Ebitani, *Appl. Catal. Gen. A*, **458**, 55 (2013).
- 2013ACAG(464-465)305 N.-T. Le, P. Lakshmanan, K. Cho, Y. Han, and H. Kim, *Appl. Catal. A*, **464-465**, 305 (2013).

- 2013BJOC602 L. Möhlmann, S. Ludwig, and S. Blechert, *Beilstein J. Org. Chem.*, **9**, 602 (2013).
- 2013CCCC284 I. Sádaba, Y.Y. Gorbanev, S. Kegnaes, S.S. Reddy Putluru, R.W. Berg, and A. Riisager, *ChemCatChem*, **5**, 284 (2013).
- 2013CEJ14215 J. Cai, H. Ma, J. Zhang, Q. Song, Z. Du, Y. Huang, and J. Xu, *Chem. Eur. J.*, **19**, 14215 (2013).
- 2013CRV1499 R.-J. van Putten, J.C. van der Waal, E. de Jong, C.B. Rasrendra, H.J. Heeres, and J.G. de Vries, *Chem. Rev.*, **113**, 1499 (2013).
- 2013CSC1158 J. Jae, W. Zheng, R.F. Lobo, and D.G. Vlachos, *ChemSusChem*, **6**, 1158 (2013).
- 2013CSC1348 Y.-B. Huang, Z. Yang, M.-Y. Chen, J.-J. Dai, Q.-X. Guo, and Y. Fu, *ChemSusChem*, **6**, 1348 (2013).
- 2013CSC1631 C.M. Nicklaus, A.J. Minnaard, B.L. Feringa, and J.G. de Vries, *ChemSusChem*, **6**, 1631 (2013).
- 2013CSC1737 E. Jansen, L.S. Jongbloed, D.S. Tromp, M. Lutz, B. De Bruin, and C.J. Elsevier, *ChemSusChem*, **6**, 1737 (2013).
- 2013CSC2103 K. Pupovac and R. Palkovits, *ChemSusChem*, **6**, 2103 (2013).
- 2013CSC2236 D.J. Liu and E.Y.-X. Chen, *ChemSusChem*, **6**, 2236 (2013).
- 2013CSC383 X. Zhou and T.B. Rauchfuss, *ChemSusChem*, **6**, 383 (2013).
- 2013CSC609 A. Villa, M. Schiavoni, S. Campisi, G.M. Veith, and L. Prati, *ChemSusChem*, **6**, 609 (2013).
- 2013CSC826 M. Krystof, M. Pérez-Sánchez, and P. Domínguez de Maria, *ChemSusChem*, **6**, 826 (2013).
- 2013FR3008409 C. Laugel, J. Lebras, S. Markinkovic, J. Muzart, B. Estrine, and N. Hoffmann, FR3 008 409, to Agro Industrie Recherche et Developpements (A.R.D.) and Centre National de Recherche Scientifique (2015).
- 2013GC1975 C. Aellig, D. Scholz, S. Conrad, and I. Hermans, *Green Chem.*, **15**, 1975 (2013).
- 2013GC2240 H.A. Rass, N. Essayem, and M. Besson, *Green Chem.*, **15**, 2240 (2013).
- 2013JC(299)316 B. Saha, D. Gupta, M.M. Abu-Omar, A. Modak, and A. Bhaumik, *J. Catal.*, **299**, 316 (2013).
- 2013JC(301)83 J. Nie, J. Xie, and H. Liu, *J. Catal.*, **301**, 83 (2013).
- 2013JCSCC7034 M. Tamura, K. Tokonami, Y. Nagakawa, and K. Tomishige, *Chem. Commun.*, **49**, 7034 (2013).
- 2013JIEC(19)1056 C.A. Antonyraj, J. Jeong, B. Kim, S. Shin, S. Kim, K.-Y. Lee, and J.K. Cho, *J. Ind. Eng. Chem.*, **19**, 1056 (2013).
- 2013RSCA1033 J. Ohyama, A. Esaki, Y. Yamamoto, S. Arai, and A. Satsuma, *RSC Adv.*, **3**, 1033 (2013).
- 2013WO093322 L. Dambriane, and M. Ibert, WO2013/093322, to Roquette Frères (2013).
- 2014ACAG(472)64 B. Liu, Z. Zhang, K. Lv, K. Deng, and H. Duan, *Appl. Catal. A*, **472**, 64 (2014).
- 2014ACAG(482)231 X. Jia, J. Ma, M. Wang, Z. Du, F. Lu, and F. Wang, *Appl. Catal. A*, **482**, 231 (2014).
- 2014CSC2089 F. Liu, M. Audemar, K. De Oliveira Vigier, J.-M. Clacens, F. De Campo, and F. Jérôme, *ChemSusChem*, **7**, 2089 (2014).
- 2014ACBE(147)293 G.D. Yadav and R.V. Sharma, *Appl. Catal. B*, **146**, 293 (2014).
- 2014ACSC2175 X. Wan, C. Zhou, J. Chen, W. Deng, Q. Zhang, Y. Yang, and Y. Wang, *ACS Catal.*, **4**, 2175 (2014).

- 2014ACSC2718 Y. Nakagawa, K. Takada, M. Tamura, and K. Tomishige, *ACS Catal.*, **4**, 2718 (2014).
- 2014ACSSCE173 S. Yao, X. Wang, Y. Jiang, F. Wu, X. Chen, and X. Mu, *ACS Sustainable Chem. Eng.*, **2**, 173 (2014).
- 2014AEM1082 W.P. Dijkman and M.W. Fraaije, *Appl. Environ. Microbiol.*, **80**, 1082 (2014).
- 2014AGE6515 W.P. Dijkman, D.E. Groothuis, and M.W. Fraaije, *Angew. Chem. Int. Ed.*, **53**, 6515 (2014).
- 2014AGE9306 L. Cisneros, P. Serna, and A. Corma, *Angew. Chem. Int. Ed.*, **53**, 9306 (2014).
- 2014AGE9755 Q.-N. Xia, Q. Cuan, X.-H. Liu, X.-Q. Gong, G.-Z. Lu, and Y.-Q. Wang, *Angew. Chem. Int. Ed.*, **53**, 9755 (2014).
- 2014CATO(234)59 H. Cai, C. Li, A. Wang, and T. Zhang, *Catal. Today*, **234**, 59 (2014).
- 2014CC(57)60 M.O. Kompanets, O.V. Kusch, Y.E. Litvinov, O.L. Pliekhov, K.V. Novikova, A.O. Novokhatko, A.N. Shendrik, A.V. Vasilyev, and I.O. Opeida, *Catal. Commun.*, **57**, 60 (2014).
- 2014CC(57)64 C.A. Antonyray, B. Kim, Y. Kim, S. Shin, K.-Y. Lee, I. Kim, and J.K. Cho, *Catal. Commun.*, **57**, 64 (2014).
- 2014CCC1195 C. Laugel, B. Estrine, J. Le Bras, N. Hoffmann, S. Marinkovic, and J. Muzart, *ChemCatChem*, **6**, 1195 (2014).
- 2014CCC1701 L. Yu, L. He, J. Chen, J. Zheng, L. Ye, H. Lin, and Y. Yuan, *ChemCatChem*, **7**, 1701 (2015).
- 2014CCC3174 J. Chen, Y. Guo, J. Chen, L. Song, and L. Chen, *ChemCatChem*, **6**, 3174 (2014).
- 2014CCC758 B. Karimi, H.M. Mirzaei, and E. Farhangi, *ChemCatChem*, **6**, 758 (2014).
- 2014CCC848 J. Jae, W. Zheng, A.M. Karim, W. Guo, R.F. Lobo, and D.G. Vlachos, *ChemCatChem*, **6**, 848 (2014).
- 2014CL(144)498 B. Siyoo, M. Schneider, M.-M. Pohl, P. Langer, and N. Steinfeldt, *Catal. Lett.*, **144**, 498 (2014).
- 2014CPC1448 R. Liu, J. Chen, L. Chen, Y. Guo, and J. Zhong, *ChemPlusChem*, **79**, 1448 (2014).
- 2014CSC1068 Y.-B. Huang, M.-Y. Chen, L. Yan, Q.-X. Guo, and Y. Fu, *ChemSusChem*, **7**, 1068 (2014).
- 2014CSC2131 G. Yi, S.P. Teong, X. Li, and Y. Zhang, *ChemSusChem*, **7**, 2131 (2014).
- 2014CSC2266 A.J. Kumalaputri, G. Bottari, P.M. Erne, H.J. Heeres, and K. Barta, *ChemSusChem*, **7**, 2266 (2014).
- 2014CSC268 D. Scholz, C. Aellig, and I. Hermans, *ChemSusChem*, **7**, 268 (2014).
- 2014CSC2742 B.J. Wegenhart, L. Yang, S.C. Kwan, R. Harris, H.I. Kenttämä, and M.M. Abu-Omar, *ChemSusChem*, **7**, 2742 (2014).
- 2014CSC3095 B. Saha, C.M. Bohn, and M.M. Abu-Omar, *ChemSusChem*, **7**, 3095 (2014).
- 2014CSC3334 J. Deng, H.-J. Song, M.-S. Cui, Y.-P. Du, and Y. Fu, *ChemSusChem*, **7**, 3334 (2014).
- 2014CSC96 J. Tuteja, H. Choudhary, S. Nishimura, and K. Ebitani, *ChemSusChem*, **7**, 96 (2014).
- 2014CST1174 P.J. Deuss, K. Barta, and J.G. de Vries, *Catal. Sci. Technol.*, **4**, 1174 (2014).

- 2014CST2326 C. Aellig, F. Jenny, D. Scholz, P. Wolf, I. Giovinazzo, F. Kollhoff, and I. Hermans, *Catal. Sci. Technol.*, **4**, 2326 (2014).
- 2014FEBSJ(282)3218 J. Carro, P. Ferreira, L. Rodríguez, A. Prieto, A. Serrano, B. Balcells, A. Ardá, J. Jiménez-Barbero, A. Gutiérrez, R. Ullrich, M. Hofrichter, and A.T. Martínez, *FEBS J.*, **282**, 3218 (2014).
- 2014GC4110 F. Liu, M. Audemar, K. De Oliveira Vigier, J.-M. Clacens, F. De Campo, and F. Jérôme, *Green Chem.*, **16**, 4110 (2014).
- 2014GC1543 M. Chatterjee, T. Ishizaka, and H. Kawanami, *Green Chem.*, **16**, 1543 (2014).
- 2014GC2762 Z. Zhang, B. Liu, K. Lv, J. Sun, and K. Deng, *Green Chem.*, **16**, 2762 (2014).
- 2014GC3778 D.J. Chadderton, L. Xin, J. Qi, Y. Qiu, P. Krishna, K.L. More, and W. Li, *Green Chem.*, **16**, 3778 (2014).
- 2014GC4734 M. Chatterjee, T. Ishizaka, and H. Kawanami, *Green Chem.*, **16**, 4734 (2014).
- 2014IECR1313 Y. Wang, B. Liu, K. Huang, and Z. Zhang, *Ind. Eng. Chem. Res.*, **53**, 1313 (2014).
- 2014IECR5820 S. Wang, Z. Zhang, B. Liu, and J. Li, *Ind. Eng. Chem. Res.*, **53**, 5820 (2014).
- 2014JC(315)67 S. Siankevich, G. Savoglidis, Z. Fei, G. Laurency, D.T.L. Alexander, N. Yan, and P.J. Dyson, *J. Catal.*, **315**, 67 (2014).
- 2014JC(316)57 J. Nie and H. Liu, *J. Catal.*, **316**, 57 (2014).
- 2014JC(317)206 T. Passini, A. Lolli, S. Albonetti, F. Cavani, and M. Mella, *J. Catal.*, **317**, 206 (2014).
- 2014JC(319)61 F. Menegazzo, T. Fantinel, M. Signoretto, F. Pinna, and M. Manzoli, *J. Catal.*, **319**, 61 (2014).
- 2014JCS(D)10224 T. Pasini, G. Solinas, V. Zanotti, S. Albonetti, F. Cavani, A. Vaccari, A. Mazzanti, S. Ranieri, and R. Mazzoni, *Dalton Trans.*, **43**, 10224 (2014).
- 2014JCSCC5633 J. Ohyama, R. Kanao, A. Esaki, and A. Satsuma, *Chem. Commun.*, **50**, 5633 (2014).
- 2014JMCA(388–389)123 S.E. Davis, A.D. Benavidez, R.W. Gosselink, J.H. Bitter, K.P. de Jong, A.K. Datye, and R.J. Davis, *J. Mol. Catal. A Chem.*, **388–389**, 123 (2014).
- 2014KJCE1362 N. Mittal, G.M. Nisola, L.B. Malihan, J.G. Seo, S.-P. Lee, and W.-J. Chung, *Korean J. Chem. Eng.*, **31**, 1362 (2014).
- 2014NATC4123 R.V. Jagadeesh, H. Junge, and M. Beller, *Nat. Commun.*, **5**, 4123 (2014).
- 2014OBC9324 J.A.S. Coelho, A.F. Trindade, V. André, M.T. Duarte, L.F. Veiros, and C.A.M. Afonso, *Org. Biomol. Chem.*, **12**, 9324 (2014).
- 2014PNA8363 J.J. Pacheco and M.E. Davis, *PNAS*, **111**, 8363 (2014).
- 2014RKMC(112)173 R. Sahu and P.L. Dhepe, *React. Kinet. Mech. Cat.*, **112**, 173 (2014).
- 2014RSCA59083 Z. Xu, P. Yan, W. Xu, S. Jia, Z. Xhía, B. Chung, and Z.C. Zhang, *RSC Adv.*, **4**, 59083 (2014).
- 2014RSCA60469 X. Kong, Y. Zhu, H. Zheng, F. Dong, Y. Zhu, and Y.-W. Li, *RSC Adv.*, **4**, 60467 (2014).
- 2014USP0142326 A.S. Shaikh, K.R. Parker, M.E. Janka, and L.R. Partin, US2014/0142326, to Eastman Chemical Company (2014).

- 2014WO086702 M. Breuer, and B. Blank, WO2014/086702 to BASF SE (2014).
- 2014WO122142 J.-M. Clacens, F. Decampo, F. Grasset, B. Katryniok, F. Dumeignil, S. Paul, and V. Rataj, WO2014/122142, to Rhodia Operations (2014).
- 2014WO198057 F. Decampo, and P. Li, WO2014/198057 to Rhodia Operations & Rhodia (China) Co., Ltd. (2014).
- 2015ACAG(504)408 A. Lolli, S. Albonetti, L. Utili, R. Amadori, F. Ospitali, C. Lucarelli, and F. Cavani, *Appl. Catal. A*, **504**, 408 (2015).
- 2015ACAG(506)206 F. Kerdi, H. Ait Rass, C. Pinel, M. Besson, G. Peru, B. Leger, S. Rio, E. Monflier, and A. Ponchel, *Appl. Catal. A*, **506**, 206 (2015).
- 2015ACBE520 S. Albonetti, A. Lolli, V. Morandi, A. Migliori, C. Lucarelli, and F. Cavani, *Appl. Catal. B*, **163**, 520 (2015).
- 2015CSC1862 J. Tuteja, S. Nishimura, H. Choudhary, and K. Ebitani, *ChemSusChem*, **8**, 1862 (2015).
- 2015ACSC2035 J. Lan, J. Lin, Z. Chen, and G. Yin, *ACS Catal.*, **5**, 2035 (2015).
- 2015ACSC5636 G. Lv, H. Wang, Y. Yang, T. Deng, C. Chen, Y. Zhu, and X. Hou, *ACS Catal.*, **5**, 5636 (2015).
- 2015ACSC5904 J.J. Pacheco, J.A. Labinger, A.L. Sessions, and M.E. Davis, *ACS Catal.*, **5**, 5904 (2015).
- 2015ACSC6907 L. Wang and E.Y.-X. Chen, *ACS Catal.*, **5**, 6907 (2015).
- 2015ACSC788 Z. Xu, P. Yan, W. Xu, X. Liu, Z. Xia, B. Chung, S. Jia, and Z.C. Zhang, *ACS Catal.*, **5**, 788 (2015).
- 2015ACSSCE406 S. Wang, Z. Zhang, and B. Liu, *ACS Sustainable Chem. Eng.*, **3**, 406 (2015).
- 2015AGE9837 J.D. Lewis, S. van de Vyver, and Y. Román-Leshkov, *Angew. Chem. Int. Ed.*, **54**, 9835 (2015).
- 2015AICEJ590 J. Luo, L. Arroyo-Ramírez, R.J. Gorte, D. Tsoulaki, and D.G. Vlachos, *AIChE J.*, **61**, 590 (2015).
- 2015AOG152 Y. Zhu, M. Shen, Y. Xia, and M. Lu, *Appl. Organomet. Chem.*, **29**, 152 (2015).
- 2015CC(58)179 A. Jain, S.C. Jonnalagadda, K.V. Ramanujachary, and A. Mugweru, *Catal. Commun.*, **58**, 179 (2015).
- 2015CC(63)21 Y. Zhu, X. Liu, M. Shen, Y. Xia, and M. Lu, *Catal. Commun.*, **63**, 21 (2015).
- 2015CC(63)37 Y. Zhu, M. Shen, Y. Xia, and M. Lu, *Catal. Commun.*, **63**, 37 (2015).
- 2015CC(66)55 P. Yang, Q. Cui, Y. Zu, X. Liu, G. Lu, and Y. Wang, *Catal. Commun.*, **66**, 55 (2015).
- 2015CCCC4050 A.D. Dwivedi, K. Gupta, D. Tyagi, R.K. Rai, S.M. Mobin, and S.K. Singh, *ChemCatChem*, **7**, 4050 (2015).
- 2015CCCC1701 L. Yu, L. He, J. Chen, J. Zheng, L. Ye, H. Lin, and Y. Yuan, *ChemCatChem*, **7**, 1701 (2015).
- 2015CCCC2853 C. Zhou, W. Deng, X. Wan, Q. Zhang, Y. Yang, and Y. Wang, *ChemCatChem*, **7**, 2853 (2015).
- 2015CCL1265 C. Fang, J.-J. Dai, H.-J. Xu, Q.-X. Guo, and Y. Fu, *Chin. Chem. Lett.*, **26**, 1265 (2015).
- 2015CEJ(270)444 L. Gao, K. Deng, J. Zheng, B. Liu, and Z. Zhang, *Chem. Eng. J.*, **270**, 444 (2015).
- 2015CSC1206 H. Ait Rass, N. Essayem, and M. Besson, *ChemSusChem*, **8**, 1206 (2015).

- 2015CSC1323 G. Bottari, A.J. Kumalaputri, K.K. Krawczyk, B.L. Feringa, H.J. Heeres, and K. Barta, *ChemSusChem*, **8**, 1323 (2015).
- 2015CSC1648 T.S.A. Heugebaert, C.V. Stevens, and C.O. Kappe, *ChemSusChem*, **8**, 1648 (2015).
- 2015CSC3590 G. Chieffi, M. Braun, and D. Eposito, *ChemSusChem*, **8**, 3590 (2015).
- 2015CSC3832 J. Artz and R. Palkovits, *ChemSusChem*, **8**, 3832 (2015).
- 2015CSC672 J. Artz, S. Mallmann, and R. Palkovits, *ChemSusChem*, **8**, 672 (2015).
- 2015CST1314 Z. Miao, Y. Zhang, X. Pan, T. Wu, B. Zhang, J. Li, T. Yi, Z. Zhang, and X. Yang, *Catal. Sci. Technol.*, **5**, 1314 (2015).
- 2015CST3108 J. Shi, M. Zhang, W. Du, W. Ning, and Z. Hou, *Catal. Sci. Technol.*, **5**, 3108 (2015).
- 2015CST3194 N. Mei, B. Liu, J. Zheng, K. Lv, D. Tang, and Z. Zhang, *Catal. Sci. Technol.*, **5**, 3194 (2015).
- 2015CST4208 Y. Zhu, X. Kong, H. Zheng, G. Ding, Y. Zhu, and Y.-W. Li, *Catal. Sci. Technol.*, **5**, 4208 (2015).
- 2015GC1308 Z. Zhang, J. Zhen, B. Liu, K. Lv, and K. Deng, *Green Chem.*, **17**, 1308 (2015).
- 2015GC1610 B. Liu, Y. Ren, and Z. Zhang, *Green Chem.*, **17**, 1610 (2015).
- 2015GC2504 X. Kong, R. Zheng, Y. Zhu, G. Ding, Y. Zhu, and Y.-W. Li, *Green Chem.*, **17**, 2504 (2015).
- 2015GC2714 J. Donnelly, C.R. Müller, L. Wiermans, C.J. Chuck, and P. Domínguez de Maria, *Green Chem.*, **7**, 2714 (2015).
- 2015GC2849 S. Subbiah, S.P. Simeonov, J.M.S.S. Esperança, L.P.N. Rebelo, and C.A.M. Afonso, *Green Chem.*, **15**, 2849 (2013).
- 2015GC307 J. Mitra, X. Zhou, and T. Rauchfuss, *Green Chem.*, **17**, 307 (2015).
- 2015GC3271 S.M. McKenna, S. Leimkühler, S. Herter, N.J. Turner, and A.J. Carnell, *Green Chem.*, **17**, 3271 (2015).
- 2015GC3310 P.P. Upare, D.W. Hwang, Y.K. Hwang, U.-H. Lee, D.-Y. Hong, and J.-S. Chang, *Green Chem.*, **17**, 3310 (2015).
- 2015GC3718 Y.-Z. Qin, Y.-M. Li, M.-H. Zong, H. Wu, and N. Li, *Green Chem.*, **17**, 3718 (2015).
- 2015GC3746 P.-F. Koh and T.-P. Loh, *Green Chem.*, **17**, 3746 (2015).
- 2015GC4618 K. Gupta, D. Tyagi, A.D. Dwivedi, S.M. Mobina, and S.K. Singh, *Green Chem.*, **17**, 4618 (2015).
- 2015ICP546 A.S. Amarasekara, T.B. Singh, E. Larkin, M.A. Hasan, and H.-J. Fan, *Ind. Crops Prod.*, **65**, 546 (2015).
- 2015JC(326)1 F. Menegazzo, M. Signoretto, D. Marchese, F. Pinna, and M. Manzoli, *J. Catal.*, **326**, 1 (2015).
- 2015JMCAC(404-405)106 N. Mittal, G.M. Nisola, J.G. Seo, S.-P. Lee, and W.-J. Chung, *J. Mol. Catal. A*, **404–405**, 106 (2015).
- 2015JOC10404 R.F.A. Gomes, J.A.S. Coelho, R.F.M. Frade, A.F. Trindade, and C.A.M. Afonso, *J. Org. Chem.*, **80**, 10404 (2015).
- 2015OL5244 S. Sowmiah, L.F. Veiros, J.M.S.S. Esperança, L.P.N. Rebelo, and C.A.M. Afonso, *Org. Lett.*, **17**, 5244 (2015).
- 2015RCBIE1069 V.P. Kashparova, E.A. Khokhlova, K.I. Galkin, V.M. Chernyshev, and V.P. Ananikov, *Russ. Chem. Bull. Int. Ed.*, **64**, 1069 (2015).
- 2015RSCA69238 J.-N. Tan, M. Ahmar, and Y. Queneau, *RSC Adv.*, **5**, 69238 (2015).

- 2015USP0051412 M.E. Janka, D. Lange, M.C. Morrow, B.R. Bowers, K.R. Parker, A. Shaik, L.R. Partin, and C. Sumner, US2015/0051412, to Eastman Chemical Company (2015).
- 2015USP0314272 S.S. Stahl, A.B. Powell, T.W. Root, D.S. Mannel, and M.S. Ahmed, US2015/0314272 to Wisconsin Alumni Research Foundation (2015).
- 2015USP0336090 N. Kanna, S.V.V. Chilukuri, G.D. Kokate, and L. Gurralla, US2015/0336090, to Council of Scientific & Industrial Research (2015).
- 2015WO056270 S.K.M. Konduri, S.K. Thoota, P.R. Muddasani, K.S.B.R. Adibhatla, and V.C. Nannapaneni, WO2015/056270, to Natco Phram Limited (2015).
- 2015WO155784 S.K.M. Konduri, S.K. Thoota, C. Javvadi, P.R. Muddasani, K.S.B.R. Adibhatla, and V.C. Nannapaneni, WO2015/155784 (2015).
- 2016ACBE(180)751 F. Neațu, R.S. Marin, M. Florea, N. Petrea, O.D. Pavel, and V.I. Pârvulescu, *Appl. Catal. B*, **180**, 751 (2016).
- 2016ACSC381 T. Yan, B.L. Feringa, and K. Barta, *ACS Catal.*, **6**, 381 (2016).
- 2016ACSC3784 Z. Xu, P. Yan, H. Li, K. Liu, X. Liu, S. Jia, and Z.C. Zhang, *ACS Catal.*, **6**, 3784 (2016).
- 2016AGE8338 K.I. Galkin, E.A. Krivodaeva, L.V. Romshov, S.S. Zalesskiy, V.V. Kachala, J.V. Burykina, and V.P. Ananikov, *Angew. Chem. Int. Ed.*, **55**, 8338 (2016).
- 2016CEJ(238)1315 X. Liu, J. Xiao, H. Ding, W. Zhong, Q. Xu, S. Su, and D. Yin, *Chem. Eng. J.*, **283**, 1315 (2016).
- 2016CSC521 N. Perret, A. Grigoropoulos, M. Zanella, T.D. Manning, J.B. Claridge, and M.J. Rosseinsky, *ChemSusChem*, **9**, 521 (2016).
- 2016CSC1209 W.-P. Wu, Y.-J. Xu, R. Zhu, M.-S. Cui, X.-L. Li, J. Deng, and Y. Fu, *ChemSusChem*, **9**, 1209 (2016).
- 2016F(163)74 J. Liu, L. Arroyo-Ramírez, J. Wei, H. Yun, C.B. Murray, and R.J. Gorte, *Appl. Catal. A*, **508**, 86 (2015).
- 2016GC1855 S. Higson, F. Subrizi, T.D. Sheppard, and H.C. Hailes, *Green Chem.*, **18**, 1855 (2016).
- 2016GC2302 G. Lv, H. Wang, Y. Yang, T. Deng, C. Chen, Y. Zhu, and X. Hou, *Green Chem.*, **18**, 2302 (2016).
- 2016GC487 M. Chatterjee, T. Ishizaka, and H. Kawanami, *Green Chem.*, **18**, 487 (2016).
- 2016GC643 X. Li and Y. Zhang, *Green Chem.*, **18**, 643 (2016).
- 2016GC676 J. Ohyama, R. Kanao, Y. Ohira, and A. Satsuma, *Green Chem.*, **18**, 676 (2016).
- 2016GC974 X. Jia, J. Ma, M. Wang, H. Ma, C. Chen, and J. Xu, *Green Chem.*, **18**, 974 (2016).
- 2016GC979 G. Yi, S.P. Teong, and Y. Zhang, *Green Chem.*, **18**, 979 (2016).
- 2016JTICE92 S. Wang, B. Liu, Z. Yuan, and Z. Zhang, *J. Taiwan Inst. Chem. Eng.*, **58**, 92 (2016).
- 2016SC1245 V.V. Martichonok, P.K. Chiang, P.J. Dornbush, and K.M. Land, *Synth. Commun.*, **44**, 1245 (2014).
- 2016WO004867 P. Li, and F. Decampo, WO2016/004867 to Rhodia Operations (2016).



# INDEX

'Note: Page numbers followed by "f" indicate figures and "t" indicate tables.'

## A

- Acetone peroxide, 91
- Achmatowicz rearrangement, 285–286
- 3-Acyl-2-aminobenzofurans, 219–220
- 3-Acyl-2-(*N*-acylamino)benzofurans, 219–220
- $\beta$ -Alkylation, 136
- Amberlyst-15, 183
- 5-Amino-3-nitro-1,2,4-triazole (ANTA), 111
- $\beta$ -Amino thiones, 45
- Aryl chlorides, 211–212
- Avantium's process, 248–249, 251
- Azabicyclo[2.2.1]heptanes, 24–25, 25f
- Azabicyclo[3.1.0]hexanes, 24, 24f
- Azabicyclononanes, 26–27
- Azabicyclo[3.2.1]octanes, 25–26, 26f
- Azetidines, 15–16, 15f
- Aziridines, 175–176
- Azole-based high energy density materials
  - explosophores, 89–90
  - imidazole-based energetic materials, 104–105
    - 2,4-dinitroimidazole, 105
    - 1-nitramino-2,4-dinitroimidazole, 105, 107
    - N*-nitrobenzyl imidazole derivatives, 108–109
    - N,N'*-nitroamino 4,4',5,5'-tetranitro-2,2'-biimidazole, 107–108
    - N*-trinitroethylamination, 105–106
  - nucleophilic aromatic substitution, 108–109
  - pyrazole-based energetic materials, 92–104
  - representative energetic compounds, 90–91
  - tetrazole-based energetic materials, 123–127
  - triazole-based energetic materials, 109–121

## B

- Baeyer–Villiger (BV) oxidation, 200
- Benclonthiaz, 77f, 78–79
  - discovery, 79
  - structure-activity relationships, 80
  - synthesis, 79–80
- Benthiavalicarb, 59f, 64
  - discovery, 65, 65f
  - structure-activity relationships, 66, 66f
  - synthesis, 65
- Benzimidazoles, 190–191
- Benzisothiazoles, 48–49
- Benzodiazoles, 146–148
- Benzodithiophenes, 142–144
- Benzotriazole, 148
- Biaryls, 5–6
- Bioisosteric replacement, 42–44, 43f

## C

- $\epsilon$ -Caprolactam (CPL), 200
- Carbazoles, 148–149
- CC chemokine receptor-1 (CCR1), 21
- 5-Chloromethylfurfural (CMF), 251
- 2-Chlorothiazol-5-ylmethyl chloride (CCT), 51
- Clothianidin, 49f, 53
  - discovery, 53, 54f
  - structure-activity relationships, 54–55, 55f
  - synthesis, 54
- Cook–Heilborn's synthesis, 44–45
- Cyclopenta[1,2-*b*:5,4-*b'*]dithiophenes (CPDT), 142
- Cyclopenta[1,2-*b*:5,4-*b'*]dithiophen-4-one (CDT), 141–142
- Cyclotrimethylenetrinitramine (RDX), 90–91
- Cyperus difformis*, 75

## D

- 1,1-Diamino-2,2-dinitroethene (FOX-7), 91

2,2-Diaryltetrahydrofuran, 19  
Dibenzothiophene (DBT), 140–141  
Dicloromezotiaz, 49f  
  discovery, 55, 56f  
  structure-activity relationships, 58, 58f  
  synthesis, 57  
  triflumezopyrim, 55  
Diels–Alder reaction, 277  
2,5-Diformylfuran (DFF), 260–262  
Dimethylfuran, 281–284, 282t–283t  
Dimethyl sulfoxide (DMSO), 248–249  
2,4-Dinitroimidazole, 105  
Dipeptidyl peptidase 4 (DPP4), 21  
Dithieno[3,2-*b*:20,3'-*d*]pyrrole (DTP),  
  149  
DNA methyltransferase inhibitors, 19  
Drugs/drug candidates  
  biaryls, 5–6, 6f–7f  
  heterocyclic pharmacophores, 7–8, 8f–9f  
  major influencers, drug structures, 2, 2f  
  method, 3  
  palladium-catalyzed cross-coupling  
    reactions, 6–7, 8f  
  ring containing compounds/molecules,  
    3–5, 4f–5f  
  Suzuki couplings, 10–11  
  synthetic accessibility, 10–11  
  transition metal catalyzed crosscoupling  
    reactions, 5–6, 6f

## E

Epoxides, 179  
3,4-Epoxy-1-butene (EpB), 179  
Ethaboxam, 59f  
  discovery, 63, 63f  
  structure-activity relationships, 64, 64f  
  synthesis, 63–64  
3,4-Ethylenedioxythiophene (EDOT),  
  136–137  
Explosophores, 89–90

## F

Fibroblast activation protein (FAP), 18–19  
Five-membered heterocycles  
  amberlyst-15, 183  
  amorphous SiO<sub>2</sub>-Al<sub>2</sub>O<sub>3</sub>, 189  
  benzimidazoles, 190–191

  benzothiazole derivatives, 192  
  cyclic carbonates, 191  
  furan-2,5-dicarboxylic acid (FDCA), 186  
  gold catalysts, 183  
  5-hydroxymethylfurfural (HMF),  
    185–186  
  imidazole, 190  
  maleic anhydride (MA), 183–185  
  *N*-acylindoles, 189  
  olefinic acids, 186–187  
  Paal–Knorr synthesis, 183  
  phthalic anhydride (PA), 185  
  pyrazole synthesis, 187–188  
  solid-acid SSA, 187  
  Sonogashira coupling, 189–190  
  γ-valerolactone, 186  
  vapor-phase synthesis, 191  
Fluensulfone, 77, 77f  
  discovery, 78  
  structure-activity relationships, 78  
  synthesis, 78  
Four-membered heterocycles, 182  
Friedlander quinoline synthesis, 195–196  
Fungicides, 58, 59f  
  benthiavalicarb, 64–66  
  ethaboxam, 63–64  
  isotianil, 66–67  
  oxathiapiprolin, 68–69  
  thiabendazole, 58–60  
  thifluzamide, 60–62  
2,5-Furandicarboxylic acid (FDCA),  
  185–186, 248–249  
5-hydroxymethylfurfural  
  catalyzed oxidation, 256,  
    257t  
  enzymatic oxidation, 256, 259t  
  oxidation, other oxidants, 256, 258t  
  oxidation/pathways, 252, 253t–254t,  
    255  
Fused thiophenes, 138–145  
  benzodithiophenes, 142–144  
  cyclopenta[1,2-*b*:5,4-*b'*]dithiophenes  
    (CPDT), 142  
  cyclopenta[1,2-*b*:5,4-*b'*]dithiophen-4-  
    one (CDT), 141–142  
  dibenzothiophene (DBT), 140–141  
  isothianaphthene (ITN), 138–139

- naphthodithiophenes (NDTs), 143–145, 144f  
thienothiophenes (TTs), 139–140
- G**  
Glucagon-like peptide-1 (GLP-1), 20  
G-protein bile receptor 1, 15  
G-protein-coupled receptor (GPCR) 119, 20  
Green syntheses. *See also*  
5-Hydroxymethylfurfural (HMF)  
hydrogenation products  
diamines and aminoalcohols, 270–272  
diols and triols, 262–267  
1-hydroxy-2,6-hexanedione, 267–270  
nylon intermediates, 272–276  
monomers, polymers  
hydrogenation products, 262–276  
oxidation products, 252–262
- H**  
Hantzsch's dihydropyridine synthesis, 194–195, 197–198  
Herbicides, 69–71, 73f  
mefenacet, 74–77  
methabenzthiazuron, 71–74  
Heterobicyclo systems  
amantidine derivatives, 27  
azabicyclo[2.2.1]heptanes, 24–25, 25f  
azabicyclo[3.1.0]hexanes, 24, 24f  
azabicyclononanes, 26–27  
azabicyclo[3.2.1]octanes, 25–26, 26f  
nicotinamide phosphoribosyltransferase, 27  
Heterocyclic building blocks, 134–135  
BODIPY, 160–161  
nitrogen-containing building blocks, 145–146  
benzodiazoles, 146–148  
benzotriazole, 148  
carbazoles, 148–149  
dithieno[3,2-*b*:20,3'-*d*]pyrrole (DTP), 149  
imide-based building blocks, 150–156  
quinoxaline, 146  
thieno[3,4-*b*]pyrazines (TPZs), 146  
phosphole derivatives, 159–160  
silole derivatives, 157–159  
thiophene-related building blocks  
fused thiophenes, 138–145  
selenophenes, 135–138  
tellurophenes, 135–138  
thiophenes, 135–138  
Heterogeneous catalysts, 174–175, *See also specific heterocycles*  
catalyst choice, 175–176  
five-membered heterocycles, 183–192  
four-membered heterocycles, 182  
metallo-silicates, 176–177  
microporous zeolites, 176, 177t  
process and economic considerations, 201–202  
reaction chemistry, classification, 178  
seven-membered heterocycles, 199–201  
six-membered heterocycles, 192–199  
solid-base materials, 178  
sulfuric acid-treated montmorillonite clays, 177  
three-membered heterocycles, 178–182  
3,3,6,6,9,9-Hexamethyl-1,2,4,5,7,8-hexaoxacyclononane (TATP), 91  
Hexanitrohexaazaisowurtzitane (HNIW), 90–91  
High energy density materials (HEDMs), 92  
High fructose corn syrup (HFCS), 251–252  
HMF. *See* 5-Hydroxymethylfurfural (HMF)  
HMX. *See* Octahydro-1,3,5,7-tetranitro-1,3,5,7-tetrazocine (HMX)  
Hoiamide A, 38  
Hydrogenation products  
diamines and aminoalcohols, 270–272, 275  
diols and triols, 262–267, 268t–269t, 271t  
1-hydroxy-2,6-hexanedione, 267–270, 272, 273t–274t  
nylon intermediates, 272–276  
1-Hydroxy-2,6-hexanedione (HHD), 267–270, 272, 273t–274t  
5-Hydroxymethyl-2-furancarboxylic acid (HMFA), 260, 261t

5-Hydroxymethylfurfural (HMF), 185–186  
to carbocycles, 275–277  
C–C bond formation  
  aldol condensation reactions, 279–281  
  arylations, 279–280  
  Baylis–Hillman reaction, 281  
  benzoin condensation, 278–279  
  coupling, 278  
  Diels–Alder reaction, 277  
dimethylfuran, 281–284, 282t–283t  
hydrogenation, 267  
  diamines and aminoalcohols, 270–272, 275  
  nylon intermediates, 272–276  
oxidation products, 284–285  
  bis-imidate and bis-amidinium salt, 260  
  from renewable resources, 248–250  
transformations, 285–286

## I

Imidazole-based energetic materials,  
  104–105  
  2,4-dinitroimidazole, 105  
  1-nitramino-2,4-dinitroimidazole, 105, 107  
  *N*-nitrobenzyl imidazole derivatives, 108–109  
  *N,N'*-nitroamino 4,4',5,5'-tetranitro-2,2'-biimidazole, 107–108  
  *N*-trinitroethylamination, 105–106  
  nucleophilic aromatic substitution, 108–109  
Imide-based building blocks, 155f  
  benzodipyrroledione (BPD), 152  
  3,7-bis(2-oxoindolin-3-ylidene)benzo[1,2-*b*:4,5-*b'*]difuran-2,6(3*H*,7*H*)-dione, 154  
  diketopyrrolopyrrole (DPP), 151–152  
  with thiophene and pyridine wings, 151–152  
  dithienocoronene diimide from 1,7-bromopyrene diimide, 156–157  
  isoindigo (IID), 153–154  
  *N*-alkylated phthalimides from phthalic anhydride, 150

  naphthalene diimide derivatives from naphthalene dianhydride, 154–155  
  pyrene diimide derivatives from pyrene dianhydride, 156  
  semiconducting polymer with pyrene diimide moiety, 156  
  thieno[3,4-*c*]pyrrole-4,6-dione from 3,4-dibromothiophene, 151  
  thienoisoindoleone (TIO), 152–153  
Insecticides, 49, 49f  
  clothianidin, 53–55  
  dicloromezotiaz, 55–58  
  thiamethoxam, 50–53  
International Zeolite Association (IZA), 176  
Isoindigo (IID), 153–154  
Isoindoloquinazolinones, 214–216  
Isothianaphthene (ITN), 138–139  
Isotianil, 59f, 66  
  discovery, 66–67  
  structure-activity relationships, 67  
  synthesis, 67

## J

Janus kinases (JAKs), 16

## L

$\gamma$ -Lactones, 213  
Lewis acidity, 276  
Lignocellulose, 248

## M

Maleic anhydride (MA), 183–185  
MDDR database, 3  
Mefenacet, 73f, 74  
  discovery, 74–75, 74f  
  structure-activity relationships, 75–77, 76f  
  synthesis, 73, 75  
Metallosilicates, 176–177  
Methabenzthiazuron, 71–73, 73f  
  discovery, 73  
  structure-activity relationships, 74  
  synthesis, 73–74  
Microporous zeolites, 176, 177t

**N**

Naphthodithiophenes (NDTs), 143–145, 144f

Nematicides, 77

benclonthiaz, 78–80

fluensulfone, 77–78

Nitrogen-containing building blocks, 145–146

benzodiazoles, 146–148

benzotriazole, 148

carbazoles, 148–149

dithieno[3,2-*b*:20,3'-*d*]pyrrole (DTP), 149

imide-based building blocks,

150–156

quinoxaline, 146

thieno[3,4-*b*]pyrazines (TPZs), 146

Nitroglycerine, 90–91

*N,N'*-ethylene-bridged 4,4'-

diaminobis(pyrazole), 96–97

*N,N'*-ethylene-bridged 5,5'-

diaminobis(pyrazole), 97–98

*N,N'*-ethylene-bridged 4,4'-

diazidobis(pyrazole), 97–98

*N,N'*-nitroamino 4,4',5,5'-tetranitro-

2,2'-biimidazole, 107–108

**O**

Octahydroacridines, 196

Octahydro-1,3,5,7-tetranitro-1,3,5,7-tetrazocine (HMX), 90–91

Octanitrocubane (ONC), 91

Olefinic acids, 186–187

Organic semiconductors. *See* Heterocyclic building blocks

Oxathiapiprolin, 59f, 68

discovery, 68, 68f

structure–activity relationships,

69, 72f

synthesis, 69–71

Oxetanes, 16–17, 17f

Oxidation products

2,5-diformylfuran, 260–262

FDCA, *See-also* 2,5-Furandicarboxylic acid (FDCA)

palladium, 252–255

terephthalic acid, 252

5-hydroxymethyl-2-furancarboxylic acid (HMFCFA), 260, 261t

Oxone<sup>®</sup>, 94–95

**P**

Paal–Knorr synthesis, 183

Palladium-catalyzed carbonylative synthesis, 207

alkoxycarbonylative macrolactonization, 242–243

2,3-dihydrobenzodioxepinones, 241, 243

five-membered heterocycles

acenaphthoimidazolylidene palladium, 208–209

3-acyl-2-aminobenzofurans, 219–220

3-acyl-2-(*N*-acylamino)benzofurans, 219–220

1,2,4- and 1,3,4-oxadiazole, 215–216

aryl chlorides, 211–212

*t*-butylamine, 208

carbonylative annulation to  $\gamma$ -lactones, 213–214

*o*-chloroketimines to isoindolin-1-ones, 212

1,2-dibromobenzene, 211

isoindoloquinazolinones, 214–216

$\gamma$ -lactones, 213

*N*-unprotected arylethylamines to five-membered benzolactams., 212

oxidative carbonylation of hydrazides, 217–218

oxidative O–H/*N*–H carbonylation of hydrazides, 217–218

sequential one-pot synthesis, 211

vinyl C(sp<sup>2</sup>)-H bond, 213–215

six-membered heterocycles, 232, 237, 240

amino esters to six-membered benzolactams, 221–222

2-aminopyridine to quinazolinone, 235

*o*-arylaniline, 224–225

aryl bromides to quinazolines, 230–232

2-bromoanilines, 228–229

carbonylative cycloamidation of ketoimines, 234–235

- Palladium-catalyzed carbonylative synthesis  
(*Continued*)  
 carbonylative Sonogashira cross-coupling to 4-quinolones, 230–231  
 C–H activation/carbonylation,  
 2-arylphenols, 222–223  
 $\alpha$ -chloroketones to 3-acyl-4-hydroxy-2-pyranone, 239–240  
 double carbonylative synthesis, quinazolinones, 229–230  
 enamides to 1,3-oxazin-6-ones, 226  
 2-fluorobromobenzene to quinazolinone, 235  
 2-fluorobromobenzene with DBU, 236–237  
 icarbonylative synthesis, tetracyclic quinazolinones, 229–230  
*o*-iodoanilines to isatoic anhydrides, 238–239  
 isatoic anhydride, 238  
 linear and angular fused quinazolinones, 236  
 multicomponent synthesis of uracil analogs, 239–240  
*N*-arylpyridine-2-amine to 11*H*-pyrido[2,1-*b*]quinazolin-11-one, 233–234  
*N*-arylpyridine-2-amine with internal alkyne to 2-quinolinone, 232–233  
*N*-(2-bromophenyl)pyridine-2-amines, 234  
*N*-(*o*-bromoaryl)amides to benzoxazinones, 227  
*N*-sulfonyl-2-aminobiaryls to phenanthridinones, 224–225  
 3-phenylquinolin-4(1*H*)-one, 223–224  
 quinazolines, 238–239  
 salicylic aldehyde and benzyl chloride to chromenone, 225–226  
 2-vinylanilines to 2(1*H*)-quinolinones, 227–228  
 Pechmann condensation, 198–199  
 Pentaerythritol tetranitrate (PETN), 90–91  
 Phenylmethylcarbinol (PhMeCHOH), 180  
 Phosphole derivatives, 159–160  
 Phthalic anhydride (PA), 185  
 $\beta$ -Picoline, 193  
 Picric acid, 90–91  
 Piperidines, 20–21, 21f  
 Platform chemicals, 248–249  
 Polyhydroxylated piperidines, 21  
 Pyrazole-based energetic materials  
 amination, 95–96  
 4-(4'-amino-3,5'-dinitro-1'-pyrazol)-3,5-dinitro-1*H*-pyrazolate, 101–103  
 4-amino-3,7,8-trinitropyrazolo-[5,1-*c*][1,2,4]triazine, 100–101  
 bis(heterocycle), 101–102  
 3,4-dinitro- and 3,5-dinitro-1-(trinitromethyl)pyrazoles, 101  
 hexanitrobenzene, 92–93  
 monocationic 5-nitramino 3,4-dinitropyrazolates, 98–100  
 multifunctionalized nitraminopyrazoles, 98–100  
 4-nitramino-3,5-dinitropyrazole, 97–99  
 1,4-nitramino 3,5-dinitropyrazole-based salts, 98–100  
*N,N'*-azo-bridged bispyrazoles, 104  
*N,N'*-ethylene-bridged 4,4'-diaminobis(pyrazole), 96–97  
*N,N'*-ethylene-bridged 5,5'-diaminobis(pyrazole), 97–98  
*N,N'*-ethylene-bridged 4,4'-diazidobis(pyrazole), 97–98  
*N,N'*-2-nitrazapropyl-bridged bis(pyrazoles), 102–104  
 Oxone<sup>®</sup>, 94–95  
 polynitro-substituted bispyrazoles, 101–102  
 3,4,5-trinitro-1*H* pyrazole (TNP), 92–93  
 3,4,5-trinitro-1*H*-pyrazol-1-ol, 94–95  
 Pyrrolidines, 17–19, 18f
- Q**  
 Quinoxaline, 146
- R**  
 RDX. *See* Cyclotrimethylenetrinitramine (RDX)  
 ROUTINE<sup>™</sup>, 66

**S**

Saturated heterocycles, 14  
  heterobicyclo systems, 24–27  
  one heteroatom ring systems, 15–22  
  spirocyclic heterocyclic ring systems,  
  22–24

*Scirpus juncooides*, 75

Seven-membered heterocycles, 199–201

SGLT. *See* Sodium-dependent glucose  
  transporter (SGLT)

SHARID™, 66

Sharpless epoxidation, 182

Silole derivatives, 157–159

Six-membered heterocycles

  Friedlander quinoline synthesis, 195–196

  Hantzsch dihydropyridine synthesis, 194–  
  195, 197–198

  lactic acid (LA), 199

  octahydroacridines, 196

  Pechmann condensation, 198–199

  picolines, 193

  polyarylpyridines, 194

  pyrazine, 197

  Sc-USY catalyst, 196–197

  s-triazines, 198

  Ti-Pd-MFI catalyst, 192–193

Sodium-dependent glucose transporter  
  (SGLT), 21

Spirocyclic heterocyclic ring systems, 22

  spirooxetanes, 22

  spiropiperidines, 23–24, 23f

  spiropyrrolidines, 22–23, 23f

Spirooxetanes, 22

Spiropiperidines, 23–24, 23f

Spiropyrrolidines, 22–23, 23f

Sulfuric acid-treated montmorillonite  
  clays, 177

Suzuki couplings, 10–11

Synthetic accessibility, 10–11

**T**

Tetrahydrofurans, 19–20, 19f

Tetrahydropyrans, 21–22, 21f

Tetrazole-based energetic materials

  5-aminotetrazole-1-ol, 125–127

  5,5'-bistetrazole-1,1'-diol dihydrate,  
  125–126

  1,5-di(nitramino)tetrazole, 124

  5-nitro-2-nitratomethyl-tetrazole, 127

*N,N'*-ether-bridged tetrazoles, 123

  potassium 1,1'-dinitramino-5,5'-  
  bistetrazolate, 124–125

Terephthalic acid, 252

Thiabendazole, 58–59, 59f

  discovery, 59

  structure-activity relationships, 60

  synthesis, 59–60

Thiamethoxam, 49f

  discovery, 50, 51f

  neonicotinoids, 50

  structure-activity relationships, 52–53, 52f

  synthesis, 51–52

Thiazole/isothiazole ring containing  
  compounds, 80–81

  benzothiazoles and benzisothiazoles, 37f, 38

  bioisosteric replacement, 42–44, 43f

  in crop protection, 40f

  aromatic heterocyclic rings, 39, 42f

  occurrence, 39, 41t

  fungicides, 58, 59f

  benthiavalcarb, 64–66

  ethaboxam, 63–64

  isotianil, 66–67

  oxathiapiprolin, 68–69

  thiabendazole, 58–60

  thifluzamide, 60–62

  generic structures, 37, 37f

  herbicides, 69–71, 73f

  mefenacet, 74–77

  methabenzthiazuron, 71–74

  hoiamide A, 38

  insecticides, 49, 49f

  clothianidin, 53–55

  dicloromezotiaz, 55–58

  thiamethoxam, 50–53

  nematicides, 77

  benclonthiaz, 78–80

  fluensulfone, 77–78

  synthesis

    benzisothiazoles, 48–49

    benzothiazoles, 47–48

    isothiazoles, 45–47

    thiazoles, 44–45

  thiazole moiety, 38

- Thieno[3,4-*b*]pyrazines (TPZs), 146
- Thienoisindole-dione (TID), 152–153
- Thienothiophenes (TTs), 139–140
- Thiufuzamide, 59f
- discovery, 61, 61f
  - structure-activity relationships, 61–62, 62f
  - succinate dehydrogenase inhibitors (SDHI), 60–61
  - synthesis, 61–62
- Thiophene-related building blocks
- fused thiophenes, 138–145
    - benzodithiophenes, 142–144
    - cyclopenta[1,2-*b*:5,4-*b'*]dithiophenes (CPDT), 142
    - cyclopenta[1,2-*b*:5,4-*b'*]dithiophen-4-one (CDT), 141–142
    - dibenzothiophene (DBT), 140–141
    - isothianaphthene (ITN), 138–139
    - naphthodithiophenes (NDTs), 143–145, 144f
    - thienothiophenes (TTs), 139–140
  - selenophenes, 135–138
  - tellurophenes, 135–138
  - thiophenes, 135–138
- Thiophenes, 135–138
- Three-membered heterocycles
- Ag-catalyzed vapor-phase processes, 180
  - aziridines, 175–176
  - bifunctional epoxidation catalysts, 181
  - epoxides, 179
  - 3,4-epoxy-1-butene (EpB), 179
  - H<sub>2</sub>O<sub>2</sub> production, 180–181
  - sharpless epoxidation, 182
  - t*-BuOH and PhMeCHOH, 180
  - TS-1 catalyst, 180–181
  - vapor-phase EO production, 179
- TNT. *See* 2,4,6-Trinitrotoluene (TNT)
- 2,4,6-Triamino-1,3,5-trinitrobenzene (TATB), 91
- 2,4,6-Triarylpyridines, 194
- Triazole-based energetic materials, 109
- ammonium perchlorate (AP), 109–110
  - azo-bridged trinitromethyl 1,2,4-triazoles, 110–111
  - 4,4'-bis(5-nitro-1,2,3-*2H*-triazole), 120–122
  - 3,3'-diamino-4,4'-azobis-1,2,4-triazole, 117
  - 5,5'-diamino-4,4'-dinitramino-3,3'-bi-1,2,4-triazole, 119–120
  - 1,3-dichloro-2-nitrazapropene, 111–112
  - dinitro-bis-1,2,4-triazole-1,1'-diol, 113–114
  - 3-dinitromethyl-1,2,4-triazolone, 120
  - energetic bis(1,2,4-triazole) derivatives, 112–113
  - high-dense 5,5'-dinitromethyl bis(1,2,4-triazole), 112–113
  - 1-methyl-5-nitramino-3-nitro-1,2,4-triazole, 111–112
  - N-functionalized 1,2,4-triazoles, 113–115
  - 3-nitro-1-(2*H*-tetrazol-5-yl)-1*H*-1,2,4-triazol-5-amine, 114, 116
  - 5-nitro-1,2,3-*2H*-triazole, 120–121
  - 3-nitro-5-nitramino-1*H*-1,2,4-triazole, 111–112
  - polysubstituted derivatives, 115–116
  - 4,4',5,5'-tetraamino-3,3'-bi-2,4-triazolium cation, 118–119
  - 3,6,7-triamino-[1,2,4]triazolo[4,3-*b*][1,2,4]triazole, 117–118
  - 1,2,3-triazole to 1,2,3,4-tetrazine, 121, 123
  - trinitromethyl and dinitromethyl 1,2,4-triazoles, 110
  - 3,4,5-Trinitro-1*H* pyrazole (TNP), 92–93
  - 2,4,6-Trinitrotoluene (TNT), 90–91
  - TTs. *See* Thienothiophenes (TTs)
- V**
- γ-Valerolactone, 186
- W**
- WNT signaling, 23